Mapping ENU-induced thymic lymphoma susceptibility loci in C57BL/6 mice

A dissertation presented by Pedro Romao in fulfilment of the requirements for the degree of Doctor of Veterinary Medicine in the subject of Laboratory Animal Medicine to the School of Veterinary Medicine and Science, University of Nottingham.

November, 2016

Acknowledgements

I would like to express my deep gratitude and appreciation to my supervisor, Dr Paul Potter, for the all the support and guidance in conducting this work, for being available at every moment and for having a such a friendly approach. I also thank you to Professor Cheryl Scudamore, my co-supervisor, for guiding me though the pathology territories of this work and through my first steps in murine histopathology.

I express my deepest gratitude to Janet Rodgers – your wisdom has led me into a much higher level of professional fulfilment. I also want to thank Maggie Lloyd for the ever refreshing and vibrant spark she brought to my learning process during the residency element of this programme.

I also want to thank Professor Sarah Wolfensohn and Professor Tim Morris for creating the Oxford/Nottingham Laboratory Animal Doctoral Programme and the Wellcome Trust for funding it. Thanks to Professor David Haig and Dr Mark Bowen for their support and guidance throughout the programme.

To David Whittaker, Paul West, Dr Caroline Bergman, Dr Wairimu Gatome, Dr Manuel Berdoy, Dr Kathy Murphy and Madalena Gallagher, my honest thank you for making me feel at home, showing me the art and science of being the Named Veterinary Surgeon and, above all, for your friendship. I will always remember my years at Oxford.

To Dr Paul Schroeder and Dr Lindsay Benson, thank you for having been great “old brothers”. Loreen Chan, my doctorate colleague - thank you for sharing along the way – it would not have been as fun without you.

At the Medical Research Council, I would like to express my gratitude to my colleagues Sara Falcone, Thomas Nicol, Andy Blease, Andy Haynes and Heena Lad for their support. Tom and Sara, you were exceptionally friendly and your willingness to help was inspiring - thank you ever so much. Simon Greenaway from Bioinformatics processed the genotyping data, for which I am very thankful.

This work would not have been possible without the highly professional support of Mary Lyon Centre Ward 3 team, Marie Hutchinson, Rosie Hillier, Craig Tizzard, Bonnie Wood, Steven Andrews, Natalie Rivers, Gemma Law and Anna Domenech. Thank you very much guys!

To Paras Pathak, Helen Natukunda and Sarah Vivers, from MRC Harwell, Clinical Pathology, thank you very much. Your generosity in sharing your knowledge was priceless. Helen, seeing you leading by example and making that extra effort to achieve more and better, in work and in life, was truly inspiring - thank you for inspiring me. In the statistical department, I would like to thank George Nicholson from the University of Oxford and Kayleigh Leigh and Jennifer Thomas from Envigo for their incredible support and guidance with the statistical analysis of the data.

My appreciation naturally extends to those good friends with whom life outside work was enjoyable and even special – to my friend Dragos Lordean, to Luis Santos, Tom Agnew, Samantha Laber and Hugo Oliveira, I will not forget the good times! An extended thank you to Dragos Lordean, Thomas Nicol and Sara Falcone for helping with the proof reading. To Margarida Avillez, my eternal gratitude for your support.

Finally, to my parents Rosa and Jose Romao, for being a pillar of strength in my life.

Declaration

I declare that the work in this thesis was carried out in accordance with the regulations of the University of Nottingham. The work is original and no part of the thesis has been submitted for any other academic award. Any views expressed in the thesis are those of the author.

Ethical note

The research was approved by the Ethics Committee at the Medical Research Council Harwell, by the University of Nottingham and conducted humanely under a Project Licence, UK Home Office.

Table of contents

Acknowledgements 2

Declaration 4

Ethical note 4

Table of contents 5

Abbreviations 18

1. Introduction 20

1.1. Introduction 21

1.2. Background 21

1.3. Neoplasia and genetics 23

1.3.1. Lymphoid neoplasms 25

1.3.1.1. Classification of lymphoid neoplasms in humans 25

1.3.1.2. Epidemiology 29

1.3.1.3. Precursor T-cell lymphoblastic leukaemia/lymphoma (T-ALL) 31

1.3.1.3.1. Thymocyte differentiation 33

1.3.1.3.2. Clinical features and sites of involvement 34

1.3.1.3.3. Morphology of T-ALLs 34

1.3.1.3.4. Immunophenotype 35

1.3.1.3.5. Molecular pathogenesis 39

1.3.1.3.6. Gene expression profiling 44

1.3.1.3.7. Prognosis 45

1.3.1.4. Lymphoma in laboratory mice 46

1.3.1.4.1. Spontaneous lymphoid neoplasms in laboratory mice 47

1.3.1.4.2. ENU-induced lymphoid neoplasms in laboratory mice 48

1.3.1.4.3. Classification of mouse lymphoid neoplasms 52

1.3.1.4.3.1. B-cell neoplasms 52

1.3.1.4.3.2. T-cell neoplasms 53

1.3.1.4.4. Clinical signs 54

1.3.1.4.5. Necropsy gross findings of thymic lymphomas 55

1.3.1.4.6. Gold standards for diagnosis of lymphoma 55

1.3.1.4.7. Immunophenotype 58

1.3.1.4.7.1. Antigen expression during mouse T-cell development 59

1.3.1.4.7.2. T-cell-associated antigens used in flow cytometry 60

1.3.1.4.7.3. Other cluster differentiation (CD) markers associated with normal and neoplastic T-cells 61

1.3.1.4.7.4. B-cell-associated antigens 62

1.3.1.4.7.5. Selection of antibodies for the current study 62

1.3.1.4.8. Genetic determinants of lymphoid neoplasms 63

1.4. Quantitative trait loci (QTL) analysis 64

1.5. Translational potential 66

1.6. Aims of the study 69

2. Materials and Methods 70

2.1. Introduction 71

2.2. Animal model: two generation outcross-intercross (C57BL/6 x A/J) 71

2.2.1. Statistical determination of sample size 71

2.3. Housing and husbandry 73

2.3.1. Diet 73

2.3.2. Health status 74

2.4. Chemical induction of lymphoma with ENU 74

2.4.1. Preparation for injection before making up ENU 74

2.4.2. Preparation of ENU (prepared immediately before use, in fume hood) 75

2.4.3. Spectrophotometric determination of ENU concentration 75

2.4.4. Calculation of concentration 76

2.4.5. Calculation of volume to inject 76

2.4.6. Intraperitoneal Injection 76

2.5. ENU dosage regimen planned 77

2.5.1. Animal welfare assessment during the injection protocol 77

2.6. Experimental groups according to ENU dosage 78

2.7. Experimental endpoint 79

2.7.1. Collection of data 79

2.7.1.1. Harvesting of organs and tissues of interest 81

2.7.1.1.1. Peripheral blood 81

2.7.1.1.2. Necropsy and tissue harvesting 82

2.7.1.2. Analysis of biometric and haematology data 84

2.7.1.2.1. Methodology 84

2.7.1.2.2. Body weight and haematology parameters 84

2.7.1.2.3. Thymus and spleen weight 87

2.7.1.2.4. Data handling 87

2.8. Histopathological evaluation of samples 88

2.8.1. Distinguishing lymphoma from reactive hyperplasia in mice 88

2.9. Flow cytometry immunophenotyping 88

2.9.1. Cytometer configuration 89

2.9.2. Application settings 89

2.9.2.1. Sample preparation specific steps 90

2.9.2.2. Software configuration 90

2.9.3. Antibody conjugates 91

2.9.4. Antibody dilutions 92

2.9.4.1. Thymus 92

2.9.4.2. Spleen 94

2.9.5. Compensation analysis 96

2.9.5.1. Compensation analysis protocol 96

2.9.5.1.1. FACSDiva settings 97

2.9.6. Fluorescence minus one (FMO) analysis 98

2.9.6.1. FACSDiva configuration for FMO analysis 98

2.9.7. Establishing MFI reference intervals for each cell type in the thymus .. 98

2.9.8. Establishing MFI reference intervals for each cell type in the spleen ... 99

2.9.9. Flow cytometry protocol ... 99

2.9.9.1. Reagents ... 99

2.9.9.2. Preparation on the morning of analysis ... 100

2.9.9.3. Organ collection ... 100

2.9.9.4. Organ dissociation ... 101

2.9.9.5. Cell counting ... 102

2.9.9.6. Red blood cell lysis, blocking and staining ... 102

2.9.9.7. Sample analysis ... 103

2.9.9.7.1. FC of thymus ... 103

2.9.9.7.2. FC of spleen ... 106

2.10. DNA extraction ... 109

2.11. Genotyping ... 110

2.12. Quantitative Trait Loci (QTL) analysis ... 110

3. Results ... 113

3.1. ENU Protocol ... 114

3.1.1. Introduction ... 115

3.1.2. Background data ... 115

3.1.3. Haematology ... 116

3.1.4. Clinical chemistry ... 116

3.1.5. Necropsy 117

3.1.6. Histology 117

3.1.7. Animals culled of welfare grounds per cohort 117

3.1.8. Overview of treatment protocol per cohort 119

3.2. Pathology 120

3.2.1. Introduction 121

3.2.2. Thymic lymphoma diagnosis and incidence 121

3.2.3. Spleen metastasis of thymic lymphoma 123

3.2.4. Extramedullary haematopoiesis 125

3.2.5. Necropsy findings 126

3.3. Biometric and Haematology 129

3.3.1. Introduction 130

3.3.2. Results – biometric data 131

3.3.2.1. Body weight (BW) 131

3.3.2.1.1. Males 132

3.3.2.1.2. Females 132

3.3.2.2. Organ weight adjusted to body weight 133

3.3.2.2.1. Thymus 133

3.3.2.2.1.1. Males 133

3.3.2.2.1.2. Females 134

3.3.2.2.2. Spleen 135

3.3.2.2.2.1. Males 135

3.3.2.2.2.2. Females 135

3.3.3. Results - haematology data 136

3.3.3.1. White Blood Cell count Baso (WBCB) 136

3.3.3.1.1. Males 136

3.3.3.1.2. Females 137

3.3.3.2. Absolute neutrophil count 138

3.3.3.2.1. Males 138

3.3.3.2.2. Females 138

3.3.3.3. Absolute lymphocyte count 139

3.3.3.3.1. Males 139

3.3.3.3.2. Females 139

3.3.3.4. Absolute monocyte count 140

3.3.3.4.1. Males 140

3.3.3.4.2. Females 141

3.3.3.5. Absolute eosinophil count 141

3.3.3.5.1. Males 141

3.3.3.5.2. Females 142

3.3.3.6. Absolute Large Unstained Cells count 142

3.3.3.6.1. Males 143

3.3.3.6.2. Females 143

3.3.3.7. Absolute basophil count 144

3.3.3.7.1. Males 144

3.3.3.7.2. Females 144

3.3.3.8. Red Blood Cell count (RBC) 145

3.3.3.8.1. Males 145

3.3.3.8.2. Females 146

3.3.3.9. Haemoglobin Concentration (HGB) 147

3.3.3.9.1. Males 147

3.3.3.9.2. Females 148

3.3.3.10. Haematocrit (HCT) 149

3.3.3.10.1. Males 149

3.3.3.10.2. Females 150

3.3.3.11. Mean Cell Volume (MCV) 151

3.3.3.11.1. Males 151

3.3.3.11.2. Females 152

3.3.3.12. Mean Cell Haemoglobin Concentration (MCHC) 152

3.3.3.12.1. Males 152

3.3.3.12.2. Females 153

3.3.3.13. Platelet count 154

3.3.3.13.1. Males 154

3.3.3.13.2. Females 155

3.4. Flow cytometry 157

3.4.1. Thymus 158

3.4.1.1. Controls 158

3.4.1.1.1. Percentage of lymphocyte populations 159

3.4.1.1.2. Analysis of cellular size 159

3.4.1.1.3. Median Fluorescence Intensity reference intervals 160

3.4.1.1.4. Unstained control samples 161

3.4.1.2. Treated 161

3.4.1.2.1. Analysis of cellular size 161

3.4.1.2.2. Unstained control samples 162

3.4.1.2.3. Thymic lymphoma immunophenotypes 162

3.4.1.2.3.1. Lymphomas of predominantly CD8+CD4+ cells 164

3.4.1.2.3.2. Lymphomas of predominantly CD8+CD4+- cells 165

3.4.1.2.3.3. Lymphomas of predominantly CD8+-CD4+ cells 167

3.4.1.2.3.4. Lymphomas of predominantly CD8+-CD4+- cells 168

3.4.1.2.3.5. Lymphomas of predominantly CD4 cells 171

3.4.1.2.3.6. Lymphomas of predominantly CD8 cells 172

3.4.1.2.3.7. Lymphomas of predominantly double negative cells 174

3.4.1.2.3.8. Lymphomas of mixed cells 177

3.4.2. Spleen 179

3.4.2.1. Controls 180

3.4.2.1.1. Percentage of lymphocyte populations 180

3.4.2.1.2. Establishing MFI reference intervals 180

3.4.2.2. Treated 181

3.4.2.2.1. Spleen metastasis of a CD8+CD4+- thymic lymphoma 182

3.4.2.2.2. Spleen metastasis of a DP CD8+CD4+ thymic lymphoma..... 184

3.4.2.2.3. Spleen metastasis of a CD8+-CD4+ thymic lymphoma 185

3.4.2.2.4. Spleen metastasis of CD8+-CD4+- thymic lymphomas 186

3.4.2.2.5. Spleen metastasis of a CD8+ thymic lymphoma 188

3.5. Genetic analysis 190

3.5.1. DNA extraction 191

3.5.2. QTL analysis 192

3.5.2.1. Interval Mapping Analysis 193

3.5.2.2. Composite Interval Mapping 194

3.5.3. Identification of candidate genes 194

3.5.3.1. Single nucleotide polymorphisms 195

3.5.3.2. Insertions/deletions 197

4. Discussion 198

4.1. ENU Protocol 199

4.1.1. Introduction 200

4.1.2. Pathology findings 200

4.1.3. Animal welfare 201

4.1.4. Changes in treatment protocol 201

4.1.4.1. Weight control 201

4.1.4.2. Diet 202

4.1.4.3. Treatment dosage 202

4.1.4.4. Time between treatments 202

4.1.4.5. Age at commencement 202

4.1.4.6. Selection of animals to carry through treatment 202

4.1.5. Impact on the study 203

4.2. Pathology 204

4.2.1. Histology 205

4.2.2. Necropsy 205

4.3. Biometric and Haematology 207

4.3.1. Biometric data 208

4.3.1.1. Body weight 208

4.3.1.2. Organ weight 208

4.3.1.2.1. Thymus 208

4.3.1.2.2. Spleen 208

4.3.2. Haematology data 208

4.3.2.1. White blood cell-related parameters 208

4.3.2.2. Red blood cell-related parameters and platelets 210

4.4. Flow Cytometry 212

4.4.1. Thymus 213

4.4.2. Spleen 215

4.5. Genetic analysis 218

4.5.1. Physical distance and linkage distance 219

4.5.2. Selection of the quantitative trait to analyse 219

4.5.3. A QTL in chromosome 3 220

4.5.4. Single nucleotide polymorphisms 221

4.5.4.1. *Fcrls, Fcrl1* and *Fcrl5* 221

4.5.4.2. *Cd5l* 223

4.5.4.3. *Etv3* 224

4.5.4.4. *Sh2d2a* 226

4.5.4.5. *Gon4l* 226

4.5.4.6. *Ecm1* 226

4.5.4.7. *Cd160* 227

4.5.4.8. *Trim45* 227

4.5.4.9. *Vangl1* 227

4.5.5. Insertions/deletions 228

4.5.5.1. *Nras* 228

4.5.6. Single nucleotide polymorphisms and insertions/deletions 229

4.5.6.1. *Rit1* 229

4.5.6.2. *Selenbp1* 229

4.5.6.3. *Rfx5* 230

4.5.6.4. *Anp32e* 231

4.5.6.5. *Wdr3* 231

4.5.6.6. *Hipk1* 231

4.5.6.7. *Ptpn22* 232

4.5.6.8. *St7l* 232

4.5.7. Conclusion 233

5. Conclusions and future work 234

6. References 240

7. Appendix 1 - List of materials and reagents 256

8. Appendix 2 - Tables and figures 258

Abbreviations

ALT	Alanine aminotransferase
AST	Aspartate aminotransferase
BASO	Basophils
bp	Base pair
CK	Creatine Kinase
CIM	Composite Interval Mapping
cM	Centimorgan
DN	Double negative
DP	Double positive
EDTA	Ethylenediaminetetraacetic
ENU	*N*-ethyl-*N*-nitrosourea
EOSIN	Eosinophil
F1	First generation
F2	Second generation
FI	Fluorescence intensity
FMO	Fluorescence minus one
FRCPath	Fellow of the Royal College of Pathologists
FSC	Forward scatter
FSC-A	Forward scatter area
FSC-H	Forward scatter height
GWAS	Genome-wide association studies
H&E	Haematoxylin and eosin
HCT	Haematocrit or Packed Cell Volume
HGB	Haemoglobin Concentration
IM	Interval Mapping
IMPC	International Mouse Phenotyping Consortium
IQR	Inter quartile range
IVC	Individual ventilated cage
LAF	Laminar air flow
LUC	Large Unstained Cells
LYMPH	Lymphocyte
Mbp	Mega base pairs
MCHC	Mean Cell Haemoglobin Concentration
MCV	Mean Cell Volume
MONO	Monocyte
MRC	Medical Research Council
NACWO	Named Animal Care and Welfare Officer
NEUT	Neutrophil
NHL	Non-Hodgkin’s lymphoma
OD	Optical density
PLT	Platelet Count
QTL	Quantitative trait loci
RBC	Red Blood Cell Count
RCVS	Royal College of Veterinary Surgeons
RI	Reference interval
rSDEN	Electronic Noise Robust Standard Deviation
SD	Standard deviation
SD	Standard deviation
SNP	Single nucleotide polymorphism
SOP	Standard Operating Procedure
SP	Single positive
SPF	Specific pathogen free
SSC	Side scatter
SSC-H	Side scatter height
SSC-W	Side scatter width
T-ALL	T-cell acute lymphoblastic leukaemia
T-LBL	T-cell acute lymphoblastic lymphoma
WBCB	White Blood Cell Count (Baso)

1. Introduction

1.1. Introduction

Tumour development is a complex process involving susceptibility loci (oncogenes) and the accumulation of spontaneous somatic mutations in tumour suppressor genes that interact to result in cancer. Tumours may require the accumulation of a variety of mutations before developing but the general principle is that the mutations result in an imbalance between the oncogene and tumour suppressor gene function (Berger et al., 2011). This multi-hit process can be tested by subjecting strains of mice susceptible to certain types of tumours to chemical mutagens, thereby inducing further mutations. This technique is used in this study to identify loci resulting in the susceptibility to thymic lymphoma in the C57BL/6J strain in order to further our understanding of the processes involved in the development of such tumours.

1.2. Background

A recent study on *N*-ethyl-*N*-nitrosourea (ENU) treated mice, (Smith et al., 2009), indicated that the majority of C57BL/6J males injected with ENU develop lymphomas. At a 3 x 100 mg/kg injection regime, 100% of the G_0 C57BL/6J males developed lymphomas, and more than 75% of the experimental group morbidity was attributable to the development of T-lymphoblastic lymphoma. Other studies have indicated that there is a strain-specific variation in the susceptibility to ENU-induced lymphomas (Fenske et al., 2006a, Shimada et al., 2003b), albeit under different dosing regimens, and that C57BL/6J mice are susceptible to the development of lymphomas in response to ENU-induced somatic mutations. The BALB/c strains tested are not particularly resistant to lymphoma development - approximately 50% of ENU treated BALB/cAnNCrl males develop early T-lymphoblastic lymphoma (Smith et al., 2009). On the other hand, strains such as A/J and C3H/HeJ are less susceptible to ENU-induced lymphomas (Fenske et al., 2006a, Shimada et al., 2003b). According to The

Jackson Laboratory, the reported frequency of spontaneous lymphomas was negligible in A/J mice (Krupke et al., 2008). The interaction of several factors, both genetic and environmental, resulting in tumorigenesis is expected (Knudson, 1971, Knudson, 1993), and there is increasing evidence for susceptibility loci in many cancers, including lymphoma (Skibola et al., 2007).

Previous work by Shimada et al. (2003a) determined that C57BL/6J mice had a statistically higher incidence of thymic lymphoma, and that these lymphomas had an increased level of *ras* mutations, compared to C3H/He mice (45% vs 8%) in response to ENU treatment. In addition to the frequency of *ras* mutations, the spectrum of mutations differed between strains. These results suggest there is a genetic interaction between the background strain and somatic mutations resulting in the accumulation of *ras* mutations in ENU treated mice and a concomitant increase in the development of lymphomas in C57BL/6J mice. Further substantiation of the genetic control of ENU-induced lymphoma susceptibility comes from the evidence that *Runx1*-deficient mice and mice transgenic for a *Runx1* fusion protein (AML1-ETO), associated with acute myeloid leukaemia in humans, have an increased incidence of ENU-induced malignancies (Kundu et al., 2005b, Yuan et al., 2001b). ENU-induced mutations at the *Ikaros* and *p53* loci may also contribute to disease by acting as dominant negative mutations in tumour suppressor genes (Kakinuma et al., 2005a). A similar approach has been successful in determining susceptibility to acute myeloid leukaemia.

The susceptibility may have several causes including a reduced DNA repair efficiency or the presence of an oncogene; Msh2 deficient (Claij et al., 2003) and Pim-1 transgenic mice (Breuer et al., 1989) both exhibit an increased incidence of ENU-induced lymphomas. QTL analysis of intercrossed resistant and susceptible strains has

successfully identified susceptibility loci in ENU-induced (Shimada et al., 2003b) and radiation-induced (Boulton et al., 2003) disease.

1.3. Neoplasia and genetics

The genome of normal cells is in a dynamic equilibrium, representing a balance between processes that generate mutations and processes that maintain the normal nucleotide sequence (Loeb et al., 2003). Several lines of evidence indicate that tumorigenesis in humans is a multistep process and that these steps reflect genetic alterations that drive the progressive transformation of normal human cells into highly malignant cells (Hanahan and Weinberg, 2000). Evidence now indicates that for a large number of cancer types there are environmental influences, but also hereditary predispositions (Kumar et al., 2010e). Still according to the same author, genetic predisposition to cancer can be divided into three categories: autosomal dominant-inherited cancer syndromes, defective DNA repair syndromes and familial cancers. In the first category, the inheritance of a single autosomal dominant gene, usually a tumour suppressor, greatly increases the risk of developing a tumour. In the second category, DNA instability results from conditions characterized by defects in DNA repair genes. As for the third category, in which lymphomas are included, the transmission pattern is not clear; siblings have a risk between two and three times greater than unrelated individuals. Furthermore, segregation analyses usually show that predisposition to the tumours is dominant, but multifactorial inheritance cannot be ruled out. It is likely that familial susceptibility to cancer may depend on multiple low-penetrance alleles, each contributing to only a small increase in the risk of tumour development. Additionally, the interaction between genetic and non-genetic factors is

particularly complex when tumour development depends on the action of multiple genes.

There are many distinct types and subtypes of cancer and, although the factors contributing to neoplastic transformation are complex, Hanahan and Weinberg (2000) suggested that the vast catalog of cancer cell genotypes is a manifestation of essential alterations in cell physiology that collectively dictate malignant growth: self-sufficiency in growth signals, insensitivity to growth-inhibitory (antigrowth) signals, evasion of programmed cell death (apoptosis), limitless replicative potential, sustained angiogenesis, tissue invasion and metastasis, and defects in DNA repair. An additional common trait shared by most tumours, escape from the immune system, was added to this list following on the work of several authors (Zitvogel et al., 2006, Kim et al., 2007, Dunn et al., 2006), who point out the role of the immune system not only in eliminating neoplastic cells but also in selecting for tumour variants.

Many specific rearrangements such as chromosomal translocations and other acquired mutations are associated with particular neoplasms, suggesting a critical role in their genesis. In some instances, the result of the aberration is to produce a "dominant-negative" protein that interferes with normal function (loss of function). In others, the result is an inappropriate increase in some normal activity (gain of function), and in certain tumours, different aberrations have the same functional consequence as a result of their convergence on a common critical signaling pathway. Oncoproteins created by genomic aberrations often block normal maturation, and frequently at a stage when cells are proliferating rapidly (Kumar et al., 2010e). Although multiple abnormal chromosomes are found in most solid tumours, they are seldom diagnostic of tumour type. An exception is the characteristic translocations involving rearrangements of

specific chromosomes that have been instrumental in the diagnosis of several haematological malignancies (Loeb et al., 2003).

Proto-oncogenes, tumour suppressor genes, genes that regulate apoptosis and those involved in DNA repair are the principal targets of genetic damage in the pathogenesis of cancer. Proto-oncogene mutations are considered dominant, whereas in most cases, a mutation in both alleles of tumour suppressor genes is required before transformation can occur (Hanahan and Weinberg, 2000). Defective DNA repair genes can predispose cells to widespread mutations and thus to neoplasia. Cells with mutations in DNA repair genes are said to have developed a *mutator phenotype* (Zhang et al., 2007). According to Goldsby et al. (2001), DNA polymerase appears to be the major DNA polymerase that catalyses eukaryotic DNA replication and the replacement of a wild-type DNA pol-δ with a mutated allele that lacks proofreading activity results in both lymphomas and epithelial cancers in mice. MicroRNAs, a class of regulatory molecules, can act as oncogenes or tumour suppressor genes by affecting the translation of other genes (Rana, 2007).

1.3.1. Lymphoid neoplasms

1.3.1.1. Classification of lymphoid neoplasms in humans

According to Kumar et al. (2010c), lymphoid malignancies are clinically the most important disorders of white blood cells. These diseases fall into several broad categories: (1) lymphoid neoplasms, which include a diverse group of tumours of B-cell, T-cell and NK-cell origin, (2) myeloid neoplasms, in which three categories, acute myeloid leukaemias, myelodysplastic syndromes and chronic proliferative disorders, are recognized, and (3) histiocytosis which include uncommon proliferative lesions of macrophages and dendritic cells. The World Health Organization (WHO)

scheme uses morphologic, immunophenotypic, genotypic and clinical features to classify the lymphoid neoplasms. According to the 2008 WHO classification, lymphoid neoplasms were classified into five broad categories according to the cell of origin (Table 1): precursor B-cell neoplasms (of immature B cells), peripheral B-cell neoplasms (of mature B cells), precursor T-cell neoplasms (of immature T cells), peripheral T-cell and NK-cell neoplasms (of mature T cells), and Hodgkin lymphoma (of Reed-Sternberg cells and variants), (Harris et al., 1999a).

Precursor B-cell neoplasm (neoplasm of immature B cells)
B-cell acute lymphoblastic leukaemia/lymphoma (B-ALL)
Peripheral B-cell neoplasms (neoplasms of mature B cells)
Chronic lymphocytic leukaemia/small lymphocytic lymphoma
B-cell prolymphocytic leukaemia
Lymphoblastic lymphoma
Splenic and nodal marginal zone lymphomas
Extranodal marginal zone lymphoma
Mantle cell lymphoma
Follicular lymphoma
Marginal zone lymphoma
Hairy cell leukaemia
Plasmacytoma/plasma cell myeloma
Diffuse large B-cell lymphoma
Burkitt lymphoma
Precursor T-cell neoplasm (neoplasm of immature T cells)
T-cell acute lymphoblastic leukaemia/lymphoma (T-ALL)
Peripheral T-cell and NK-cell neoplasms (neoplasms of mature T cells and NK
T-cell prolymphocytic leukaemia
Large granular lymphocytic leukaemia
Mycosis fungoides/Sézary syndrome
Peripheral T-cell lymphoma, unspecified
Anaplastic large-cell lymphoma
Angioimmunoblastic T-cell lymphoma
Enteropathy-associated T-cell lymphoma
Panniculitis-like T-cell lymphoma
Hepatosplenic ϒδ T-cell lymphoma
Extranodal NK/T-cell lymphoma
NK-cell leukaemia
Hodgkin lymphoma (neoplasms of Reed-Sternberg cells and variants)
Classical subtypes
Nodular sclerosis
Mixed cellularity
Lymphocyte-rich
Lymphocyte depletion
Lymphocyte predominance

Table 1: 2008 WHO classification of lymphomas.

In 2016, the WHO published an updated classification of lymphoid neoplasms (Table 2 and Table 3) although there were only limited alterations in the classification compared with 2008 (Swerdlow et al., 2016) and not affecting lymphoblastic lymphomas.

Mature B-cell neoplasms	
Chronic lymphocytic leukemia/small lymphocytic lymphoma	Large B-cell lymphoma with IRF4 rearrangement*
Monoclonal B-cell lymphocytosis*	Primary cutaneous follicle center lymphoma
B-cell prolymphocytic leukemia	Mantle cell lymphoma
Splenic marginal zone lymphoma	In situ mantle cell neoplasia*
Hairy cell leukemia	Diffuse large B-cell lymphoma (DLBCL), NOS
Splenic B-cell lymphoma/leukemia, unclassifiable	Germinal center B-cell type*
Splenic diffuse red pulp small B-cell lymphoma	Activated B-cell type*
Hairy cell leukemia-variant	T-cell/histiocyte-rich large B-cell lymphoma
Lymphoplasmacytic lymphoma	Primary DLBCL of the central nervous system (CNS)
Waldenstr¨om macroglobulinemia	Primary cutaneous DLBCL, leg type
Monoclonal gammopathy of undetermined significance (MGUS), IgM*	EBV1 DLBCL, NOS*
m heavy-chain disease	EBV1 mucocutaneous ulcer*
g heavy-chain disease	DLBCL associated with chronic inflammation
a heavy-chain disease	Lymphomatoid granulomatosis
Monoclonal gammopathy of undetermined significance (MGUS), IgG/A*	Primary mediastinal (thymic) large B-cell lymphoma
Plasma cell myeloma	Intravascular large B-cell lymphoma
Solitary plasmacytoma of bone	ALK1 large B-cell lymphoma
Extraosseous plasmacytoma	Plasmablastic lymphoma
Monoclonal immunoglobulin deposition diseases*	Primary effusion lymphoma
Extranodal marginal zone lymphoma of mucosa-associated lymphoid tissue	HHV81 DLBCL, NOS*
(MALT lymphoma)	Burkitt lymphoma
Nodal marginal zone lymphoma	Burkitt-like lymphoma with 11q aberration*
Pediatric nodal marginal zone lymphoma	High-grade B-cell lymphoma, with MYC and BCL2 and/or BCL6 rearrangements*
Follicular lymphoma	High-grade B-cell lymphoma, NOS*
In situ follicular neoplasia*	B-cell lymphoma, unclassifiable, with features intermediate between DLBCL and
Duodenal-type follicular lymphoma*	classical Hodgkin lymphoma
Pediatric-type follicular lymphoma*	

*Table 2: The WHO update on the classification of lymphoid neoplasms in 2016. Provisional entities are listed in italics. *Changes from the 2008 classification.*

Mature T and NK neoplasms	
T-cell prolymphocytic leukemia	Primary cutaneous CD301 T-cell lymphoproliferative disorders
T-cell large granular lymphocytic leukemia	Lymphomatoid papulosis
Chronic lymphoproliferative disorder of NK cells	Primary cutaneous anaplastic large cell lymphoma
Aggressive NK-cell leukemia	Primary cutaneous gd T-cell lymphoma
Systemic EBV1 T-cell lymphoma of childhood*	Primary cutaneous CD81 aggressive epidermotropic cytotoxic T-cell lymphoma
Hydroa vacciniforme–like lymphoproliferative disorder*	Primary cutaneous acral CD81 T-cell lymphoma*
Adult T-cell leukemia/lymphoma	Primary cutaneous CD41 small/medium T-cell lymphoproliferative disorder*
Extranodal NK-/T-cell lymphoma, nasal type	Peripheral T-cell lymphoma, NOS
Enteropathy-associated T-cell lymphoma	Angioimmunoblastic T-cell lymphoma
Monomorphic epitheliotropic intestinal T-cell lymphoma*	Follicular T-cell lymphoma*
Indolent T-cell lymphoproliferative disorder of the GI tract*	Nodal peripheral T-cell lymphoma with TFH phenotype*
Hepatosplenic T-cell lymphoma	Anaplastic large-cell lymphoma, ALK1
Subcutaneous panniculitis-like T-cell lymphoma	Anaplastic large-cell lymphoma, ALK2*
Mycosis fungoides	Breast implant–associated anaplastic large-cell lymphoma*
S´ezary syndrome	
Hodgkin lymphoma	
Nodular lymphocyte predominant Hodgkin lymphoma	Lymphocyte-rich classical Hodgkin lymphoma
Classical Hodgkin lymphoma	Mixed cellularity classical Hodgkin lymphoma
Nodular sclerosis classical Hodgkin lymphoma	Lymphocyte-depleted classical Hodgkin lymphoma
Posttransplant lymphoproliferative disorders (PTLD)	
Plasmacytic hyperplasia PTLD	Polymorphic PTLD
Infectious mononucleosis PTLD	Monomorphic PTLD (B- and T-/NK-cell types)
Florid follicular hyperplasia PTLD*	Classical Hodgkin lymphoma PTLD
Histiocytic and dendritic cell neoplasms	
Histiocytic sarcoma	Follicular dendritic cell sarcoma
Langerhans cell histiocytosis	Fibroblastic reticular cell tumor
Langerhans cell sarcoma	Disseminated juvenile xanthogranuloma
Indeterminate dendritic cell tumor	Erdheim-Chester disease*
Interdigitating dendritic cell sarcoma	

*Table 3: (continued from previous page) - The WHO update on the classification of lymphoid neoplasms in 2016. Provisional entities are listed in italics. *Changes from the 2008 classification.*

1.3.1.2. Epidemiology

Taken together, the diverse lymphoid neoplasms constitute a complex clinically important group of cancers, with about 100,000 new cases being diagnosed each year

in the United States (Kumar et al., 2010c). In the UK in 2010, around 12,200 new cases of non-Hodgkin's lymphoma (NHL) were registered and 4,400 people were recorded as having died from the disease, with NHL being the 6th most common cancer and the 12th most common cause of cancer death. NHL is primarily a disease of older people (60% of cases are diagnosed in the over-65s), and slightly more common in men than in women, the age and sex profile varying between NHL subtypes. Survival has improved markedly in recent decades, and more than six in ten NHL patients are expected to survive their disease for five years or more after diagnosis. However, survival rates vary markedly with subtype (Cancer Research UK, 2013).

According to Clarke and Glaser (2002), and Cartwright et al. (1999), in line with other developed countries, NHL (all subtypes combined) registrations have increased almost three-fold in Great Britain since the mid-1970s, with much of the rise occurring before the mid-1990s. Improvements in diagnostic techniques and data registration for NHL have likely contributed to these trends, so interpretation of these trends should be undertaken with caution (Adamson et al., 2007). Furthermore, with the exception of HIV, no established aetiological factors are known to have changed over time.

Within neoplasms arising from precursor B and T lymphocytes, acute T-cell lymphoblastic leukaemia (T-ALL) is less common than acute B-cell lymphoblastic leukaemia (B-ALL), accounting for approximately 15% of childhood and 25% of adult acute lymphoblastic leukaemias. Precursor T-cell lymphoblastic lymphoma (T-LBL) comprises 85-90% of all lymphoblastic lymphomas and similarly to its leukemic counterpart (T-ALL), is more frequent in adolescent males (Swerdlow et al., 2008).

According to Kumar et al. (2010c), about 85% of ALLs (B and T) are B-ALLs. Also, many T-ALL present with, or evolve to, a leukemic picture. Together with B-ALL, they account for approximately 2500 new cases diagnosed each year in the United States, most occurring in individuals under 15 years of age, being three times more common in Caucasians than in Afro-Carribeans, and slightly more frequent in males compared to females. Hispanics have the highest incidence of any ethnic group, again emphasising the importance of genetic background in this disease.

Lymphoid neoplasms are often associated with immune abnormalities. Both a loss of protective immunity (susceptibility to infection) and a breakdown of tolerance (autoimmunity) can be seen, sometimes in the same patient (Kumar et al., 2010c). Associations between NHL and HIV/AIDS are well documented (Grulich et al., 2007). Since the introduction of highly active antiretroviral therapy (HAART) in 1996, the risk of NHL overall for HIV patients has decreased. In comparison with B-cell malignancies, T-cell neoplasms are relatively rare and, importantly, are overall characterized by an inferior treatment outcome (de Leval et al., 2009).

No risk factors have been clearly identified in lymphoblastic lymphomas but a number of cases have been reported in studies assessing the carcinogenic activity of viruses, oncogenes, immunodeficiency, chemicals, and radiations (Cortelazzo et al., 2011). Also, factors known to have the most impact on NHL incidence at the population level are age and, for most subtypes, male gender (Oliver et al., 2013).

1.3.1.3. Precursor T-cell lymphoblastic leukaemia/lymphoma (T-ALL)

Although T-ALL and T-LBL present differently, primarily with respect to involvement of bone marrow and blood (Hoelzer and Gökbuget, 2009), they are very

closely-related diseases. According to the WHO 2008 classification, they are considered as one disease entity (Harris et al., 1999b).

One confusing aspect of the lymphoid neoplasms concerns the use of the terms *leukaemia* and *lymphoma*. *Leukaemia* is used for neoplasms that present with widespread involvement of the bone marrow and usually, but not always, the peripheral blood. *Lymphoma* is used for proliferations that arise as discrete tissue masses. However, many entities called "lymphoma" occasionally have leukemic presentations, and evolution to "leukaemia" is not unusual during the progression of incurable "lymphomas". Conversely, tumours identical to "leukaemias" sometimes arise as soft tissue masses unaccompanied by bone marrow disease. Hence, when applied to particular neoplasms, the terms *leukaemia* and *lymphoma* merely reflect the usual tissue distribution of each disease at presentation (Kumar et al., 2010c). This is aligned with the "World Health Organization classification of tumours of haematopoietic and lymphoid tissues", which states that with extensive marrow and blood involvement, acute lymphoblastic leukaemia is the appropriate term and if the patient presents with a mass lesion and 25% or fewer lymphoblasts in the marrow, the designation lymphoma is preferred, and also that this is an arbitrary distinction and exceptions may apply (Swerdlow et al., 2008).

According to Uyttebroeck et al. (2007), although there is a considerable overlap between the immunophenotype of both T-cell lymphoblastic neoplasms, T-ALL have a more immature phenotype and T-LBL have a more mature phenotype, which may suggest that T-ALL derive from a T-cell progenitor in the bone marrow, while thymocytes represent the normal counterpart in T-LBL, which offers a possible explanation for the differential patterns in both disease distribution (bone marrow

involvement versus mediastinal mass) and immunophenotype (earlier versus latter stages of T-cell differentiation).

When studying the gene expression profile of both T lymphoblastic neoplasms, T-ALL and T-LBL samples segregated into distinct clusters, which suggest underlying differences in their biology (Uyttebroeck et al., 2007, Raetz et al., 2006).

Concerning the gene expression profiling of childhood versus adult of the various T-ALL/LBL subtypes, adult cases showed a shift to more immature stages of maturation arrest which might be related to age-related thymic atrophy, predominantly affecting αβ-lineage precursors and inducing a progressive change in the thymocyte population at risk of oncogenic transformation (Asnafi et al., 2004). In mice, according to Jacoby et al. (2002b), the thymus reaches maximum size around the time of sexual maturity and involutes between 35 and 80 days of age.

1.3.1.3.1. Thymocyte differentiation

Normal T cells develop in the thymic cortex from common lymphoid progenitor cells originated in the bone marrow. In the thymic cortex, mature T-cell receptor (TCR) αβ or γδ positive T-cells develop from common CD4-CD8- double negative (DN) progenitor cells (Aifantis et al., 2006, Hoffmann and Melchers, 2003, Saito and Watanabe, 1998, von Boehmer et al., 2003). The differentiation process proceeds through sequential stages defined according to the expression of CD4 and CD8, from double negative to double positive (DP) in the thymic cortex, to single positive (SP) thymocytes in the medulla. Subgroups of T-cell lymphoblastic neoplasms have been defined by immunophenotyping and can be matched to the various stages of normal thymocyte development. Immature T-cell lymphoblastic neoplasms (expression of

CD3 and TCR absent or circumscribed to the cytoplasm) occur more frequently in adults, whereas mature T-cell lymphoblastic neoplasms (with cellular membrane expression of CD3 and TCR) are more frequent in children (de Leval et al., 2009).

1.3.1.3.2. Clinical features and sites of involvement

Precursor T-cell lymphoblastic neoplasms are aggressive diseases that mainly develop in children, particularly in adolescent males, although also affects adults. It manifests either with an extensive bone marrow and blood involvement (T-ALL), which is the most frequent clinical presentation, or less commonly as a mass lesion (often in the thymus/anterior mediastinum, but also in lymph nodes and, rarely, extra nodal sites) (de Leval et al., 2009). Precursor T-ALL typically presents with a high leukocyte count, and often a large mediastinal mass or other tissue mass. Precursor T-LBL frequently presents with a mass lesion in the mediastinum often exhibiting rapid growth. Pleural effusions are common. According to the same source, the blood and marrow are involved in all cases of T-ALL. According to Swerdlow et al. (2008), approximately 50% of T-lymphoblastic lymphomas present as a mediastinal mass; other possible sites include peripheral lymph nodes, skin, liver, spleen, Waldeyer's ring, central nervous system and gonads.

1.3.1.3.3. Morphology of T-ALLs

As described in Kumar et al. (2010c), mediastinal thymic masses occur in 50% to 70% of all T-ALLs, which are also more likely to be associated with lymphadenopathy and splenomegaly. In both B- and T-ALL, the tumour cells have scant basophilic cytoplasm and nuclei somewhat larger than those of small lymphocytes. The nuclear chromatin is delicate and finely stripped, and nucleoli are either absent or inconspicuous. In many cases the nuclear membrane is deeply subdivided, imparting a

convoluted appearance. In keeping with the aggressive clinical behaviour, the mitotic rate is high. As with other rapidly growing lymphoid tumours, interspersed macrophages ingesting apoptotic tumour cells may impart a “starry sky” appearance.

According to Swerdlow et al. (2008) in smears T-ALL/LBL cells are of medium size with a high nuclear cytoplasmic ratio; there may be a considerable size range from small lymphoblasts with very condensed nuclear chromatin and no evident nucleoli to larger blasts with finely dispersed chromatin and relatively prominent nucleoli. Cytoplasmic vacuoles may be present. The number of mitotic figures is reported to be higher in T-ALL than in B-ALL. In T-LBL the lymph node generally shows complete effacement, with involvement of the capsule. Partial involvement in a paracortical location with sparing of germinal centres may occur. In some cases, the predominant population of blasts has convoluted nuclei; mitotic figures may be numerous.

1.3.1.3.4. Immunophenotype

A flow cytometer evaluates the physical and/or chemical characteristics of single cells and other particles as they pass individually through a measuring device and sensing point in a fluid stream and are illuminated by an incident laser light of specific frequencies (Shapiro, 2003). Physical properties such as cellular size and granularity can be measured by simple forward and side scatter while various cellular components, such as surface receptors, intracellular molecules and DNA, are targeted by antibodies bound with fluorescent dyes allowing their detection and evaluation (Macey, 1988).

The flow cytometer consists of four systems: fluidics, optics, electronics and computer interface. Cellular suspensions are the most common source of material used in flow cytometry for disease characterisation (Betters, 2015). In this study, cell suspensions

were obtained from thymi and spleens harvested at necropsy. Cells are collected from the well and delivered onto the fluidics system, which leads them through a very narrow passage, where each cell is individually interrogated by a laser beam. The optic component is a laser that emits light of a specified wavelength. Two initial parameters are assessed while cells pass the laser beam: forward scatter (FSC) and side scatter (SSC). Forward scatter is the light that scatters in the same direction as the laser and is indicative of cell size whereas SSC is the light scattered at 90° angle from the direction of the laser and is proportional to cell granularity (Pedreira et al., 2013). For example, granulocytes, such as neutrophils, have a higher intracellular granularity and therefore higher SSC than lymphocytes, and the two populations show as two distinct clusters on a SSC plot. The electronics involve the conversion of photons by the flow cytometer's photomultiplier tubes into electrical signals that can be interpreted (Betters, 2015).

A set of optical filters assures that light reaches the correct photomultiplier tube as it filters it according to its wavelength. Finally, a computer is used to store data relative to each cell and also to regulate the flow cytometer and specific software such as FACSDiva™ or FlowJo™ are used for the analysis of the data generated.
Fluorescence is produced when an incident light of one wavelength excites electrons of certain molecules from their ground state to higher energy levels with subsequent return of electrons to lower energy levels by emitting light of a longer wavelength (Carter NP and Ormerod MG, 2000, Ormerod MG, 2000). Flow cytometers detect the characteristics of cells/particles by measuring the amount of light reflected by these particles and by detecting the fluorescence produced by fluorochromes conjugated

either directly with cell components or conjugated to antibodies directed against cells components (Kaleem, 2006).

Most lymphoid neoplasms resemble some recognizable stage of B or T-cell differentiation, and this aspect is used in their classification. Markers recognized by antibodies used in the characterization of B- and T-cell lymphomas and leukaemias are listed below; adapted from Kumar et al. (2010c).

- Markers primarily associated with T cells
    - CD3: thymocytes, mature T cells
    - CD4: helper T cells, subset of thymocytes
    - CD8: Cytotoxic T cells, subset of thymocytes, and some NK cells
- Markers primarily associated with B cells
    - CD19: Pre-B cells and mature B cells
- Present in all leukocytes
    - CD45: all leukocytes; also known as leukocyte common antigen (LCA)

T-ALL and T-LBL are morphologically undistinguishable (Raetz et al., 2006, de Leval et al., 2009, Uyttebroeck et al., 2007, Cortelazzo et al., 2011) and therefore other techniques have to be used when wanting to identify them accurately. According to Swerdlow et al. (2008), the lymphoblasts in T-ALL/LBL are terminal deoxynucleotidyl TdT positive and variably express CD1a, CD2, CD3, CD4, CD5, CD7 and CD8. Of these, CD7 and cytoplasmic CD3 are most often detected, and only CD3 is considered lineage specific. CD4 and CD8 are frequently co-expressed on the blasts, and CD10 may be present. CD79a positivity has also been observed in some cases.

T-ALL/LBL can be stratified into different stages of intrathymic differentiation according to other number and sequence of antigens expressed (cytoplasmic CD3, CD2 and CD7 expressed early, followed by CD5, CD1a, followed by membrane CD3).

T-ALLs are arrested at various stages of pre T-cell development. In most cases cells are positive for CD1, CD2, CD5 and CD7. The more immature tumours are usually negative for the surface markers CD3, CD4, and CD8, whereas the "late" pre-T cell tumours are positive for these markers (Kumar et al., 2010c).

According to the expression pattern of specific markers, the following categories of T-LBL/ALL could be identified (Bernard et al., 1981, Cortelazzo et al., 2011):

- Pro-T (cytoplasmic CD3+, CD7+, CD2-, CD1a-, CD4-, CD8-, CD34±)
- Pre-T (cytoplasmic CD3+, CD7+, CD2+, CD1a-, CD4-, CD8-, CD34±)
- Cortical-T (cytoplasmic CD3+, CD7+, CD2+, CD1a+, CD4+, CD8+, CD34-)
- Medullary-T (cytoplasmic CD3+, CD7+, CD2+, CD1a+, CD4±, CD8+, CD34- and surface CD3+).

T-ALL includes a heterogeneous group of malignancies defined by the expansion of immature T-cell precursors blocked at specific stages of maturation, typically deviated from normal differentiation pathways (Uckun et al., 1997, Aifantis et al., 2008, Chiaretti and Foà, 2009). T-cells develop primarily in the thymus and identification of immature T-cells in peripheral blood, bone marrow or tissues other than thymus is abnormal (van Dongen et al., 2012). According to van Dongen et al. (2012), among other markers, TdT is used to indicate the precursor nature of T cells and can be used concomitantly with staining for cytoplasmic CyCD3.

However, because of asynchronous and aberrant antigen expression in neoplastic lymphoblasts, many cases of T-ALL/LBL cannot be correlated unambiguously to a thymic differentiation stage (de Leval et al., 2009). Interestingly, the aberrant expression of T-cell markers such as CD4, CD7, and CD8 has been observed on B-cell non-Hodgkin lymphomas. In their study, Kaleem et al. (2001) have shown that from nine cases of well-characterized B-cell non-Hodgkin lymphoma, CD2 was the most commonly expressed (in five cases), CD8 and CD7 were identified in two cases each. Furthermore, in a control group of fifty-nine cases of benign lymph nodes analysed during the same period, there was no aberrant expression of T-cell-associated antigens, which indicated that such an expression was not a feature of benign lymphoid proliferations. Loss of surface CD3 is not unusual in T-cell lymphomas, but cytoplasmic CD3 expression is consistently seen in these cases (Swerdlow et al., 2008).

The other commonly used T-cell markers such as CD1, CD2, CD4, CD5, CD7 and CD8 have their selective usage and expression patterns. In general, all the above T-cell-associated markers should be run in addition to CD16, CD56, and CD57 for evaluation of T/NK-cell lymphomas (Kaleem, 2006).

1.3.1.3.5. Molecular pathogenesis

Over the past decade, high throughput genome-wide analytical methods, such as gene expression profiling using DNA or oligonucleotide microarrays and array-based comparative genomic hybridization (aCGH), emerged as powerful tools to characterize genetic and molecular features of cancers and provided important information about lymphoma biology, classification and prognosis (de Leval et al., 2009). In T-ALL, leukaemic transformation in maturing thymocytes is caused by a

multistep pathogenesis involving numerous genetic abnormalities that drive normal T-cells into uncontrolled cell growth and clonal expansion (van Vlierberghe et al., 2008). Dominant-negative mutations involving transcription factors that interfere with early stages of lymphoid or myeloid cell differentiation often collaborate with activating mutations in tyrosine kinases that increase cell survival and proliferation. A different type of regulated genomic instability is unique to precursor B and T cells, which express a V(D)J recombinase that cuts DNA at specific sites within the immunoglobulin (Ig) and T-cell receptor loci, respectively. This process is essential for the assembly of productive antigen receptor genes but sometimes goes awry, leading to joining of portions of other genes to antigen receptor gene regulatory elements. Particularly in tumours of precursor T-cells, proto-oncogenes are often deregulated by their involvement in such aberrant recombination events (Kumar et al., 2010e). Furthermore, chromosomal translocations are found in many human hematopoietic neoplasms and are responsible for the activation of proto-oncogenes or the generation of fusion proteins (Kumar et al., 2010c, Herbert C. Morse et al., 2002).

Although genetic aberrations in T-ALL have been extensively studied, the molecular genetics of T-LBL is yet not well characterized (Cortelazzo et al., 2011). However, according to Swerdlow et al. (2008), cytogenetic abnormalities are present in 50-70% of T-LBL patients and according to the evidence found by Lones et al. (2007), and Thomas and Kantarjian (2001), the most common cytogenetic abnormalities, found in 47% of T-LBL, involve 14q11-13. This corresponds to the site of TCR $\alpha\delta$, including inv(14)(q11,q32) and deletions or translocations involving chromosomes 9, 10 and 11 corresponding to sites of TCR α, β and γ-subunit genes. More, translocation

(9;17)(q34;q23) occurs only in LBL, perhaps indicating the existence of subsets of LBL that are distinct from T-ALL.

T lymphoblasts may demonstrate clonal rearrangement of the T-cell receptor genes (TCR) but this is not lineage specific (Swerdlow et al., 2008, Cortelazzo et al., 2011). Compared with ALL, there is relatively little data on the role of cytogenetics or molecular analysis of particular translocations (Cortelazzo et al., 2011). Many of the genes that are involved in chromosomal translocations in T-ALL become activated due to disturbances in the rearrangement process of the TCR genes (van Vlierberghe et al., 2008). In T-ALL/LBL, molecular subgroups delineated by gene expression profiling correlate with leukemic arrest at specific stages of normal thymocyte development and different oncogenic pathways, and seem to be of interest for prognosis prediction (de Leval et al., 2009). The most common genetic aberrations encountered in T-ALL/LBL were compiled (Table 4). The structural alterations comprise mostly translocations, but also deletions and duplications.

Cytogenetic abnormalities	Involved genes	Frequency
Translocation involving *TCR* Loci (*TCRA* and *TCRD*, 14q11; *TCRB*, 7q35: and *TCRG*, 7p15)	*HOX11* (*TLX1*) (10q24)	35%
	HOX11L2 (*TLX3*) (5q35)	
	HOXA cluster (7p15)	
	MYC (8q24.1)	
	TAL1 (*SCL*) (1p32)	
	LMO1 (*RBTN1*) (11p15)	
	LMO2 (*RBTN2*) (11p13)	
	LYL1 (19p13)	
	LCK (1p34.3-35)	
	NOTCH1 (9q34.3)	
	CCND2 (12p13)	
Fusion genes	*SIL-TAL1* (del(1p32))	9-30% of pediatric T-ALL, with decreasing frequency in adults
	CALM-AF10 (*PICALM-MLLT10*) (t(10;11)(p13;q14))	10%
	MLL-ENL (t(11;19)(q23;p13)) and variants	8% of adult T-ALL
	NUP214-ABL1 (t(9;9)(q34;q34), episomal amplification) and variants	6%
Deletions	*INK4/ARF* (*CDKN2A,P16*) (del(9p21))del(6q) (candidate gene: GRIK2)	30-65%
Gene duplications	*MYB* (dup(6q23))	8-15%
	Dup(9q34)(including *NOTCH1*, *MRLP41*, *SSNA1* and *PHPY1*)	33% of pediatric T-ALL
Mutations	*NOTCH1* (9q34)	50%
	JAK1 (1p31)	20%

Table 4: The most common genetic aberrations encountered in T-cell lymphoblastic neoplasms (adapted from de Leval et al., 2009).

In most cases, the translocations juxtapose the regulatory region of the TCR loci and transcription factor genes, leading to their aberrant expression in the developing thymocytes. Other chromosomal breaks cause gene fusions encoding chimeric proteins. In general, TCR translocations and gene fusions are mutually exclusive

(de Leval et al., 2009). Furthermore, some recurrent chromosomal aberrations occur as cryptic rearrangements, evidenced only by fluorescence *in situ* hybridization (FISH) or molecular studies. T-LBL almost always shows clonal rearrangements of the T-cell receptor *beta* or *gamma* chain genes, but there is simultaneous presence of clonal rearrangements of the Ig heavy chain (Rosenquist et al., 1997, Szczepanski et al., 1999) and therefore these rearrangements are not helpful for lineage assignment (Cortelazzo et al., 2011).

Activating mutations have been found in genes normally involved in T-cell development. Mutations of NOTCH1, which plays an essential role in regulation and commitment of haematopoietic progenitors to the T-cell lineage and the subsequent assembly of pre-T cell receptor complexes, were found in more than 50% of T-ALL cases (Weng et al., 2004). Activating mutations of JAK1, which plays a major role in mediating biological responses induced by cytokines controlling lymphoid cell precursor development, were found in approximately 20% of adult T-ALL (Flex et al., 2008).

Approximately 90% of ALLs (B and T) have numerical or structural chromosomal changes. Most common is hyperploidy (> 50 chromosomes), but hypoploidy and a variety of balanced chromosomal translocations are also seen. These alterations frequently correlate with immunophenotype and sometimes prognosis. For example, hyperploidy and hypoploidy are seen only in B-ALL. In addition, T-ALL are associated with completely different sets of translocations, indicating that they are pathogenetically distinct (Kumar et al., 2010c).

A large variety of somatic genetic markers contribute to T-ALL oncogenesis (Aifantis et al., 2008). According to R. D. Brunning et al. (2008), in one third of T-ALL/LBL, translocations have been detected involving the alpha and delta T-receptor loci at 14q11.2, the beta locus at 7p14-15, with a variety of partner genes. Genes include the transcription factors MYC (8q24.1), TAL1 (1p32), RBTN1 (11p15), RBTN2 (11p13), and HOX11 (10q24), and the cytoplasmic tyrosine kinase LCK (1p34.3-35). In most of cases, these translocations lead to a dysregulation of transcription of the partner gene by juxtaposition with the regulatory region of one of the T-cell receptor loci. In about 25% of T-ALL the TAL 1 locus is dysregulated by a microscopic deletion in its 5' regulatory region, rather than by translocation. The deletion del(9p), resulting in loss of tumour suppressor gene CDKN2A (an inhibitor of the cyclin-dependent kinase CDK4), occurs more frequently in T-ALL, (about 30% of cases by cytogenetics, a higher percentage by molecular testing) than in other immunological subsets. These genetic features are identical to those in T-LBL and have no evident specific clinical significance.

Some studies suggest there is a potential diagnostic, pathogenic and/or prognostic role for some genes in T-ALL but these features deserve to be further investigated in lymphoblastic lymphoma (Cortelazzo et al., 2011). The genes in question are: BCL2L13 (Yang et al., 2010), LMO2 (McCormack et al., 2010), NOTCH1 (Ferrando, 2009), and ETV6-RUNX1 (Konn et al., 2010)

1.3.1.3.6. Gene expression profiling

The molecular subgroups defined according to the expression of T-cell transcription factors appear to correlate with genetic rearrangements of the corresponding genes, hence the designation "molecular-cytogenetic subgroups" (de Leval et al., 2009).

Concordant findings have been reported by two groups, (Ferrando et al., 2002, Soulier et al., 2005) which identified several molecular signatures defined by the aberrant expression of T-cell-specific transcription factors. According to de Leval et al. (2009), these molecular subgroups are indicative of leukemic arrest at specific stages of normal thymocyte development and differentiation, and might reflect different oncogenic pathways involved in the pathogenesis of T-ALL. Furthermore, the *LYL1+* signature is characterized by expression on early thymocyte genes, the *HOX11+*, *HOX11L2+* and *HOXA+* signatures correspond to early cortical thymocytes, and the *TAL1+* signature reflects arrest at the late cortical stage of thymocyte differentiation.

The gene expression signature in cases with the *MLL-ENL* fusion gene shows asynchronous expression of early and more mature thymocyte genes in association with high levels of TCRG TCRD, suggesting that *MLL-ENL+* cases are blocked at an early stage of thymocyte differentiation after commitment to the γδ lineage (Soulier et al., 2005, Ferrando and Look, 2003, Ferrando et al., 2002).

Besides TCR translocations and gene fusions associated with specific molecular signatures are thought to represent a primary genetic event, other genetic abnormalities encountered across the full range of molecular subgroups, are suspected to play a secondary synergizing role in the pathogenesis of lymphoblastic neoplasms (e.g. NOTCH1 activating mutations) (van Vlierberghe et al., 2008).

1.3.1.3.7. Prognosis

Some studies have shown a correlation between the stages of T-cell differentiation and survival but no definite genetic correlation has been found (Brunning RD et al., 2008) (Brunning RD et al., 2008). With aggressive chemotherapy about 95% of children with ALL obtain clinical remission, and 75% to 85% are cured. However, ALL

remains the leading cause of cancer deaths in children, and only 35% to 40% of adults are cured. T-ALL may be less differentiated than T-LBL, but the groups overlap. Prior to the advent of current therapeutic protocols, the prognosis of T-ALL was unfavourable; with the current treatment regimens, survival is comparable to B-ALL (Swerdlow et al., 2008). Some of the "molecular-cytogenetic subgroups" defined by distinct gene signatures found to correlate with cytogenetic alterations seem to be associated with prognostic significance, suggesting they might be ultimately used for guiding patient stratification and treatment decision (de Leval et al., 2009).

1.3.1.4. Lymphoma in laboratory mice

The very origins of the laboratory mouse were promulgated by an interest in the genetic basis of cancer, and this interest has accelerated with genetically engineered mice. Many of the common inbred strains of mice were originally developed because of their propensity to develop tumours, such as mammary tumours in C3H/H2 mice, testicular teratomas in 129/Sv mice, multicentric lymphomas in BALB/c mice, and thymic lymphomas in AKR mice (Percy D.H. and S.W., 2007, Percy and Barthold, 2007).

Although conventional morphology remains the gold standard for evaluation of hematolymphoid proliferations in paraffin-embedded tissue, immunophenotyping is playing an ever-greater role in the diagnosis and classification of these proliferations (Morse et al., 2002b, Kunder et al., 2007, Swerdlow et al., 2008). Most of the present knowledge of mouse haematopoietic neoplasms is based in studies of such diseases in inbred and outbred mice occurring either spontaneously or following induction with irradiation, chemicals, or exogenous infection with murine leukaemia viruses

(MuLVs). There is a considerable strain dependence of disease and incidence, with much of the differences being genetically determined (Wood et al., 2007).

According to Ward (2006), lymphomas are among the most common tumours in many strains and stocks of mice, especially those used in safety assessment: CD-1, C57BL/6 and B6;129 mice develop 10-50% incidences in aging mice. According to current evidence, it is widely accepted that cancer has a relevant genetic component and that there are non-heritable variables influencing the phenotype. Even though in modern biomedical research context, environmental variables are very well controlled, aspects such as stress or epigenetic modification of gene expression may play a role in phenotypic expression.

1.3.1.4.1. Spontaneous lymphoid neoplasms in laboratory mice

The most common causes and contributors to death in ageing C57BL/6J mice were, at the time the study was carried out by Blackwell et al. (1995), and recently, as revised by Brayton et al. (2012), lymphoma and hematopoietic neoplasms in general. The most common spontaneous lymphoma in many common used inbred strains is the follicular B-cell lymphoma (Wood et al., 2007, Percy D.H. and S.W., 2007), which presents, on necropsy, an enlarged spleen with prominent white pulp that can be seen as white mottling or nodules representing individual enlarged follicles (Figure 1), sometimes nodular enlarged mesenteric lymph nodes, sometimes enlarged Peyer's patches (Wood et al., 2007).



Figure 1: Sagittal section of an enlarged spleen harbouring a follicular B-cell lymphoma, showing the internal surface on the top and the external surface on the bottom.

Lymphomas of mice can be found in specific gross distributions and T-cell lymphomas are originated primarily in the thymus and are commonly systemic (generalized), whereas B-cell lymphomas originate commonly in the spleen, Peyer's patches or mesenteric lymph node and rarely have a systemic gross distribution (Ward, 2006). Lymphomas arise spontaneously in AKR/J, C58/J and other strains of mice by somatic recombination of latent murine leukaemia viruses that activate oncogenes or inactivate tumour suppressor genes via insertional mutagenesis (Mucenski et al., 1988b).

1.3.1.4.2. ENU-induced lymphoid neoplasms in laboratory mice

ENU is a potent mutagen used mutagenesis screening programs since 1970 and at typical doses (100-400 mg/kg), ENU induces point mutations roughly once every 1000 loci (~20-30 per mouse genome) (Hitotsumachi et al., 1985). The most common reported ENU-induced tumours in mice occur in the lung, thymus and liver, and there is some evidence that genetic variability contributes to susceptibility in these tumours (Malkinson, 1989).

ENU is widely used within the biomedical research community as a way of blindly and randomly inducing mutations on germ line cells in order to investigate possible phenotypes on the offspring and their relation with the mutations that originated them. Alongside with its mutagenic properties, ENU is carcinogenic and these two properties in combination seem to be at the basis of the necessary shifts occurring along the lymphocyte differentiation pathway that will result in lymphoma. ENU is used in this study as a way to chemically induce thymic lymphoma and also because there is a wealth of expertise at the Medical Research Council Harwell institute in dealing with ENU in the context of the Harwell ENU-mutagenesis DNA archive (Quwailid et al., 2004). As an alkylating agent its ethyl group is transferred to nucleophilic sites on each of the four nucleotides of DNA. This results in mispairing at the next round of DNA replication. ENU predominantly mutates A:T base pairs, and in the mouse phenotypic screens approximately 60% of the mutations detected are A:T to T:A transitions or A:T to G:C transversions. In descending order of occurrence, ENU produces missense, nonsense and splice-site mutations and these tend to occur in genes with longer coding sequences and higher exon numbers (Acevedo-Arozena et al., 2008). It would be interesting to further classify the mentioned missense mutations, since depending on whether they are conservative or non-conservative, the impact on protein function will differ dramatically.

Most of the potent chemical carcinogens require only a single injection in young mice to induce a high incidence of lymphomas, often thymic T-cell lymphoblastic lymphomas (Ward, 2006). Although the exact dose that produces the highest mutation frequency may vary from one strain to another when administered in a single dose, increasing the dose increases the mutation rate, but this effect does not remain linear

at high doses. Instead, the maximum efficiency is achieved when high doses are administered in a fractionated form with a period separating each injection, typically a week (Acevedo-Arozena et al., 2008). In their study, Justice et al. (2000) concluded that, overall, a 3x100 mg/kg dose is well tolerated by several inbred stains and by all F1 hybrid animals tested. Furthermore, this dose produced a high mutation rate and it is recommended as a starting dose.

Based on the National Toxicology Programme database, there are two patterns of induction of lymphomas in mice. These types include: (1) early induction associated with increased mortality and decreased survival and (2) increased incidence of lymphomas at the end of the two-year bioassay. The early induced tumours are often thymic T-cell lymphomas while the later are typical naturally occurring B-cell lymphomas from the spleen, Peyer's patches or mesenteric lymph node.

Given the relatively high incidence of lymphomas in mice, it is important to compare the type of lymphoma in the control group to those in treated animals. The follicular/pleomorphic lymphoma is the most common lymphoma in most strains of mice (Ward, 2006, Percy D.H. and S.W., 2007, Percy and Barthold, 2007). It most commonly arises in the spleen, mesenteric lymph node and/or Peyer's patches of small intestine. Follicular lymphoma is often composed of variable populations of centroblasts and centrocytes in various proportions. These cells are the main cell types in follicles and germinal centres. Besides these blasts and mature lymphocytes, some cells have cleaved (folded) nuclear membranes, hence the term "cleaved" lymphocytes. Tumour cells often express CD45R (B220) and Pax-5 and can produce immunoglobulins, which can react with antibodies to human kappa light chains (Morse et al., 2002b).

In their study, Fenske et al. (2006b) injected mice from 20 inbred strains (n=240) with 100 mg/kg at weeks 9 and 10 and found that the most common tumours induced where hematopoietic, with the lymphoid lineage affected more that the myeloid lineage.

The most common lymphoid tumour induced by viruses, chemicals and radiation is a precursor T-cell lymphoblastic lymphoma/leukaemia (pre-TLBL) (Wood et al., 2007) and still according to the same authors, this neoplasm is characterised by:

- Other nomenclature: Thymoma, lymphoblastic lymphoma, thymic lymphoma
- Necropsy findings: Enlarged thymus, variable splenomegaly and lymphadenopathy
- Cell size: Medium, uniform
- Cytoplasm: Scant
- Nuclei: Round; chromatin fine
- Nucleoli: Multiple, small/prominent; some with central, prominent nucleoli
- Mitoses: Numerous
- Pattern: Diffuse, starry sky (appearance conferred by tangible body macrophages)
- Phenotype: Immature T-cell $CD3^{+}$, $CD4^{-}/CD8^{-}$ double negative, $CD4^{+}/CD8^{+}$ double positive, or CD4 or CD8 single positive, TCR^{+}, $cytTdT^{+}$
- Molecular: Clonal T-cell, TCRβ R/R
- Characteristic: High grade, moderate starry sky, sheets of cells, perivascular infiltration of lung, liver, soft tissue

- Presumed cell of origin: Precursor intra-thymic T cell but could derive from precursor cells in the bone marrow that home to the thymus
- Differential diagnosis: Histologically indistinguishable from precursor B-cell lymphoblastic lymphoma/leukaemia but $CD3^+$; also very similar to Burkittlike lymphomas but sIg^-
- Human counterpart and commentary: Precursor T-cell lymphoblastic lymphoma

1.3.1.4.3. Classification of mouse lymphoid neoplasms

The nomenclature of lymphomas and leukaemias in mice has evolved over the past 30 years (Ward, 2006). The justification for the existence of the laboratory mouse is to model and understand human disease. Thus nomenclature of mouse neoplasia continues to evolve in an effort to align mouse neoplasia with that of the human (Percy D.H. and S.W., 2007, Percy and Barthold, 2007). An international panel of scientists with expertise in mouse and human haematopathology joined with the haematopathology subcommittee of the Mouse Models for Human Cancers Consortium (MMHCC) to develop criteria for definition and classification of these diseases together with a standardized nomenclature. The fundamental elements contributing to the scheme are clinical features, morphology, immunophenotype, and genetic characteristics. The resulting classifications has numerous parallels to the World Health Organization classification of human lymphoid tumours while recognizing differences that may be species specific (Wood et al., 2007).

1.3.1.4.3.1. B-cell neoplasms

- Precursor B-cell neoplasm
    - Precursor B-cell lymphoblastic lymphoma/leukaemia (pre-B LBL)

- Mature B-cell neoplasms
    - Small B-cell lymphoma (SBL)
    - Splenic marginal zone B-cell lymphoma (SMZL)
    - Follicular B-cell lymphoma (FBL)
    - Diffuse large B-cell lymphoma (DLBCL)
        - Morphologic variants
            - Centroblastic (CB)
            - Immunoblastic (IB)
            - Histiocyte associated (HA)
            - Subtypes: Primary mediastinal (thymic) diffuse large B-cell lymphoma (PM)
    - Classic Burkitt lymphoma (BL)
    - Burkittlike lymphoma (including mature B-cell lymphomas with lymphoblastic morphology) (BLL)
    - Plasma cell neoplasm
        - Plasmacytoma (PCT)
        - Extraosseous plasmacytoma (PCT-E)
        - Anaplastic plasmacytoma (PCT-A)
    - B-natural killer cell lymphoma (BNKL)

1.3.1.4.3.2. T-cell neoplasms

- Precursor T-cell neoplasm
    - Precursor T-cell lymphoblastic lymphoma/leukaemia (pre-T LBL)
- Mature T-cell neoplasms
    - Small T-cell lymphoma (STL)

    - T-natural killer cell lymphoma (TNKL)
- T-cell neoplasm, character undetermined
    - Large cell anaplastic lymphoma (TLCA)

There are considerably less subtypes of T-cell lymphomas in mice than in humans. In any case, according to Morse et al. (2002b), the most common chemically induced lymphoma in mice, precursor T-cell lymphoblastic lymphoma/leukaemia, is the counterpart of human precursor T-cell lymphoblastic lymphoma.

1.3.1.4.4. Clinical signs

One important aspect to consider is to distinguish lymphoma from reactive hyperplasia. According to Morse et al. (2002), several aspects can be considered when establishing the difference in mice. Clonal TCR rearrangements, indicated by strong non-germline bands, are detected by Southern blot in lymphoma. Expression of surface antigens sharply modal and often different from the range for normal cells can be detected by flow cytometry or immunohistochemistry. Also, at cytology, monomorphic populations of lymphocytes and frequently numerous mitotic figures are more related with lymphoma than with reactive hyperplasia.

Mice developing leukaemia/lymphoma can present with a variety of signs. They are mainly enlargement of lymph nodes and spleen, hunched posture, ruffled fur, laboured breathing, paralysis and ataxia (Morse et al., 2002a). Table 5 summarises the frequency at which tissues are involved in precursor T-cell lymphoblastic lymphoma in the mouse. In addition to this, precursor and mature T-cell neoplasms in mice have very identical behaviour in terms of organs and tissues involved and the leukemic phase is seen in one third of lymphoblastic lymphomas.

Organs and tissues involved in Precursor T-cell Lymphoblastic Lymphoma in mice			
Most frequent → **Less frequent**			
Thymus Abdominal lymph nodes: splenic, renal, lumbar Peripheral lymph nodes Mesenteric lymph nodes	Spleen Thoracic lymph nodes Liver Lungs Kidney	Gut-associated lymphoid tissue	Bone marrow

Table 5: Organs and tissues involved in precursor T-cell lymphoblastic lymphoma in mice, adapted from (Herbert C. Morse et al., 2002).

1.3.1.4.5. Necropsy gross findings of thymic lymphomas

The earliest gross lesions of thymic lymphoma are enlargement or reduced size of one thymic lobe followed by enlargement of the other lobe (Wood et al., 2007). Care must be taken to distinguish and dissect the thymus from mediastinal lymph nodes. Thymic lymphomas spread to thoracic non-lymphoid tissues and mediastinal lymph nodes and subsequently to peripheral nodes, spleen, liver, and other tissues. They can sometimes fill most of the thoracic cavity, causing dyspnoea. In their study, Fenske et al. (2006b) the ENU-induced lymphoid neoplasms observed were highly aggressive, there was symptomatic mediastinal involvement and the latency for these lymphomas was relatively short - about 20 weeks.

1.3.1.4.6. Gold standards for diagnosis of lymphoma

In Morse et al. (2002a), detailed morphologic features for the diagnosis of lymphoma are presented. For samples fixed with formalin or in Bouin's, embedded in paraffin and stained with H&E, the following morphologies and characteristics are described: size and shape, cytoplasm – quantity and colour, nucleus – size, chromatin pattern, membrane features and shape, and finally, nucleolus – number, size, prominence, colour and location. As for size and shape, tissue histiocytes, phagocytic macrophages and red blood cells within the same tumour or tissues can be used for size

comparisons with tumour cells. For example, a small lymphocyte is one and a half the diameter of a red blood cell. Nevertheless, this relationship is less clear-cut when applied to neoplastic lymphocytes, as there is a significant variation in cell size of specific types of lymphoma in different mice. Concerning the cytoplasm, it varies from scant, with only a thin rim surrounding the nucleus, to abundant, which is twice the nuclear size. When comparing tissues from animals exposed to the same experimental conditions, as it happened here, it is important to consistently use the same fixative and stains, since they can have an impact of the quantity of cytoplasm: cells stained with Wright-Giemsa or fixed with Bouin's seem to have more cytoplasm than those stained with H&E or fixed with formalin. The size of the nucleus is usually given in terms of size relative to that of histiocytes or endothelial cells and described as small, medium or large, when smaller than, the same size, or larger than those of histiocytes or endothelial cells. Again, this may vary with the fixative employed. As for the chromatin pattern, it can be described as vesicular (open), coarse, or clumped (condensed). Lymphomas resembling immature lymphocytes can have various chromatin patterns. The nuclear shape can vary from round, to oval, multilobated, angulated and cleaved. Finally, the location and number of nucleoli can be associated with specific types of lymphoma. For example, a single central nucleolus is common in lymphoblastic tumours.

The diagnostic criteria for the classification of T-ALL/LBL in humans, defined by the WHO, was published in Swerdlow et al. (2008). In smears T-ALL/LBL cells are of medium size with a high nuclear cytoplasmic ratio; there may be a considerable size range from small lymphoblasts with very condensed nuclear chromatin and no evident nucleoli to larger blasts with finely dispersed chromatin and relatively prominent

nucleoli. Cytoplasmic vacuoles may be present. In marrow sections, the lymphoblasts have high nuclear-cytoplasmic ratio, finely stippled chromatin and inconspicuous nucleoli. The number of mitotic figures is reported to be higher in T-ALL than in B-ALL. In T-LBL the lymph node generally shows complete effacement, with involvement of the capsule. Partial involvement in a paracortical location with sparing of germinal centres may occur. In some cases, the predominant population of blasts has convoluted nuclei and mitotic figures may be numerous. Other authors have also described the morphological characteristics of this lymphoma sub-type in similar terms. For example, in Kumar et al. (2010c), mediastinal thymic masses occur in 50% to 70% of all T-ALLs, which are also more likely to be associated with lymphadenopathy and splenomegaly. Additionally, in both B- and T-ALL, the tumour cells have scant basophilic cytoplasm and nuclei somewhat larger than those of small lymphocytes, the nuclear chromatin is delicate and finely stripped. In many cases the nuclear membrane is deeply subdivided, imparting a convoluted appearance. In keeping with the aggressive clinical behaviour, the mitotic rate is high. As with other rapidly growing lymphoid tumours, interspersed macrophages ingesting apoptotic tumour cells may impart a "starry sky" appearance. In You et al. (2015), T-All/T-LBL is characterised by a proliferation of lymphoblasts that can show a spectrum of cytologic features and the designations L1 and L2 used for the characterisation of lymphoblasts, while not having clinical relevance, are helpful for describing this spectrum: L1-type blasts are small with a high nucleus/cytoplasm ration and small nucleoli, whereas L2-type are larger, with prominent nucleoli and more abundant cytoplasm. Furthermore, cytoplasmic vacuoles can be seen in lymphoblast in a subset of cases.

In the murine arena, the WHO international classification of mouse tumours was published in Frith et al. (2001). There, lymphoblastic lymphoma cells, medium in size, with moderate amount of basophilic and sometimes vacuolated cytoplasm, form non-cohesive but homogeneous sheets, often with a starry-sky appearance, tangible macrophages and apoptosis. Their nucleus is round, with a high nuclear to cytoplasm ratio and a central and prominent nucleolus is described. Furthermore, lymphoblastic lymphoma is described as aggressive, with infiltration of the liver kidneys, ovaries and along the vascular tree in the lungs, with numerous mitotic figures and with the potential of turning leukemic.

An international panel of scientists with expertise in mouse and human haematopathology joined with the hematopathology subcommittee if the Mouse Models for Human Cancer Consortium to develop criteria for definition and classification of mouse lymphoid neoplasm together with standardised nomenclature (Morse et al., 2002b). According to their publication, T-cell lymphoblastic lymphoma is also known as thymic lymphoma, denoting its preferable and primary location. Furthermore, microscopically, Pre-T LBL is composed of medium and uniform sheets of cells, with scant cytoplasm, round nuclei and fine chromatin, small/prominent nucleoli and numerous mitotic figures. The same pattern of diffuse starry sky, conferred by tangible body macrophages, mentioned in humans, is also seen in mice.

1.3.1.4.7. Immunophenotype

Molecules expressed on the surface or cytoplasm of hematopoietic cells play important roles in their development and function and have facilitated the understanding the immune system.

1.3.1.4.7.1. Antigen expression during mouse T-cell development

As in humans, T-cells in mice arise from bone marrow and differentiate in the thymus. T-cell development is characterized by distinct and sequential patterns of antigen expression, as summarised on Table 6, which is a composite of data based on flow cytometry from multiple sources (Rehg et al., 2012).

Antigen expression during mouse T-cell development							
	Thymus-cortex					**Thymus-medulla**	
Antigen	Pro-T1	Pro-T2	Pre-T1	Pre-T2	DP	SP	Mature peripheral lymphoid tissue
CD7	+	+	+	+	+	+	+/-
CD5	-	+	+	+	+	+	+
CD2	-	+	+	+	+	+	+
CD3	C	C	C	C	C	S	S
CD43	+	+	+	+	+	+	+
TdT	+	+	+	+	+	-	-
CD117 (KIT)	++	++	+	+	Low	-	-
CD4	-	-	-	-	+	+ or -	+ or -
CD8	-	-	-	-	+	+ or -	+ or -
CD44	+	+	-	-	-	-	-
CD25	-	+	+	-	-	-	-

Table 6: Antigen expression during mouse T-cell development. Abbreviations: C= cytoplasm; S= surface; DP= double positive; SP= single positive. Expression is semi-quantitative; + present; ++ high. Adapted from (Rehg et al., 2012).

Thymocytes are subdivided as double negative (DN), double positive (DP), or single positive (SP) based on the expression of CD4 and CD8 receptors. In mice, the DN stage is heterogeneous and can still be subdivided into four distinct subsets ($ProT_1$, $ProT_2$, Pre-T_1 and Pre-T_2) based on expression of CD2, CD3, CD5, CD7, CD43, CD44, CD25, and CD117 as well as TdT (Godfrey et al., 2012).

The laboratory diagnosis of non Hodgkin lymphoma is usually complemented by immunophenotyping either by immunohistochemistry (IHC) or flow cytometry (FC). Flow cytometry and other techniques with adjunctive roles in diagnosis and classification of hematopoietic neoplasms must, however, be reconciled with morphology for such diagnosis (Kaleem, 2006). Flow cytometry offers many

advantages in comparison to IHC for the same roles and provides uses that are either not possible or not preferable by IHC, such as multiparameter evaluation of single cells and detection of clonality in T cells (Kaleem, 2006).

1.3.1.4.7.2. T-cell-associated antigens used in flow cytometry

CD3 is a lineage specific protein considered a pan-T-cell marker. It is a multi-domain component of the T-cell receptor complex that is normally located in the cytoplasm of immature T-lymphocytes and on the surface of mature T-lymphocytes (Rehg et al., 2012). According to Lai et al. (1998), there are four subunits of CD3 identified in mice: CD3d, CD3e, CD3g and CD3z, coded by four distinct genes, located in two distinct chromosomes, chromosome 9 for subunits d, e and g, and chromosome 1 for subunit z. Apart from playing a role in TCR subunits, CD3 is involved in receptor complex assembly/traffic and signal transduction. CD3 is not expressed in B-cells, macrophages, myeloid cells, or their neoplasms (Kunder et al., 2007). If a flow cytometry laboratory labels only for surface antigens, the majority of T-lymphoblastic lymphomas will be negative for CD3, since T-lymphoblastic lymphomas rarely express surface CD3 units (Rehg et al., 2012).

CD4 and CD8 are glycoproteins expressed on the surface membrane of mutually exclusive, functionally distinct T-cell populations. CD4 is expressed on T-cells, monocytes, macrophages, Langerhans cells, and other dendritic cells, but not B-cells (Rehg et al., 2012), at least in normal circumstances. It is coded by the *cd4* gene located on chromosome 6 in the mouse and plays a role in TCR co-receptor, Major Histocompatibility Complex (MHC) class II receptor and is involved in signal transduction (Lai et al., 1998). In peripheral T cells, CD4 and CD8 have mutually exclusive expression patterns, although a very small fraction of peripheral T cells may

show expression of both antigens (Nah et al., 1997). CD8 antigen is expressed on cytotoxic T-cells and a subset of NK cells (Rehg et al., 2012). It is composed of two subunits: a and b, coded respectively by *Cd8a* and *Cd8b* genes located on mouse chromosome 6. CD8 plays a role in TCR co-receptors, MHC class I receptor and is involved in signal transduction (Lai et al., 1998).

1.3.1.4.7.3. Other cluster differentiation (CD) markers associated with normal and neoplastic T-cells

According to Morse et al. (2002), it is suggested that routine FC analysis include the following antigen-specific receptors: IgM, IgD, IgG, Igκ, Igλ, TCRα/β, TCRγ/δ), CD3, CD4, CD5, CD8, CD11b, CD19, CD45R(B220), CD90, and CD138. CD79a was initially claimed to be exclusively expressed on B lineage cells but has also been reported in T-lymphoblastic lymphomas (Kaleem, 2006). In their study, Pilozzi et al. (1998), looked at the co-expression of CD79a (JCN117) and CD3 in 149 cases of T-cell and 68 cases of B-cell lymphoblastic leukaemia/lymphoma and co-expression was reported in 10% of T-lymphoblastic leukaemia/lymphoma cases, using immunohistochemistry. In another study, Hashimoto et al. (2002), used immunohistochemistry to look at the expression of CD79a, a B-cell marker, and found evidence that low-level expression of CD79a is common in thymocytes and transiently expressed in immature T-lineage cells.

It is not uncommon for T-cell lymphomas to lose one or more of the four (CD2, CD3, CD5, CD7) pan T-cell antigens. Antigen loss is defined by some as staining less than 50% of the total T-cells (Rehg et al., 2012). Given that there is a very strong evidence in the literature that the most common ENU-induced lymphoma is a precursor T-cell lymphoblastic lymphoma (Morse et al., 2002b, Kakinuma et al., 2005b, Shimada et al., 2003a, Smith et al., 2009, Borowsky et al., 2004, Herbert C. Morse et al., 2002,

Morse et al., 2002a), the antibody panel of markers used here was thought for this specific type of lymphoma.

1.3.1.4.7.4. B-cell-associated antigens

Among the B-cell-associated surface markers, CD19 is the most sensitive and specific. Given that B-cell follicular lymphoma is the main spontaneous lymphoma in mice and that it can affect the spleen, which is also a possible target for metastatic precursor T-cell lymphoblastic lymphoma, CD19 was used in flow cytometric analysis of spleens.

1.3.1.4.7.5. Selection of antibodies for the current study

Even though there is an effort to standardise the nomenclature and classification criteria across human and mouse models of human disease, there seems to be a considerable variety of opinions in the literature on which markers characterise the phenotype of such a complex clinical entity as lymphoma. Apart from that, there is erroneous expression of some markers by neoplastic cells. In this study, the decision of which antibodies to use was made with the intention of identifying the stage of development at which the thymocytes were arrested, whilst differentiating immature from mature forms of T-cell lymphoma, given that they have a close immunophenotype. As stated above, there is evidence for the importance of an accurate classification since it influences treatment strategy. According to Rehg et al. (2012), to diagnose a T-lymphoblastic lymphoma by surface markers, a FC laboratory must use antibodies that label CD44 and CD25, which are early T-cell surface antigens, and alternatively the cells can be permeabilized to allow the polyclonal antibody to penetrate the cell membrane and label the CD3 epsilon antigen. Nevertheless, according to the same authors, in mice, CD117 is present across all

stages of immature T-lymphocytes and disappears when cells reach maturity and migrate from the thymic cortex to the medulla.

In conclusion, the panel of antibodies chosen for detection of surface markers by FC to immunophenotype lymphoma in the experimental population included: CD3, CD4, CD8, CD25, CD44, and CD117. CD45, a pan-leukocyte antigen, was used to identify the initial gate from which all cells were acquired by the cytometer FACSCANTO II^{TM}. The decision was mainly substantiated on the studies carried out in mice by (Rehg et al. (2012), with human lymphocytes by von Boehmer et al. (2003) and the cytometer manufacturer specifications in the application note (Wang et al., 2012a).

1.3.1.4.8. Genetic determinants of lymphoid neoplasms

Research conducted by Shimada et al. (2003a) has shown that *ras* oncogenes activation were frequently associated with ENU-induced thymic lymphoma in C57BL/6 mice. The mutations of K-*ras* in neoplastic thymi were predominantly GGT to GAT in codon 12. On the other hand, neoplastic thymi from C3H/He mice given the same treatment had significantly lower frequency of *ras* mutations, which suggest that the spectrum of *ras* mutations in ENU-induced thymic lymphoma is genetically determined.

Work conducted on the effect of ENU on tumour suppressor genes by Kakinuma et al. (2005b) has shown that *p53* and *Ikaros*, both mapped on chromosome 11, harboured point mutations in 30% (8/27) and 19% (5/27), respectively. The same authors have also shown that 90% (10/11) of the tumours with point mutations retained the wild-type alleles of *p53* and *Ikaros*. Additional work on p53 gene has shown that the majority of p53 knockout mice succumb to thymic CD4+CD8+ T-cell lymphomas (Donehower et al., 1992). The p53 protein functions as a transcription factor to induce

cell arrest, apoptosis and senescence following genotoxic stress (Dudgeon et al., 2014).

In their work, Kundu et al. (2005a) and Yuan et al. (2001a), further substantiated the genetic control of ENU-induced lymphoma susceptibility - *Runx1* deficient mice and mice transgenic for a *Runx1* fusion protein (AML1-ETO), associated with acute myeloid leukaemia in humans, have an increased incidence of such malignancies upon ENU treatment. The susceptibility may have several causes including a reduced DNA repair efficiency or the presence of an oncogene; Msh2 deficient (Claij et al., 2003) and Pim-1 transgenic mice (Breuer et al., 1989) both exhibit an increased incidence of ENU induced lymphomas.

There is also a possible viral component in the pathogenesis of lymphoma in mice. The somatic recombination of latent murine leukaemia viruses that activate oncogenes or inactivate tumour suppressor genes via insertional mutagenesis was described by Mucenski et al. (1988a) in spontaneous occurring lymphomas in AKR/J and C58/J mice. Furthermore, mice pre-TLL was found to be associated with murine leukaemia virus (MuLV) insertional mutagenesis at common integration sites at *Myc*, *Mycn* and *Pim1* genes (Morse et al., 2001).

1.4. Quantitative trait loci (QTL) analysis

Two parental inbred strains are crossed to produce an F1, the starting point for the two most common mapping strategies. Intercrossing the F1 generates an F2 and backcrossing to one or other of the parental strains produces a backcross (Flint et al., 2005). In this study, the experimental population of F2 mice resulted from outcrossing two inbred strains that showed a very distinct trait (incidence of lymphoma) when exposed to ENU: the susceptible strain (C57BL/6J) and the resistant strain (A/J),

followed by an intercross of the F1 offspring. The two-generation outcross-intercross series is the second major breeding protocol used today for linkage analysis in mice. According to Mendel's first law, the offspring from an intercross will be distributed among three genotypes at any single locus — 50% will be heterozygous *A/a*, 25% will be homozygous *A/A*, and 25% will be homozygous *a/a* (Silver and Silver, 1995).

Quantitative trait loci analysis is a statistical analysis that aims to identify loci associated with a specific phenotype. The principal goal of QTL analysis has been to find out whether phenotypic differences are primarily associated with a few loci with fairly large effects, or to many loci, which with minute effects (Miles and Wayne, 2008). The first scenario is more common when dealing with phenotypes of Mendelian inheritance, such as Huntingdon's disease or cystic fibrosis, in which a single gene is responsible for the effect. The gene associated with cystic fibrosis, for example, was initially found to be located in chromosome 7 by linkage analysis (Wainwright et al., 1985, Knowlton et al., 1985). The linkage analysis was the foundation for the discovery of the responsible gene four years later by (Kerem et al., 1989). After identifying large regions in the genome harbouring genes potentially responsible for the phenotype, more refined techniques can be used to narrow down the region of interest to the level of the gene. The quest for individual genes within a QTL is assisted by the identification of *a priori* candidate genes using classical reverse genetics or bioinformatics (Miles and Wayne, 2008).

The aim of this study is to identify hypothetical loci associated with an increased susceptibility to ENU-induced thymic lymphoma in C57BL/6 mice. Cancer is a complex disease and in most cases, there seem to be several genes of minor effect contributing for the disease. In the past decade, studies of mice showed that many

genes with relatively small effects control cancer susceptibility. Nevertheless, in his review, Demant (2003), has compiled information about more than 100 cancer-susceptibility loci associated with several types of cancer, from intestinal cancer, to lung cancer, mammary gland, skin, ovarian, liver, etc. There, he also shows cancer-susceptibility loci associated with lymphoma, although not specifically related to precursor T-cell thymic lymphoma: *Pctm* on chromosome 1 (Le Voyer et al., 2000), *Lyr2* on chromosome 4 (Shisa et al., 1996), *Tlsm1* in chromosome 7 (Yoshihiro Yamada et al., 1994), *Mlsmr1* in chromosome 17 and *Msmr2* in chromosome 18 (Pataer et al., 1996).

Genome-wide association studies (GWAS) are an excellent complement to QTL mapping. Whereas QTL contain many linked genes, which are challenging to separate, GWAS produce many unlinked individual genes, but are associated with large numbers of false positives - combining the two techniques can make the most of both approaches and help provide the ultimate deliverable: individual genes or even nucleotides that contribute to the phenotype of interest (Miles and Wayne, 2008).

1.5. Translational potential

The outcome for patients affected with T-ALL, lymphoma and leukaemia forms included, has improved markedly in recent years owing to the application of intensive chemotherapy regimens. However, such intensive chemotherapy comes at the cost of significant short-term and potentially long-term side effects and therefore a molecular targeted and tumour-specific drugs demand for a deeper understanding of the molecular mechanisms of these neoplasms. Mouse models are powerful tools to screen for novel genetic factors that underlie complex traits such as susceptibility to drug induced cancer (Fenske et al., 2006b) and inbred mouse strains represent unique

genetic resources for the identification of alleles or quantitative trait loci that predispose to oncogenesis (Naf et al., 2002).

The iterative nature of the list and definitions of disease entities in the mouse derives from the increasingly well-supported presumption that carefully defined and validated model systems can provide fundamental insights into human disorders with attendant implications for prevention and intervention. The Haematopathology Subcommittee of the Mouse Models of Human Cancer Consortium was given the charge of developing a consensus list of haematopoietic neoplasms with descriptions and criteria for diagnosis. The goal was to define disease entities that could be recognized by pathologists and related to human disorders where possible (Wood et al., 2007).

A prominent goal of studying mouse tumours is to develop an understanding of the pathogenesis that would provide opportunities for preventing or treating similar disorders of humans. It has, therefore, been important to determine whether disease in the two species is homologous and deserve identical names (Wood et al., 2007). The same authors found this decision is often difficult to make and the reasons are related to fundamental differences between the species in the characteristics of primary and secondary lymphoid organs. Uniquely in mice, extramedullary haematopoiesis continues in the red pulp of the spleen throughout life (Percy and Barthold, 2007). Also, according to Steiniger et al. (2001) and (2006), the splenic marginal zone of mice has also been shown to differ significantly from that in humans. Some mouse lymphomas have strong histological similarities to the human NHL subsets including precursor B- and T-cell lymphoblastic (Hori et al., 2001) and human T-cell acute lymphoblastic leukaemia/lymphoma (T-ALL) is believed to have a counterpart in

mice, precursor T-cell lymphoblastic lymphoma/leukaemia (pre-T LBL) (Morse et al., 2002b), making this a reliable model of the human disease.

The classification of the ENU-induced lymphoma in mice according to distinct stages of thymocyte development may have the potential of refining the mouse model of pre-T ALL/LBL. In humans, there is a tendency to differentiate these two forms. Furthermore, the therapeutic approach differs between T-LBL and T-ALL (Hoelzer and Gokbuget, 2009, Jabbour et al., 2006). At the moment there is no clear distinction between T-ALL and T-LBL in mice and this clinical entity is defined as "Precursor T-cell lymphoblastic lymphoma/leukaemia (pre-T LBL)", alternating between lymphoma and leukaemia mainly based on the distribution of neoplastic cells. If cells are mainly circumscribed to a cellular mass, the preferred term is lymphoma, and if affecting the bone marrow and peripheral blood, the preferred term is leukaemia, similarly to what was established by the WHO for lymphomas in humans. As previously stated, there is evidence that T-ALL and T-LBL have distinct phenotypes, and that they could be segregated in distinct molecular subgroups, and such distinction is relevant when defining a treatment strategy.

Treatment-related lymphoid malignancies are rare in humans but do occur (van Leeuwen et al., 1994). Radiation therapy and certain forms of chemotherapy used to treat cancer increase the risk of subsequent myeloid and lymphoid neoplasms (Fenske et al., 2006b, Travis et al., 1991, Curtis et al., 1992, Kaldor et al., 1990) due to the mutagenic effects of ionizing radiation and chemotherapeutic drugs on hematolymphoid progenitor cells (Kumar et al., 2010c). Secondary malignancies may arise as a consequence of chemotherapeutic protocols using alkylating agents and it is believed that genetics play a role on this process. Knowing which genes may

predispose to increased susceptibility to secondary malignancies, by mapping the susceptibility alleles for ENU-induced lymphomas, may help to make more informed decisions on the therapy to use and improve human health (Fenske et al., 2006b).

Apart from the translational aspects, this project has the potential of improving the welfare of C57BL/6 mice, commonly chemically mutagenized, by identifying the loci associated with increased susceptibility to lymphoma. This can become a foundation for future refinement, by identifying contributing genes and possibly leading to the creation of a transgenic model that is less susceptible to lymphomas.

1.6. Aims of the study

This project intends to identify hypothetical loci that result in an increased incidence of lymphoma development in C57BL/6J mice by carrying out a quantitative trait loci analysis of cohorts of F2 mice treated with ENU. According to Fenske et al. (2006b), lymphoma susceptibility mapped to two regions on chromosomes 3 and 15, one of which contains the gene encoding Sprouty1, an antagonist of fibroblast growth factor signalling. Also, according to the same authors, although several interesting candidate regions were identified, these studies need to be validated and complemented using traditional intercross mapping strategies, which will be carry out in this study.

One of the objectives of this study is to characterize ENU-induced thymic lymphoma in mice by flow cytometry, haematology and biometric variables such as body weight and organ weight analysis. Flow cytometry immunophenotyping allows identification of distinct stages of thymocyte development, as well as malignant cells. Tissue samples from tumour masses were stored for later analysis of sequence changes in oncogenes and other candidate loci.

2. Materials and Methods

2.1. Introduction

Mice were grouped in ENU-treated and non-treated control groups. Following ENU challenge, the animals were clinically monitored daily. Biometric and haematology data were collected at culling and analysed, thymic lymphomas and spleen metastasis were diagnosed histologically using haematoxylin and eosin stained sections and immunophenotyped by flow cytometry. DNA from a selection of both lymphoma positive and negative mice was extracted, sent out for genotyping and a linkage analysis was done.

2.2. Animal model: two generation outcross-intercross (C57BL/6 x A/J)

C57BL/6J and A/J are inbred strains - they were developed by at least 20 crosses between siblings and are virtually homozygous at every single locus. Mice were outcrossed and subsequently F1 generations were intercrossed yielding an F2 in which thymic lymphoma was chemically induced.

2.2.1. Statistical determination of sample size

There was a limitation in the power calculation for an experiment of this nature, as it was not possible to predict how many loci would account for the differences in the phenotype. Furthermore, although it is possible to calculate power when there is one locus intervening, it is not the case when several loci are involved, which was likely to be the case here. The approach presented next is therefore an attempt to have an approximate idea of the sample size needed to test the hypothesis.

According to Flint et al. (2005), the number of animals (n) needed to map an additive QTL in an F2 can be calculated using Equation 1, where α is the significance level, β is the power required and V_{QTL} is the proportion of variance associated with the QTL. The Z values are obtained from the standard tables of the normal distribution.

$$n = \left(\frac{1 - V_{QTL}}{V_{QTL}}\right)\left(\frac{Z_{1-\alpha/2}}{(1 - V_{QTL})^{1/2}} + Z_{1-\beta}\right)^2 \qquad (1)$$

Equation 1

An α significance level of 0.01 was used and a power (β) of 90% was selected by Flint et al. (2005), although power is typically considered at 80%. The α significance level has been chosen at 0.01 relating to a genome-wide significance. The corresponding Z values from the standard table of the normal distribution are 3.89 and 1.28 for α and β respectively. For a purely additive QTL that explains 5% of the variance, the calculation yields Equation 2.

$$\left(\frac{0.95}{0.05}\right)\left(\frac{3.89}{0.97} + 1.28\right)^2 = 532$$

Equation 2

By increasing sample size to approximately N=500, it would be possible to detect a single QTL explaining at least 5% of variation of trait in F2. Hypothesized loci should account for more than 8% of the variation of the trait in F2 population since the incidence at which parental inbred strains used in this study developed lymphoma when challenged with ENU in similar environmental conditions was very different, as reported in Fenske et al. (2006b).

The experimental population of F2 intercrosses was bred in three separate cohorts and two major experimental groups were defined: ENU-treated (n= 300-400), and non-treated controls (n=60). The study included both sexes, at identical numbers in both groups. Although this was the initial plan, for animal welfare reasons, five groups had

to be created: four groups treated at different ENU dosages and a control group. Details are given further ahead.

2.3. Housing and husbandry

The humane care and use of mice in this research was conducted under the Animals (Scientific Procedures) Act 1986, Home Office, United Kingdom.

C57BL/6 x A/J F2 intercross mice bred at the Mary Lyon Centre (MLC), Harwell, Oxfordshire, were kept in individually ventilated cages (IVCs) (Charles River Laboratories UK, Margate, UK), high health status, mouse only, in a specific pathogen free (SPF) barrier facility, the MLC. The centre has digital record-keeping for all relevant data associated with individual mice and procedures carried out on them.

They were protected from exposure to infectious agents and housed in a 12 h light/dark (07:00–19:00 light phase) cycle at 19–23°C and 5°–65% relative humidity on grade 6 sawdust bedding (Datesand Ltd, Manchester, UK).

2.3.1. Diet

On a regular basis, mice were fed rat and mouse No. 3 Breeding Diet (Special Diets Services, Witham, Essex, UK) and provided with chlorinated water *ad libitum*. During ENU administration, in addition to the regular diet, TransBreed (Special Diets Services, Witham, Essex, UK) pellets were placed on the cage floor. This is a formula with high fat content (10% by weight, 24% by energy) that supplies more energy than a standard diet and contains very digestible raw materials. The objective of using this diet was to counterbalance the weight loss systematically observed during ENU

administration explained below. Whenever used for the ENU-treated group, SDS TransBreed was also added on the cage floor of control animals.

2.3.2. Health status

The microbiological screening programme in the MLC involves sending mice from sentinel cages (one per 56 cages) that are challenged with samples of dirty bedding from separate columns in each rack on an eight-week rotation. Live mice are submitted to an outside laboratory for microbiological testing based on FELASA recommendations (Nicklas et al., 2001). Health screening has shown that the Specific Pathogen Free (SPF) status has been maintained throughout the period of this research.

2.4. Chemical induction of lymphoma with ENU

Given its toxic, mutagenic and carcinogenic properties, only highly trained personnel are allowed to handle, prepare and perform intraperitoneal injections of ENU in mice. All work was carried out in a class II biological safety cabinet and strictly followed the relevant Standard Operational Procedure (SOP), including the spectrophotometric determination of ENU concentration (Table 94, Appendix 2 - Tables and figures).

2.4.1. Preparation for injection before making up ENU

ISOPAC® containing 1 g of ENU was removed from the freezer the night before injection, covered with foil to protect it from light and placed in the fume hood. On the day of injection, all mice were weighed and their weights recorded. In the laminar air flow (LAF) cabinet, inactivation solution in a 500 ml spray bottle and a 1-liter plastic beaker containing approximately 400 ml of inactivating solution were prepared.

2.4.2. Preparation of ENU (prepared immediately before use, in fume hood)

A 1000 ml beaker container with 500 ml of deactivation solution was prepared. This was used for any waste materials. More than 10 ml of absolute ethanol were aliquoted into a universal tube and 10 ml withdrawn using a 10ml syringe. A venting needle (21G) was inserted into the top of the ISOPAC® and the ethanol injected using a 21G needle. Both needles were removed and the ISOPAC® was agitated until all of the large ENU crystals dissolved. A venting needle was replaced in the top of the ISOPAC® and 1 x 30 ml aliquots of phosphate/citrate buffer were injected into the ENU ISOPAC® using a 50ml syringe. The venting needle was removed. This step was repeated twice more, making a total of 90 ml of phosphate/citrate buffer. 15–20 ml of air was injected and 15–20 ml of ENU solution were withdrawn from the ISOPAC® using a 20ml syringe. A single use mini filter was attached on to the syringe and the solution injected slowly into a universal tube. Filters were disposed of into the beaker containing inactivating solution. This was repeated until there was enough filtered ENU to inject all the mice.

2.4.3. Spectrophotometric determination of ENU concentration

4 ml of citrate/phosphate buffer were aliquoted into a cuvette (control cuvette) and placed in cuvette holder. 3.2ml of phosphate/citrate buffer were aliquoted into a cuvette. 800µl of filtered ENU were pipetted into the cuvette and carefully mixed. The first two steps were repeated producing a total of two samples, A and B, and placed in the cuvette holder. A wavelength of 398 nm and mode ABS were confirmed. The control cuvette was placed in the spectrophotometer while holding the opaque sides and ensuring the triangle marker on the cuvette was on the left hand side. Calibrate function was

pressed - the Optical Density (OD) read 0 as it was supposed. Control cuvette was removed, replaced in holder and moved to fume hood. Sample A was then carefully placed in the slot in the spectrophotometer in the same way as the control cuvette, the reading was recorded and the step repeated for sample B. The OD of sample A and B were within 0.1 nm of each other.

2.4.4. Calculation of concentration

(OD_{398}(sample A) + OD_{398}(sample B)) x 3.6 = ENU concentration (mg/ml)

2.4.5. Calculation of volume to inject

Using the formulae below, the correct dose for each mouse was calculated according to their individual weight. The maximum volume never exceeded 15 ml/kg.

- For a dose of 100mg/kg: volume (ml) to inject = $\frac{\text{weight of mouse (g) x 0.1}}{\text{ENU concentration (mg/ml)}}$
- For a dose of 90mg/kg: volume (ml) to inject = $\frac{\text{weight of mouse (g) x 0.09}}{\text{ENU concentration (mg/ml)}}$
- For a dose of 80mg/kg: volume (ml) to inject = $\frac{\text{weight of mouse (g) x 0.08}}{\text{ENU concentration (mg/ml)}}$

2.4.6. Intraperitoneal Injection

The beaker containing waste deactivation solution was placed into the LAF cabinet along with the first cage of mice to be treated. For each mouse to be injected, the weight was checked on cage card and the correct volume to administer was read out. A second person injected the mouse with the specified volume of ENU solution intraperitoneally, discarded the needle and expelled any ENU left in the syringe into the deactivation solution. Treated mice were individually placed in a clean cage. Injected mice were monitored throughout the injection session before returning to ward. Spectrophotometric determination of ENU concentration was repeated and recorded.

2.5. ENU dosage regimen planned

Based on in house experience and on literature (Weber et al., 2000, Justice et al., 2000, Hitotsumachi et al., 1985, Acevedo-Arozena et al., 2008), a typical dose of 3 x 100 mg/kg was considered well-tolerated and balanced between the scientific criteria of maximizing mutation load and the detrimental effects of high doses of ENU on the animal, and established as the dose to be administered intraperitoneally at weeks 12, 13 and 14 of age.

2.5.1. Animal welfare assessment during the injection protocol

The animals were assessed daily and on manifestation of signs of disease such as loss of body weight, laboured breathing, hunched posture, piloerection, absence of normal grooming behaviour, loss of inquisitive behaviour, inappetence and detectable lumps on visual exam, were euthanized, necropsied and relevant tissues harvested. These clinical signs are good indicators of ill-health (Sewell et al., 2015).

ENU was diluted in an ethanol solution and, as such, mice were inspected at least twice on the day of injection and any showing signs of tissue damage at the site of injection were euthanized. Stress during administration was minimized by careful handling. The volume of any substance given was as small as practicable. Unexpected adverse effects during or after the administration resulted in euthanasia under Schedule 1, unless the effect was mild or could be promptly controlled by veterinary treatment or reduction of the dose administered.

As for humane end-points, any animal whose weight fell more than 20% below that expected from its starting weight was killed humanely. After the initial treatment, animals underwent additional daily welfare checks during their lifetime. Such animals (e.g. showing severe weight loss and/or signs of suffering and/or tumours) were culled

under Schedule 1 by an overdose of barbiturate administered intraperitoneally, weighed, necropsied, gross pathology findings recorded, and samples collected for haematology and histopathology.

2.6. Experimental groups according to ENU dosage

Although the initial plan was to treat all animals with exactly the same ENU dosage in order to get a consistent group with little variability, a compromise between scientific output and animal welfare had to be found, as explained in section 4.1, page 199. As a consequence, four distinct treatment groups of mice were created and studied, as detailed in Table 7.

ENU Protocol	Age (weeks) at each treatment	Number of animals			Total
		Cohort 1	Cohort 2	Cohort 3	
100+100+80 mg/kg	12, 13, 15	43	-	-	43
100 mg/kg	14, 16, 18	-	13	10	23
100+90 mg/kg	14, 16, 18	-	71	46	117
100+90+80 mg/kg	14, 16, 18	-	127	98	225
Total		43	211	154	408

Table 7: Experimental units per ENU dosage.

There were mice from different cohorts exposed to the same ENU dosage, but since the remaining variables that could have had an effect on the scientific outcome, such as temperature, humidity, diet, age at commencement, and time between treatments were virtually the same for all mice, they were grouped according to the only variable that was different - treatment dose. Five groups were created: 1 or control, consisting of untreated mice; 2, mice treated at (100+90) mg/kg; 3, treated at (100+90+80) mg/kg;

4, treated at (100+100+80) mg/kg; and 5, treated at 100 mg/kg (that were not included in the analysis). Not knowing in advance whether animals treated with lower doses such as 100 mg/kg or 100+90 mg/kg would develop lymphoma, they were kept in the

experiment. At the end of the experimental period, animals treated at 100 mg/kg did not provide valuable information as only one animal developed lymphoma - not representative enough to be included in the analysis.

2.7. Experimental endpoint

According to the survivability analysis on Smith et al. (2009), less than 20% of the mice treated with ENU were alive around day 330 of age, and according to Justice et al. (2000), males will live an average of 1 year after treatment in a clean colony, rather than the normal 18 months to 2 years. The experimental endpoint was set when mice would reach approximately 12 months of age.

2.7.1. Collection of data

Data was collected from animals that fulfilled the following inclusion criteria: have at least one month after last treatment was administered, had no dubious identification and were not found dead.

The histopathological analysis of H&E-stained sections of the thymus was a keystone to compare lymphoma positive with lymphoma negative phenotypes. Apart from the control group, within each ENU dosage group there were mice that had developed lymphoma and others that had not. To compare data from those three groups (control, ENU-treated lymphoma negative and ENU-treated lymphoma positive), only data from mice whose thymi were subject to histological examination, the gold standard method for diagnosing this pathology, were included.

In the most numerous group (Group 3) the aim was to get as many thymi processed histologically as possible. In smaller groups, such as Group 2 and 4, the number of animals from which data was analysed depended primarily on the number of

lymphoma positive mice found. A similar number of mice with increased thymi (strongly indicative of the presence of thymic lymphoma) and normal thymi were histologically processed in order to obtain a balanced number of lymphoma negative animals to act as control for the analysis. For example, in Group 2, from a total of 113 animals treated at 100+90 mg/kg, only 18 developed thymic lymphoma and therefore only 17 normal weight thymi were prepared for histopathological examination, resulting in a group of 35 mice from which relevant data could be obtained. In the same way, in Group 4, from a total of 43 mice that lived throughout the experimental period, only 13 developed lymphoma and therefore data from 12 lymphoma negative mice were also collected. The cost of processing all tissues from all animals would have largely outweighed the scientific benefit. Biometric variables such as body and organ weights (thymus and spleen) measured at culling were analysed.

In conclusion, there was a considerable difference between number of animals treated and number of animals that provided information for the final analysis of biometric and haematology parameters (Table 8). That difference can be explained by several aspects: (1) the nature of the study, which included an element of unpredictably, as it was not possible to tell in advance how many treated mice would develop lymphoma, (2) an unknown variable, as the number of loci accounting for the difference in phenotypes was unknown, making difficult the process of calculating sample size needed to achieve power, (3) the nature of QTL analysis, which requires a high number of experimental units to deliver, (4) animals humanely terminated for welfare reasons, and (5) a cost-benefit analysis as explained before.

ENU dosage	Total	Included in biometric analysis
100 mg/kg	23	0
100+90 mg/kg	117	35
100+90+80 mg/kg	225	178
100+100+80 mg/kg	43	25
Total	408	238

Table 8: Animals included in the analysis of biometric and haematology data.

Biometric data collected and analysed included body weight at culling, thymus weigh, spleen weight and thymic lymphoma incidence. Thymus and spleen weights were measured before fixation and after removing any adjacent tissues.

2.7.1.1. Harvesting of organs and tissues of interest

During necropsy, the main focus was to assess the thymus for any gross lesions indicative of the presence of thymic lymphoma, by assessing its size and weight. A full necropsy was carried out for each mouse and organs of the lymphoreticular system such as lymph nodes and the spleen were carefully examined. Before necropsy, a sample of peripheral blood was collected.

2.7.1.1.1. Peripheral blood

Peripheral blood was collected as a terminal procedure. Mice were overdosed with anaesthetic, weighed and upon reaching a deep anaesthetic plane, assessed by the complete absence of pedal withdrawal reflex, a sample of peripheral blood was collected from the retro-orbital sinus using a capillary tube.

A sample of at least 200 µl of peripheral blood from each animal was collected in a tube with EDTA and processed with ADVIA Haematology Analyser. On rare occasions, when the required volume of blood could not be collected, a dilution was made with sheath solution or 0.9% saline to reach the minimum volume required to run the sample and the results compensated for the dilution. In order to prevent false results, based on haemodilution or clot formation, the ratio of anticoagulant to

collected blood volume was taken into consideration. A blood smear of most samples was made. This was done to help with the interpretation when the analyser presented an error message or misinterpreted one cell type for another; e.g.: platelet clumps as eosinophils. Diff Quick was used to stain these smears.

2.7.1.1.2. Necropsy and tissue harvesting

After blood collection and confirmation of death by cessation of circulation, a full necropsy was carried out. Macroscopic findings were recorded for each mouse and sample organs and tissues were harvested.

When harvesting the thymus, in most cases, as exemplified in Figure 2, macroscopic findings were good indicators of the presence of thymic lymphoma.

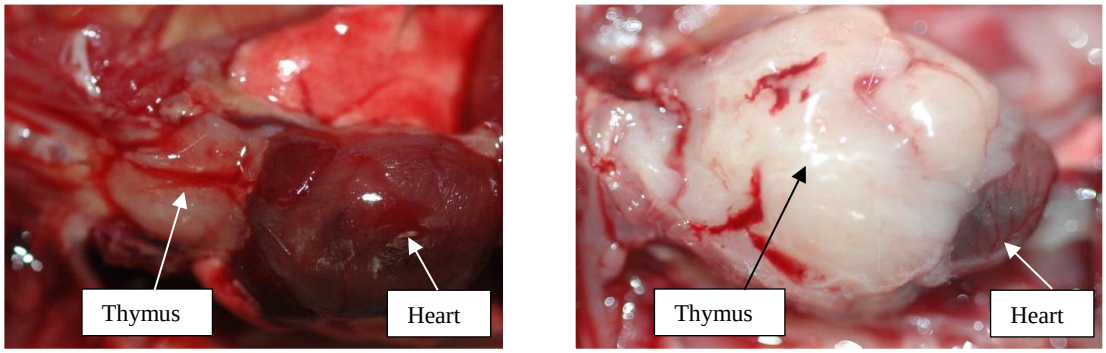


Figure 2: Picture of a normal thymus on the left and of a thymic lymphoma on the right.

In mice, according to Jacoby et al. (2002b), the thymus reaches maximum size around the time of sexual maturity and involutes between 35 and 80 days of age. The age in days (mean±SD) of mice at culling was above 80 days, when no considerable involution was expected to have occurred: 342.86±49.71 in Group 1 (control), 291.74±49.5 in Group 2, 302.94±50.98 in Group 3, and 292.04±53.88 in Group 4. Thymus weight is a good indicator of whether a proliferative process is present and in 10 week mice it weighs (mean±SD) 41.9±10.8 mg and 24.2±6.72 mg in female and male C57BL/6J (n= 19) respectively, and 41.8±8.64 mg and 36.3±11.1 in female and

male A/J (n= 20), respectively, (Deschepper CF and Gallo-Payet N, 2004). A threshold for thymus weight was established at 100 mg: (1) if weighing more than 100 mg, was cut in two halves of identical size by a transversal section, one half fixed in 10% buffered formalin and processed by histology and one half kept in a 1 ml centrifuge tube containing 1 ml RPMI, incubated on ice for posterior flow cytometry analysis, and (2) if weighing 100 mg or less, the whole organ was fixed in 10% buffered formalin for histological processing for possible and H&E-stained slides evaluation.

During the process of preparing a cell suspension for flow cytometry, a sample of approximately 250 µL from each thymus was kept in a 1.5 ml centrifuge tube and frozen at -80°C for future DNA extraction, sequencing and possible analysis of sequence changes in oncogenes and other candidate loci.

Because thymic lymphomas may spread to thoracic non-lymphoid tissues and mediastinal lymph nodes and subsequently to peripheral nodes, spleen, liver, and other tissues, a careful dissection was observed to distinguish and separate the thymus from surrounding tissues.

As for the spleen, weight was measured and if 500 mg or less, the whole organ was fixed in 10% buffered formalin. If higher than 500 mg, it was cut in to halves of identical size by a sagittal section, one half fixed in 10% buffered formalin and one half kept for flow cytometry analysis in a 1 ml centrifuge tube containing 1 ml RPMI and stored at 4° C or incubated on ice until further processing.

Furthermore, approximately 1 cm of distal tail was cut, kept in a 1 ml centrifuge tube, and stored at -20° C, for DNA extraction.

2.7.1.2. Analysis of biometric and haematology data

2.7.1.2.1. Methodology

As stated above, the main endpoint here was to study the hypothetical association between loci and increased susceptibility to thymic lymphoma. Nevertheless, the analysis of terminal body weight, organ weights and blood parameters was done as a way to increase the data obtained from the experiment, aiming to increase the scientific output whilst keeping the cost, as far as animal welfare is concerned. Hence, a pilot study, designed to characterize the effect of ENU on those biometric variables was not carried out and, as a consequence, the variability of the responses was not known before the data was analysed. Although the sample was considerably large, in some cases the variability was marked and, therefore, in the absence of an *ad hoc* power calculation, the results presented should be taken as indicative and the conclusions as assumptions. The analysis was carried out on each parameter and sex separately.

2.7.1.2.2. Body weight and haematology parameters

A two-way analysis of variance (ANOVA) was applied to the data. The factors in the analyses were dose group, thymus lymphoma status (animal positive or negative for lymphoma) and their interaction. Comparisons were made between the groups using two-tailed Student's *t*-tests based on the error mean square from the analysis of variance. Levene's test for homogeneity of variance (Levene, 1960) was performed following the ANOVA described above. If Levene's test was significant at the 1% level, then this indicated a difference between the variances. Data were transformed using a logarithmic transformation (base 10) and the ANOVA and Levene's test were performed on the transformed data. If Levene's test was again significant at the 1% level, the same process was performed using a square-root transformation. Where

Levene's test was still significant, the ANOVA analysis was performed upon the rank transformed data. Given the marked variability in most responses, the data had to be transformed in order to comply with the assumptions for the ANOVA analysis. The transformations applied to the data are not statistical tests and do not have an impact on the occurrence of Type I and Type II errors. On the other hand, it has to be acknowledged that by running several *t*-tests after the ANOVA, the chances of false positives (Type I errors) are increased. Although adjustments for multiple comparisons could have been applied to reduce Type I errors, they would have increased Type II errors. To counteract the risk, the results were reviewed by looking at their biological relevance and statistical significance. Table 9 summarizes the transformation methods used in the analysis of each parameter and whether statistical significance was attained at interaction level.

Sex	Parameter	Dataset used in final analysis	Significant interaction
Males	BW	Untransformed	No
	Thymus Weight (includes BW as a covariate)	Log transformed	No
	Spleen Weight (includes BW as a covariate)	Rank transformed	No
	WBCB	Rank transformed	No
	RBC	Rank transformed	No
	HGB	Rank transformed	No
	HCT	Rank transformed	No
	MCV	Rank transformed	No
	MCHC	Rank transformed	No
	PLT	Rank transformed	No
	Neutro	Rank transformed	No
	Lymph	Rank transformed	No
	Mono	Rank transformed	No
	Eos	Rank transformed	No
	LUC	Rank transformed	No
	Baso	Rank transformed	No
Females	BW	Untransformed	No
	Thymus Weight (includes BW as a covariate)	Rank transformed	No
	Spleen Weight (includes BW as a covariate)	Log transformed	No
	WBCB	Rank transformed	No
	RBC	Rank transformed	Yes
	HGB	Rank transformed	Yes
	HCT	Rank transformed	Yes
	MCV	Rank transformed	No
	MCHC	Rank transformed	Yes
	PLT	Untransformed	No
	Neutro	Rank transformed	No
	Lymph	Rank transformed	No
	Mono	Untransformed	No
	Eos	Untransformed	No
	LUC	Rank transformed	No
	Baso	Rank transformed	No

Table 9: Summary data transformation methods used and significance at interaction level.

Table 10 shows the haematology variables analyzed in this study. Other variables, such as the percentage of each leucocyte population and white blood cells perox (WBCP) were collected. WBCP and WBCB (white blood cell baso) of each result was compared to validate white blood cell count - both results had to be similar. WBCB was selected to be included in the analysis. Results for each leucocyte are presented as absolute count.

Variable	Meaning	Units
WBCB	White Blood Cell Count (Baso)	10^3/µL
NEUT	Neutrophil	10^3/ µL
LYMPH	Lymphocyte	10^3/µL
MONO	Monocyte	10^3/µL
EOSIN	Eosinophil	10^3/µL
BASO	Basophils	10^3/µL
LUC	Large Unstained Cells	10^3/µL
RBC	Red Blood Cell Count	10^6/ µL
HGB	Haemoglobin Concentration	g/dL
HCT	Haematocrit or Packed Cell Volume	%
MCV	Mean Cell Volume	fL
MCHC	Mean Cell Haemoglobin Concentration	g/dL
PLT	Platelet Count	10^3/µL

Table 10: Haematology variables analysed, their abbreviations and units.

2.7.1.2.3. Thymus and spleen weight

Analysis of covariance was performed using body weight as a covariate (Angervall and Carlström, 1963). The treatment comparisons were made on adjusted group means in order to allow for differences in body weight which might influence the organ weights.

The factors in the analyses were dose group, thymus lymphoma status, their interaction and body weight as a covariate. Comparisons were made between the groups using two-tailed Student's *t*-tests based on the error mean square from the analysis of covariance.

2.7.1.2.4. Data handling

The data were analyzed using SAS 9.1.3 (SAS, 2002).

2.8. Histopathological evaluation of samples

The samples for histological evaluation were fixed in 10% buffered formalin, the sections were embedded in paraffin and staining was done with H&E. Histological assessment of the slides was done by the author and reviewed by an FRCPath and RCVS specialist in Laboratory Animal Pathology.

2.8.1. Distinguishing lymphoma from reactive hyperplasia in mice

According to Ward et al. (2012), aging mice may develop medullary hyperplasia and when pronounced, thymic medullary hyperplasia can mimic neoplasia in aging mice. However, these lesions, composed of B-cells, which can form germinal centres and plasma cells, are not as large as tumour masses seen in thymic lymphomas. The cortex generally shows patchy atrophic changes, and epithelial and lymphoid hyperplasia may be present together (Frith et al., 2001). According to the same author, benign and malignant thymomas are listed as differential diagnosis, but the epithelial component is at the base of their histogenesis, whereas in thymic lymphomas there is no evidence of an epithelial component. The epithelial component is positive for keratin, seems to be derived from the epithelial cells in thymic (Hassal's) corpuscles or thymic reticular tissue, and varies from a minor component to the majority of the tumour mass (Ward et al., 1999). It was critical for this project to accurately diagnose thymic lymphoma and to that end it was important to distinguish lymphoma from reactive hyperplasia. This was done by histological analysis of H&E sections, as per Morse et al. (2002b).

2.9. Flow cytometry immunophenotyping

Although histological examination is the gold standard method to diagnose thymic lymphoma, it is not possible to obtain information about the specific immunophenotype from an H&E stained slide. In order to characterise the immunophenotype(s) of thymic lymphoma, cell suspensions of enlarged thymi and

spleens were analysed by flow cytometry. Most spleens weighing more than 0.5 g were analysed using largely the same panel of antibodies used for thymus, with the addition of CD19.

2.9.1. Cytometer configuration

FACS CANTO II was the cytometer used for the acquisition. It has three lasers (blue, red and violet) and its configuration is shown in Table 11.

Cytometer Configuration												
Software Version	BD FACSDiva 8.0											
Export Time	07/08/2014 10:17											
User												
Cytometer	FACSCantoII											
Serial Number	V96300196											
Configuration Name	IMPC											
Folder Name	New Folder											
Comments												
Window Extension	7											
Laser Name	Type	Wavelength	Power	Detector Array	Detector	Channel	Mirror	Filter	Parameter	Fsc Channel	Reference	Position
Blue	Blue	488	20	Octagon	A	1	735 LP	780/60 BP	PE-Cy7	0	Y	2
					B	2	600 LP	616/23 BP	PE-CF594			
					C		610 LP					
					D	3	556 LP	585/42 BP	PE			
					E	4	502 LP	530/30 BP	Alexa Fluor 488			
									FITC			
					F	5		488/10 BP	SSC			
					G							
					H							
Red	Red	633	17	Trigon	A	6	735 LP	780/60 BP	APC-Cy7			3
					B		685 LP					
					C	7		660/20 BP	APC			
Violet	Violet	405	25	Trigon	A	9	502 LP	510/50 BP	AmCyan			1
					B	8		450/50 BP	Pacific Blue			
					C							

Table 11: Flow cytometer configuration.

2.9.2. Application settings

During the flow cytometry analysis, electronic noise is one of the aspects that has to be taken into account, particularly when having to compare results obtained from analysis carried out in a long period of time. The aim of creating and saving "application settings" at the start of any experiment involving a new cell-type is to have the negative population of interest above electronic noise. This is the first step in standardizing flow cytometry results, creating the experimental conditions that allowed comparison of results in time. It is the first of a series of steps required to setup a FC experiment, in combination with others such as finding the best working

dilution of antibodies, compensation analysis and fluorescence minus one analysis, all of which were done for both thymus and spleen.

2.9.2.1. Sample preparation specific steps

Three thymi and one spleen from ENU-treated C57BL/6 males with approximately one year of age were harvested. The F2 population is heterozygous and therefore there is no animal that could act as a model for all the other animals. The choice of establishing application settings with C57BL/6 thymi, not being ideal, did not seem to have compromised the outcome.

1. From the point at which the cell suspension is obtained on a 1.5 ml centrifuge tube, already digested, 500 µL of lysis buffer were added and left to act for 1 minute, after which equal volume of FC buffer was added;
2. The tube was spun at 290 G, for 5 minutes at 8° Celsius;
3. The pellet was re-suspended in 1 ml of FC buffer in a FC tube. When cell concentration was too high, the suspension was further diluted into another FC tube with 1 ml of FC buffer.

2.9.2.2. Software configuration

1. In cytometer reports, the latest "cytometer baseline" was selected;
2. Electronic Noise Robust Standard Deviation (rSDEN) value was used to calculate 2.5 X rSDEN. The objective was to have the negative population of interest above this value, which was achieved by manipulating the voltages for each fluorochrome;
3. The analyser was set to acquire 20 000 events. Forward scatter (FSC) was set to 300 and side scatter (SSC) to 430. Threshold was set to 50 000 events;
4. Sample acquisition and setting up the gates

a. P1 was SSC vs Time. It was set to ignore the first 10 seconds to ensure the flow was stable at acquisition;
b. P2 was a size gate, that is FSC vs SSC
    i. Next 2 gates were the singlets gates: P3 was side scatter singlets gate (SSC-H vs SSC-W, height vs width), and P4 was forward scatter singlets gate (FSC-H vs FSC-W, again, height vs width);
    ii. And 2 more plots (these had to be relabelled when testing for each fluorochrome): FSC-H vs fluorochrome and a histogram.

The plots were set to display bi-exponential mode. From plot P4 "Statistics view" was generated. Sample was acquired and rSDEN of the fluorochrome being tested checked on stats box. The objective is to have a value higher than the electronic noise. If the value was lower, the voltage was increased in intervals of 5-10, in more than one attempt if needed. When the voltage was adequate for any given fluorochrome, "record" function was activated. The number of events to record from P4 (stopping gate) was 20 000 at a medium flow rate. The process was repeated for each fluorochrome; the labels on the SSC vs fluorochrome and histogram plots were changed accordingly. At each attempt, the rSDEN value for the previous fluorochrome have occasionally changed and therefore had to be refined again and overwritten. The aim was to be, at most, 10 units above electronic noise. Once completed, application settings were saved.

2.9.3. Antibody conjugates

The panel of antibody conjugates (Table 12) was the same for thymi and spleens, except CD19 that, being a B-cell marker was only used for the analysis of spleens. CD16 was used to block non-specific sites and not subject to titration analysis.

Antibody	Fluorochrome
CD3	Pac Blue
CD4	FITC
CD8a	APC-Cy7
CD19	AmCyan
CD25	PE
CD44	PE-CF594
CD45	PE-Cy7
CD117	APC

Table 12: Antibody panel used in FC analysis.

2.9.4. Antibody dilutions

This experiment was done for each cell-type and the objective was to ascertain the dilution at which each antibody-fluorochrome conjugate provided the best differentiation of positive and negative cells in the samples analysed. Typical dilutions starting from 1:100 up to 1:3200 were tested.

2.9.4.1. Thymus

The antibody dilutions that provided the best differentiation between positive and negative events for each antibody-conjugate in thymus analysis are presented in Table 13.

Antibody conjugate	Optimal dilution
CD3	1:100
CD4	1:1600
CD8	1:200
CD25	1:200
CD44	1:3200
CD45	1:8000
CD117	1:100

Table 13: Optimal antibody dilutions found for thymus analysis.

An initial dilution of 1:1600 was found to be ideal for CD44 on C57BL/6 thymus, used in the antibody dilution experiments, but the results were off scale when this dilution was used in the F2 intercross. A dilution of 1:3200 proved to work best.

For CD45, a pan leucocyte marker, the dilution of choice was 1:8000 since lower dilutions produced results off scale. Being a pan leucocyte maker, all cells stained positive, not allowing differentiating between CD45 negative and CD45 positive cells.

CD117 is rarely expressed and since dilutions were tested in a normal thymus, it was nearly impossible to gate. A low dilution (1:100) was defined, subject to further testing in neoplastic thymi. Figure 3 shows the stain index of each antibody conjugate at each dilution tested.

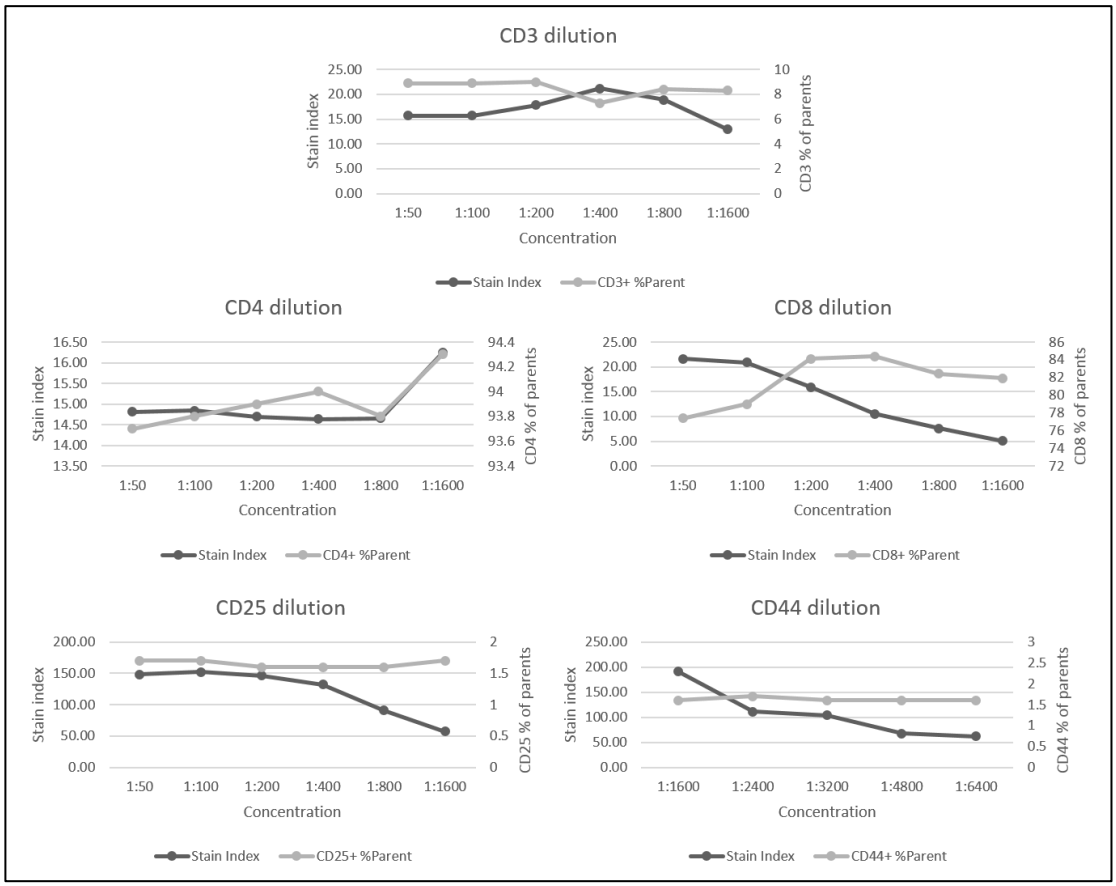


Figure 3: Stain index using median fluoresce intensities for each antibody used in flow cytometry analysis of thymi.

2.9.4.2. Spleen

The antibody dilutions that provided the best differentiation between positive and negative events for each antibody-conjugate in spleen analysis are shown in Table 14.

Antibody conjugate	Optimal dilution
CD3	1:100
CD4	1:800
CD8	1:200
CD19	1:200
CD25	1:200
CD44	1:3200
CD45	1:8000
CD117	1:200

Table 14: Optimal antibody dilutions found for spleen analysis.

Figure 4 shows the stain index of each antibody conjugate at each dilution tested.

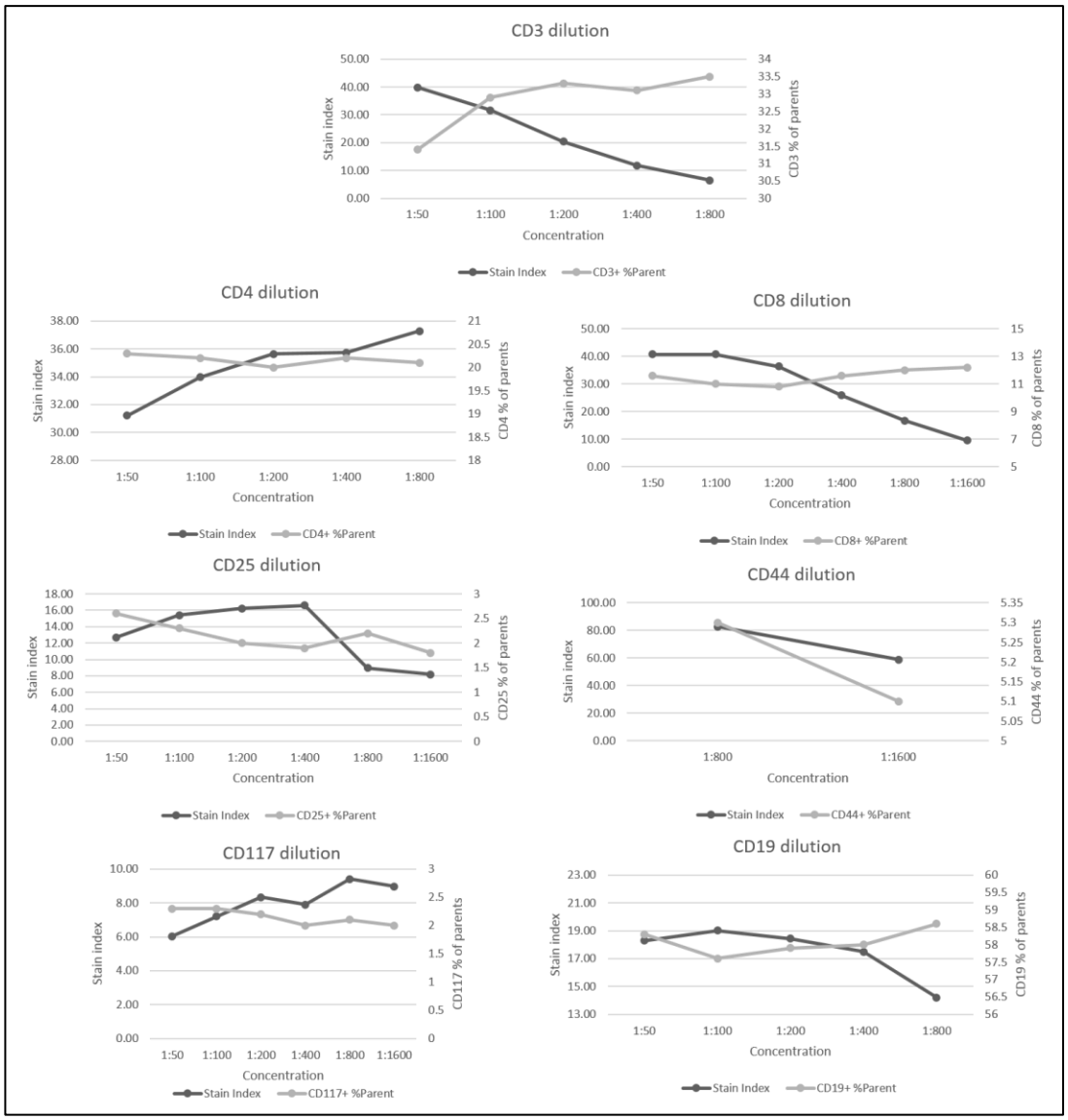


Figure 4: Stain index using median fluoresce intensities for each antibody used in flow cytometry analysis of spleen

2.9.5. Compensation analysis

Because fluorochromes can emit fluorescence in nearby wavelengths, there is an overlap phenomenon that has to be compensated in order to determine with accuracy to which fluorochrome a given emission belongs to. This was achieved by using specific software resources after determining which dilution of each antibody conjugate produces the best results and before start running the samples. FACSDiva™ and FloJo™ are two commonly used software programmes capable of doing this. In this study both were used, the former during acquisition and the latter for the analysis.

2.9.5.1. Compensation analysis protocol

1. A new experiment was created using a new plate (96 V bottom);
2. "Inspector" window was opened and on "cytometer settings", all fluorochromes not being used were deleted;
3. "Well" was selected and, on "Experiment", "Compensation setup" was chosen, followed by "Create compensation controls", which generates a window with "Create compensation controls". "Include separate unstained control tube/well" was selected and "Generic" mode was left by default;
4. Wells were automatically generated in the plate configuration, one for each fluorochrome used and one for the blank. When scrolling over each well, an indication of what fluorochrome had to be added on each well was shown and the correct sequence was followed when adding the antibodies conjugates;
5. On "Global Worksheet" window, "normal worksheets" was selected. It contained:
    a. Sheet 1, where any plots could be created; all other sheets had predefined plots;

b. “Unstained control” sheet, with a SSC/FSC plot plus 5 histograms, one for each antibody conjugate;
c. A separate sheet per fluorochrome, each displaying 2 plots, SSC/FSC and Count/Fluorochrome;

6. The unstained control sheet was opened when running the setup control;
7. A small volume of the “setup control” was run to define the lymphocyte gate (P1) and to adjust voltages of side and forward scatter. “Apply to all compensation controls” was applied to P1
8. On “Experiment layout”, “Acquisition”, 20 000 events were set to be recorded;
9. One well at the time was run at the lowest speed (0.5 µL/sec);
10. At the end of the experiment, compensation was calculated.

2.9.5.1.1. FACSDiva settings

One worksheet per fluorochrome, each containing the following: Time plot, Size plot, FSC singlets plot, SSC singlets plot, Histogram for cell count vs fluorochrome being excited.

Loader Settings: sample volume, 150 µL; mixing volume, 100 µL; mixing speed, 200 µL/sec; number of mixes, 2; wash volume, 400 µL.

Cytometer configuration: parameters, as defined from application settings; threshold 25000.

Acquisition dashboard: stopping gate, FSC Singlets; storage gate, all events; events to record, 100000; events to display, 5000; flow rate, medium.

2.9.6. Fluorescence minus one (FMO) analysis

This analysis has allowed an accurate positioning of the gates for each population of cells and it was done for both spleen and thymus. For a single sample, eight wells were singly-stained, one per antibody conjugate, another eight wells stained with all antibody conjugates except one. Two extra wells, a negative control with no staining at all and a positive control stained with all antibody conjugates were also included. The preparation of the antibodies for this experiment is illustrated in Table 95 for thymus and Table 96 for spleen, Appendix 2 - Tables and figures. The MFI of each cell population identified during the FMO experiment is presented in Figure 40 to Figure 46 for thymus and Figure 47 to Figure 54 for spleen, Appendix 2 - Tables and figures

2.9.6.1. FACSDiva configuration for FMO analysis

300000 events were acquired in the live gate, the threshold was set to 25000, on standard throughput mode, with a flow rate of 1 µL/Sec, a sample volume of 150 µL, mixing volume of 100 µL, mixing speed set to 200, 2 mixes and a wash volume of 400 µL.

2.9.7. Establishing MFI reference intervals for each cell type in the thymus

The Median Fluorescence Intensity values of thymic lymphocytes from control mice (N= 21) was used to establish reference intervals for the subsequent characterisation of neoplastic cells. A normality test for each variable was carried out using D'Agostino & Pearson Omnibus tests. Where data were normally distributed, reference intervals were created using mean +- 2 x standard deviation, and where data were not normally distributed, using median and interquartile range. The results of MFI, FSC and frequency of each cell type, as well as of the normality test and

measures of central tendency and variation are presented (Table 97 to Table 105, Appendix 2 - Tables and figures).

2.9.8. Establishing MFI reference intervals for each cell type in the spleen

The same analysis carried out for the MFI reference intervals of T-cells in the thymus was done using data from spleens harvested from control mice (N= 18). A normality test for each variable was carried out using D'Agostino & Pearson Omnibus tests. Where data were normally distributed, reference intervals were created using mean +/- 2 x standard deviation, and where data were not normally distributed, using median and interquartile range. The results of MFI, FSC and frequency of each cell type, as well as of the normality test and measures of central tendency and variation are presented (Table 106 to Table 116, Appendix 2 - Tables and figures).

2.9.9. Flow cytometry protocol

2.9.9.1. Reagents

Table 15 shows the reagents used during the preparation of a cell suspension, before being read by the flow cytometer.

Reagent	Preparation
RPMI buffer, for organ preservation after harvesting and during transport to the laboratory	Already prepared from seller
FC buffer	PBS 1X (Sigma); EDTA 5mM; 0.5% FCS (v/v)- stable for 1 month at 8° Celsius
Red blood cell lysis buffer	requires a dilution of 1:10 of "10X eBiosciences solution" in deionized water
Stopping reaction buffer	PBS 1X/EDTA 0.1 M (37.5g in one litre). Required 300 µL per sample
Buffer for organ preservation in the laboratory, before processing	RPMI with 2% FCS (v/v)
Collagenase II (70 µg/ml)	1 mg in 14 ml RPMI/2% FSC frozen into 500 µL aliquots

Table 15: Reagents used in flow cytometry.

2.9.9.2. Preparation on the morning of analysis

1. Antibody cocktail, protected from direct light and kept at 4° Celsius;
2. Read/dead cell exclusion dye (Sytox blue) at a concentration of 1:20000, 230 µl required per well;
3. Enzyme solution (7X)
    a. 2% FCS in RPMI. Aliquots of frozen FCS added to RPMI in the laboratory and not at the Animal House where organs were harvested biosecurity reasons;
    b. 4 ml of (RPMI and 2% of FCS solution) into a 15 ml centrifuge tube; 500 µl of collagenase added;
    c. Mixed on cylinders and brought up to room temperature for optimal enzyme performance;
4. Stopping buffer allowed to achieve room temperature;
5. 50 ml centrifuge tubes, C tubes and 1 ml centrifuge tubes identification;
6. 2.6 ml of RPMI with 2% FCS added to C tubes, kept on wet ice;
7. 1.5 ml centrifuge tubes identified (twice as much the number of organs to process) with 897 µl of FC buffer on each;
8. Preparation of the antibody cocktail;

2.9.9.3. Organ collection

The procedure to harvest the thymus and the spleen was described in 2.7.1.1.2 Necropsy and tissue harvesting. To preserve cell integrity and antigenic expression, samples have to be fresh; 48 hours is generally considered the maximal storage time for retaining adequate viability and antigen expression (McCoy, 2001, McKenna et al., 2009, Mustafa et al., 2008). Samples from neoplastic tissues with high cell turnover, such as some types of lymphoma, may be more prone to disintegration

before 48 hours and should probably be analysed within 24 hours of collection (Reggeti and Bienzle, 2011). During the course of this project, samples were always processed within 24 hours. Given the laborious nature involved, the following routine was established and followed throughout. Samples harvested when the mice were euthanized were preserved on a 1.5ml centrifuge tube with 1 ml of RPMI incubated on ice until being moved to the laboratory where they were transferred into a C-tube with RPMI enriched with foetal calf serum (FCS) at 2%. This was then followed by mechanical and enzymatic digestion, filtration, spinning and resuspension of cells in FC buffer will take place. Cells were then kept in a 1.5 ml centrifuge tube in the fridge overnight. In the following morning cells were brought to room temperature and the protocol resumed and completed on that same day.

2.9.9.4. Organ dissociation

1. Enzymatic and mechanical dissociation: collagenase was vortexed and 400 µl added to each C tube before being attached to GentleMacs and processed for 20 minutes;
2. After successful dissociation and before adding the stop solution to inactivate collagenase and stop the enzymatic digestion, a sample of 100 µL from each cell suspension was collected into 1.5 ml centrifuge tubes for future DNA extraction of lymphoma cells. Samples were centrifuged (290 G, 5 minutes, 4° degrees Celsius), the supernatant was discharged and the tubes stored at -80° Celsius.
3. 300 µL of Stopping buffer were added to the C tube containing the cell suspension. The stopping buffer blocks enzymatic digestion and dissociate T-cell-dendritic cell interactions;

4. Cell suspension was filtered using 70 µm filters to eliminate fibrous tissue and aggregates of cells and span for 5 minutes at 4° Celsius, 290 g;
5. The supernatant was discharged, a volume cell suspension of about 150 µl was left in the bottom and about 850 µl of FC buffer were added to achieve a final volume of 1 ml, re-suspended, transferred into a 1.5 ml centrifuge tube and kept in the fridge overnight.

2.9.9.5. Cell counting

The following morning, the cell suspension was brought to room temperature and mixed. A Moxi Z Mini Automated Cell Counter was used to assess the cell concentration in each cell suspension using 75 µl of a 1:300 dilution, and the volume required to contain 4 million cells for the analysis was calculated. Whenever an automatic count was not provided, manual gates were created (3-26 µm, 3-18 µm, and 3-10 µm) and the lowest cell count was used to calculate the volume required to run in the flow cytometer. According to in house experience, a suspension containing 4 million cells would be enough to acquire 300 000 cells.

2.9.9.6. Red blood cell lysis, blocking and staining

After adding the cell suspension containing approximately 4 million cells into a dedicated well on a 96 V bottom plate, adding FC buffer, spinning and eliminating the supernatant, 100 µL of lysis buffer were added since the cells of interest were lymphocytes. After 1 minute of incubation, followed by washing with FC buffer, spinning, discarding the supernatant and repeating until the pellet was no longer red, cells were incubated with 100 µL of 1:100 FC blocker (CD16), on ice, for 15 minutes. In the meantime, the antibody cocktail tubes were vortexed and centrifuged at 20 000G, for 8 minutes at 4° Celsius. After washing out the lysis buffer, 100 µL of the

antibody cocktail were added, followed by incubation period at 4° C, protected from light for 20 minutes. The antibody cocktail was then washed out and the pellet re-suspended in 230 µL of read buffer Sytox blue.

2.9.9.7. Sample analysis

A cleaning plate was run each morning, followed by Cytometer Setup and Tracking (CS&T). Compensation was linked to the new analysis, depending on the tissue under analysis (thymus or spleen), and application settings were applied.

Loader Settings: sample volume, 150 µL; mixing volume, 100 µL; mixing speed, 200 µL/sec; number of mixes, 2; wash volume, 200 µL.

Cytometer configuration: parameters, according to what was set by application settings; threshold, starts at 5000 by default and usually was set at 25000, but tested for each plate.

Acquisition dashboard: stopping gate, live; storage gate, all events; events to record, 300000; events to display, 5000; flow rate, medium.

2.9.9.7.1. FC of thymus

The thymus was the organ of choice to phenotype lymphoma in treated mice, given precursor T-cell lymphoblastic lymphomas, also frequently designated by thymic lymphomas, are the most common ENU-induced lymphomas. Cell surface markers such as CD3, CD4, CD8, CD25, CD44 and CD117 were used to determine the subset of malignant T-cells present in thymic lymphomas. Sytox blue, a live/dead marker was used to identify dead cells and remove them from the analysis. The first step in the gating hierarchy was to look at the stability of the flow of cells in time. Cells selected to the next step were collected from a period of stable flow. Subsequently,

live leucocytes were separated from dead leucocytes using CD45, a pan-leucocyte marker and Sytox blue (Figure 5), a dye that links to DNA, which would happen if cell membrane were ruptured and therefore the cell viability was compromised.

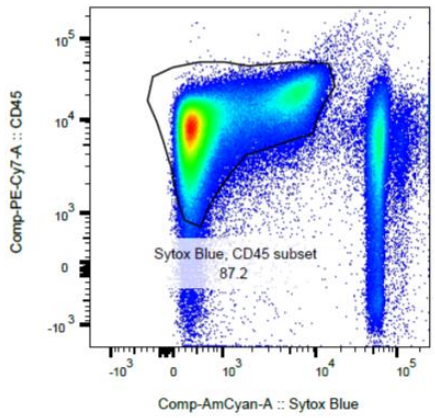


Figure 5: Gate with live leucocytes, CD45+, Sytox blue -, comprising 87.2% of all cells analysed on this sample.

The next step was to use only non-aggregated cells in order to count individual cells as one event. To achieve this, two singlet gates were created, FSC-H versus FSC-A, followed by SSC-H versus SSC-W, as shown in Figure 6.

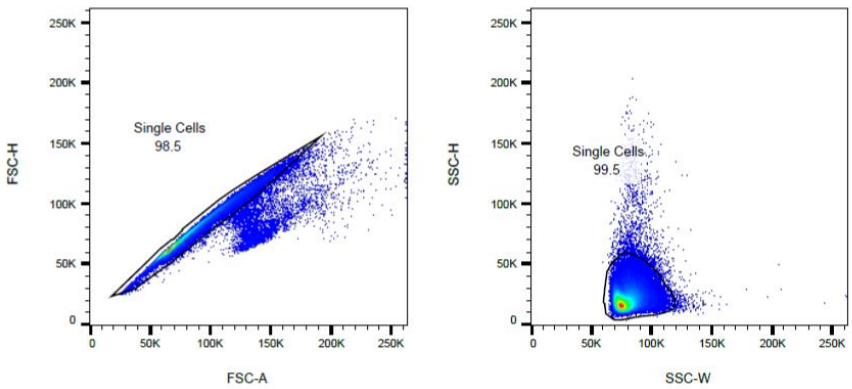


Figure 6: Gating of single cells by forward scatter on the left and side scatter on the right.

Among CD45+ thymic lymphocytes, there were four main groups which had to be identified next, depending on their expression of surface antigens CD8 and CD4:

double negative (CD8-CD4-), double positive (CD8+CD4+), single positive CD8 (CD8+

CD4-) and single positive CD4 (CD8-CD4+) and that was achieved gating CD8 against CD4 and measuring the fluorescence captured at APC-Cy7 and FITC detectors as shown in Figure 7.

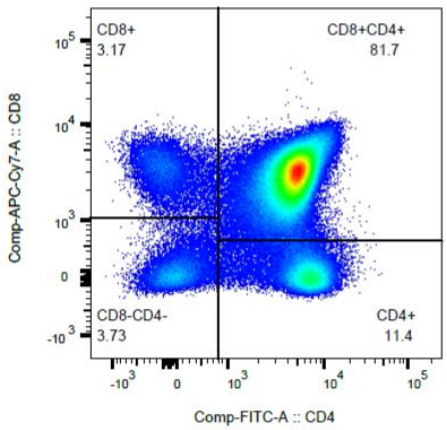


Figure 7: Identification of lymphocytes in a control F2 intercross according to their expression of surface CD4 and CD8 antigens, revealed by the fluorescence captured at APC-Cy7 and FITC channels, respectively.

The first two groups, DN and DP, include all precursor, immature, T-cells. The first group in particular, includes four of the existing five subtypes of precursor T-cells and their identification was assessed by their expression of surface antigens CD25 and CD44, as shown in Figure 8.

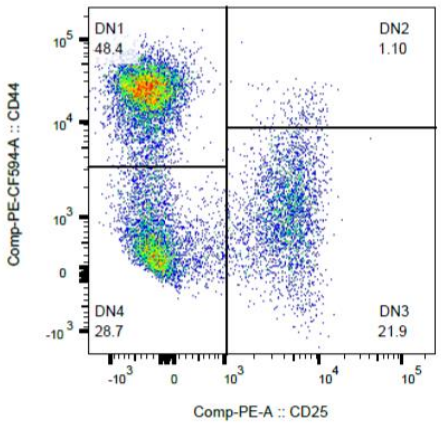


Figure 8: Gating of immature lymphocytes according to their surface expression of surface CD25 and CD44 antigens, revealed by the fluorescence captured at PE and PE-CF594 channels, respectively.

CD3, only present at the surface of mature lymphocytes, being intracellular marker in immature lymphocytes, and CD117 did not prove to be useful - their use would have an effect of increasing the complexity of the analysis without adding relevant information, and although they were used in all samples and data was collected, they were not included in the analysis.

2.9.9.7.2. FC of spleen

The spleen can be involved in cases of precursor T-cell lymphoblastic lymphoma (Morse et al., 2002b). Whenever there was a suspicion that it had been colonised by thymic lymphoma cells, based on gross evaluation and absolute weight at necropsy, it was immunophenotyped by FC. To assess if histologically confirmed cases of thymic lymphoma metastases in the spleen were correlated with the subset of neoplastic cells originally found in the thymus, a similar approach in gating T-lymphocytes used for thymus phenotyping was used for the spleen.

Similar to what was done for thymus analysis, the gating strategy started by looking at the stability of the flow of cells in time. Cells selected from a period of stable flow were subsequently challenged by CD45 against Sytox blue, as seen in Figure 9.

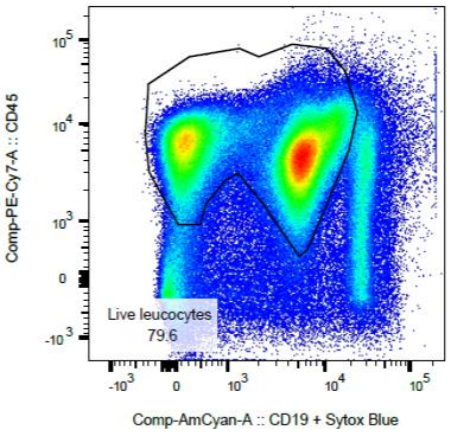


Figure 9: Gate with live leucocytes, CD45+, Sytox blue-, comprising 79.6% of all cells analysed on this sample.

Because there is a wider diversity of cell types in the spleen then in the thymus, an additional gate was created to isolate lymphocytes from other leucocytes by forward and side scatter profile, as seen in Figure 10.

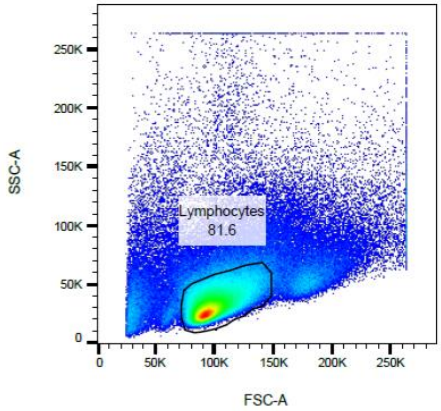


Figure 10: Isolation lymphocytes from other leucocytes present in the spleen.

The next step was to identify and positively select lymphocytes that were not aggregated to other lymphocytes, which was done using side scatter and forward scatter gates as shown in Figure 11.

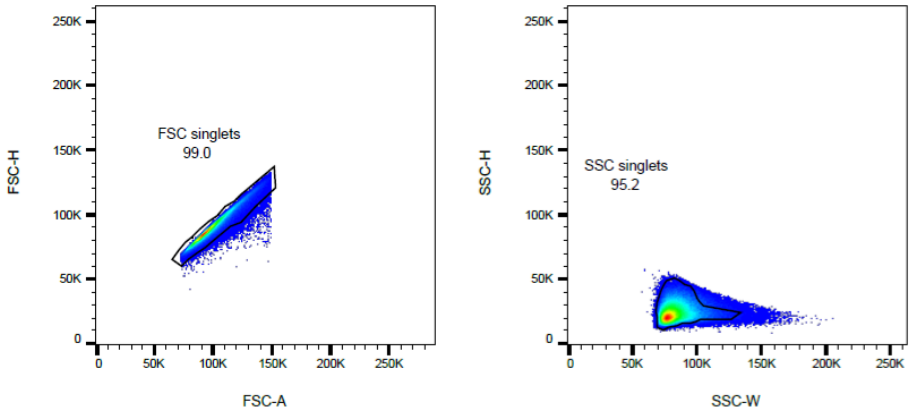


Figure 11: Isolation of single cells by forward scatter on the left and side scatter on the right.

Since the main cells of interest were T-lymphocytes, cell surface marker CD19, a B-cell marker was used against SSC to identify B-cells and separate them from T-cells as shown in Figure 12. CD19 was also used to identify possible B-cell neoplasms affecting the spleen, since the relative proportion of T-cells/B-cells would be affected. Then, CD4 and CD8 were used to differentiate the main types of T-lymphocytes (Figure 13).

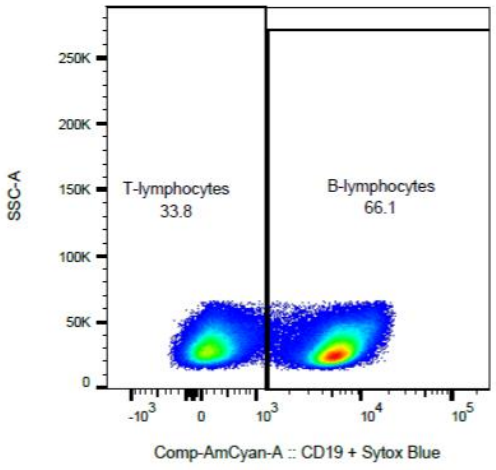


Figure 12: Identification of T and B-lymphocytes.

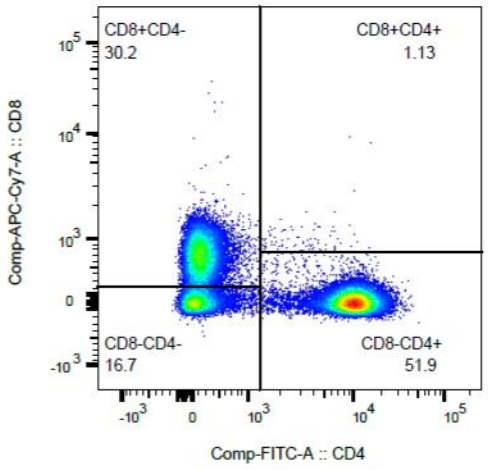


Figure 13: Splenic T-lymphocytes according to their expression of surface markers CD4 and CD8.

Finally, data from CD25PE and CD44PE-CF594, initially thought to be used to determine the subset of double negative malignant T-cells in the presence of a DN tumour metastasis, were not included in the analysis since their expression, and therefore meaning, in the spleen and the thymus are different, as further explained in 4.4.2, page 215. Likewise, although CD3 and CD117 were used in the antibody cocktail, their value, while considerably increasing the complexity of the analysis, did not prove to be relevant and therefore were not included in the analysis.

2.10. DNA extraction

DNA was extracted from tail tips stored at -20 ° C using DNeasy Blood & Tissue Kit. The procedure was performed according to the manufacturer's instructions (Qiagen, 2015). After extraction, DNA concentration and purity were measured using NanoDrop 8000. The volume required to achieve 350 ng of DNA was calculated, samples were prepared and the dried down at 45 °C in an incubator before being sent at room temperature for mapping. DNA concentrations obtained from each tail tip can be seen in section 3.5.1, Table 90 and Table 91.

2.11. Genotyping

DNA extracted from tail tips was used for genotyping using a Single Nucleotide Polymorphism (SNP) array, Illumina GigaMUGA third-generation mouse genotyping array with a density of 150K markers.

Informative SNPs, in each chromosome of parental strains C57BL/6 and A/J were identified and used to create a panel with informative SNPs with a distance between each SNP of approximately 10 million base pairs (Mbp). Each panel, one for each chromosome, was then used to look at the selected SNPs at exactly the same location across the genotype of the experimental population, and only those were used for the initial linkage analysis.

Gender	Treatment	Lymphoma -	Lymphoma +	Total
Female (n= 91)	(100+100+80) mg/kg	6	10	16
	(100+90+80) mg/kg	30	38	68
	(100+90) mg/kg	0	7	7
Male (n= 101)	(100+100+80) mg/kg	5	4	9
	(100+90+80) mg/kg	58	23	81
	(100+90) mg/kg	11	0	11
Total		110	82	192

Table 16: Overview of DNA mapped by gender, treatment group and histology diagnosis of the thymus

As seen in Table 16, a similar number of males (n=101) and females (n= 91), as well as a similar number of and lymphoma negative (n= 110) and lymphoma positive (n= 82) were studied. Furthermore, a total of 37 thymi of lymphoma positive mice included in the mapping analysis were also immunophenotyped by flow cytometry.

2.12. Quantitative Trait Loci (QTL) analysis

For each chromosome, informative Single Nucleotide Polymorphisms (SNPs), which allowed to differentiate between C57BL/6 and A/J regions, were selected at a distance of approximately 10 million base pairs from each other. A map with informative SNPs

was created for all 19 autosomal chromosomes and for X chromosome. Genotyping data obtained from chromosome Y was incomplete and therefore not used for the QTL analysis.

For each chromosome, genotyping results, obtained from GigaMUGA third-generation mouse genotyping array, were narrowed down so that only information relative to the genotype at each informative SNPs was kept. The genotyping data was generated in base pair (bp) and for the QTL analysis had to be converted to centimorgan (cM) - approximately 2000 kb (2000000 bp) per centimorgan (Lee M. Silver, 1995).

Data relative to 20 chromosomes, 304 markers positioned at approximately 10 mega base pairs (Mbp), or 5 cM, from each other across the whole genome, genotyping data from 192 mice in approximately all 304 markers, and absolute thymus weight were organised in five separate files. The files consisted of: (1) labels attributed to each chromosome and indication of the number of markers used to map them, (2) labels attributed to each marker, (3) position, in cM, of each marker, (4) genotype of each animal on each marker and, (5) phenotype information, indicating absolute thymus weight of each mouse at culling. Thymus weight at culling was the quantitative trait selected for the QTL analysis. According to the results (section 3.3.2.2.1, page 133) obtained here, this trait was strongly associated with the presence of thymic lymphoma and not associated with ENU.

The QTL analysis was done on WINQTL 2.5 (Wang S. et al., 2012). The first analysis performed on the dataset was an Interval Mapping (IM), followed by a Composite Interval Mapping (CIM). The threshold at which significance was established for each

analysis was defined by a permutation test, with a walk speed of 1cM, 1000 permutation times, at a 0.05 significance level. For the CIM, a standard model was selected. As for background controls, the analysis was done with the default 5 control marker numbers, a window size of 10 cM and a forward regression, as regression method. To extract the information of identified QTLs for both IM and CIM, the software was set to locate QTLs automatically, with a minimum distance of 5cM between them and a 1 LOD support interval.

The possible identification of a QTL will lead to the investigation of candidate genes located in the region between the markers positioned immediately before and after the QTL. The Sanger sequencing database, (Wellcome Trust Sanger Institute, 2011), based on Keane et al. (2011) and Yalcin et al. (2011), will be used for that purpose. This is a database of several inbred strains and lists the variants between these strains and the reference strains (C57BL/6) allowing to investigate particular genes or regions and get a list of the sequence variants that exist. Candidate genes would be genes already described in the literature as being associated with cancer in general and T-cell lymphomas in particular. The search will focus on SNPs that affect protein sequence. The implications on amino acid substitution were assessed on Yates et al. (2016) and their impact on protein function predicted according to Sim et al. (2012).

3. Results

3.1. ENU Protocol

3.1.1. Introduction

Although the ENU protocol planned for this study was designed based on evidence, it proved to be inadequate for the animal model used as it caused severe body weight loss. In this section, the toxic effects of the original protocol and the improvements following the implementation of a set of measures are shown.

3.1.2. Background data

According to unpublished data from the MLC, when treating A/J mice and F1 from outcross with C57BL/6 with ENU at a conventional dosage, only one mouse had to be culled due to reaching the weight loss limit of 20% imposed by the Project License (Table 17).

Batch	Date	Strain	Dose	N	Comments
ENU 187	Jul-09	AJM	3 x 100 mg/kg	10	1 culled 20% weight loss
ENU 191	Aug-09	AJ-B6MF1	3 x 100 mg/kg	10	
ENU 199	Sep-09	AJ-B6MF1	3 x 100 mg/kg	10	
ENU 210	Nov-09	AJ-B6MF1	3 x 100 mg/kg	5	
ENU 223	May-10	AJM	3 x 100mg/kg	14	

Table 17: Body weight loss associated after ENU treatment in A/J and AJB6M F1.

The figures for the administration of ENU to C57BL/6J mice alone are very similar, with low levels of morbidity and mortality associated to treatment even at slightly higher dosages (100+100+120 mg/kg). Both inbred strains and F1 tolerated well ENU at 3 x 100 mg/kg given intraperitoneally between weeks 10 - 16 of age.

To further investigate why the F2 population had a higher body weight loss than expected, necropsies were performed and blood was collected for haematology and clinical chemistry analysis.

3.1.3. Haematology

The peripheral blood cell analysis (Table 18) was performed with ADVIA Haematology Analyzer and clinical chemistry with a Beckam Coulter AU680.

Variable	F2 culled (Mean±SD)	Control (Mean±SD)[1]
White blood cells (x10E03 cells/µL)	0.9±0.4	2.48±1.34
Red blood cells (x10E06 cells/µL)	8.64± 1.99	9.95±0.65
Haemoglobin (g/dL)	12.24±3.84	14.36±1.03
Haematocrit(L/L)	0.45±0.1	0.47±0.03
Lymphocyte count (x10E03 cells/µL)	0.47±0.29	1.83±1.22

Table 18: Altered haematology parameters after ENU administration (100 mg/kg at 10 and 12 weeks of age), N=24.
[1] Control data displayed was obtained at the end of the experiment from animals with about 1 year of age.

Results showed a decrease in white blood cells, particularly in lymphocytes, and red blood cells with implication on haemoglobin and haematocrit.

3.1.4. Clinical chemistry

A basic panel of clinical chemistry variables was used to assess liver function and integrity, kidney function, pancreatic endocrine function, and muscle tissue integrity. The results are presented in Table 19.

Variable	Mean	SD	Reference intervals[1]
Urea	5.46	0.92	8.4-13.3
Creatinine	10.93	1.62	6.7 -11.3
ALT	35.85	30.09	27 -60
AST	60.92	20.64	36 - 66
Total Protein	46.43	1.09	46.0 -53.1
Albumin	22.22	2.40	21.9 -27.3
Glucose	11.60	1.45	10.88 -16.85
CK	267.00	197.79	28 -400

Table 19: Generic assessment of clinical chemistry variables in decedent mice (N=14).
[1] Reference intervals presented here are from adult C57BL/6 mice.

A word of caution has to be said when interpreting the results - clinical chemistry reference intervals used here are those described on the literature for adult C57BL/6 mice (Jacoby et al., 2002a) since no specific reference intervals for C57BL/6 x A/J intercross were published.

3.1.5. Necropsy

At necropsy there were no outstanding findings.

3.1.6. Histology

At the histological examination, a decreased cellularity in the bone marrow and lymph nodes was seen (Table 20).

Tissues examined	Findings
Lungs, larynx, trachea, thyroid, parathyroid, salivary glands (submandibular, sublingual, parotid), heart, tongue, liver, pancreas, spleen, duodenum, oesophagus, colon, rectum, stomach, jejunum, uterus, skeletal muscle, skin, eyes, brain (4 sections), pituitary, peripheral nerve (sciatic), nasal cavity (three sections), ovaries and oviducts	No abnormalities found.
Kidneys	Focal minimal corticomedullary mineralization, minimal inflammatory cell infiltrate renal pelvis, which can all be seen as a background changes.
Adrenals	Slight vacuolation of X-zone, which can be seen as a background change in mice.
Mesenteric lymph node	Decreased cellularity.
Bone/bone marrow (sternum and tibiofemoral joint)	Decreased cellularity.

Table 20: Summary of microscopic findings identified in decedent F2 mice.

3.1.7. Animals culled of welfare grounds per cohort

A set of measures implemented (section 4.1.4, page 201) in cohort 1 resulted in a descrease in morbidity and mortality seen at the third injection, from 38% to 11% (Figure 14).

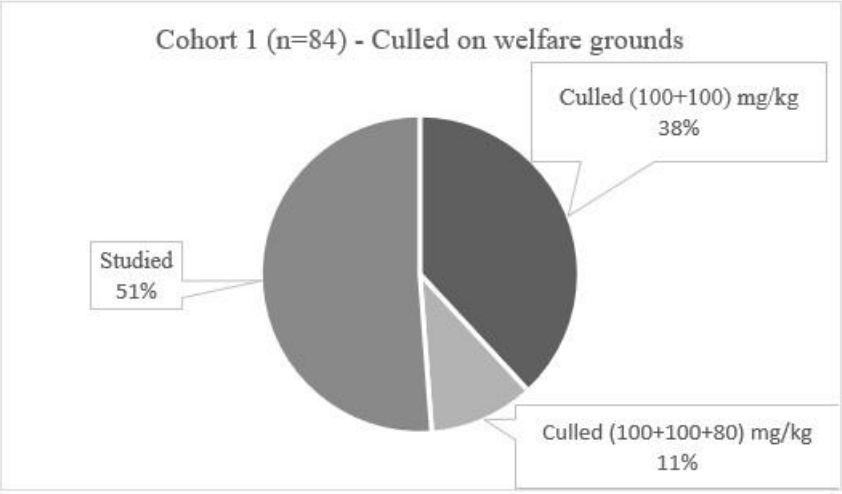


Figure 14: Cohort 1, percentage of mice culled on welfare grounds after 2nd (100+100 mg/kg)

Figure 15 shows the percentage of mice euthanized for welfare reasons after each treatment.

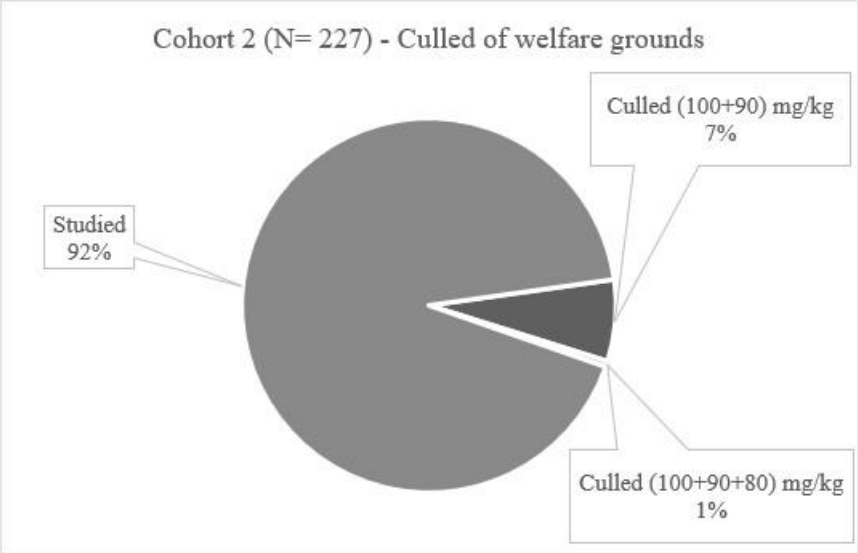


Figure 15: Cohort 2, percentage of mice culled on welfare grounds.

Figure 16 shows the percentage of mice euthanized for welfare reasons after each treatment.

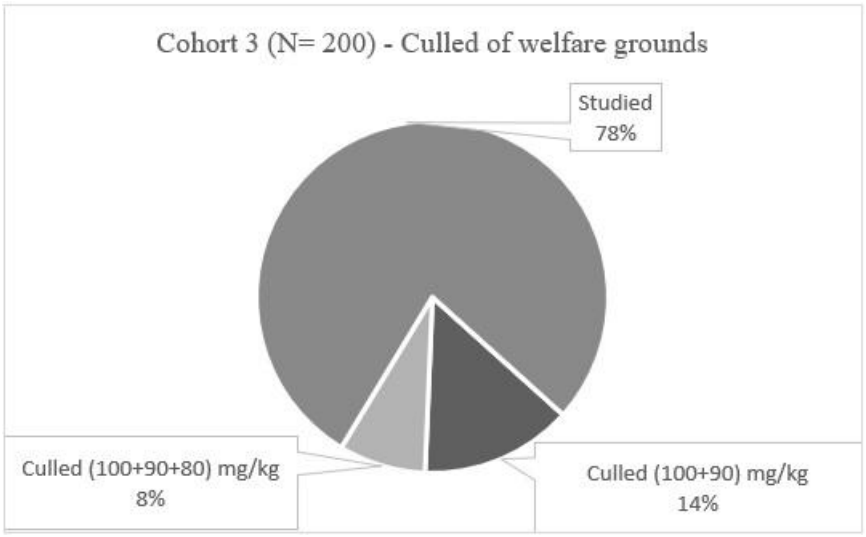


Figure 16: Cohort 3, percentage of mice culled on welfare grounds

3.1.8. Overview of treatment protocol per cohort

In summary, due to unexpected ENU related toxicity in F2 intercross, treatment was not homogeneous across the three cohorts. The major differences affecting the smallest cohort (cohort 1) were: age at commencement, ENU dosages and time between treatments, as summarised in Table 21. Furthermore, twenty animals from each cohort, ten males and 10 females, were randomly selected to act as non-treated controls.

Cohort	**Number of animals**	**ENU Protocol**		
		1st treatment Age (weeks), dose	**2nd treatment Age (weeks), dose**	**3rd treatment Age (weeks), dose**
1	43	12 weeks, 100 mg/kg	13 weeks, 100 mg/kg	15 weeks, 80 mg/kg
2	211	14 weeks, 100 mg/kg	16 weeks, 90 mg/kg	18 weeks, 80 mg/kg
3	154	14 weeks, 100 mg/kg	16 weeks, 90 mg/kg	18 weeks, 80 mg/kg

Table 21: Overview of differences in treatment across groups.

3.2. Pathology

3.2.1. Introduction

Necropsy was performed in all mice and the main gross findings comparing lymphoma negative and lymphoma positive mice are briefly presented here. Haematoxylin and eosin (H&E) sections of thymi were evaluated, as this is the gold standard method of diagnosing thymic lymphoma. Diagnostic criteria and the incidence of thymic lymphoma are presented. Other findings, such as metastasis of the primary thymic tumour invading the spleen and extramedullary haematopoiesis are also shown, as the spleens were also histologically evaluated.

3.2.2. Thymic lymphoma diagnosis and incidence

Lymphoblastic lymphomas are characterized by homogeneous sheets of variably (usually medium) sized but uniform non-cohesive cells with scant cytoplasm, round distinct and often multiple nucleoli, and intermediate to high numbers of mitotic figures (Haley, 2013). These features can be appreciated at microscopic examination of H&E slides, which is the gold standard method of diagnosing thymic lymphoma (Figure 17).

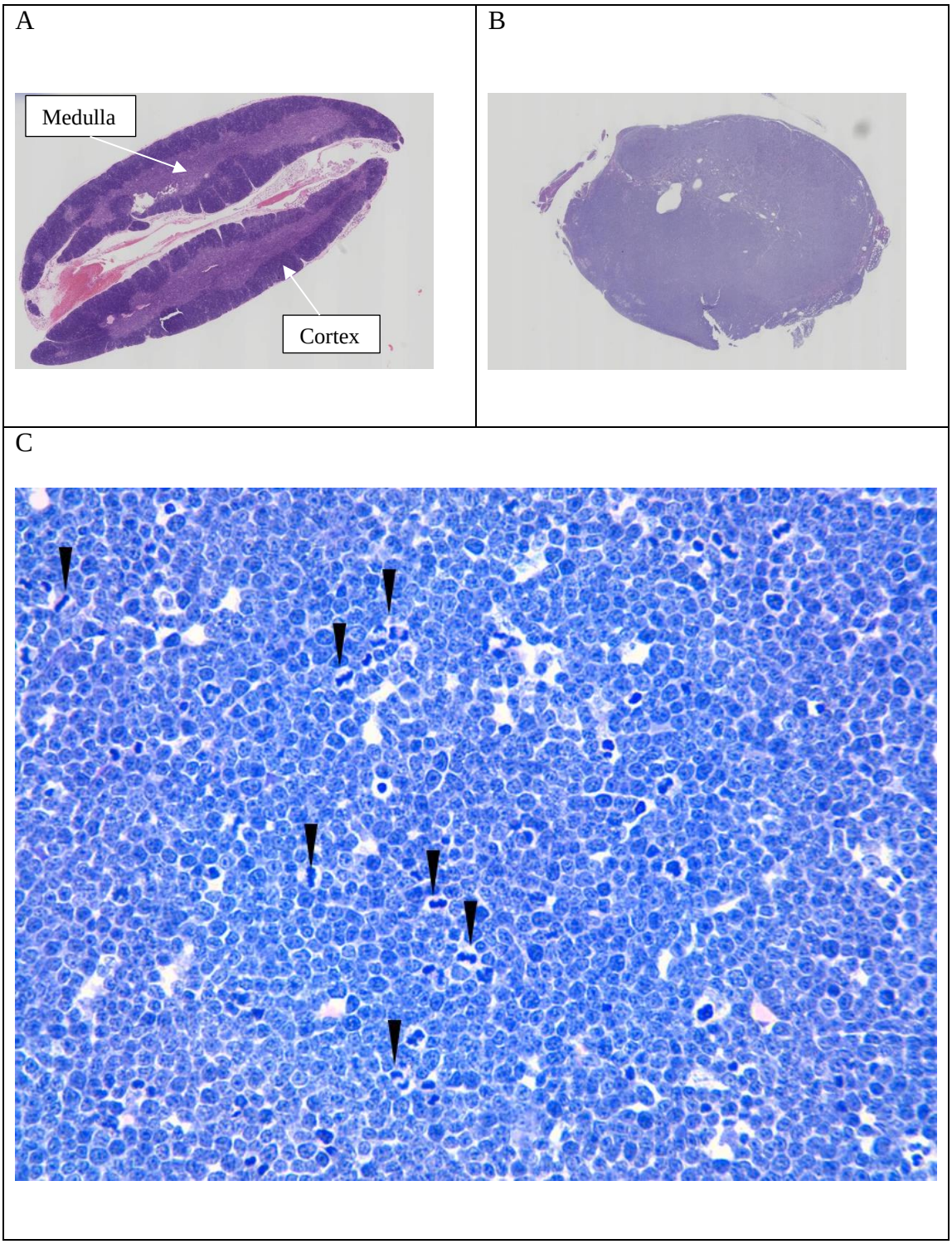


Figure 17: A, low power transverse section normal thymus; B, low power transverse section of thymus with thymic lymphoma, showing loss of normal architecture and invasion by a uniform population of lymphocytes. C, 40X thymic lymphoma, showing a homogeneous sheet of uniform cells with scant cytoplasm, round distinct nucleoli and multiple mitotic figures (arrow heads).

For the purpose of analysing the incidence of lymphoma data, the most numerous group (Group 3) was used. From a total of 178 mice treated at (100+90+80) mg/kg,

110 males and 68 females, 63 (36%) developed thymic lymphoma (Figure 18). There was no significant difference in the incidence of thymic lymphoma between sexes, as assessed by Chi-square test (P= 0.731).

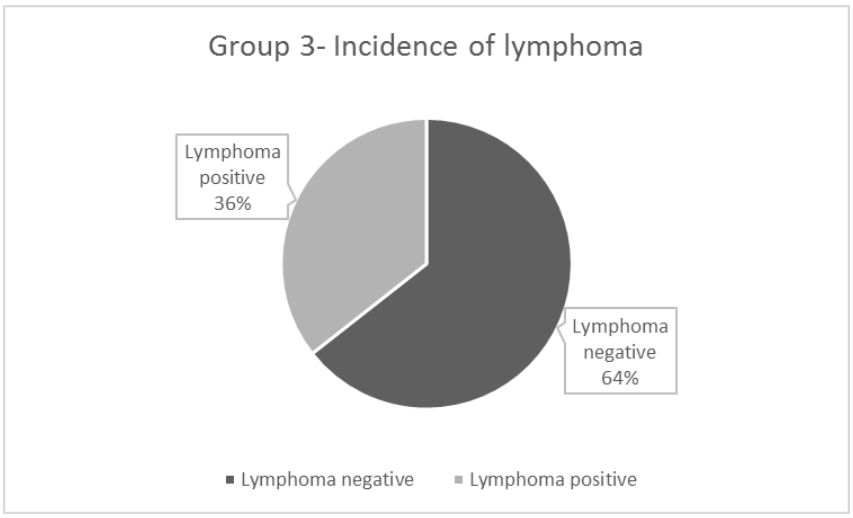


Figure 18: Global incidence of lymphoma in mice treated at (100+90+80) mg/kg.

3.2.3. Spleen metastasis of thymic lymphoma

Results presented here are from treated mice (n= 94, 56 females and 38 males) from groups 2, 3 and 4, with histological confirmation of both the primary tumour on the thymus and presence or absence of metastasis on the spleen (Figure 19).

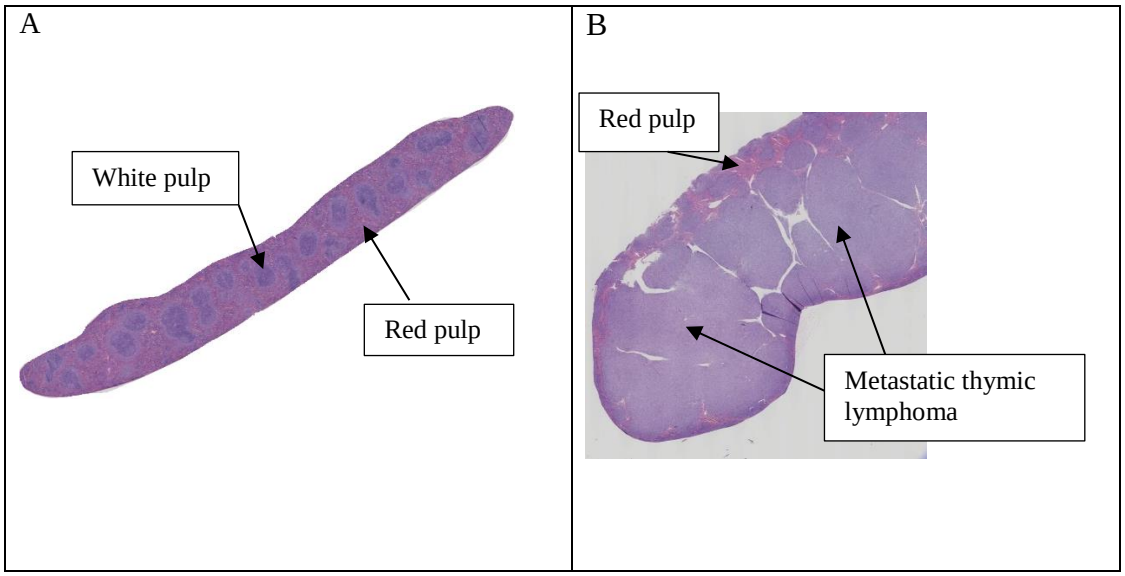


Figure 19: A, Sagittal section of normal spleen with clear demarcation between white pulp and red pulp; B, splenic metastatis of thymic lymphoma with the parenquima colonised by a sheet of neoplastic lymphocytes.

In 46 mice (49%) with thymic lymphoma, the tumour has spread to the spleen (Figure 20). There was no significant difference in the rate of metastization of thymic lymphoma between sexes, as assessed by Chi-square test (P= 0.802).

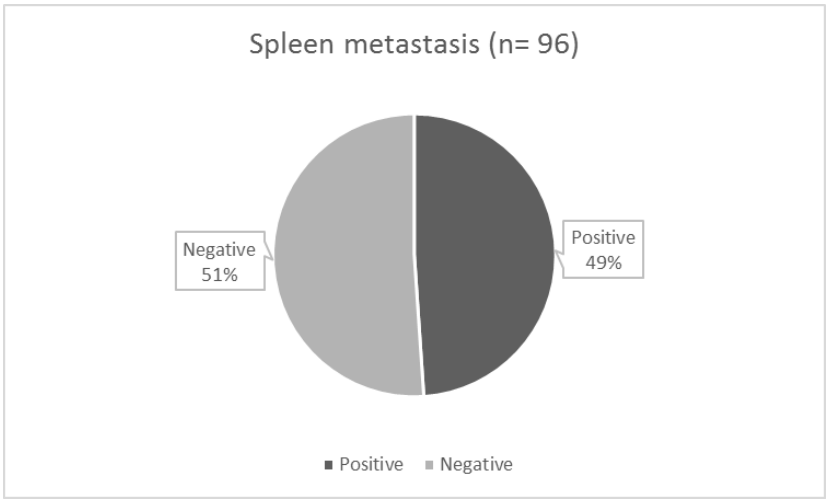


Figure 20: Overall incidence of splenic metastasis of thymic lymphoma.

3.2.4. Extramedullary haematopoiesis

Although assessing the degree of extramedullary haematopoiesis was not the focus of this study, the spleens were prepared for routine microscopic examination to assess for the presence of metastases of thymic lymphoma, and EMH was frequently seen in treated animals (Figure 21).

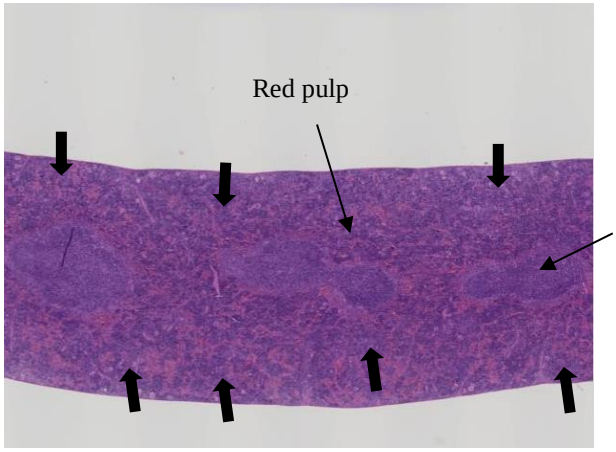


Figure 21: Sagittal section of spleen showing dark foci of increased extramedullary haematopoiesis (thick arrows) scattered throughout the red pulp.

From a total of 238 ENU-treated mice from groups 2, 3 and 4 with a histological evaluation of the spleen, 125 males and 113 females, 60% had an increase in extramedullary haematopoiesis (Figure 22). There was no significant difference between sexes as assessed by Chi-square test (P= 0.195). In the control group (n= 57), only one mouse (1.75%) had increased EMH.

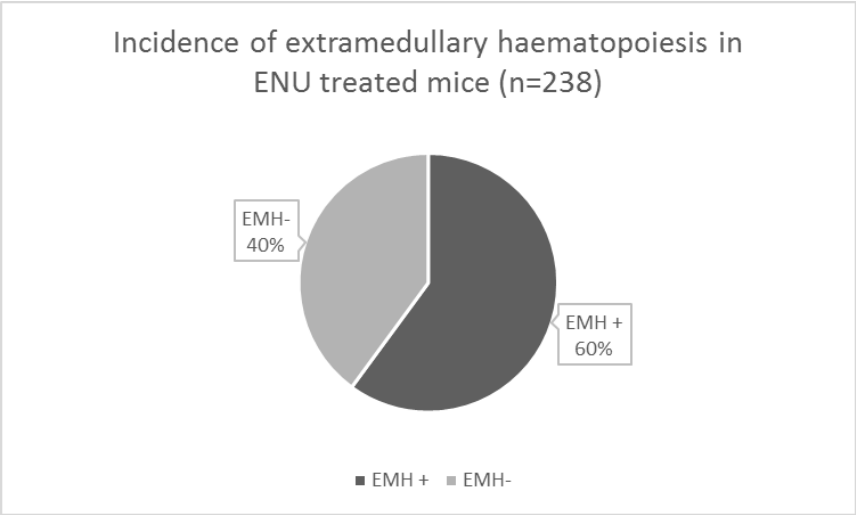


Figure 22: Incidence of EMH in ENU-treated mice.

3.2.5. Necropsy findings

Gross pathology findings at necropsy in ENU-treated mice with a histological evaluation of the thymus (n= 238) were recorded and summarised (Table 22). The most common finding in the thymus and spleen was increased size and these data are presented separately (section 3.3.2.2, page 133).

			Lymphoma negative (n= 144)		Lymphoma positive (n=94)	
			Count	%	Count	%
GI Tract	Stomach	Growth	3	2.08	1	1.06
	Intestines	Growth	14	9.72	3	3.19
		Intussusception	3	2.08	1	1.06
	Anus	Prolapse	1	0.69		
		Blood	21	14.58	9	9.57
Urinary System	Kidneys	Discoloration, Pale			2	2.13
		Cysts	4	2.78		
		Enlarged			5	5.32
Liver	Discoloration	Pale	3	2.08	6	6.38
		Dark-red	1	0.69	1	1.06
		Mottled	1	0.69		
	Other	Enlarged	1	0.69	7	7.45
		Cysts	6	4.17		
		Growth	3	2.08		
Abdominal cavity		Growth	5	3.47		
		Ascitis	2	1.39	1	1.06
Thoracic cavity		Growth			2	2.13
		Adhesions	1	0.69	6	6.38
		Haemothorax	4	2.78	10	10.64
		Chilothorax	1	0.69		
Heart		Enlarged			1	1.06
Hemolymphoreticular	Lymph nodes	Enlarged	16	11.11	18	19.15
	Spleen	discoloration, dark-red areas	2	1.39	2	2.13
		Growth	1	0.69	1	1.06
Lungs		Growth	98	68.06	39	41.49
		Discoloration, Pale	3	2.08	3	3.19
		Lobe, Enlarged	1	0.69		
Female Reproductive	Vagina	Growth	3	2.08	1	1.06
		Blood	1	0.69	1	1.06
		Discharge	1	0.69	1	1.06
	Uterus	Prolapse	2	1.39		
		Growth	2	1.39		
		Enlarged	1	0.69		
	Ovaries	Cystic	1	0.69	3	3.19
		Growth	3	2.08		
Male Reproductive		Preputium, Growth	1	0.69		
		Prostate, Growth	1	0.69	2	2.13
Skin	Subcutaneous	Growth	6	4.17	2	2.13
	Skin	Erosion/ulceration	5	3.47	2	2.13
Head and neck		Growth	5	3.47		

Table 22: Incidence of gross findings at necropsy by lymphoma status.

The most common finding across treated mice were growths of pale colouration with varied diameters (between 2-3 mm on average) affecting the lungs.

Enlargement of lymph nodes was also seen at high frequency in both lymphoma negative (11.1%) and positive (19.15%) mice.

The presence of blood in the perianal region was one of the most common findings at routine clinical examination and one of the most common justifications for euthanasia.

It was seen in 14.58% of lymphoma negative and 9.57% of lymphoma positive mice. Equally more frequent in lymphoma negative mice was the presence of growths with 2-3 mm in diameter in the intestinal tract, 14%, compared with 3% in mice that have developed lymphoma.

3.3. Biometric and Haematology

3.3.1. Introduction

Having an experimental population in which thymic lymphoma was induced also provided an opportunity to study how several variables differ in lymphoma negative and lymphoma positive mice. This was achieved by measuring several biometric and haematology parameters at culling and analyzing them. Absolute body weight and organ weights (spleen and thymus) adjusted to body weight at culling were analysed and designated here as biometric data. The following haematology parameters were also measured and analysed: white blood cells, lymphocytes, neutrophils, eosinophils, basophils, monocytes, large unstained cells, red blood cells, haemoglobin, hematocrit, mean cell volume, mean cell haemoglobin concentration and platelets.

ENU has detrimental effects and allocating animals only to two groups (lymphoma negative and positive) for the statistical analysis would not be adequate since ENU administration was likely to have had an effect on its own. Therefore, "treatment dose", "lymphoma status" and their "interaction" were considered in order to identify the root of the effect detected on the variables studied, in particularly those associated with the presence of thymic lymphoma. "Treatment dose" groups were: group 1 (control), group 2 treated at (100+90) mg/kg, group 3 at (100+90+80) mg/kg and group 4 at (100+100+80) mg/kg. As for "lymphoma status", there were two possible outcomes: lymphoma negative (defined as 0 on tables) or lymphoma positive (defined as 1 on tables). A positive "interaction" on any given variable meant that the effect of "treatment dose" on the variable was influenced by whether a lymphoma had developed or not. For example, a positive interaction found in red blood cell count meant that there was a statistically significant difference between the groups under comparison and that the effect of "treatment dose" on red blood cell count varied

depending on “lymphoma status” - whether the animals were lymphoma positive or negative. The reverse holds true: the impact of “lymphoma status” on the variable depended on “treatment dose” received. Where the interaction was statistically significant, an analysis of the interaction between the three treatment doses (100+90) mg/kg, (100+90+80) mg/kg and (100+100+80) mg/kg and two lymphoma statuses (lymphoma positive and lymphoma negative) was done; and analysis of each main effect (treatment dose and lymphoma status) on their own was not. Where no statistical significance was attained at interaction level, the effect of each main level, “treatment dose” and “lymphoma status” on their own, were assessed, with particular emphasis on “lymphoma status”, since the aim was to compare the phenotypes lymphoma positive and negative.

Each parameter was analysed by sex and, unless otherwise specified, analysis was performed upon the rank-transformed dataset. When reporting the results, data are mean ± standard deviation, unless otherwise stated. The results of each variable by treatment group, lymphoma status and, where the interaction was positive, by lymphoma status within each group are presented. For clarification, “level of group” and “level of status” mentioned on the tables are equivalent with “treatment dose” and “lymphoma status”, respectively.

3.3.2. Results – biometric data

3.3.2.1. Body weight (BW)

Body weight was measured at culling to see if there were differences between lymphoma positive and negative animals and what was associated with it, if thymic lymphoma or ENU.

3.3.2.1.1. Males

For body weight in males, analysis was performed upon the untransformed dataset. The interaction term was not statically significant, suggesting the effect of treatment on body weight at culling between the groups did not vary depending on whether there was a thymic lymphoma or not. On its own, "treatment dose" had a significant impact on body weight: in all treated groups, males weighed less at culling than control males, Table 23. Likewise, "lymphoma status" had a significant impact on body weight, although not as strong as "treatment dose", with lymphoma positive males weighing less (32.62 ± 4.89) than lymphoma negative males (40.18 ± 8.51), (Table 24).

Level of Group	N	BW	
		Mean	Std Dev
1	28	51.39	6.42
2	22	34.68	5.37
3	93	35.48	5.74
4	10	35.87	3.89

Table 23: Body weight by group in males.

Level of Status	N	BW	
		Mean	Std Dev
0	115	40.18	8.51
1	38	32.62	4.89

Table 24: Body weight by lymphoma status in males.

3.3.2.1.2. Females

As with males, body weight analysis in females was performed upon the untransformed dataset, the interaction term was not statically significant and on their own, both "treatment dose" and "lymphoma status" were significant, with the former having a particularly strong impact on reducing body weight gain (Table 25). Lymphoma positive females weighed (27.15 ± 4.16), less than lymphoma negative females (36.07 ± 9.48), (Table 26).

Level of Group	N	BW	
		Mean	Std Dev
1	29	45.99	7.33
2	13	33.75	6.74
3	85	28.71	5.03
4	15	27.31	3.64

Table 25: Body weight by group in females.

Level of Status	N	BW	
		Mean	Std Dev
0	86	36.07	9.48
1	56	27.15	4.16

Table 26: Body weight by lymphoma status in females.

The ANOVA results for body weight in both sexes are presented in Table 27.

Body weight	Source	Result
Males	Interaction	F (2, 146) = 0.62, P= 0.541
	Treatment dose	F (3, 146) = 43.21, P< 0.0001
	Lymphoma status	F (1, 146) = 5.04, P= 0.026
Females	Interaction	F (2, 135) = 0.91, P= 0.404
	Treatment dose	F (3, 135) = 47.75, P< 0.0001
	Lymphoma status	F (1, 135) = 5.94, P= 0.016

Table 27: ANOVA results for body weight.

In summary, in both sexes, ENU and lymphoma were found to be, on their own, associated with decrease in body weight gain.

3.3.2.2. Organ weight adjusted to body weight

3.3.2.2.1. Thymus

3.3.2.2.1.1. Males

For thymus weight in males, the analysis was performed upon the log transformed dataset. Both “interaction” and “treatment dose” were not significant. As expected, there was a strong statistical significant difference in thymus weight at “lymphoma status” level, with log thymus weight in lymphoma positive males (-0.46 ± 0.37 for a body weight of 32.62 ± 4.89) being significantly higher than in lymphoma negative males (-1.72 ± 0.27 for a body weight of 40.18 ± 8.51), (Table 28).

Level of Status	N	logThymus_W		BW	
		Mean	Std Dev	Mean	Std Dev
0	115	-1.72	0.27	40.18	8.51
1	38	-0.46	0.37	32.62	4.89

Table 28: Log-transformed thymus weight adjusted to body weight by lymphoma status in males.

3.3.2.2.1.2. Females

No significant "interaction" was seen between "treatment dose" and "lymphoma status" in females. On its own, "treatment dose" did not account for differences on thymus weight. On the other hand, and similarly to what was seen in males, "lymphoma status" strongly accounted for an increase on thymus weight in lymphoma positive (231.7 ± 51.91 for a body weight of 27.15 ± 4.16) when compared with lymphoma negative females (107.39 ± 58.48 for a body weight of 36.07 ± 9.48), (Table 29).

Level of Status	N	RANK_Thymus_W		BW	
		Mean	Std Dev	Mean	Std Dev
0	86	107.39	58.48	36.07	9.48
1	56	231.70	51.91	27.15	4.16

Table 29: Rank-transformed thymus weight adjusted to body weight by lymphoma status in females.

Results for the analysis of adjusted thymus weight in both sexes are presented in Table 30.

Thymus weight	Source	Result
Males	Interaction	F (2, 145) = 0.32, P= 0.723
	Treatment dose	F (3, 145) = 1.54, P= 0.208
	Lymphoma status	F (1, 145) = 241.41, P< 0.0001
Females	Interaction	F (2, 134) = 0.46, P= 0.631
	Treatment dose	F (3, 134) = 1.42, P= 0.241
	Lymphoma status	F (1, 134) = 50.91, P< 0.0001

Table 30: ANOVA results for adjusted thymus weight.

In summary and as expected, judging by the enlarged thymi seen at necropsy, the thymi of lymphoma positive mice weighed significantly more than the thymi of mice

without thymic lymphoma, in both sexes. ENU was not directly associated with this difference.

3.3.2.2.2. Spleen

Being an important organ of the lymphoreticular system, as thymus is, and a common site where thymic lymphomas metastasize, the spleen weight was also recorded at culling.

3.3.2.2.2.1. Males

In males, the difference in spleen weight at culling between lymphoma positive and negative mice was associated with "treatment dose", with an increased spleen weight being observed across all treated groups when compared with control (Table 31). Both the "interaction" term and "lymphoma status" were not associated with spleen weight changes.

Level of Group	N	RANK_Spleen_W		BW	
		Mean	Std Dev	Mean	Std Dev
1	28	49.68	26.56	51.39	6.42
2	22	157.34	78.56	34.68	5.37
3	93	168.21	73.07	35.48	5.74
4	10	144.15	88.83	35.87	3.89

Table 31: Rank-transformed spleen weight adjusted to body weight by group in males.

3.3.2.2.2.2. Females

In females, the analysis was done upon log transformed dataset. As with males, the effect of "treatment dose" was statistically significant and an increase in spleen weight was seen across all treated groups when compared with control (Table 32). Both the "interaction" and "lymphoma status" were not significant.

Level of Group	N	Log_Spleen_W		BW	
		Mean	Std Dev	Mean	Std Dev
1	29	-0.85	0.30	45.99	7.33
2	13	-0.31	0.43	33.75	6.74
3	85	-0.44	0.33	28.71	5.03
4	14	-0.41	0.37	27.32	3.78

Table 32: Log-transformed spleen weight adjusted to body weight by group in females.

Results for the analysis of adjusted spleen weight in both sexes are presented in Table 33.

Spleen weight	Source	Result
Males	Interaction	F (2, 145) = 1.6, P= 0.206
	Treatment dose	F (3, 145) = 7.30, P< 0.0001
	Lymphoma status	F (1, 145) = 0.22, P= 0.642
Females	Interaction	F (2, 133) = 0.93, P= 0.396
	Treatment dose	F (3, 133) = 3.24, P= 0.024
	Lymphoma status	F (1, 133) = 3.19, P= 0.076

Table 33: ANOVA results for adjusted spleen weight.

In summary, in both sexes, despite a splenic metastization rate of nearly 50% (n=96) found amongst the lymphoma positive mice in this study, the presence of lymphoma was not associated with the significant increase in spleen weights - ENU was.

3.3.3. Results - haematology data

Although this study was done on a model of lymphoma and not a model of leukaemia, lymphomas can and do become leukaemic, invading the blood stream and eventually colonizing organs. Blood parameters were measured to investigate differences between lymphoma positive and negative in the experimental population.

3.3.3.1. White Blood Cell count Baso (WBCB)

3.3.3.1.1. Males

The interaction between “treatment dose” and “lymphoma status” was not significant, as it was not “treatment dose”. A statistical significant difference at “lymphoma status” level was attained - white blood cell mean in lymphoma positive males

(184.7 ± 74.8) was significantly higher than in lymphoma negative males (120.29 ± 60.73), (Table 34).

Level of Status	N	RANK_WBCB	
		Mean	Std Dev
0	72	93.12	59.40
1	48	163.40	85.71

Table 34: Rank-transformed white blood cell count by lymphoma status in males.

3.3.3.1.2. Females

There were no statistically significant differences in white blood cells at the interaction level and the main effect "treatment dose" was not statistically significant. A statistical significant difference at "lymphoma status" level was attained - white blood cell mean in lymphoma positive females (163.4 ± 85.71) was significantly higher than in lymphoma negative females (93.12 ± 59.4), (Table 35).

Level of Status	N	RANK_WBCB	
		Mean	Std Dev
0	72	93.12	59.40
1	48	163.40	85.71

Table 35: Rank-transformed white blood cell count by lymphoma status in females.

The ANOVA results for the analysis of WBC in both sexes are presented in Table 36.

WBC	Source	Result
Males	Interaction	F (2, 130) = 1.74, P= 0.179
	Treatment dose	F (3, 130) = 1.93, P= 0.128
	Lymphoma status	F (1, 130) = 5.63, P= 0.019
Females	Interaction	*F* (2, 113) = 0.46, *P* = 0.632
	Treatment dose	F (3, 113) = 1.06, P= 0.369
	Lymphoma status	F (1, 113) = 6.42, P= 0.013

Table 36: ANOVA results for WBC count.

In summary, there was a statistically significant increase in WBC in lymphoma positive mice, in both sexes, that was associated with the presence of thymic lymphoma.

3.3.3.2. Absolute neutrophil count

3.3.3.2.1. Males

The interaction between "treatment dose" and "lymphoma status" was not significant, as it was not the main effect "lymphoma status". At "treatment dose" level, a significant increase on neutrophils count was seen in treated mice (Table 37).

Level of Group	N	RANK_Neutro	
		Mean	Std Dev
1	28	92.05	53.34
2	17	181.76	67.03
3	82	136.85	67.60
4	10	111.80	73.36

Table 37: Rank-transformed absolute neutrophil count by group in males.

3.3.3.2.2. Females

There was no interaction between "treatment dose" and "lymphoma status" on neutrophil count in females. The main effect "treatment dose" did not attain statistically significance. The main effect "lymphoma status" was statistically significant: lymphoma positive (161.56 ± 79.67) had an increased neutrophil count when compared with lymphoma negative (102.65 ± 70.64) females (Table 38).

Level of Status	N	RANK_Neutro	
		Mean	Std Dev
0	72	102.65	70.64
1	48	161.56	79.67

Table 38: Rank-transformed absolute neutrophil count by lymphoma status in females.

The ANOVA results for the analysis of neutrophil count in both sexes are presented in Table 39.

Neutrophils	Source	Result
Males	Interaction	F (2, 130) = 0.98, P= 0.379
	Treatment dose	F (3, 130) = 5.15, P= 0.002
	Lymphoma status	F (1, 130) = 3.84, P= 0.052
Females	Interaction	F (2, 113) = 0.53, P= 0.589
	Treatment dose	F (3.113) = 2.10, P= 0.104
	Lymphoma status	F (1, 133) = 5.27, P= 0.023

Table 39: ANOVA results for neutrophil count.

Overall, there was a difference in how the neutrophil count varied in lymphoma positive mice between males and females. In males, the increase in neutrophils seen in lymphoma positive mice was associated with ENU treatment, whereas in females it was associated with lymphoma.

3.3.3.3. Absolute lymphocyte count

3.3.3.3.1. Males

The effect of "treatment dose" on absolute lymphocyte count in males did not vary depending whether a lymphoma has developed or not - the interaction was not statistically significant. When looking at each main effect, "treatment dose" effect on absolute lymphocyte count was not significant, whereas "lymphoma status" was associated with an increase in lymphocyte count: lymphoma positive (184.38 ± 72.64) had a significant increase on lymphocyte count when compared with and lymphoma negative (122.12 ± 61.9) males, (Table 40).

Level of Status	N	RANK_Lymph	
		Mean	Std Dev
0	104	122.12	61.90
1	33	184.38	72.64

Table 40: Rank-transformed absolute lymphocyte count by lymphoma status in males.

3.3.3.3.2. Females

The findings seen on absolute lymphocyte count in females were similar to those seen in males. There were no significant differences at "interaction" and "treatment dose"

levels, whereas “lymphoma status” was associated with a significant difference between groups. Absolute lymphocyte count in lymphoma positive females (162.33 ± 85.42) was significantly higher than in lymphoma negative females (91.34 ± 58.92), (Table 41).

Level of Status	N	RANK_Lymph	
		Mean	Std Dev
0	72	91.34	58.92
1	48	162.33	85.42

Table 41: Rank-transformed absolute lymphocyte count by lymphoma status in females.

The ANOVA results for the analysis of lymphocyte count in both sexes are presented in Table 42.

Lymphocytes	Source	Result
Males	Interaction	F (2, 130) = 1.34, P= 0.264
	Treatment dose	F (3, 130) = 1.54, p=0.208
	Lymphoma status	F (1, 130) = 6.10, P= 0.015
Females	Interaction	F (2,113) = 0.83, P= 0.438
	Treatment dose	F (3, 113) = 0.88, P= 0.455
	Lymphoma status	F (1, 113) = 7.17, P= 0.009

Table 42: ANOVA results for lymphocyte count.

In summary, the statistically significant increase in lymphocyte count in lymphoma positive animals, seen in both sexes, was associated with the presence of thymic lymphoma.

3.3.3.4. Absolute monocyte count

3.3.3.4.1. Males

There was no significant interaction between “treatment dose” and “lymphoma status” on monocyte count in males. Likewise, on its own, “treatment dose” did not have a significant effect on monocyte count. On the other hand, “lymphoma status” was associated with a significant difference in monocyte count: lymphoma positive had an

increased monocyte count (167.92 ± 79.17) when compared with lymphoma negative males (126.18 ± 66.63), (Table 43).

Level of Status	N	RANK_Mono	
		Mean	Std Dev
0	104	126.18	66.63
1	33	167.92	79.17

Table 43: Rank-transformed absolute monocyte count by lymphoma status in males.

3.3.3.4.2. Females

Levene's test on untransformed monocyte data was not significant and therefore the analysis was done on raw data. There were no significant effects of "interaction", "treatment dose", and "lymphoma status", on monocyte absolute count in females.

Table 44 shows the ANOVA results for the analysis of monocyte count in both sexes.

Monocytes	Source	Result
Males	Interaction	F (2, 130) = 0.07, P= 0.9351
	Treatment dose	F (3, 130) = 2.6, P=0.055
	Lymphoma status	F (1, 130) = 7.13, P= 0.009
Females	Interaction	F (2, 113) = 0.3, P= 0.744
	Treatment dose	F (3, 113) = 0.21, P= 0.892
	Lymphoma status	F (1, 113) = 2.95, P= 0.089

Table 44: ANOVA results for monocyte count.

Overall, in females, there was no difference in monocyte count regardless of whether the animals had developed lymphoma or not. In males, there was a significant increase in animals with thymic lymphoma.

3.3.3.5. Absolute eosinophil count

3.3.3.5.1. Males

There was no significant interaction between "treatment dose" and "lymphoma status" on eosinophil count in males. The main effect "lymphoma status" was not statistically significant. There was a significant effect at the level of "treatment dose", which

seemed to be particularly evident in group 3 (117.1 ± 80.35) when compared with control males (160.13 ± 53.38), (Table 45).

Level of Group	N	RANK_Eos	
		Mean	Std Dev
1	28	160.13	53.38
2	17	163.94	70.68
3	82	117.10	80.35
4	10	149.55	88.54

Table 45: Rank-transformed absolute eosinophil count by group in males

3.3.3.5.2. Females

Eosinophil count in treated females was not significantly affected. No significant effect was found neither at "interaction" level, nor at "treatment dose" level, nor at "lymphoma status" level.

Table 46 shows the ANOVA results for the analysis of eosinophil count in both sexes.

Eosinophils	Source	Result
Males	Interaction	F (2, 130) = 0.03, P= 0.966
	Treatment dose	F (3, 130) = 3, P= 0.033
	Lymphoma status	F (1, 130) = 3.11, P= 0.08
Females	Interaction	F (2, 113) = 0.31, P= 0.733
	Treatment dose	F (3, 113) = 0.28, P= 0.839
	Lymphoma status	F (1, 113) = 2.89, P= 0.092

Table 46: ANOVA results for eosinophil count.

In summary, eosinophil count did not seem to be particularly affected by ENU nor thymic lymphoma, although in the biggest group, group 3, males had an increase in eosinophil count at culling associated with "treatment dose" when compared with control males.

3.3.3.6. Absolute Large Unstained Cells count

Large unstained cells are identified by some haematology analysers and they are generally thought to represent large lymphocytes or monocytes (Robert L. Hall, 2013).

3.3.3.6.1. Males

There was no statistically significant interaction between "treatment dose" and "lymphoma status" on large unstained cells count, but both main effects attained statistical significance. At "treatment dose" level, data indicates that there was an increase in LUC in treated males (Table 47). At "lymphoma status" level, a significant increase in LUC in lymphoma positive was found (193 ± 66.57) when compared with lymphoma negative males (110.94 ± 59.49), (Table 48).

Level of Group	N	RANK_LUC	
		Mean	Std Dev
1	28	87.18	58.26
2	17	173.29	70.40
3	82	138.06	67.38
4	10	119.90	72.16

Table 47: Rank-transformed absolute LUCs count by group in males.

Level of Status	N	RANK_LUC	
		Mean	Std Dev
0	104	110.94	59.49
1	33	193.00	66.57

Table 48: Rank-transformed absolute LUCs count by lymphoma status in males.

3.3.3.6.2. Females

Large unstained cell count in females was not affected neither by an interaction between "treatment dose" and "lymphoma status", nor "treatment dose" on its own. On the other hand, LUC were significantly increased in lymphoma positive (178.78 ± 72.65) when compared with lymphoma negative females (92.56 ± 60.36), (Table 49).

Level of Status	N	RANK_LUC	
		Mean	Std Dev
0	72	92.56	60.36
1	48	178.78	72.65

Table 49: Rank-transformed absolute LUCs count by lymphoma status in females.

Table 50 shows the ANOVA results for the analysis of LUC count in both sexes.

LUC	Source	Result
Males	Interaction	F (2,130) = 0.91, P= 0.404
	Treatment dose	F (3, 130) = 3.87, P= 0.011
	Lymphoma status	F (1, 130) = 11.91, P< 0.001
Females	Interaction	F (2,113) = 0.3, P= 0.742
	Treatment dose	F (3, 113) = 1.6, P= 0.194
	Lymphoma status	F (1, 113) = 17.52, P< 0.0001

Table 50: ANOVA results for LUC count.

In summary, LUC were elevated in both sexes and the association with the presence of thymic lymphoma was strong.

3.3.3.7. Absolute basophil count

3.3.3.7.1. Males

There was neither a significant effect at "interaction" between "treatment dose" and "lymphoma status" nor at "treatment dose" on its own. On the other hand, the presence of lymphoma was associated with increased basophil count in lymphoma positive (198.8 ± 57.79), when compared with lymphoma negative (104.11 ± 53.81) males (Table 51), as expressed by the significance attained at "lymphoma status" level.

Level of Status	N	RANK_Baso	
		Mean	Std Dev
0	104	104.11	53.81
1	33	198.80	57.79

Table 51: Rank-transformed absolute basophil count by lymphoma status in males.

3.3.3.7.2. Females

As with males, in females, only "lymphoma status" effect was statistically significant, with lymphoma positive basophil count (189.09 ± 62.1) increased in comparison with lymphoma negative count (92.90 ± 55.84), (Table 52). At "interaction" level and "treatment dose" level, no statistically significant differences between lymphoma positive and negative females were found.

Level of Status	N	RANK_Baso	
		Mean	Std Dev
0	72	92.90	55.84
1	48	189.09	62.10

Table 52: Rank-transformed absolute basophil count by lymphoma status in females.

The ANOVA results for the analysis of basophil count in both sexes are presented in Table 53.

Basophils	Source	Result
Males	Interaction	F (2, 130) = 0.29, P= 0.752
	Treatment dose	F (3, 130) = 0.54, P= 0.656
	Lymphoma status	F (1, 130) = 32.91, P< 0.0001
Females	Interaction	F (2, 113) = 0.15, P= 0.857
	Treatment dose	F (3, 113) = 1.09, P= 0.357
	Lymphoma status	F (1, 113) = 24.04, P< 0.0001

Table 53: ANOVA results for basophil count.

In summary, basophil count was increased in both sexes in association with thymic lymphoma.

3.3.3.8. Red Blood Cell count (RBC)

3.3.3.8.1. Males

Each main effect on their own was statistically significant, but the effect that each of them had on red blood cell count in males did not depend on the other. Looking at "treatment dose" level, data indicates that ENU had a strong and significant impact on decreasing RBC (Table 54). At "lymphoma status", red blood cell count was significantly increased in lymphoma positive (128.68 ± 69.96) when compared with lymphoma negative males (123.39 ± 74.56), (Table 55).

Level of Group	N	RANK_RBC	
		Mean	Std Dev
1	28	203.45	33.52
2	17	128.65	72.73
3	82	99.09	66.00
4	10	107.10	58.94

Table 54: Rank-transformed absolute red blood cell count by group in males

Level of Status	N	RANK_RBC	
		Mean	Std Dev
0	104	123.39	74.56
1	33	128.68	69.96

Table 55: Rank-transformed absolute red blood cell count by lymphoma status in males.

3.3.3.8.2. Females

The interaction term was statically significant, suggesting that the difference in red blood cell count between the groups depended on lymphoma status. When comparing treated females with control females, red blood cell count means were significantly lower in all treated groups. For a RBC count of 203.45 ± 33.52 in control, the RBC counts in treated females were:

a) In lymphoma negative females, group 2 (138.25 ± 77.56, P= 0.027), group 3 (87.11 ± 60.05, P< 0.0001) and group 4 (139.6 ± 68.4, P= 0.0168);
b) In lymphoma positive females, group 2 (106.93 ± 49.25), group 3 (127.92 ± 68.91) and group 4 (100.16 ± 99.76), with P< 0.0001 in all cases.

When comparing lymphoma positive with lymphoma negative females within each treatment group, RBC count in group 3 (N= 64) was significantly lower in lymphoma negative (87.11 ± 60.05) compared to lymphoma positive (127.92 ±68.91), P=0.007. In groups 2 (N= 11) and 4 (N=14), no significant difference was found; P= 0.412 and 0.246 respectively. The results are presented in Table 56.

Level of Group	Level of status	N	RANK_RBC	
			Mean	Std Dev
1	0	29	210.93	25.89
2	0	4	138.25	77.56
2	1	7	106.93	49.25
3	0	34	87.12	60.05
3	1	32	127.92	68.91
4	0	5	139.60	68.39
4	1	9	100.17	99.76

Table 56: Rank-transformed absolute red blood cell count by group and lymphoma status in females.

The ANOVA results for the analysis of RBC count in both sexes are presented in Table 57.

RBC	Source	Result
Males	Interaction	F (2, 130) = 0.87, P= 0.42
	Treatment dose	F (3, 130) = 21.39, P< 0.0001
	Lymphoma status	F (1, 130) = 7.35, P= 0.008
Females	Interaction	F (2,113) = 3.42, P= 0.036
	Treatment dose	-
	Lymphoma status	-

Table 57: ANOVA results for RBC count.

In summary, in males, RBC count was increased in lymphoma positive when compared with lymphoma negative and that was associated with the presence of lymphoma, even though ENU was strongly associated with a significant decrease in RBC. In females, treated animals had a significantly lower RBC count when compared to control animals, but lymphoma positive animals in group 3, the most numerous group, had significantly higher RBC count than lymphoma negative.

3.3.3.9. Haemoglobin Concentration (HGB)

3.3.3.9.1. Males

Following the trend seen for red blood cells, the interaction term was not statistically significant, but both main effects were. At "treatment dose" level, an overall decrease in haemoglobin in treated males when compared with control males was found (Table

58). At "lymphoma status", there was a significant increase in HGB in lymphoma positive (127.17 ± 64.86) when compared with lymphoma negative males (118.47 ± 71.34), (Table 59).

Level of Group	N	RANK_HGB	
		Mean	Std Dev
1	28	193.59	32.20
2	17	121.18	65.67
3	82	97.25	63.99
4	10	106.25	63.30

Table 58: Rank-transformed haemoglobin concentration by group in males.

Level of Status	N	RANK_HGB	
		Mean	Std Dev
0	104	118.47	71.34
1	33	127.17	64.86

Table 59: Rank-transformed haemoglobin concentration by lymphoma status in males

3.3.3.9.2. Females

Similar to what was seen for RBC, the interaction term was statistically significant. When comparing haemoglobin levels in control females (211.14 ± 30.62) with treated females:

a) That did not develop lymphoma, it was significantly lower in groups 2 (136.25 ± 77.76, P= 0.034) and 3 (92.74 ± 64.8, P< 0.0001), but not in group 4 (172.1 ± 82.03, P= 0.221);
b) That developed lymphoma, there was a significant reduction in all groups; 116.46 ± 67.29, P= 0.0008 in group 2, 132.22 ± 72.07, P< 0.0001 in group 3, and 100.89 ± 104.54, P< 0.0001 in group 4.

When looking at the difference in haemoglobin concentration between lymphoma positive and lymphoma negative females within each treatment group, there was, in line with what was reported above for RBC, a significant difference in group 3 (P= 0.016): lymphoma positive had higher levels of HGB (132.22 ± 72.07) than lymphoma negative (92.74 ± 64.8). The results are presented in Table 60.

Level of Group	Level of status	N	RANK_HGB	
			Mean	Std Dev
1	0	29	211.14	30.62
2	0	4	136.25	77.76
2	1	7	116.43	67.29
3	0	34	92.74	64.80
3	1	32	132.22	72.07
4	0	5	172.10	82.03
4	1	9	100.89	104.54

Table 60: Rank-transformed haemoglobin concentration by group and lymphoma status in females.

Table 61 shows the ANOVA results for the analysis of HGB concentration in both sexes.

HGB	Source	Result
Males	Interaction	F (2, 130) = 1.4, P= 0.251
	Treatment dose	F (3, 130) = 21.35, P< 0.0001
	Lymphoma status	F (1, 130) = 10.17, P= 0.002
Females	Interaction	F (2, 113) = 4.28, P= 0.016
	Treatment dose	-
	Lymphoma status	-

Table 61: ANOVA results for HGB concentration.

In summary, data suggest that ENU accounted for a reduction in HGB, most likely to be linked to the reduction observed in RBC, and that lymphoma was associated with higher HGB concentration in all males and most of the females.

3.3.3.10. Haematocrit (HCT)

3.3.3.10.1. Males

The interaction between "treatment dose" and "lymphoma status" was not significant in determining the effect on haematocrit in males. On the other hand, a statistical significance was attained at both main effects on their own. "Treatment dose" had an effect of reducing the haematocrit in treated males when compared with control males (Table 62). "Lymphoma status", translated as a higher haematocrit in lymphoma

positive (129.21 ± 68.86), when compared with lymphoma negative (120.86 ± 72.60) males (Table 63).

Level of Group	N	RANK_HCT	
		Mean	Std Dev
1	28	191.54	35.19
2	17	124.24	71.97
3	82	100.26	67.56
4	10	113.75	62.87

Table 62: Rank-transformed haematocrit by group in males.

Level of Status	N	RANK_HCT	
		Mean	Std Dev
0	104	120.86	72.60
1	33	129.21	68.86

Table 63: Rank-transformed haematocrit by lymphoma status in males.

3.3.3.10.2. Females

A significant interaction between both main effects was found: the effect of "lymphoma status" on haematocrit in females varied depending on "treatment dose". When comparing the haematocrit of lymphoma negative females from each treated group with control females (200.6 ± 29.78), there was a significant decrease in group 3 (94.19 ± 64.65, P< 0.0001), with no other group being affected. When comparing the haematocrit of lymphoma positive females with control females, a significant decrease was present in all treated groups: group 2 (116.86 ± 73.86, P= 0.004), group 3 (129.88 ± 75.51, P< 0.0001) and group 4 (105.56 ± 105.38, P< 0.01). When comparing HTC between lymphoma negative and lymphoma positive females within each treatment group, group 3 lymphoma positive females had a higher haematocrit (129.88 ± 75.51) than their lymphoma negative counterparts (94.19 ± 64.65). This finding is consistent with what was found for other red blood cell-related variables described above. Results shown in Table 64.

Level of Group	Level of status	N	RANK_HCT	
			Mean	Std Dev
1	0	29	200.60	29.78
2	0	4	135.25	85.49
2	1	7	116.86	73.86
3	0	34	94.19	64.65
3	1	32	129.88	75.51
4	0	5	166.90	78.29
4	1	9	105.56	105.38

Table 64: Rank-transformed haematocrit by group and lymphoma status in females.

Table 65 shows the ANOVA results for the analysis of HTC in both sexes.

HTC	Source	Result
Males	Interaction	F (2, 130) = 1.67, P= 0.193
	Treatment dose	F (3, 130) = 17.47, P< 0.0001
	Lymphoma status	F (1, 130) = 9.22, P= 0.003
Females	Interaction	F (2, 113) = 3.19, P= 0.045
	Treatment dose	-
	Lymphoma status	-

Table 65: ANOVA result for HTC.

In summary, similarly to what was seen for RBC and HGB, HTC was lower and associated with treatment but higher in lymphoma positive than in lymphoma negative mice.

3.3.3.11. Mean Cell Volume (MCV)

3.3.3.11.1. Males

The interaction term was not significant in treated males. No significant differences were found at "lymphoma status" level either. On the other hand, a significant difference was found at "treatment dose" level, in which the MCV in treated males was generally higher than in control males (Table 66).

Level of Group	N	RANK_MCV	
		Mean	Std Dev
1	28	49.98	38.29
2	17	116.82	81.16
3	82	152.99	67.97
4	10	160.45	57.80

Table 66: Rank-transformed mean cell volume by group in males.

3.3.3.11.2. Females

Similarly to was what found in males, no statistical significance was attained at neither "interaction" level nor "lymphoma status". On the other hand, "treatment dose" had a significant effect on increasing MCV (Table 67).

Level of Group	N	RANK_MCV	
		Mean	Std Dev
1	29	51.59	32.63
2	11	134.68	35.88
3	66	154.83	67.29
4	14	172.93	61.00

Table 67: Rank-transformed mean cell volume by group in females.

The ANOVA results for the analysis of MCV in both sexes are show in Table 68.

MCV	Source	Result
Males	Interaction	F (2,130) = 0.28, P= 0.757
	Treatment dose	F (3, 130) = 17.37, P< 0.0001
	Lymphoma status	F (1, 130) = 2.92, P= 0.089
Females	Interaction	F (2, 113) = 1.75, P= 0.179
	Treatment dose	F (3, 113) = 18.23, P< 0.0001
	Lymphoma status	level F (1,113) = 0.18, P= 0.671

Table 68: ANOVA results for MCV.

In summary, ENU was associated with significant increase in RBC size in both sexes.

3.3.3.12. Mean Cell Haemoglobin Concentration (MCHC)

3.3.3.12.1. Males

A significant interaction between "treatment dose" and "lymphoma status" was not found, but each main effect on their own had a significant impact on mean cell

haemoglobin concentration in males. At "treatment dose", lower MCHC values were seen across all groups when compared with control (Table 69). At "lymphoma status" level, lymphoma positive males had a significantly higher MCHC (132.98 ± 62.25) than lymphoma negative (112.03 ± 68.2), (Table 70).

Level of Group	N	RANK_MCHC	
		Mean	Std Dev
1	28	184.64	40.85
2	17	117.00	62.55
3	82	96.89	60.83
4	10	93.55	66.60

Table 69: Rank-transformed mean cell haemoglobin concentration by group in males.

Level of Status	N	RANK_MCHC	
		Mean	Std Dev
0	104	112.03	68.20
1	33	132.98	62.25

Table 70: Rank-transformed mean cell haemoglobin concentration by lymphoma status in males.

3.3.3.12.2. Females

The effect of "lymphoma status" on MCHC was dependent of "treatment dose", as shown by statistical significance attained at "interaction" level. When comparing the MCHC between lymphoma negative females and control females (215.9 ± 34.7), there was a decrease across all treated groups: group 2 (134.25 ± 58.91, P=0.019), group 3 (90.54 ± 66.23, P< 0.0001) and group 4 (150.40 ± 82.55, P= 0.037). When comparing lymphoma positive females, a similar conclusion was reached: group 2 (119.79 ± 74.85, P< 0.001), group 3 (154.17 ± 72.77, P< 0.001) and group 4 (79.22 ± 80.41, P< 0.0001).

Within each treatment group, when looking at differences between lymphoma positive and negative females, lymphoma positive in group 3 (154.17 ± 72.77, P< 0.0001) had significantly higher MCHC than their lymphoma negative counterparts (90.54 ± 66.23). This finding was consistent with findings previously reported for other red blood cell-related parameters. Although not as strong as in group 3, a significant difference was also seen in group 4, with lymphoma positive females (79.22 ± 80.41,

P= 0.049) having lower MCHC than their lymphoma negative counterparts (150.4 ± 82.55). Results of MCHC by group and lymphoma status show in Table 71.

Level of Group	Level of status	N	RANK_MCHC	
			Mean	Std Dev
1	0	29	215.90	34.70
2	0	4	134.25	58.91
2	1	7	119.79	74.85
3	0	34	90.54	66.23
3	1	32	154.17	72.77
4	0	5	150.40	82.55
4	1	9	79.22	80.41

Table 71: Rank-transformed mean cell haemoglobin concentration by group and lymphoma status in females.

Results for the ANOVA in both sexes can be seen in Table 72.

MCHC	Source	Result
Males	Interaction	F (2, 130) = 0.55, P= 0.577
	Treatment dose	F (3, 130) = 20.12, P< 0.0001
	Lymphoma status	F (1, 130) = 12.75, P< 0.001
Females	Interaction	F (2, 113) = 6.79, P= 0.002
	Treatment dose	-
	Lymphoma status	-

Table 72: ANOVA results for MCHC.

As expected, MCHC has followed the same pattern as other RBC-related variables: an overall decrease associated with ENU but higher levels in lymphoma positive than in lymphoma negative animals.

3.3.3.13. Platelet count

3.3.3.13.1. Males

No statistical significance was attained at "interaction", although both "main effects" own their own had a significant impact on platelet count in treated males. At "treatment dose" level, a general reduction in platelet count was observed across all groups when compared with control (Table 73). At "lymphoma status" level,

lymphoma positive had a significant lower platelet count (82.14 ± 79.68) than lymphoma negative males (168.27 ± 60.51), (Table 74).

Level of Group	N	RANK_PLT	
		Mean	Std Dev
1	28	196.57	39.00
2	17	115.59	85.20
3	82	137.86	75.58
4	10	143.75	77.25

Table 73: Rank-transformed platelet count by group in males.

Level of Status	N	RANK_PLT	
		Mean	Std Dev
0	104	168.27	60.51
1	33	82.14	79.68

Table 74: Rank-transformed platelet count by lymphoma status in males.

3.3.3.13.2. Females

For platelet count in females, analysis was performed upon the untransformed dataset (Levene's test not significant, P=0.014). The interaction term was not significant, and also at "treatment dose" no significance was found. Lymphoma seemed to have played a role on platelet count, expressed by the statistical significance attained at "lymphoma status": lymphoma positive had a significant decrease in platelet count (479.81 ± 310.91) when compared with lymphoma negative females (938.61 ± 331.92), (Table 75).

Level of Status	N	PLT	
		Mean	Std Dev
0	72	938.61	331.92
1	48	479.81	310.91

Table 75: Platelet count by lymphoma status in females.

ANOVA results for platelet count in both sexes can be seen in Table 76.

Platelets	Source	Result
Males	Interaction	F (2, 130) = 1.45, P= 0.239
	Treatment dose	F (3, 130) = 3.71, P=0.013
	Lymphoma status	F (1, 130) = 9.45, P= 0.003
Females	Interaction	F (2, 113) = 0.38, P= 0.684
	Treatment dose	F (3, 130) = 0.93, P= 0.431
	Lymphoma status	F (1, 113) = 21.40, P< 0.0001

Table 76: ANOVA results for platelet count.

In summary, there was a difference in sexes: in males both ENU and lymphoma were associated with a reduction in platelet count, whereas in females the association was only with lymphoma.

3.4. Flow cytometry

3.4.1. Thymus

Thymic lymphocytes from control and ENU-treated mice were stained with antibody conjugates to identify the expression of surface markers CD4, CD8, CD44 and CD25. The Median Fluorescence Intensity (MFI) of each cell was captured at APC-Cy7 and FITC channels for the characterisation of CD8 and CD4 T-cells, respectively. Immature double negative cells were characterised by MFI captured at PE and PE-CF594 channels. This has revealed the traits of each population of mature and immature T-lymphocytes in normal F2 (C57BL/6 x A/J) intercross and served as baseline to study the phenotype of thymic lymphomas. Size of each T-lymphocyte population in thymic lymphomas was also compared with their normal counterparts.

The characterisation of thymic lymphomas by flow cytometry had the potential of assessing if there was any specific stage in lymphocyte development at which differentiation was arrested and cells started replicating in a non-controlled fashion, as it is characteristic of neoplasms, therefore establishing the stage at which thymic lymphomas occur.

3.4.1.1. Controls

Cell suspensions obtained from the thymi of 21 control mice were individually analysed and provided the baseline to characterise thymic lymphoma profiles. Inclusion criteria were established in selecting the samples to include in the final analysis: must have had 70% or more live cells on CD45/Sytox blue gate and least 100000 cells on SSC singlets gate. An unstained control sample to show the intrinsic fluorescence of the cells under analysis was always included on each run (Table 119, Appendix 2 - Tables and figures).

3.4.1.1.1. Percentage of lymphocyte populations

The results obtained from the flow cytometry analysis of thymi from control mice were largely consistent throughout the study. In the thymi of control F2 intercross, 11.62±2.32% of the lymphocytes were CD4 single positive, 2.89±0.52% were CD8 single positive, 80.66±2.28% were double positive and 5.23±0.83% were double negative (Figure 23A), similar to data published by (Wang et al., 2012b) for BALB/c mice. Within the CD8CD4 double negative (DN) population, 53.77±14.84% were DN1, 0.88±0.2% were DN2, 21.69±7.33% were DN3 and 23.65±8.26% were DN4 (Figure 23B).

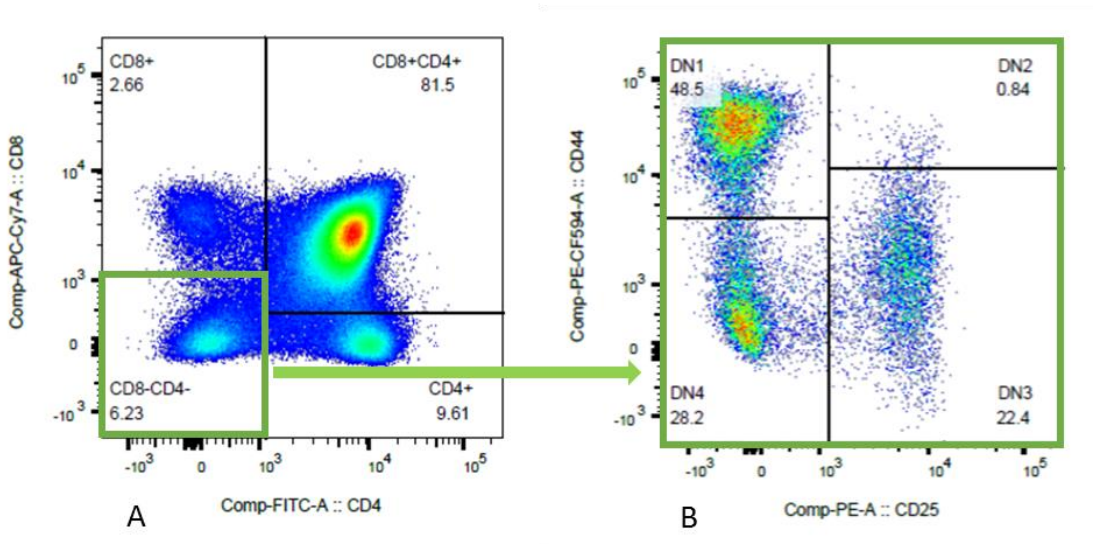


Figure 23: A) Thymic lymphocytes from control mice according to CD4 and CD8 expression, measured by fluorescence captured in APC-C7t and FITC channels. B) Further characterisation of CD8-CD4- population from A, according to CD25 and CD44 expression measured by fluorescence captured in PE-CF594 and PE channels, revealing their stage of development in the double negative differentiation process.

3.4.1.1.2. Analysis of cellular size

The analysis of size, measured using Mean FSC has revealed a value of 80634±3732 for CD4 lymphocytes, 87901±4045 for CD8, 71917±2843 for DP and 94822±4322 for DN. Within the DN population, a value of 90078±3938 was found for DN1, 120923±7620 for DN2, 101963±4638 for DN3 and 98339±6366 for DN4.

3.4.1.1.3. Median Fluorescence Intensity reference intervals

The analysis of MFI of control thymi, as explained previously (section 2.9.7, page 98) revealed the range of fluorescence that characterises as positive and negative each type of thymic lymphocyte, as seen in Table 77.

Antibody conjugate	**MFI Reference interval**
CD4+ | Median (Comp-FITC-A)	[3521 - 11137]
CD4+- | Median (Comp-FITC-A)	[279.72 - 3521]
CD8+ | Median (Comp-APC-Cy7-A)	[1374 - 4070]
CD8+- | Median (Comp-APC-Cy7-A)	[142.23 - 1374]
CD8+CD4+ | Median (Comp-APC-Cy7-A)	[1302 - 3438]
CD8+CD4+ | Median (Comp-FITC-A)	[3556.2 - 7133.8]
CD8+CD4+- | Median (Comp-APC-Cy7-A)	[1302 - 3438]
CD8+CD4+- | Median (Comp-FITC-A)	[279.72 - 3556.2]
CD8+-CD4+ | Median (Comp-APC-Cy7-A)	[142.23 - 1302]
CD8+-CD4+ | Median (Comp-FITC-A)	[3556.2 - 7133.8]
CD8+-CD4+- | Median (Comp-APC-Cy7-A)	[142.23 - 1302]
CD8+-CD4+ -| Median (Comp-FITC-A)	[279.72 - 3556.2]
CD8-CD4- | Median (Comp-APC-Cy7-A)	[29.19 - 142.23]
CD8-CD4- | Median (Comp-FITC-A)	[72.08 - 279.72]
DN1 | Median (Comp-PE-CF594-A)	[4370 - 32322]
DN2 | Median (Comp-PE-A)	[2816 - 7656]
DN2 | Median (Comp-PE-CF594-A)	[6208 - 21572]
DN3 | Median (Comp-PE-A)	[2529.2 - 6436.8]
DN4 | Median (Comp-PE-A)	[(-230.75) - (-21.55)]
DN4 | Median (Comp-PE-CF594-A)	[237.64 - 556.16]

Table 77: FC of control thymus, MFI reference intervals for each antibody conjugate.

In the same table, the intermediate phenotypes, symbolized by +-, were not present in controls but the classic characterisation of cells as “positive” and “negative” was far from sufficient to label the range of fluorescence found in neoplastic cells. A solution was attempted by creating reference intervals to accommodate intermediate expressers of CD4 FITC and CD8 APC-Cy7. For example, CD4 positive (+) lymphocytes have MFIs between 3521 and 11137, while CD4 negative (-), represented by the emission of FITC in DN gate, have MFIs between 72.08 and 279.2, which makes any CD4

FITC intermediate expressers emit between 279.2 and 3521. Characterising such diversity in immunophenotypes was complex and reference intervals were used as guides to keep consistency throughout the process.

3.4.1.1.4. Unstained control samples

Unstained thymi samples (n= 7) from control mice were run with the intent of showing the intrinsic fluorescence of cells and help with the characterisation of true negative cells. A summary of data obtained from unstained samples can be seen in Appendix 2 - Tables and figures, Table 119.

3.4.1.2. Treated

47 thymi from ENU-treated mice have fulfilled the inclusion criteria of having at least 70% of live leucocytes and at least 100000 cells on the SSC gate, of which 40 had a histological diagnosis of thymic lymphoma.

3.4.1.2.1. Analysis of cellular size

A t-Test with Welch's correction analysis of Mean FSC allowed to compare size of thymic lymphoma cells with thymic lymphocytes from control mice. Statistical significance was attained ($P<0.05$) in some lymphocyte populations (Table 78). CD4 single positive and CD4CD8 double positive thymic lymphocytes in lymphoma positive mice were significantly larger than in control, $P< 0.001$ and 0.003, respectively. On the other hand, double negative lymphocytes in treated mice were smaller than those in control mice, $P= 0.03$. No significant difference was found for CD8 single positive lymphocytes.

	Treated CD4+ vs. Control CD4+	Treated CD8+ vs. Control CD8+	Treated CD8+CD4+ vs. Control CD8+CD4+	Treated CD8-CD4- vs. Control CD8-CD4-
P value	0.0001	0.0885	0.0025	0.0279
Significantly different	Yes	No	Yes	Yes
Mean±SEM of control	80634±814.4, n=21	87901±882.7, n=21	71917±620.4, n=21	94822±943, n=21
Mean±SEM of treated	88595±1720, n=39	93785±3041, n=11	97333±6534, n=12	89966±1933, n=41

Table 78: FC of thymus, size comparison of lymphocytes (based on expression of CD4 and CD8 markers) between control and treated mice.

As for double negative populations, presented in Table 79, DN2 were significantly larger in treated mice, P< 0.001 whereas DN4 were significantly smaller in treated mice, P= 0.004.

	Treated DN1 vs. Control DN1	Treated DN2 vs. Control DN2	Treated DN3 vs. Control DN3	Treated DN4 vs. Control DN4
P value	0.3695	<0.0001	0.3433	0.0047
Significantly different	No	Yes	No	Yes
Mean±SEM of control	90078±859.3, n=21	120923±1663, n=21	101963±1012, n=21	98339±1389, n=21
Mean±SEM of treated	88406±1627, n=25	104116±3020, n=25	97672±4323, n=23	83457±4645, n=25

Table 79: FC of thymus, size comparison of DN lymphocytes between control and treated mice

3.4.1.2.2. Unstained control samples

Unstained thymi samples (n= 51) from ENU–treated mice were run in parallel with stained samples with the intent of showing the intrinsic fluorescence of cells and help with the characterisation of true negative cells. A summary of data obtained from unstained samples can be seen in Appendix 2 - Tables and figures, Table 120.

3.4.1.2.3. Thymic lymphoma immunophenotypes

According to the analysis, ENU-induced thymic lymphomas have a varied immunophenotype and intermediate expression of the main markers was very common. Results from all 40 thymi presented here had a histological confirmation of

thymic lymphoma. More than half of all tumours were of cells that had some degree of expression of both CD8 and CD4 markers followed by tumours of CD8 cells, followed by tumours of mixed cells, followed by CD4 cell tumours, with tumours of DN cells being the least frequent. Within the most common phenotype group of CD8CD4 cells, cells with intermediate expression of both CD8 and CD4 markers (CD8+-CD4+-) were the most common. Table 80 shows the distribution of all phenotypes.

Immunophenotype		**Frequency**	**Main group total**
Main group	Subgroup		
CD8CD4	CD8+CD4+	6	23 (57.5%)
	CD8+-CD4+	6	
	CD8+CD4+-	3	
	CD8+-CD4+-	8	
CD4	CD4+	2	3 (7.5%)
	CD4+-	1	
CD8	CD8+	2	8 (20%)
	CD8+-	6	
DN	DN1	1	2 (5%)
	DN2	1	
	DN3	0	
	DN4	0	
Mixed	Varied	4	4 (10%)

Table 80: Frequency of thymic lymphomas immunophenotypes.

Attributing a definitive label to each tumour was challenging given their variety and intermediate fluorescence expression, and it is arguable whether the classification used here is adequate. Tumours were grouped according to their major phenotypic traits for the purpose of objective data analysis and to allow for unbiased conclusions to be drawn. The reader may disagree with classification applied here but since the MFI of each cell type is given, they are provided with the necessary information to apply their own approach in classifying these neoplasms.

Examples of flow cytometry plots for each group of thymic lymphomas are presented next, followed by a table with the cellular populations, their frequencies, MFIs and data from control unstained samples run alongside for each tumour.

3.4.1.2.3.1. Lymphomas of predominantly CD8+CD4+ cells

Lymphomas characterised by a predominance of cells with clear positive fluorescence on CD8APC-Cy7 and CD4FITC channels were amongst the most frequent (17.5% of all tumours). Figure 24 shows the flow cytometry profile of CD8+CD4+ lymphomas. Even though they were grouped under the same category, it is clear how varied they were, not allowing in most cases the use of a simple automated 4 quadrant gating approach but requiring instead the manual identification of each cell type.

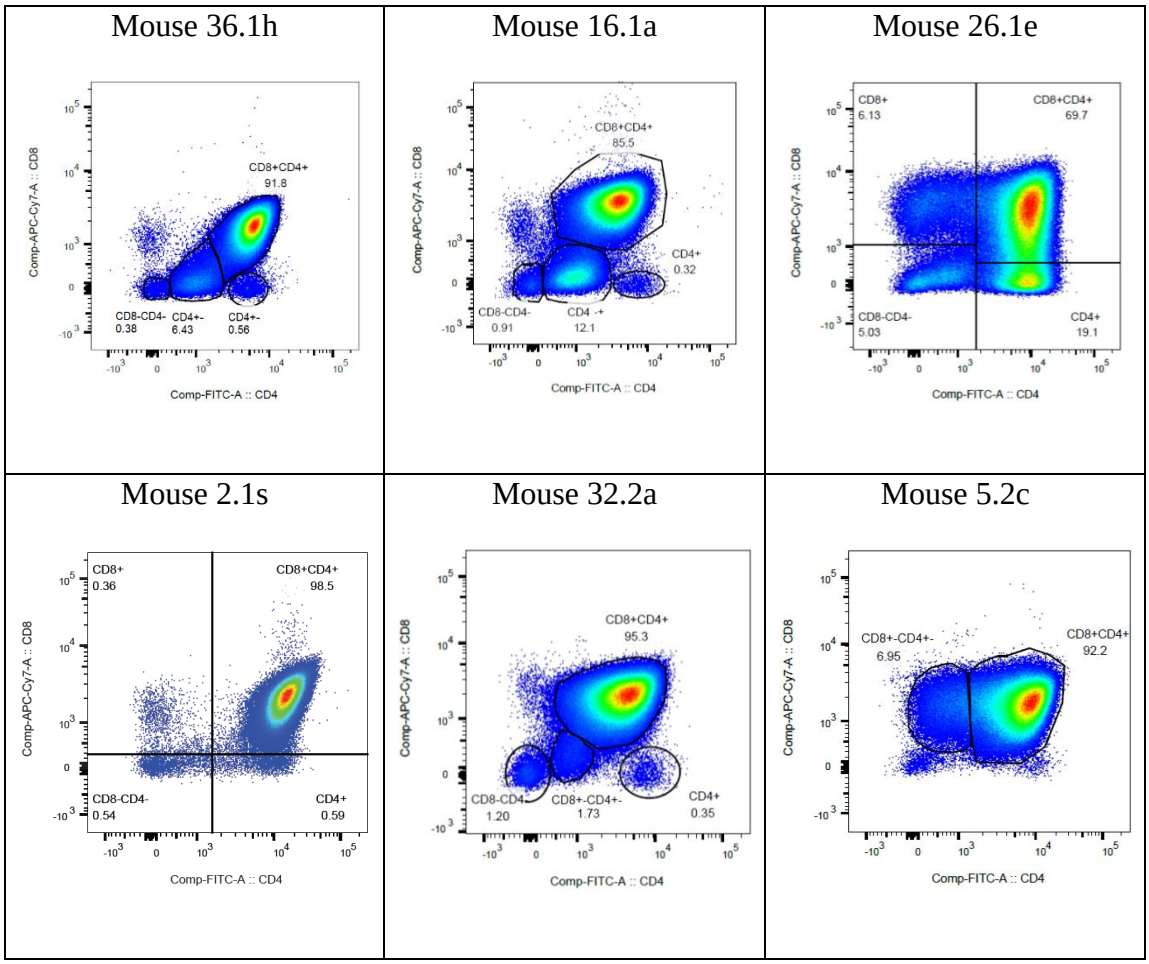


Figure 24: Flow cytometry profile of different CD8+CD4+ thymic lymphomas.

In some cases it was still possible to see the 4 classic types of thymic lymphocytes, SP, DN, SPCD8 and SPCD4, such as in mice 2.1s and 26.1e, but in most cases there was a departure from the classic classification, with the presence of cells with intermediate expression of both CD8 and CD4 markers. For the purpose of ilustrating the diversity of phenotypes, the information about the median fluoresce intensity of each cell population captured at APC-Cy-7 and FITC channels for each cell type and the unstained control run alongside are presented seperately in Table 81.

CD8+CD4+					
Mouse 36.1h	%	Mouse 16.1a	%	Mouse 26.1e	%
CD4+: APC-Cy7: 19.3 CD4+: FITC: 4882	0.56	CD4+: APC-Cy7: 5.13 CD4+: FITC: 6531	0.32	CD4+: APC-Cy7: 179 CD4+: FITC: 8171	19.1
CD4+-: APC-Cy7: 170 CD4+-: FITC: 1119	6.43	CD4+-: APC-Cy7: 190 CD4+-: FITC: 1020	12.1	CD8+: APC-Cy7: 3327 CD8+: FITC: 528	6.13
CD8+CD4+: APC-Cy7: 1642 CD8+CD4+: FITC: 5580	91.8	CD8+CD4+: APC-Cy7: 3151 CD8+CD4+: FITC: 3448	85.5	CD8+CD4+: APC-Cy7: 2575 CD8+CD4+: FITC: 8755	69.7
CD8-CD4-: APC-Cy7: -1.28 CD8-CD4-: FITC: 105	0.38	CD8-CD4-: APC-Cy7: 11.6 CD8-CD4-: FITC: -25.7	0.91	CD8-CD4-: APC-Cy7: 226 CD8-CD4-: FITC: 583	5.03
Unstained control	%	Unstained control	%	Unstained control	%
CD8-CD4-: APC-Cy7: -5.13 CD8-CD4-: FITC: 521	97.4	CD8-CD4-: APC-Cy7: -1.28 CD8-CD4-: FITC: 473	97.4	CD8-CD4-: APC-Cy7: -4.50 CD8-CD4-: FITC: 244	98.6
Mouse 2.1s	%	Mouse 32.2a	%	Mouse 5.2c	%
CD4+: APC-Cy-7: 138 CD4+: FITC: 7957	0.59	CD4+: APC-Cy7: 45.5 CD4+: FITC: 6896	0.35		
CD8+: APC-Cy-7: 1012 CD8+: FITC: 221	0.36	CD8+-CD4+-: APC-Cy7: 298 CD8+-CD4+-: FITC: 868	1.73		
CD8+CD4+: APC-Cy-7: 1979 CD8+CD4+: FITC: 14416	98.5	CD8+CD4+: APC-Cy7: 1805 CD8+CD4+: FITC: 3649	95.3	CD8+CD4+-: APC-Cy7: 1526 CD8+CD4+-: FITC: 774	6.95
CD8-CD4-: APC-Cy-7: 87.4 CD8-CD4-: FITC: 234	0.54	CD8-CD4-: APC-Cy7: 39.9 CD8-CD4-: FITC: -18.0	1.2	CD8+CD4+: APC-Cy7: 1630 CD8+CD4+: FITC: 6881	92.2
Unstained control	%	Unstained control	%	Unstained control	%
CD8-CD4-: APC-Cy7: -5.13 CD8-CD4-: FITC: 265	98.8	CD8-CD4-: APC-Cy7: -4.64 CD8-CD4-: FITC: 337	96.9	CD8-CD4-: APC-Cy7: -2.57 CD8-CD4-: FITC: 351	97.7

Table 81: Immunophenotype of all thymic lymphomas of CD8+CD4+ lymphocytes shown in Figure 24. The MFI of each cell type captured at APC-Cy7 and FITC channels is presented as well as the percentage of each cell type. For each thymus, the MFI of unstained control sample run at each experiment is also given.

3.4.1.2.3.2. Lymphomas of predominantly CD8+CD4+- cells

Within the CD8CD4 group, CD8+CD4+- was the least common phenotype, with 3 cases, but nevertheless each one was unique. In mouse 9.1o there is still a resemblance to the classic distribution in 4 quadrants, whereas in mice 7.1q and 4.2j, the cells with a CD8+CD4+- phenotype had colonized more than 90% of the thymi (Figure 25). In

mouse 4.2j, there was a second population with higher expression of CD8 but no distinction between "positive" and "highly positive" CD8 was made here. There was also slightly higher expression of CD4 but not enough to classify it as CD4+. The cells were, therefore, grouped in a single CD8+CD4+- cluster.

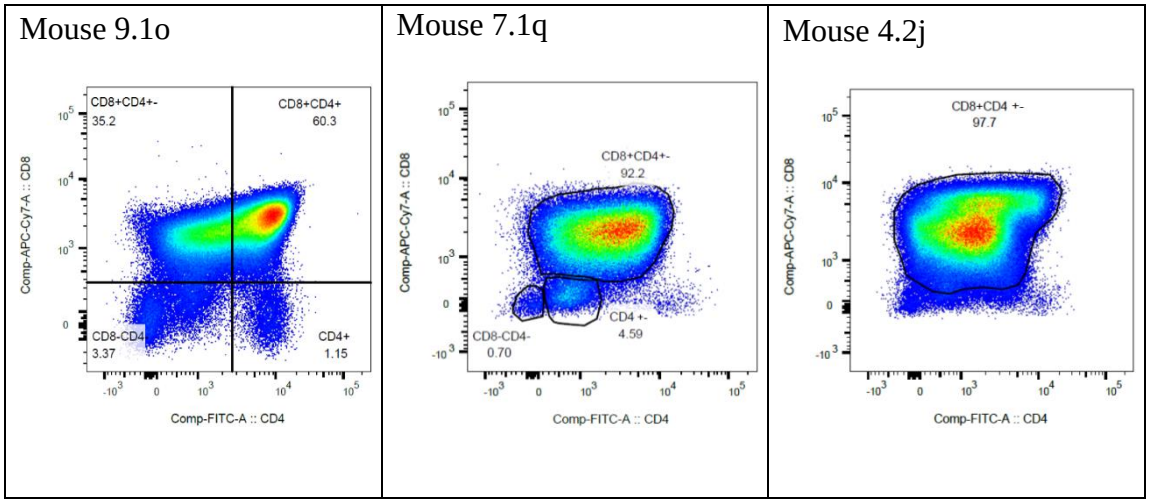


Figure 25: Flow cytometry profile of different CD8+CD4+- thymic lymphomas.

Detailed information on the MFI of each cell type composing the CD8+CD4+- tumours presented above, as well as on unstained control samples run alongside each analysis is provided in Table 82.

CD8+CD4+-					
Mouse 9.1o	%	Mouse 7.1q		Mouse 4.2j	%
CD4+: APC-Cy7: 98.4	1.15				
CD4+: FITC: 7579					
CD8+CD4+-: APC-Cy7: 1459	35.2	CD4+-: APC-Cy7: 211	4.59		
CD8+CD4+-: FITC: 1235		CD4+-: FITC: 748			
CD8+CD4+: APC-Cy7: 2413	60.3	CD8+CD4+-: APC-Cy7: 1964	92.2		
CD8+CD4+: FITC: 6762		CD8+CD4+-: FITC: 2173			
CD8-CD4-: APC-Cy7: 135	3.37	CD8-CD4-: APC-Cy7: 23.1	0.7	CD8+CD4+-: APC-Cy7: 2558	97.7
CD8-CD4-: FITC: 294		CD8-CD4-: FITC: 12.8		CD8+CD4+-: FITC: 1421	
Unstained control	%	Unstained control	%	Unstained control	%
CD8-CD4-: APC-Cy7: -6.30	97.2	CD8-CD4-: APC-Cy7: -8.98	99.2	CD8-CD4-: APC-Cy7: -5.13	96.9
CD8-CD4-: FITC: 252		CD8-CD4-: FITC: 266		CD8-CD4-: FITC: 242	

Table 82: Immunophenotype of thymic lymphomas of CD8+CD4+- lymphocytes illustrated in Figure 25 showing the MFI of each cell type captured at APC-Cy7 and FITC channels and the percentage of each cell type. For each thymus, the MFI of unstained control sample run at each experiment is also given.

3.4.1.2.3.3. Lymphomas of predominantly CD8+-CD4+ cells

Of all CD8CD4 phenotypes, six had an intermediate expression of CD8APC-Cy-7 and a positive expression of CD4FITC. In mouse 22.2h, this type of cells has colonized almost 100% of thymic lymphocyte population. In several mice, the presence of a CD4+- population was also evident (Figure 26).

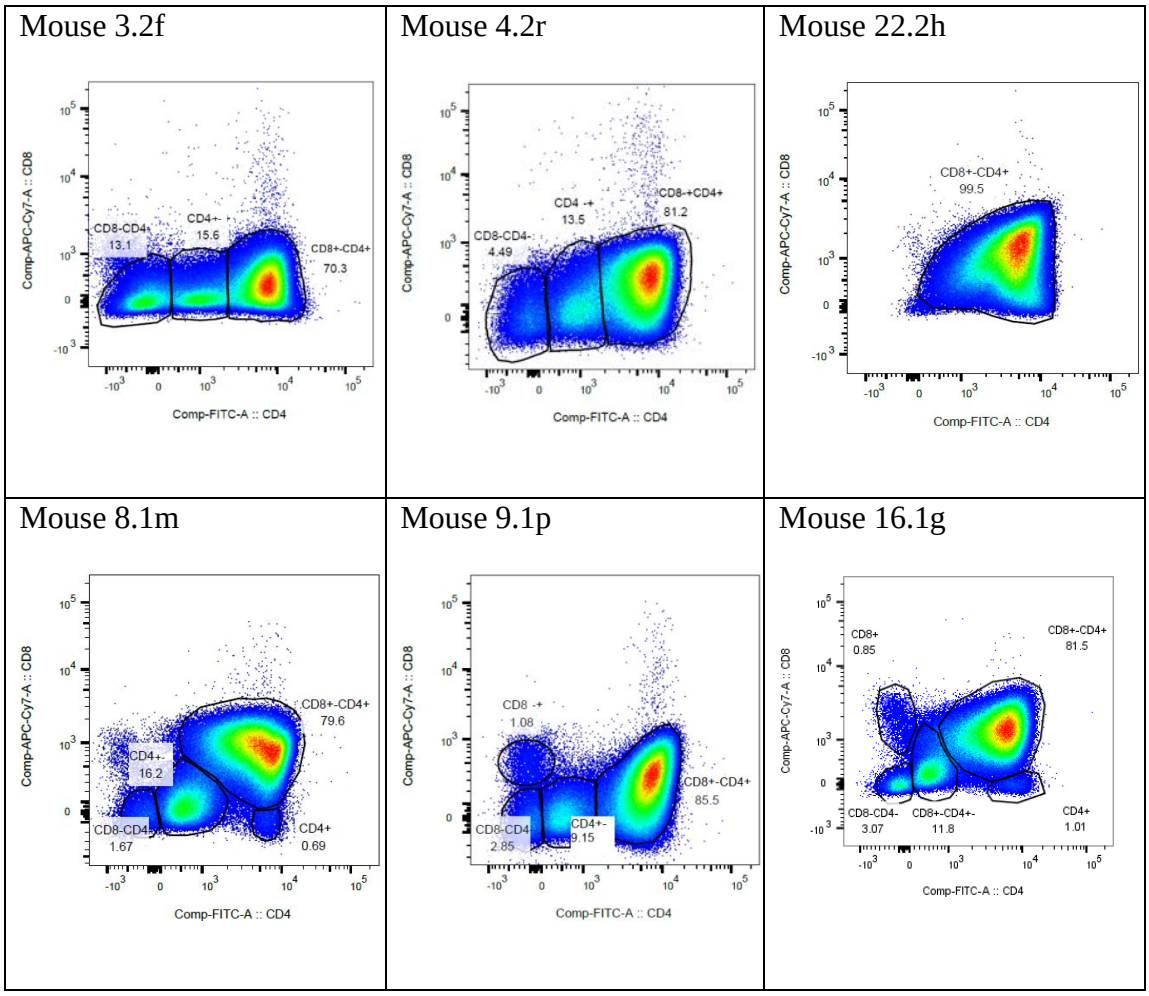


Figure 26: Flow cytometry profile of different CD8+-CD4+ thymic lymphomas.

Detailed information on the MFI of each cell type composing the CD8+-CD4+ tumours presented above, as well as on unstained control samples run alongside each analysis is provided in Table 83.

CD8+-CD4+					
Mouse 3.2f	%	Mouse 4.2r	%	Mouse 22.2h	%
CD8+-CD4+: APC-Cy7: 320	70.3	CD8+-CD4+: APC-Cy7: 295	81.2		
CD8+-CD4+: FITC: 6866		CD8+-CD4+: FITC: 6390			
CD4+-: APC-Cy7: 102	15.6	CD4+-: APC-Cy7: 93.9	13.5		
CD4+-: FITC: 1082		CD4+-: FITC: 1010			
CD8-CD4-: APC-Cy7: 47.5	13.1	CD8-CD4-: APC-Cy7: 18.5	4.49	CD8+-CD4+: APC-CY7: 1010	99.5
CD8-CD4-: FITC: -116		CD8-CD4-: FITC: -77.1		CD8+-CD4+: FITC: 4254	
Unstained control	%	Unstained control	%	Unstained control	%
CD8-CD4-: APC-Cy7: -3.85	97	CD8-CD4-: APC-Cy7: -2.50	97.3	CD8-CD4-: APC-Cy7: -7.70	98.8
CD8-CD4-: FITC: 522		CD8-CD4-: FITC: 371		CD8-CD4-: FITC: 250	
Mouse 8.1m	%	Mouse 9.1p	%	Mouse 16.1g	%
CD4+: APC-Cy7: -72.8	0.69	CD8+-CD4+: APC-Cy7: 267	85.5	CD8+: APC-Cy7: 1758	0.85
CD4+: FITC: 6213		CD8+-CD4+: FITC: 6281		CD8+: FITC: -80.9	
CD4+-: APC-Cy7: 81.6	16.2	CD4+-: APC-Cy7: 31.5	9.15	CD8+-CD4+: APC-Cy7: 1292	81.5
CD4+-: FITC: 647		CD4+-: FITC: 590		CD8+-CD4+: FITC: 4791	
CD8+-CD4+: APC-Cy7: 849	79.6	CD8+-: APC-Cy7: 492	1.08	CD8+-CD4+-: APC-Cy7: 291	11.8
CD8+-CD4+: FITC: 4771		CD8+-: FITC: -113		CD8+-CD4+-: FITC: 552	
CD8-CD4-: APC-Cy7: -10.7	1.67	CD8-CD4-: APC-Cy7: -19.9	2.85	CD8-CD4-: APC-Cy7: 8.98	3.07
CD8-CD4-: FITC: -198		CD8-CD4-: FITC: -117		CD8-CD4-: FITC: -102	
Unstained control	%	Unstained control	%	Unstained control	%
CD8-CD4-: APC-Cy7: -6.04	98.6	CD8-CD4-: APC-Cy7: -2.91	97.1	CD8-CD4-: APC-Cy7: -3.85	98.3
CD8-CD4-: FITC: 324		CD8-CD4-: FITC: 321		CD8-CD4-: FITC: 345	

Table 83: Immunophenotype of all thymic lymphomas of CD8+CD4+- lymphocytes showing the MFI of each cell type captured at APC-Cy7 and FITC channels and the percentage of each cell type. For each thymus, the MFI of unstained control sample run at each experiment is also given.

3.4.1.2.3.4. Lymphomas of predominantly CD8+-CD4+- cells

CD8+-CD4+- lymphomas were the most common phenotype of all tumours (20%) and the most common amongst tumours of CD8CD4 type (34.8%), (Figure 27). Although each tumour has a unique phenotype, they are all characterised by the presence of an increased cell population with intermediate fluorescence of both CD8APC-Cy-7 and CD4FITC conjugates. The fluorescence captured in the APC-Cy7 channel was low in mice 24.1g, 6.1d, 2.1e and the absence of a distinct DN population challenges the classification presented here. The MFI reference intervals were strong guides during this process. Furthermore, in these cases, the information provided by the unstained control helped to understand to what extent the low fluorescence levels were real and reflected some degree of presence of CD8 and CD4 markers on the surface of these cells or it was, instead, due to intrinsic cellular fluorescence. In mouse 16.2c there seems to be 2 populations of CD8+-CD4+-; the individual analysis of their

MFI has shown that both had an intermediate expression of CD8 and CD4 and therefore were grouped in a single cluster.

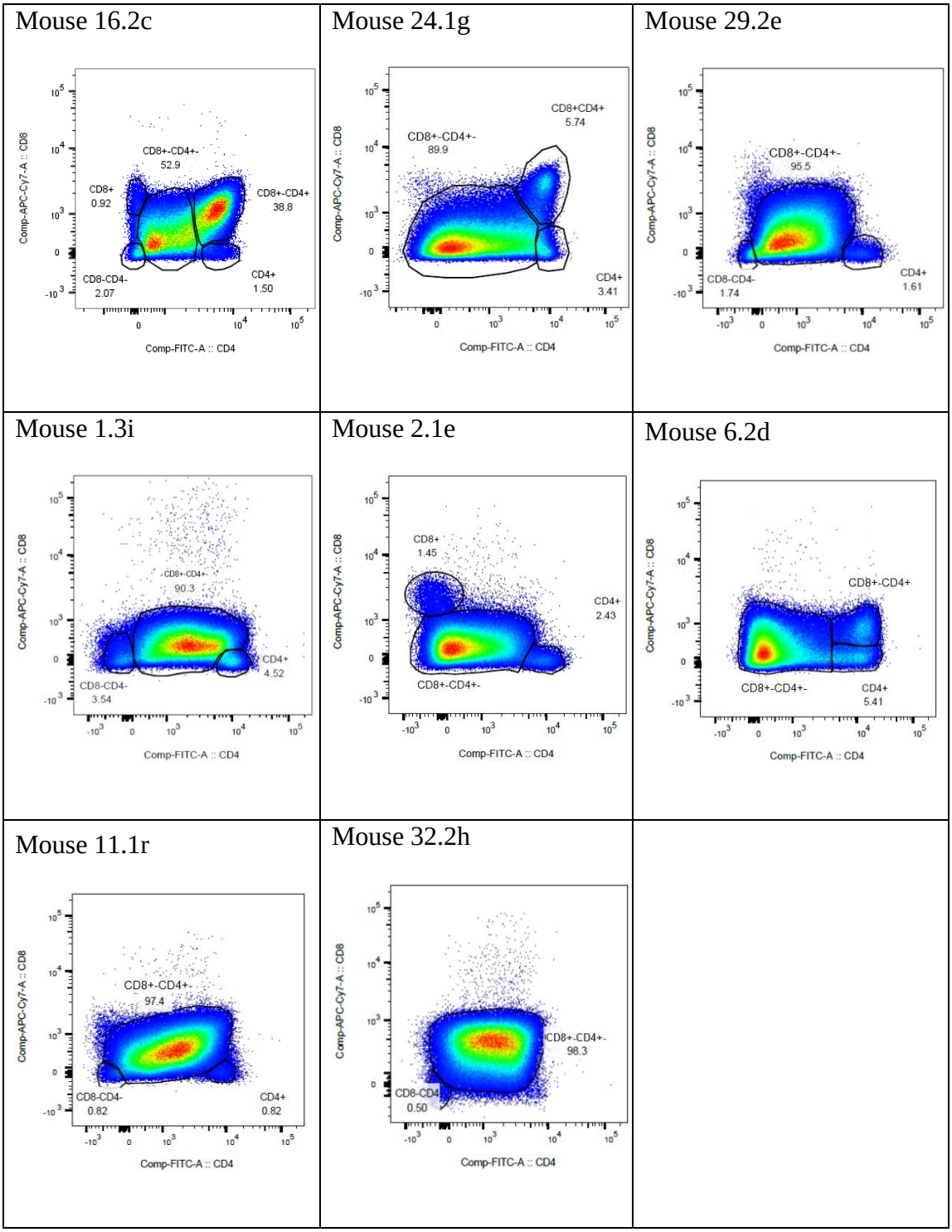


Figure 27: Flow cytometry profile of different CD8+-CD4+- thymic lymphomas.

For each flow cytometry plot presented above, detailed information on the MFI of each cell type, their percentages and unstained controls is presented in Table 84.

CD8+-CD4+-					
Mouse 16.2c	%	Mouse 24.1g	%	Mouse 29.2e	%
CD4+: APC-Cy7: 75.8	1.5				
CD4+: FITC: 4704					
CD8+: APC-Cy7: 1544	0.92	CD4+: APC-Cy7: 112	3.41	CD4+: APC-Cy7: 8.98	1.61
CD8+: FITC: 70.03		CD4+: FITC: 7597		CD4+: FITC: 8639	
CD8+-CD4+: APC-Cy7: 1059	38.8	CD8+CD4+: APC-Cy7: 2048	5.74	CD8-CD4-: APC-Cy7: -28.2	1.74
CD8+-CD4+: FITC: 4826		CD8+CD4+: FITC: 7130		CD8-CD4-: FITC: -134	
CD8+-CD4+-: APC-Cy7: 416	52.9	CD8+-CD4+-: APC-Cy7: 208	89.9	CD8+-CD4+-: APC-Cy7: 387	95.5
CD8+-CD4+-: FITC: 1092		CD8+-CD4+-: FITC: 489		CD8+-CD4+-: FITC: 939	
Unstained control	%	Unstained control	%	Unstained control	%
CD8-CD4-: APC-Cy7: -6.42	98.4	CD8-CD4-: APC-Cy7: -3.85	99.4	CD8-CD4-: APC-Cy7: 0	98.7
CD8-CD4-: FITC: 254		CD8-CD4-: FITC: 225		CD8-CD4-: FITC: 328	
Mouse 1.3i	%	Mouse 2.1e	%	Mouse 6.2d	%
CD4+: APC-Cy7: 7.70	4.52	CD4+: APC-Cy7: -12.8	2.43	CD4+: APC-Cy-7: 149	5.41
CD4+: FITC: 9197		CD4+: FITC: 8045		CD4+: FITC: 8226	
CD8+-CD4+-: APC-Cy7: 354	90.3	CD8+: APC-Cy7: 1972	1.45	CD8+-CD4+: APC-Cy-7: 784	5.89
CD8+-CD4+-: FITC: 1991		CD8+: FITC: -138		CD8+-CD4+: FITC: 11429	
CD8-CD4-: APC-Cy7: 75.8	3.54	CD8+-CD4+-: APC-Cy7: 299	95.5	CD8+-CD4+-: APC-Cy-7: 290	88.1
CD8-CD4-: FITC: -113		CD8+-CD4+-: FITC: 510		CD8+-CD4+-: FITC: 322	
Unstained control	%	Unstained control	%	Unstained control	%
CD8-CD4-: APC-Cy7: -2.57	97.1	CD8-CD4-: APC-Cy7: -5.13	98.2	CD8-CD4-: APC-Cy7: -5.13	99.1
CD8-CD4-: FITC: 362		CD8-CD4-: FITC: 240		CD8-CD4-: FITC: 217	
Mouse 11.1r	%	Mouse 32.2h	%		
CD4+: APC-Cy7: 7.70	0.82				
CD4+: FITC: 8411					
CD8+-CD4+-: APC-Cy7: 538	97.4	CD8-CD4-: APC-Cy7: -37.9	0.5		
CD8+-CD4+-: FITC: 1392		CD8-CD4-: FITC: -113			
CD8-CD4-: APC-Cy7: -19.3	0.82	CD8+-CD4+-: APC-Cy7: 406	98.3		
CD8-CD4-: FITC: -224		CD8+-CD4+-: FITC: 1337			
Unstained control	%	Unstained control	%		
CD8-CD4-: APC-Cy7: -6.42	98.9	CD8-CD4-: APC-Cy7: -5.33	97		
CD8-CD4-: FITC: 238		CD8-CD4-: FITC: 238			

Table 84: Immunophenotype of all thymic lymphomas of CD8+-CD4+- lymphocytes showing the MFI of each cell type captured at APC-Cy7 and FITC channels and the percentage of each cell type. For each thymus, the MFI of unstained control sample run at each experiment is also given.

3.4.1.2.3.5. Lymphomas of predominantly CD4 cells

Lymphomas of predominantly CD4 cells accounted only for 7.5% of all tumours. Again, the diversity of phenotypes was remarkable. In mouse 1.3g, in which clear positive CD4 cells were abnormally increased, there was some preservation of the classic distribution of cells, whereas in mice 28.1a and 5.2e, more than 90% of T-lymphocytes had some degree of expression of CD4 marker (Figure 28).

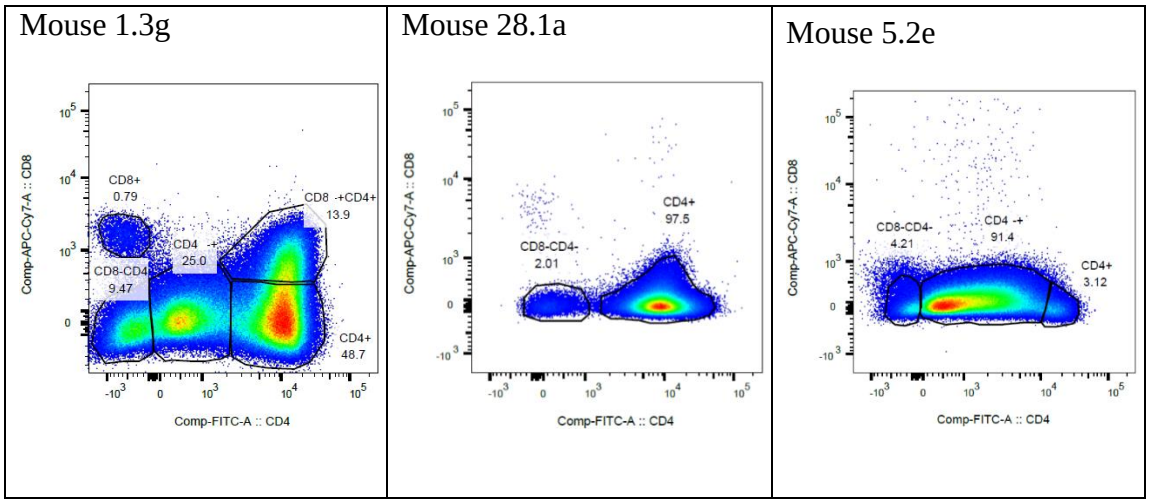


Figure 28: Flow cytometry profile of different CD4 thymic lymphomas.

Information on the MFI and frequency of each cell type is presented in Table 85.

CD4+				**CD4+-**	
Mouse 1.3g	%	Mouse 28.1a	%	Mouse 5.2e	%
CD4+: APC-Cy7: 41.4	48.7				
CD4+: FITC: 9364					
CD4+-: APC-Cy7: 44.3	25				
CD4+-: FITC: 636					
CD8+: APC-Cy7: 1529	0.79			CD4+: APC-Cy7: -14.1	3.12
CD8+: FITC: -571				CD4+: FITC: 16192	
CD8+-CD4+: APC-Cy7: 662	13.9	CD4+: APC-Cy7: 18.0	97.5	CD4+-: APC-Cy7: 114	91.4
CD8+-CD4+: FITC: 11746		CD4+: FITC: 8543		CD4+-: FITC: 1138	
CD8-CD4-: APC-Cy7: -46.0	9.47	CD8-CD4-: APC-Cy7: 1.28	2.01	CD8-CD4-: APC-Cy7: 20.5	4.21
CD8-CD4-: FITC: -395		CD8-CD4-: FITC: 230		CD8-CD4-: FITC: -126	
Unstained control	%	Unstained control	%	Unstained control	%
CD8-CD4-: APC-Cy7: -1.72	98.5	CD8-CD4-: APC-Cy7: -5.13	97.7	CD8-CD4-: APC-Cy7: -2.57	97.8
CD8-CD4-: FITC: 312		CD8-CD4-: FITC: 289		CD8-CD4-: FITC: 370	

Table 85: Immunophenotype of all thymic lymphomas of CD4 lymphocytes showing the MFI of each cell type captured at APC-Cy7 and FITC channels and the percentage of each cell type. For each thymus, the MFI of unstained control sample run at each experiment is also given.

3.4.1.2.3.6. Lymphomas of predominantly CD8 cells

20% of all neoplasms had abnormally increased CD8 cells, of which most had an intermediate expression of CD8APCy-Cy7. In mice 2.2q and 2.2h there was also a minimal increase in DN cells. Most of the CD8+- cells were vastly colonized by cells with this phenotype, giving little room for other types of lymphocytes (Figure 29).

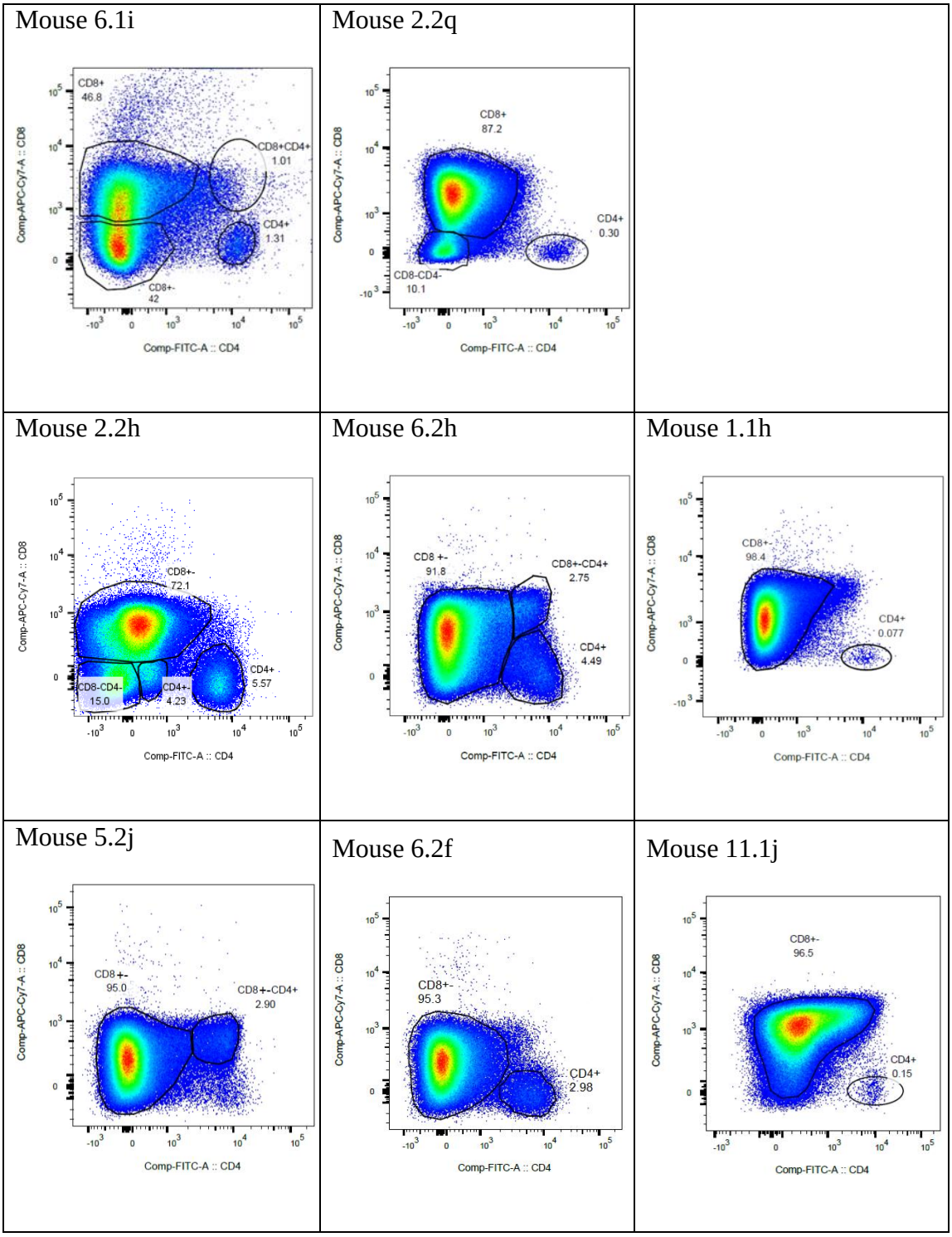


Figure 29: Flow cytometry profile of different CD8 thymic lymphomas.

The MFI and percentages of each cell population present in CD8 neoplasms are presented in Table 86. In some cases, such as in mice 5.2j and 6.2f, the fluorescence captured in APC-Cy7 channel is very low, but still distinct from the unstained control and within reference intervals for CD8+- cells.

CD8+					
Mouse 6.1i	%	Mouse 2.2q	%		
CD8+: APC-Cy7: 1419	46.8				
CD8+: FITC: -74.5					
CD4+: APC-Cy7: 233	1.31	CD4+: APC-Cy7: 55.2	0.3		
CD4+: FITC: 12018		CD4+: FITC: 13114			
CD8+CD4+: APC-Cy7: 2436	1.01	CD8+: APC-Cy7: 1853	87.2		
CD8+CD4+: FITC: 6253		CD8+: FITC: 286			
CD8+-: APC-Cy7: 250	42	CD8-CD4-: APC-Cy7: 120	10.1		
CD8+-: FITC: -156		CD8-CD4-: FITC: 57.8			
Unstained control	%	Unstained control	%		
CD8-CD4-: APC-Cy7: 5.55	97.70	CD8-CD4-: APC-Cy7: -3.85	98.4		
CD8-CD4-: FITC: 340		CD8-CD4-: FITC: 298			
CD8+-					
Mouse 2.2h	%	Mouse 6.2h	%	Mouse 1.1h	%
CD4+: APC-Cy7: -32.5	5.57				
CD4+: FITC: 5713					
CD4+-: APC-Cy7: 38.9	4.23	CD4+: APC-Cy7: 84.8	4.49		
CD4+-: FITC: 504		CD4+: FITC: 5191			
CD8+-: APC-Cy7: 586	72.1	CD8+-CD4+: APC-Cy7: 1088	2.75	CD4+: APC-Cy7: 111	0.08
CD8+-: FITC: 232		CD8+-CD4+: FITC: 3975		CD4+: FITC: 10341	
CD8-CD4-: APC-Cy7: -23.3	15	CD8+-: APC-Cy7: 424	91.8	CD8+-: APC-Cy7: 1154	98.4
CD8-CD4-: FITC: -259		CD8+-: FITC: 153		CD8+-: FITC: 228	
Unstained control	%	Unstained control	%	Unstained control	%
CD8-CD4-: -APC-Cy7: -5.33	96.6	CD8-CD4-: APC-Cy7: -4.85	97	CD8-CD4-: APC-Cy7: -3.85	98.8
CD8-CD4-: FITC: 326		CD8-CD4-: FITC: 255		CD8-CD4-: FITC: 295	
Mouse 5.2j	%	Mouse 6.2f	%	Mouse 11.1j	%
CD8+-CD4+: APC-Cy7: 503	2.9	CD4+: APC-Cy7: -13.1	2.98	CD4+: APC-Cy7: 28.6	0.15
CD8+-CD4+: FITC: 5393		CD4+: FITC: 5213		CD4+: FITC: 8548	
CD8+-: APC-Cy7: 235	95	CD8+-: APC-Cy7: 268	95.3	CD8+-: APC-Cy7: 1084	96.5
CD8+-: FITC: 35.9		CD8+-: FITC: 60.4		CD8+-: FITC: 305	
Unstained control	%	Unstained control	%	Unstained control	%
CD8-CD4-: APC-Cy7: -4.85	96.9	CD8-CD4-: APC-Cy7: -5.33	97.1	CD8-CD4-: APC-Cy7: -5.33	96.8
CD8-CD4-: FITC: 277		CD8-CD4-: FITC: 219		CD8-CD4-: FITC: 243	

Table 86: Immunophenotype of all thymic lymphomas of CD8 lymphocytes showing the MFI of each cell type captured at APC-Cy7 and FITC channels and the percentage of each cell type. For each thymus, the MFI of unstained control sample run at each experiment is also given.

3.4.1.2.3.7. Lymphomas of predominantly double negative cells

Lymphomas of double negative phenotype have accounted for only 5% of all lymphomas. As seen in Figure 30, more than 96.1% of the cells obtained from the thymus of mouse 36.2c were negative for CD8APC-Cy7 and CD4FITC, showing that the maturation was arrested at double negative phase, with no further development into CD8+CD4+ and eventually single positives CD4 and CD8. In the left lower quadrant, it is possible to identify two distinct clusters of cells; they were both negative for CD8 and CD4 and therefore considered as a single cluster. The

CD44/CD25 gates in the same figure represent a further analysis of the neoplastic DN cells to identify exactly at which stage of the double negative maturation process the differentiation was arrested. In this case almost 100% of the T-cells did not develop further from the very first stage of DN1. As it can be seen in the upper left quadrant of CD44/CD25 gates, there are two clusters of DN1 cells that could be described as CD44+ and CD44high. In mouse 1.1j, the cell suspension obtained from its thymus was composed of 80.4% of double negative T-cells and CD4+ cells were slightly increased (19.1%), as seen in CD8 v CD4 gate. Further analysis of the DN population, seen in CD44/CD25 gates, revealed the presence of cells in all four stages of development with a considerable increase in cells at DN2 stage and a decrease in both DN3 stage, suggesting the differentiation was arrested at DN2. With further development, DN2 lymphocytes would potentially colonize the whole thymus.

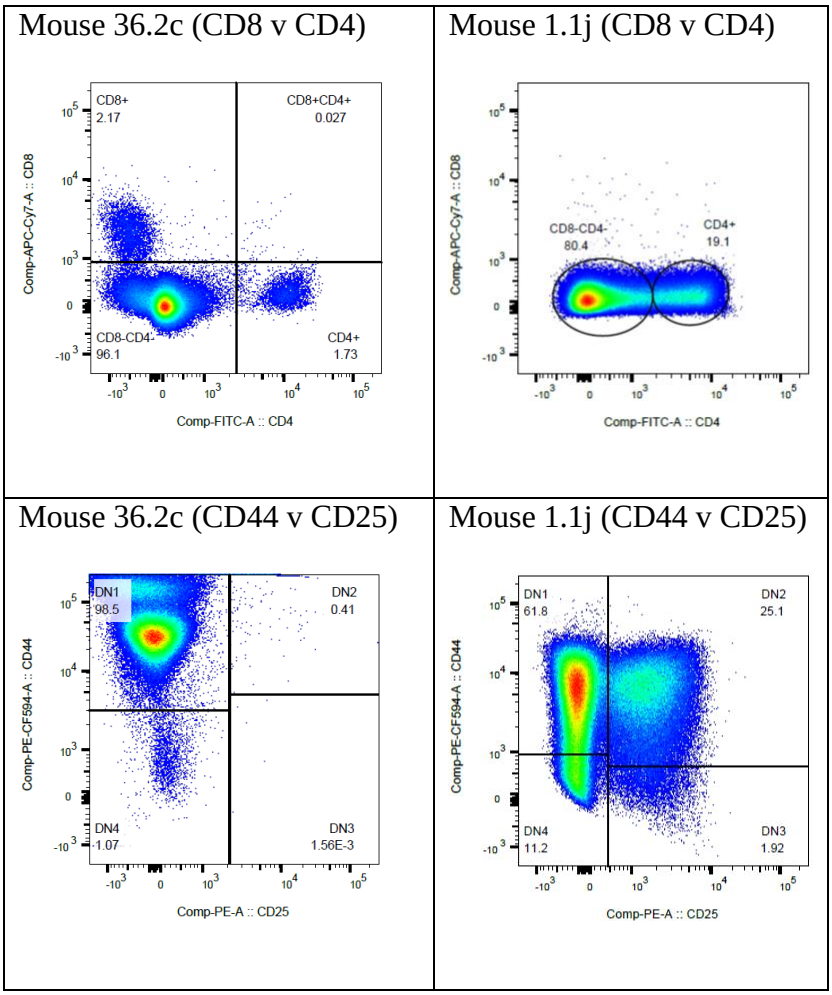


Figure 30: Flow cytometry profile of different double negative thymic lymphomas.

Information on the MFI and frequency of each cell type is presented in Table 87.

DN 1		DN2	
Mouse 1.1j	%	Mouse 36.2c	%
CD4+: APC-Cy7: 248	1.73		
CD4+: FITC: 10412			
CD8+: APC-Cy7: 2095	2.17		
CD8+: FITC: -503			
CD8+CD4+: APC-Cy7: 1327	0.03	CD4+: APC-Cy7: 219	19.1
CD8+CD4+: FITC: 4831		CD4+: FITC: 4334	
CD8-CD4-: APC-Cy7: 34.7	96.10	CD8-CD4-: APC-Cy7: 157	80.4
CD8-CD4-: FITC: 166		CD8-CD4-: FITC: 151	
DN1: PE: -19.3	**98.50**	**DN1: PE: -116**	**61.8**
DN1: PE-CF594: 33356		**DN1: PE-CF594: 5191**	
DN2: PE: 4352	**0.41**	**DN2: PE: 1544**	**25.1**
DN2: PE-CF594: 256453		**DN2: PE-CF594: 5169**	
DN3: PE: 3359	**0**	**DN3: PE: 1689**	**1.92**
DN3: PE-CF594: 2091		**DN3: PE-CF594-: 339**	
DN4: PE: 212	**1.07**	**DN4: PE: -121**	**11.2**
DN4: PE-CF594: 925		**DN4: PE-CF594: 521**	
Unstained control	%	Unstained control	%
CD8-CD4-: APC-Cy7: 8.36	98.50	Did not pass inclusion criteria	
CD8-CD4-: FITC: 261			

Table 87: Immunophenotype of all thymic lymphomas of DN lymphocytes showing the MFI of each cell type captured at APC-Cy7/FITC channels for the characterisation of CD8 and CD4 T-cells and at PE/PE-CF594 for the characterisation of DN T-cells. The percentage of each cell type. For each thymus, the MFI of unstained control sample run at each experiment is also given.

3.4.1.2.3.8. Lymphomas of mixed cells

Lymphomas in which more than one cell type was abnormally increased were grouped under this category and comprised 10% of all tumours. As shown in Figure 31, in mouse 31.2c there was an increase in CD8+, CD8+-CD4+- and of cells with a CD8+CD4+- phenotype. In mouse 10.2a, DN cells are also increased, in combination with CD4+ and subtypes of CD8CD4.

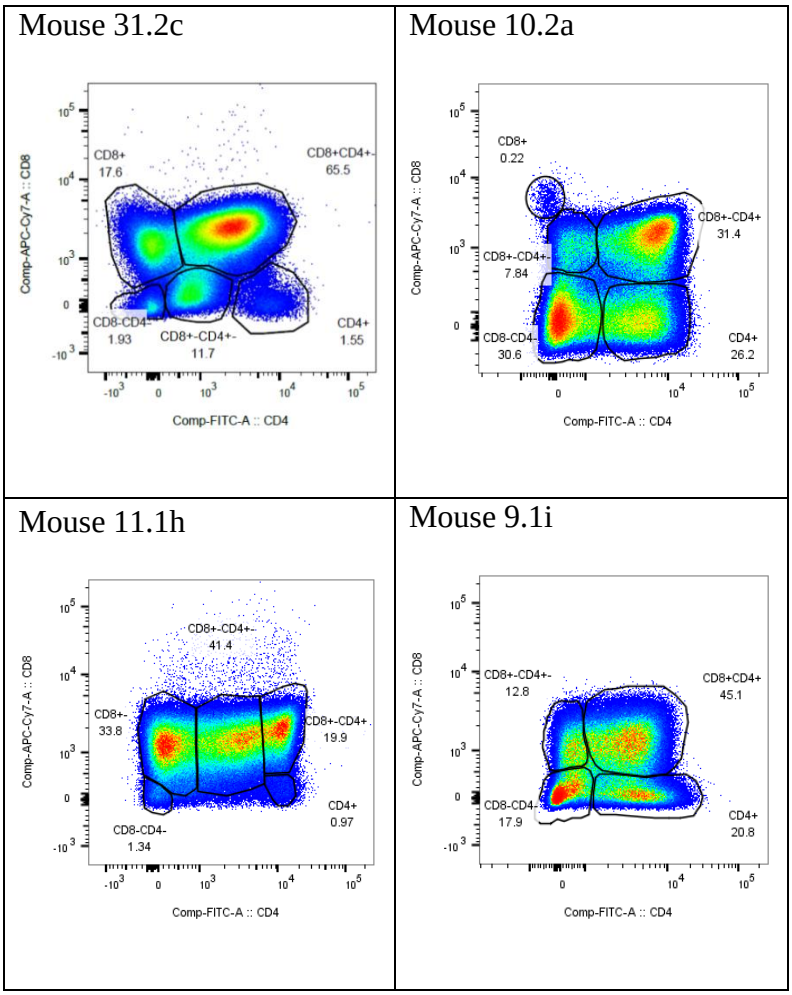


Figure 31: Flow cytometry profile of different mixed cell thymic lymphomas.

Also in mice 10.2a and 9.1i, it is arguable whether the DN cells are CD8-CD4+- instead, since there was a very low fluorescence captured in FITC channel, of 355 and 386 respectively (Table 88). The intrinsic fluorescence of cells of CD8-CD4-, provided by the analysis of unstained samples of treated mice, was 297.68+-94.73 (Appendix 2 - Tables and figures, Table 120) and supported the decision of classifying these clusters as DN.

Mixed cells			
Mouse 31.2c	%	Mouse 10.2a	%
CD4+: APC-Cy7: 107 CD4+: FITC: 6602	1.55	CD4+: APC-Cy7: 60.4 CD4+: FITC: 4301	26.2
CD8+-CD4+-: APC-Cy7: 293 CD8+-CD4+-: FITC: 823	11.7	CD8+: APC-Cy7: 4573 CD8+: FITC: -141	0.22
CD8+: APC-Cy7: 1467 CD8+: FITC: 44.9	17.6	CD8+-CD4+-: APC-Cy7: 1024 CD8+CD4+-: FITC: 627	7.84
CD8+CD4+-: APC-Cy7: 2185 CD8+CD4+-: FITC: 2144	65.5	CD8+-CD4+: APC-Cy7: 1244 CD8+-CD4+: FITC: 5419	31.4
CD8-CD4-: APC-Cy7: 11.6 CD8-CD4-: FITC: -12.8	1.93	CD8-CD4-: APC-Cy7: 62.4 CD8-CD4-: FITC: 355	30.6
Unstained control	%	Unstained control	%
CD8-CD4-: APC-Cy7: -1.28 CD8-CD4-: FITC: 270	97.50	CD8-CD4-: APC-Cy7: -4.85 CD8-CD4-: FITC: 202	99.9
Mouse 11.1h	%	Mouse 9.1i	%
CD4+: APC-Cy7: 248 CD4+: FITC: 10554	0.97		
CD8+-: APC-Cy7: 1195 CD8+-: FITC: 339	33.8	CD4+: APC-Cy7: 118 CD4+: FITC: 3726	20.8
CD8+CD4+: APC-Cy7: 1784 CD8+CD4+: FITC: 9817	19.9	CD8+-CD4+-: APC-Cy7: 1127 CD8+-CD4+-: FITC: 518	12.8
CD8+-CD4+-: APC-Cy7: 1317 CD8+-CD4+-: FITC: 2337	41.4	CD8+CD4+: APC-Cy7: 1287 CD8+CD4+: FITC: 3208	45.1
CD8-CD4-: APC-Cy7: 112 CD8-CD4-: FITC: 84.8	1.34	CD8-CD4-: APC-Cy7: 156 CD8-CD4-: FITC: 386	17.9
Unstained control	%	Unstained control	%
CD8-CD4-: APC-Cy7: -3.85 CD8-CD4-: FITC: 194	99.6	CD8-CD4-: APC-Cy7:-5.13 CD8-CD4-: FITC: 187	97.30

Table 88: Immunophenotype of all thymic lymphomas of mixed lymphocytes showing the MFI of each cell type captured at APC-Cy7/FITC channels for the characterisation of CD8 and CD4 T-cells. The percentage of each cell type and the MFI of unstained control sample is also shown.

3.4.2. Spleen

The spleen is one of the main sites for metastases of thymic lymphomas to occur. With the purpose of comparing the phenotype of the primary tumour in the thymus with the secondary tumour in the spleen, and to infer if there was a particular phenotype with higher rate of metastases, enlarged spleens found at necropsy were also collected for histology and flow cytometry analysis.

In order to include data from any spleen sample in the analysis, only samples containing 70% or more live cells in CD45/Sytox blue gate, and containing at least 100000 cells in SSC gate were included. On each plate, an unstained sample was always run.

The antibody conjugates used were mostly those used in the thymi, with the exception of CD19, a pan B-cell marker, conjugated with the fluorochrome AmCyan. As was done for the analysis of the thymi, fluorochromes APC-Cy7 and FITC, coupled with the antibodies CB8 and CD4, respectively, allowed to discriminate cells according to their expression of CD8 and CD4 surface antigens. CD44PE-CF594 and CD25PE were used but, in retrospect, their low specificity in the spleen would not allow to reach any relevant conclusions.

3.4.2.1. Controls

3.4.2.1.1. Percentage of lymphocyte populations

A total of 18 spleens have met those requirements and the results of the mean±SD of each population gated were: 67.56±5.76% of B-lymphocytes and 32.46±5.77 T-lymphocytes, and within the T-cell population, 50.75±4.34% were CD4, 28.72±5.12% were CD8, 0.45±0.24% were DP and 20.1±6.45% were DN.

3.4.2.1.2. Establishing MFI reference intervals

Based on FMO analysis and using the antibody dilutions that proved to work best, the splenic lymphocytes of control mice were characterised according to their Median Fluorescence Intensity to established reference intervals (section 2.9.8, page 99). Reference intervals revealed the range of fluorescence that characterises as positive and negative each type of splenic lymphocyte, and intermediate (+-) MFIs were established as the range of MFIs between positive and negative MFIs (Table 89).

Antibody conjugate	MFI Reference interval
B-lymphocytes | Median (Comp-AmCyan-A)	[3096.8 - 6091.2]
T-lymphocytes | Median (Comp-AmCyan-A)	[199.2 - 392.2]
CD8+ | Median (Comp-APC-Cy7-A)	[2768 - 6896]
CD8+ | Median (Comp-FITC-A)	[143.66 - 256.14]
CD4+ | Median (Comp-APC-Cy7-A)	[(-2.26) - 39.62]
CD4+ | Median (Comp-FITC-A)	[7864 - 12724]
CD8+CD4+ | Median (Comp-APC-Cy7-A)	[513.4 - 4044.6]
CD8+CD4+ | Median (Comp-FITC-A)	[741 - 6073]
CD8+CD4+- | Median (Comp-APC-Cy7-A)	[513.4 - 4044.6]
CD8+CD4+- | Median (Comp-FITC-A)	[258.64 - 741]
CD8+-CD4+ | Median (Comp-APC-Cy7-A)	[36.76 - 513.4]
CD8+-CD4+ | Median (Comp-FITC-A)	[741 - 6073]
CD8+-CD4+- | Median (Comp-APC-Cy7-A)	[36.76 - 513.4]
CD8+-CD4+ -| Median (Comp-FITC-A)	[258.64 - 741]
CD8-CD4- | Median (Comp-APC-Cy7-A)	[7.28 - 36.76]
CD8-CD4- | Median (Comp-FITC-A)	[155.76 - 258.64]

Table 89: MFI reference intervals of splenic T-lymphocytes sub-types and B-lymphocytes in control mice.

3.4.2.2. Treated

The same inclusion criteria applied to spleen samples from control animals was applied to samples from treated mice - at least 70% of live cells in CD45/Sytox blue gate, and at least 100000 cells in the SSC singlets gate. Although 58 spleens from treated mice were analysed, only results from those that have met the inclusion criteria, had a histological confirmation of thymic lymphoma with metastasis to the spleen and a flow cytometry analysis of the thymus, are presented here. The purpose was to compare the phenotype of the same tumour in the original organ and in the secondary location and indeed to assess if there was any particular phenotype with a higher metastization rate. In the limited number of samples that were selected to be presented here, there was not a phenotype of thymic lymphoma that has spread to the spleen more frequently. Examples of the flow cytometry profile of primary and secondary thymic lymphomas are presented below.

3.4.2.2.1. Spleen metastasis of a CD8+CD4+- thymic lymphoma

In Figure 32A, the flow cytometry plot of the primary tumour that was present in the thymus, it is possible to see a smaller cluster of cells with higher MFI on APC-Cy7 channel and slightly higher MFI of FITC channel, that could be classified as CD8high. This was a unique case and no distinction between positive and highly positive CD8 cells was made here. The slightly higher expression of CD4 was not enough to classify it as CD4+. A classification of CD8+CD4+ was therefore attributed to the whole group of cells. Figure 32B, C and D, refer to the spleen. In B, it is possible to see an increase in T-lymphocytes (95.9% of all splenic lymphocytes) when compared with the normal values found in controls (67.56±5.76% of B-lymphocytes and 32.46±5.77 of T-lymphocytes) indicating a departure from the normal cell composition found in this organ and highly suggestive of a T-cell neoplasia. T-cells are well differentiated from B-cells after being stained with CD19, an antibody known for being a B-cell marker. As mentioned previously, CD19 was paired with the fluorochrome AmCyan and as seen in Figure 32B, only 4.01% of all splenic lymphocytes had a positive emission on the AmCyan channel. Further investigation of this clone of splenic T-cells, by looking at their emission on the APC-Cy7 and FITC channels to assess their CD8 v CD4 composition, revealed that, as shown in Figure 32C, 97.6% were CD8CD4 double positive, a similar phenotype to the original thymic neoplasm - or arguably the same. In absolute MFI values, the emission of the primary tumour cells on the FITC channel was, as indicated in Figure 32A, 1421, rendering it a CD4 intermediate according to MFI reference intervals for the thymus, and 1741 in the metastasis, rendering it a CD4 positive, according to the reference intervals for the spleen. Additionally, it is well known that the amount of CD8CD4 DP cells found in the normal spleen is minimal, 0.45±0.24% in the controls studied during this project,

as they mature into single positive CD4 and CD8 before leaving the thymus onto the blood stream. Therefore, the presence of a cluster of lymphocytes comprised of 97.8% of double positive cells in this organ is a departure from normal. In Figure 32D, the MFI obtained from a cell suspension of the spleen from the same animal, submitted to the same steps except that did not have the antibody cocktail added to it, and therefore any fluorescence is merely due to intrinsic auto fluorescence, is presented - its use is simply to help understanding where true negative cells lie in case of doubt.

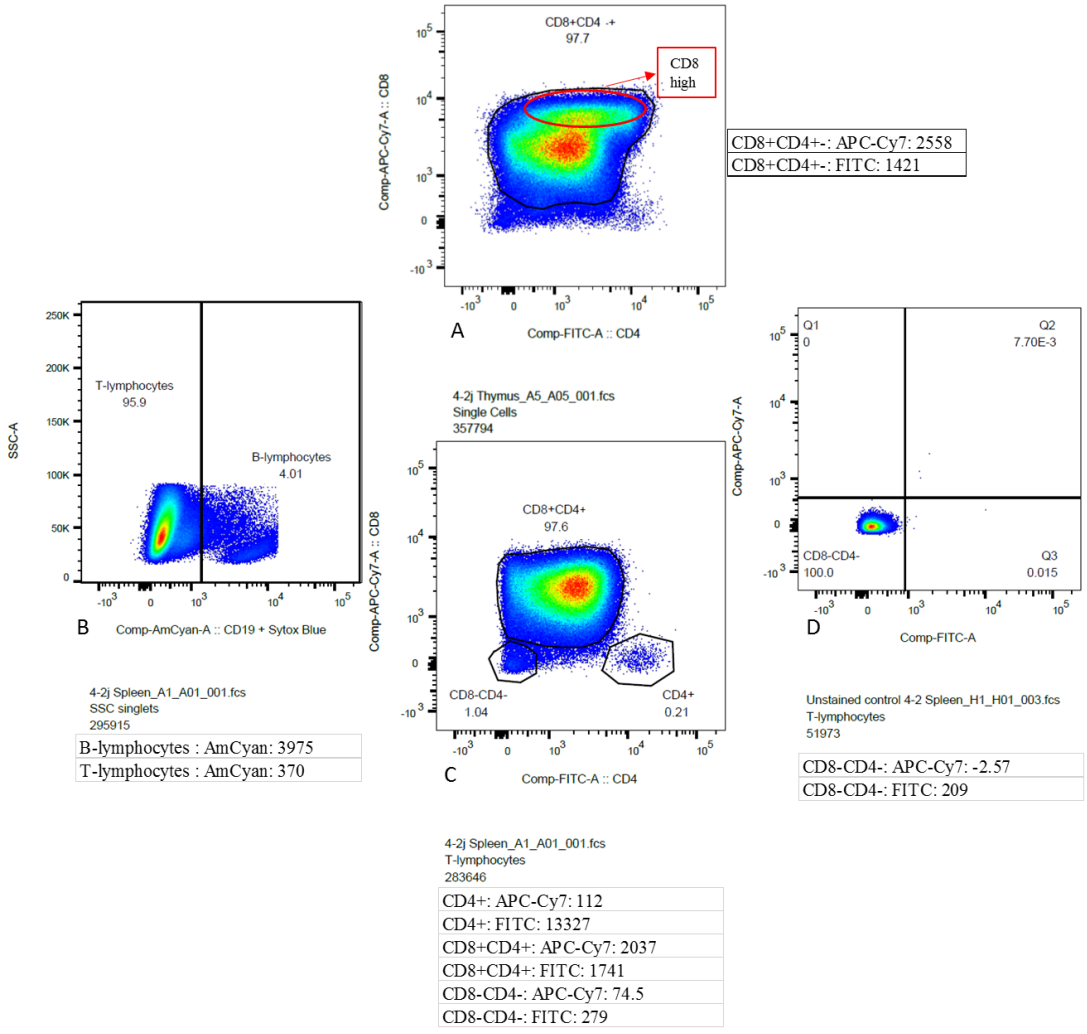


Figure 32: Flow cytometry profile of a metastatic CD8+CD4+- thymic lymphoma affecting the spleen. A) Immunophenotype of the primary tumour on the thymus according to the MFI captured at APC-Cy-7 and FITC channels allowing to classify cells according to their surface CD8 and CD4 antigen expression. B) 95.5% of all splenic lymphocytes were T-cells with only 4.01% of B-cells with a positive fluorescence (3975) captured in AmCyan channel. C) Further characterisation of T-cells from B showing a slight increase in expression on CD4 marker in comparison with the primary tumour. D) Unstained control for C.

3.4.2.2.2. Spleen metastasis of a DP CD8+CD4+ thymic lymphoma

In Figure 33, there is an example of how the FC profile of the metastasis helped with the classification of the phenotype of the primary tumour. Just by looking at the FC results in A, all 4 populations seemed to be approximately within the control values, with CD4+ lymphocytes being marginally increased, leading to the assumption that this would be a CD4+ type tumour. Nevertheless, when looking at the phenotype of the metastasis, in C, there was a very significant increase in DP cells, which are almost absent in normal spleens, showing that the differentiation of the thymic lymphocytes was arrested and tumour was formed in the thymus at double positive state.

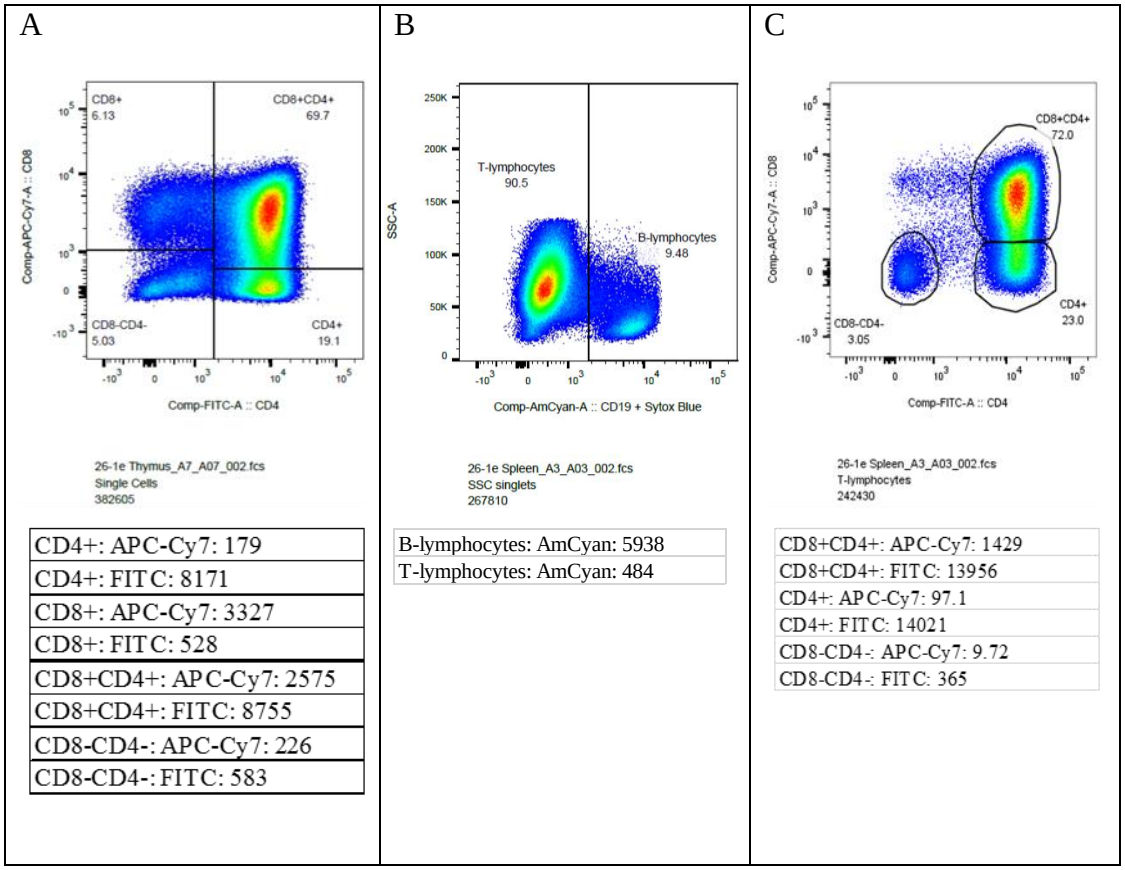


Figure 33: Flow cytometry profile of a metastatic CD8+CD4+ thymic lymphoma affecting the spleen. A) Phenotype of the primary tumour in the thymus according to the MFI captured at APC-Cy-7 and FITC channels allowing to classify cells according to their surface CD8 and CD4 antigen expression. B) 90.5% of all splenic lymphocytes were T-cells, with only 9.48% being B-cells with a positive fluorescence (5938) captured in AmCyan channel. C) Further characterisation of T-cells from B confirming the nature of the primary tumour as a DP CD4+CD8+.

3.4.2.2.3. Spleen metastasis of a CD8+-CD4+ thymic lymphoma

As in previous examples, in Figure 34A, it is possible to see the phenotype of the primary tumour on the thymus, in which the majority (79.6%) of T-lymphocytes emitted an intermediate fluorescence on the APC-Cy-7 channel (849) and positive fluorescence on the FITC channel (4771). Still in the thymus there was a slight increase in CD4intermediate lymphocytes (16.2%). In Figure 34B, it is clear that the cells suspension obtained from the spleen of the same animal had a predominance of T-lymphocytes (62.4%), characterised by a low emission on AmCyan channel. In Figure 34C, it is possible to see the phenotype of the secondary tumour on the spleen- there is a strong similarity between both primary tumour and metastasis, although in the spleen, there was a slight increase of fluorescence captured in FITC channel. The presence of a majority of CD8+-CD4+ lymphocytes in the spleen confirms that the nature of the primary tumour.

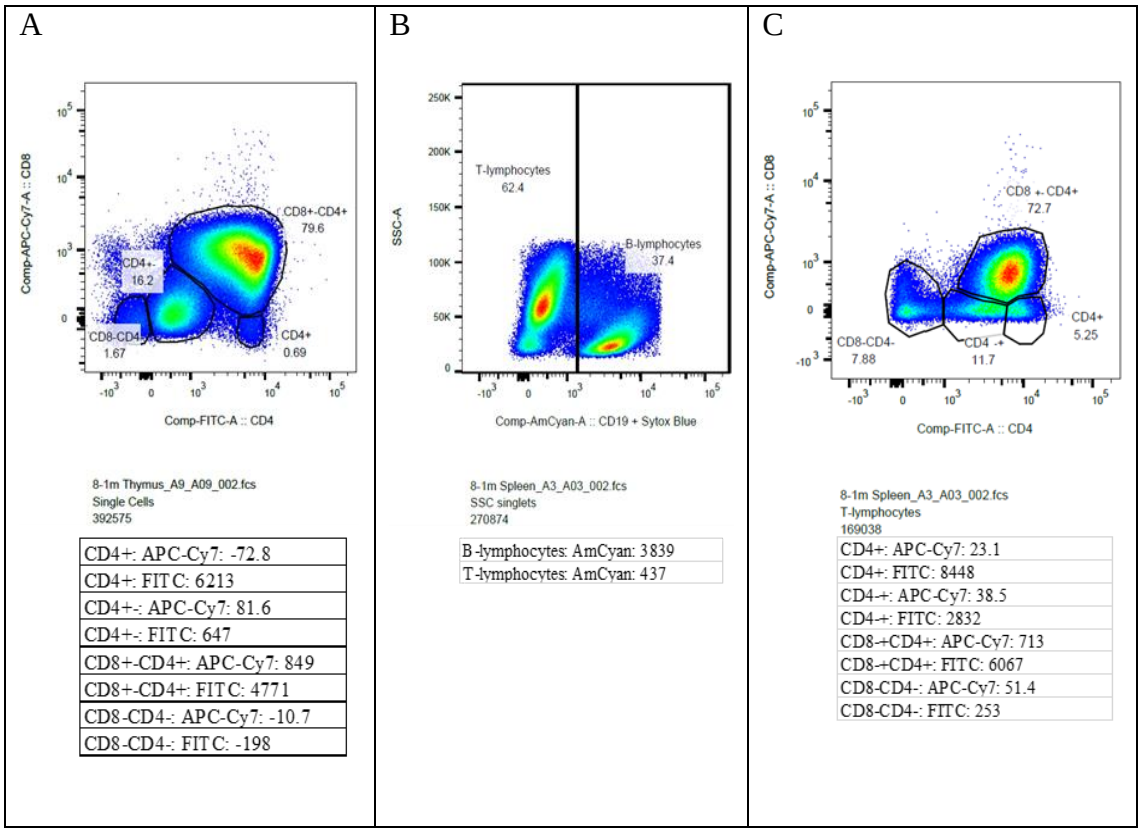


Figure 34: Flow cytometry profile of a metastatic CD8+-CD4+ thymic lymphoma affecting the spleen. A) The phenotype of the primary tumour on the thymus according to the MFI captured at APC-Cy-7 and FITC channels allowing to classify cells according to their surface CD8 and CD4 antigen expression. B) 62.4% of all splenic lymphocytes were T-cells, with 37.4% being B-cells with a positive fluorescence (3839) captured in AmCyan channel. C) Further characterisation of cells T-cells from B showing a similar profile to that of the primary tumour.

3.4.2.2.4. Spleen metastasis of CD8+-CD4+- thymic lymphomas

Figure 35A shows the phenotype of the primary thymic lymphomas, whereas Figure 35B and Figure 35C, as in previous examples, show the phenotype of the metastasis affecting the spleen. Although the phenotypes in A and C are very similar, the metastasis had slight increase of fluorescence captured at FITC channel, from 1337 to 1910, similar to what was seen with other examples of metastasis already shown. As a consequence, the classification of the primary tumour (CD8+-CD4+-) changed to CD8+-CD4+ although there is no reason to believe they are different populations. In B it is possible to see the vast colonisation of the spleen by the thymic neoplastic cells, as 93.7% of all splenic lymphocytes are T-lymphocytes, with only 6.27% of B-

lymphocytes, which is a severe departure from the cell composition normally seen in this organ.

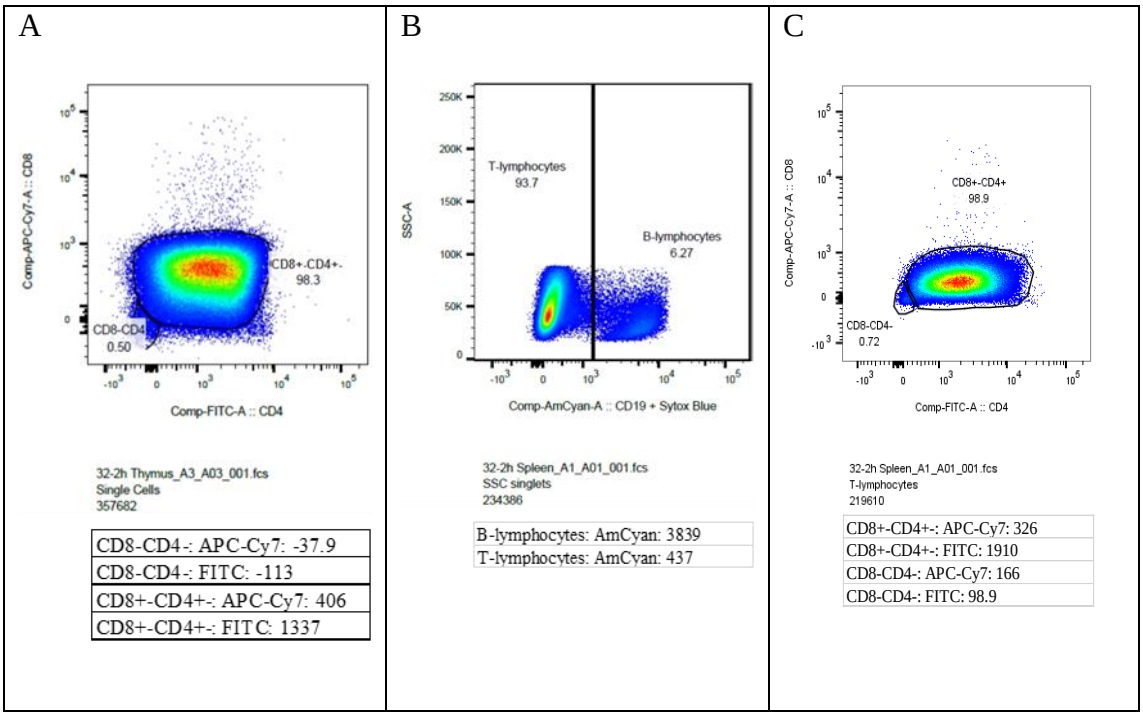


Figure 35: Flow cytometry profile of a CD8+-CD4+- thymic lymphoma affecting the spleen. A) Immunophenotype of the original thymic lymphoma according to the MFI captured at APC-Cy-7 and FITC channels allowing to classify cells according to their surface CD8 and CD4 antigen expression. B) 93.7% of all splenic lymphocytes were T-cells with only 6.27% B-cells with a positive fluorescence (3839) captured in AmCyan channel. C) Further characterisation of T-cells from B showing revealing a population with identical MFI of the primary tumour.

In Figure 36, another example of a CD8+-CD4+- thymic lymphoma (in A) that has spread into the spleen (B and C) can be appreciated. Similarly, to what was seen in other spleen metastases presented above, these cells seem to have more CD4 antigen molecules at their surface, revealed by the higher MFI captured in the FITC channel.

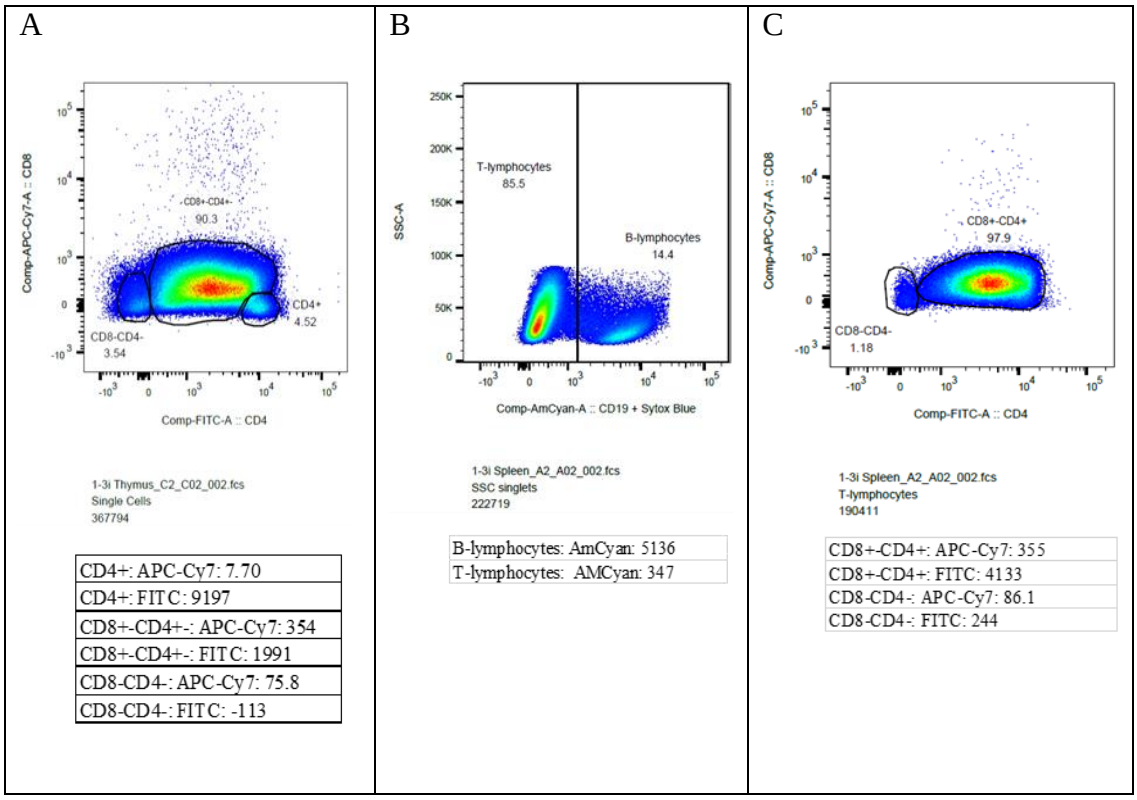


Figure 36: Flow cytometry profile of a CD8+-CD4+- thymic lymphoma affecting the spleen. A) Immunophenotype of the original thymic lymphoma according to the MFI captured at APC-Cy-7 and FITC channels allowing to classify cells according to their surface CD8 and CD4 antigen expression. B) 85.5% of all splenic lymphocytes were T-cell, with 14.4% of B-cells with a positive fluorescence (5136) captured in AmCyan channel. C) Further characterisation of T-cells from B showing a higher expression of CD4 marker then that of the primary tumour.

3.4.2.2.5. Spleen metastasis of a CD8+ thymic lymphoma

Figure 37 shows the only case of a metastasis that was not of CD8CD4, but of CD8+ cells. As shown in A, 87.2% of all thymic lymphocytes had an MFI of 1853 captured in APC-Cy7 channel and a very low MFI of 55.2 captured in the FITC channel, revealing their CD8 single positive nature. Still in A, it is possible to see a slight increase in DN cells, when compared to control. The phenotype of the metastasis also revealed an increase in CD8+ lymphocytes, but also a considerable percentage of DN cells, which are, possibly, a combination of the natural DN residents in the spleen, 20.1±6.45% as seen in controls, and DN cells found in A that might have also migrated.

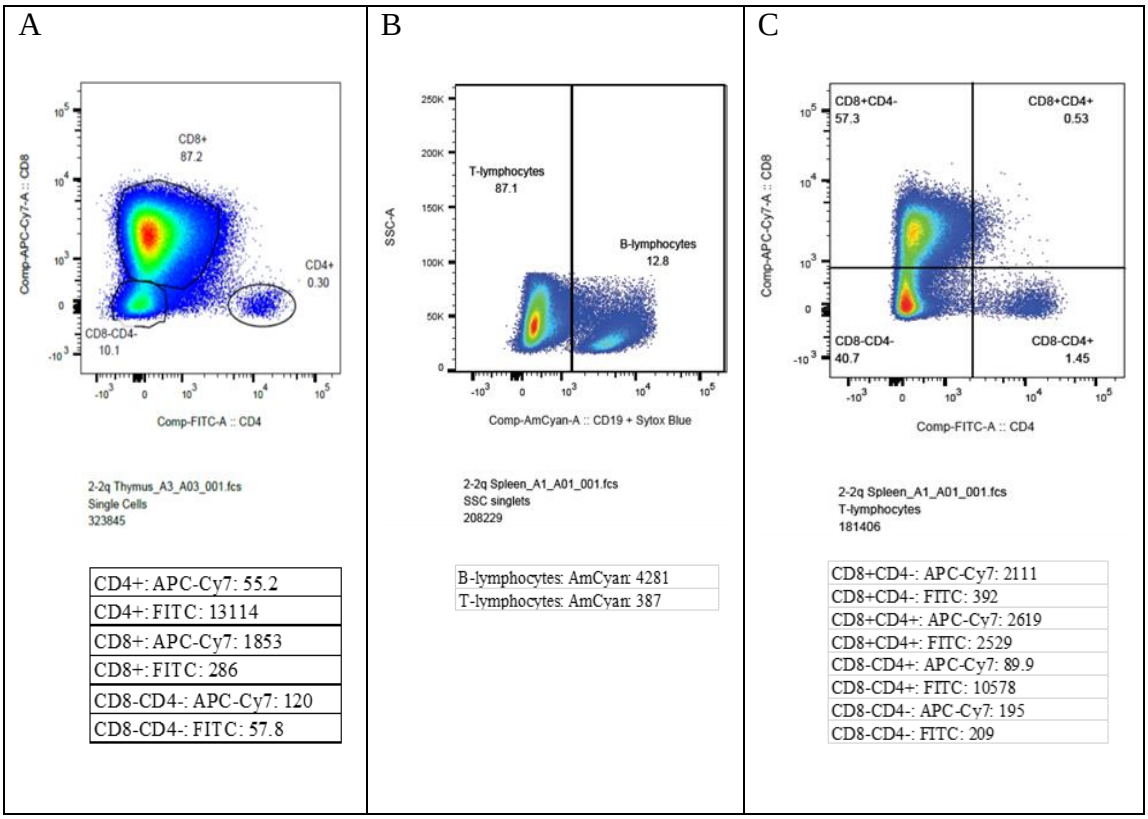


Figure 37: Flow cytometry profile of a metastatic CD8+ thymic lymphoma affecting the spleen. A) The phenotype of the primary tumour on the thymus according to the MFI captured at APC-Cy-7 and FITC channels allowing to classify cells according to their surface CD8 and CD4 antigen expression. B) 87.1% of all splenic lymphocytes were T-cells. C) Further characterisation of cells T-cells from B showing a majority of CD8+ lymphocytes.

3.5. Genetic analysis

3.5.1. DNA extraction

DNA extraction results for 192 mice are shown in tables 1 and 2. The DNA concentration obtained from each DNA suspension is expressed in ng/µl. The volume taken from each suspension needed to achieve 350 ng of DNA for genotyping is also shown. DNA was analysed using the GigaMuga SNP panel.

Column	ID	DNA (ng/µl)	Volume containing 350 ng (µl)	Column	ID	DNA (ng/µl)	Volume containing 350 ng (µl)	Column	ID	DNA (ng/µl)	Volume containing 350 ng (µl)
1	1.1B	52.71	6.6	2	11.1H	80.31	4.4	3	9.1P	89.11	3.9
	1.1F	83.15	4.2		6.2D	114.5	3.1		6.2F	96.99	3.6
	2.1L	66.85	5.2		6.2H	101.9	3.4		1.3I	94.47	3.7
	2.1R	91.22	3.8		16.2C	50.86	6.9		4.2R	109.1	3.2
	1.1H	66	5.3		11.1R	94.29	3.7		5.2E	93.06	3.8
	2.1S	47.87	7.3		9.1E	20.97	16.7		4.2J	55.72	6.3
	4.1A	74.41	4.7		12.1K	75.26	4.7		6.2A	30.44	11.5
	6.1J	74.01	4.7		8.1M	96.92	3.6		7.1D	43.56	8.0
4	16.1G	99.66	3.5	5	26.1E	82.37	4.2	6	2.2H	78.16	4.5
	5.2B	101.50	3.4		36.1A	71.55	4.9		2.2I	94.84	3.7
	36.2C	93.25	3.8		29.2B	75.55	4.6		31.1B	92.78	3.8
	9.1O	93.87	3.7		32.2C	102	3.4		36.1I	57.65	6.1
	27.2B	94.35	3.7		32.2H	81.75	4.3		26.1G	72.31	4.8
	6.2K	104.70	3.3		1.1J	87.47	4.0		29.2C	98.17	3.6
	32.2A	54.19	6.5		32.1F	37.22	9.4		10.2A	35.76	9.8
	37.1E	108.10	3.2		3.2F	20.58	17.0		37.1L	63.1	5.5
7	3.2J	78.58	4.5	8	5.1O	108.6	3.2	9	7.1G	120.5	2.9
	29.2E	117.1	3.0		9.1I	124.5	2.8		3.2G	137.1	2.6
	24.1G	115.2	3.0		6.1I	105.7	3.3		29.2I	74.12	4.7
	34.2A	94.67	3.7		6.1E	130.3	2.7		12.1C	42.27	8.3
	36.2D	89	3.9		1.3G	135.3	2.6		29.2G	98.84	3.5
	27.2F	102.1	3.4		7.1M	108.4	3.2		4.2H	46.4	7.5
	5.2J	65.93	5.3		28.1T	45.21	7.7		8.1F	61.01	5.7
	7.1Q	52.28	6.7		12.1I	56.73	6.2		29.1D	80.18	4.4
10	36.1B	64.44	5.4	11	4.2K	50.2	7.0	12	1.2I	76.83	4.6
	7.1A	108.8	3.2		4.2M	55.18	6.3		7.1B	82.28	4.3
	7.1N	116.7	3.0		14.1H	32.69	10.7		10.2E	94.97	3.7
	2.2C	98.9	3.5		5.2S	83.53	4.2		3.2D	35.96	9.7
	2.2G	113.5	3.1		6.1P	59.58	5.9		6.2B	98.14	3.6
	4.2O	104.4	3.4		6.1F	66.44	5.3		6.2C	99.53	3.5
	8.1L	41.33	8.5		3.1F	47.44	7.4		8.1H	46.54	7.5
	8.1N	102.4	3.4		6.1O	93.71	3.7		8.1J	90.83	3.9

Table 90: DNA extraction results and volume required for genotyping for plate 1

Column	ID	DNA (ng/µl)	Volume containing 350 ng (µl)	Column	ID	DNA (ng/µl)	Volume containing 350 ng (µl)	Column	ID	DNA (ng/µl)	Volume containing 350 ng (µl)
1	1.1L	50.93	6.9	2	15.1K	103.4	3.4	3	28.1N	111.2	3.1
	2.1G	38.45	9.1		35.1P	126.5	2.8		28.1L	110.6	3.2
	6.1C	45.12	7.8		24.1N	106.7	3.3		28.1K	108	3.2
	1.2G	51.01	6.9		16.1C	130	2.7		28.1I	65.34	5.4
	37.1K	85.81	4.1		36.2G	103.8	3.4		27.2A	54.67	6.4
	37.1F	100.3	3.5		35.1L	129.7	2.7		32.2I	105.5	3.3
	36.1E	114.8	3.0		23.1L	96.31	3.6		32.2D	72.38	4.8
	29.1C	74.7	4.7		28.1Q	135.2	2.6		22.2I	113.8	3.1
4	28.1U	79.23	4.4	5	3.2O	119.1	2.9	6	4.2P	72.78	4.8
	28.1S	88.75	3.9		11.1L	142.7	2.5		37.2C	94.71	3.7
	9.1F	41.76	8.4		1.2E	140.9	2.5		4.2Q	111.3	3.1
	32.2G	85.32	4.1		7.1U	74.82	4.7		27.1E	42.87	8.2
	2.2E	81.98	4.3		9.1R	82.88	4.2		35.1N	65.5	5.3
	7.1F	80.25	4.4		7.1P	132.8	2.6		3.2S	42.52	8.2
	28.1D	102.00	3.4		6.2J	112.5	3.1		28.1R	74.06	4.7
	36.1C	63.88	5.5		3.2K	52.43	6.7		9.1H	120.3	2.9
7	5.2R	70.3	5.0	8	4.2L	32.6	10.7	9	3.1H	55.49	6.3
	28.1J	29.18	12.0		3.2Q	121.7	2.9		5.1N	46.21	7.6
	8.1P	37.18	9.4		1.3F	70.33	5.0		5.1F	22.05	15.9
	31.2A	56.41	6.2		1.3J	76.37	4.6		5.1G	76.44	4.6
	2.2F	43.57	8.0		9.1N	98.95	3.5		22.2H	77.76	4.5
	8.1G	76	4.6		8.1D	77.15	4.5		36.2H	62.46	5.6
	6.2E	67.98	5.1		5.2T	82.62	4.2		29.1F	69.06	5.1
	5.2A	89.42	3.9		6.1L	95.01	3.7		11.1B	90.77	3.9
10	29.2A	76.35	4.6	11	16.1A	93.53	3.7	12	10.2C	74.42	4.7
	12.1S	60.21	5.8		12.1G	46.37	7.5		11.1J	120.3	2.9
	34.1B	98.51	3.6		2.2K	106.8	3.3		4.2S	130.9	2.7
	1.2C	112.3	3.1		11.1N	75.5	4.6		36.1D	74.8	4.7
	6.1G	70.29	5.0		12.1N	100.6	3.5		5.2H	24	14.6
	31.2C	74.1	4.7		16.1H	104	3.4		35.1M	44.97	7.8
	37.1C	86.11	4.1		2.2Q	44.18	7.9		28.1C	48.71	7.2
	36.1H	94.46	3.7		11.1E	88.3	4.0		31.1D	53.42	6.6

Table 91: DNA extraction results and volume required for genotyping for plate 2

3.5.2. QTL analysis

To determine loci associated with the development of ENU induced lymphoma, a QTL analysis was undertaken using genotyping data derived from individual mice and absolute thymus weight as the quantitative trait. As a result of loading the data into WINQTL 2.5, an error message “Marker genotype '-' in chr-1, mk-6, ind-15 isn't in Translation Table” was shown. An investigation of its meaning was not conclusive. Nevertheless, if true, being just the information on a single genotype on a single marker, it was considered not to have an impact on the result – it was 1 cell out of approximately 57000 cells. The data set was examined carefully and the information was present. Technical support was contacted but there was no response. This error message was dismissed.

Interval Mapping (IM) and Composite Interval Mapping (CIM), used for estimating the position of a QTL between two markers, were carried out. CIM adds background loci to simple IM.

3.5.2.1. Interval Mapping Analysis

The threshold of significance was established at 11.5 and a QTL was identified in chromosome 3, positioned about 48.3 cM from the left end of the chromosome, with an additive effect of 0.083, accounting for 9.3% of the variance in the trait (Figure 38 and Table 92). The additive effect is an estimate of the change in the average phenotype that would be produced by substituting a single allele of one type with that of another type (e.g. *a* replaced by *A*) in a population (Williams RW, 2015).

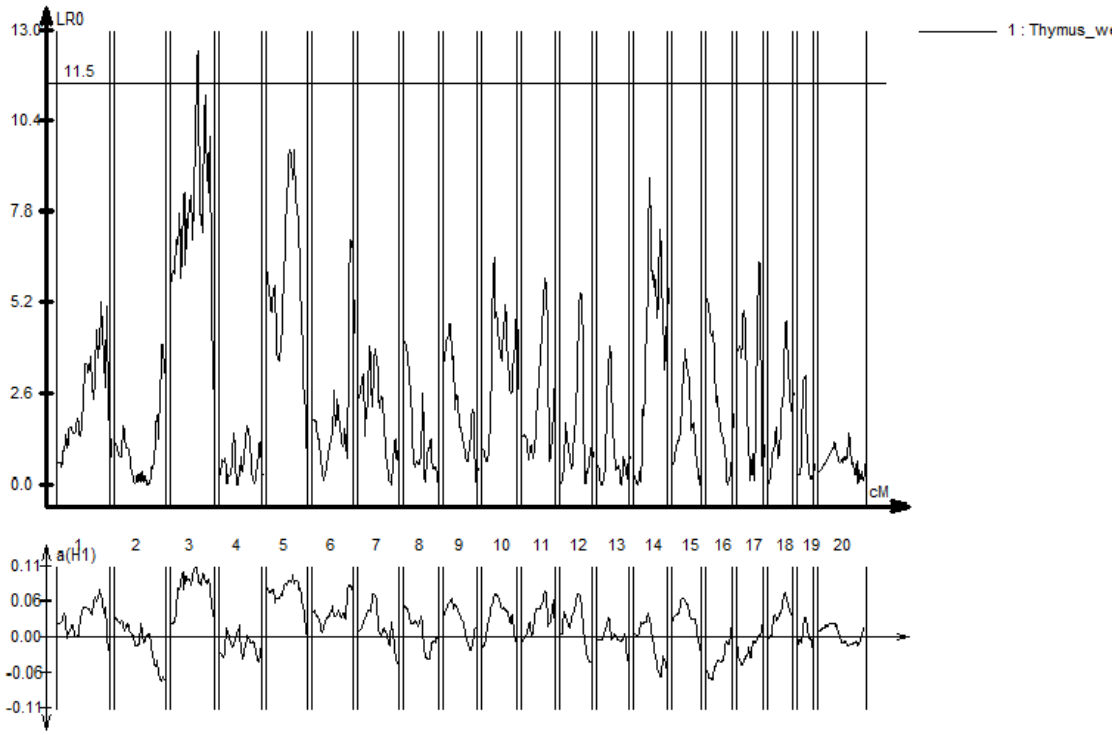


Figure 38: Interval mapping result for the continuous variable thymus weight showing a peak surpassing the significance level (horizontal line at 11.5 LR) in chromosome 3, indicating a possible QTL.

Trait	Chrom	Marker	Position	LOD Score	Additive	Dominance	R2	TR2	S
1	3	12	48.3000	2.6983	0.0830	-0.0657	0.0931	0.0984	88.8073

Table 92: EQTL result for Interval Mapping Analysis on thymus absolute weight.

3.5.2.2. Composite Interval Mapping

The threshold (LR) was established at 17.86 and no QTLs were found (Figure 39). Nevertheless, the highest peak was still at chromosome 3.

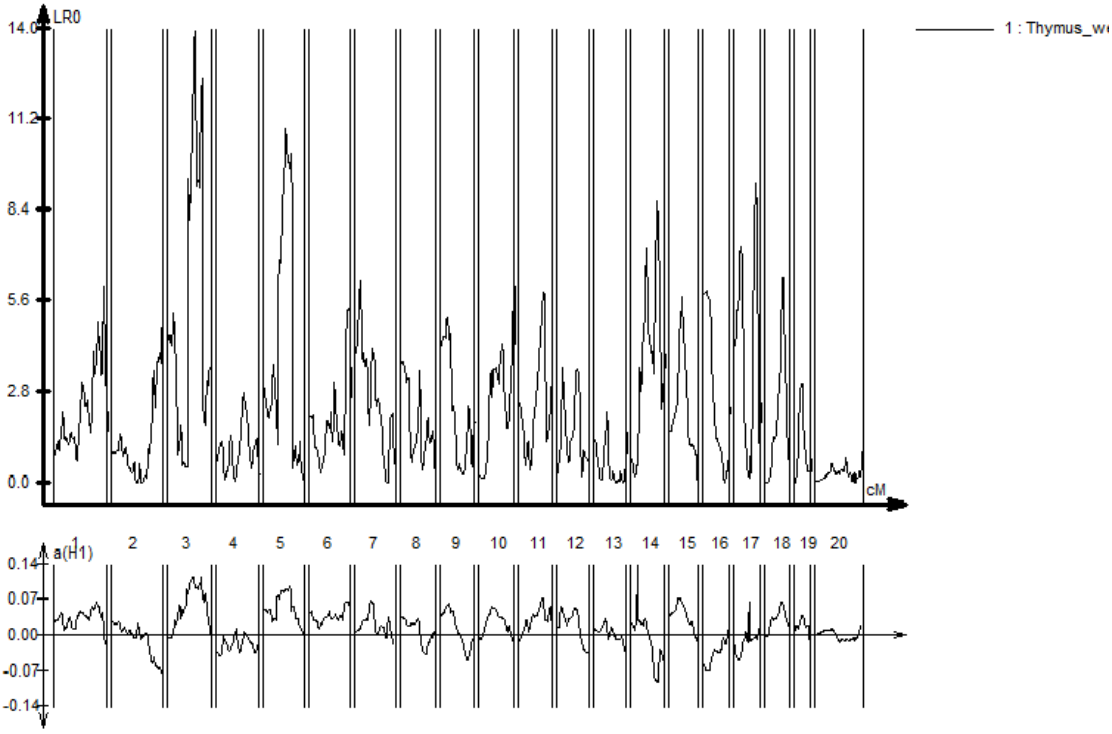


Figure 39: Composite Interval Mapping result for the continuous variable "thymus weight" showing that no QTLs were identified.

3.5.3. Identification of candidate genes

The identification of a QTL on chromosome 3 by Interval Mapping analysis led to the investigation of candidate genes located in the region between the markers positioned immediately before and after the QTL. The Sanger sequencing database, (Wellcome Trust Sanger Institute, 2011), was used to search at the vicinity of the QTL (48.3 cM, equivalent to 96525953 bp). The proximal edge of that region was defined by the marker located at 87248346 bp and the distal edge by the marker located at 105034644 bp. The search was focused on SNPs that affect protein sequence and for that, at SNP/Indel types, the following search criteria was selected: incomplete terminal codon variant, initiator codon variant, missense variant, nonsense-mediated

decay (NMD) transcript variant, splice acceptor variant, splice donor variant, splice region variant, stop gained and stop lost. As for structural variant types, complex events, copy number gains, deletion, insertion and inversion were selected.

3.5.3.1. Single nucleotide polymorphisms

One hundred and six genes were found in between the left and right edges of the QTL. Information about each gene was collected using Mouse Genome Informatics database, (Eppig et al., 2015) and the National Centre for Biotechnology Information database (NCBI, 2016), as well as the usual literature search engines. The Ensembl database (Yates et al., 2016), was used to identify if and how the change in nucleotide would result in the substitution of an amino acid in the protein, and the likelihood of having affected its function. Sorting Intolerant from Tolerant (SIFT) score (Sim et al., 2012), which predicts whether an amino acid substitution affects protein function based in sequence homology and the physical properties of amino acids was used.

Based on published information, genes found within the QTL were selected as candidates, as they have previously been related to cancer pathogenesis and/or lymphocyte biology. For each gene, at each position, the base pair present in the reference stain (C57BL/6J) is shown, followed by how it differs in A/J mice, how the variant is classified, how the new codon results in modifying the amino acid and the likelihood of causing modifications in protein function. For genes with multiple variants that did not result in amino acid replacements, an indication of how many variants were found is given (Table 93). Complete information of each variant is shown in Appendix 2 - Tables and figures. The meaning of abbreviations used for each amino acid can be found in Appendix 2 - Tables and figures, Table 122.

Position	Gene	C57BL/6	A_J	Consequences	AA	SIFT
87257389	*Fcrls*	T	C	Missense variant	-	-
87367745	*Cd5l*	A	G	Missense variant	N/S	0.58, T
87384839	*Fcrl1*	C	G	Missense variant	P/A	0.22, T
87385323	*Fcrl1*	C	T	Splice region variant	-	-
87385732	*Fcrl1*	T	C	Missense variant	L/P	0.17, T
87389383	*Fcrl1*	C	T	Missense variant	P/S	1, T
87443666	*Fcrl5* (a)	C	A	Missense variant	P/H	0.13, T
87443680	*Fcrl5*	T	C	Missense variant	F/L	0.57, T
87443684	*Fcrl5*	A	C	Missense variant	Y/S	0.41, T
87443693	*Fcrl5*	G	A	Missense variant	R/H	0.76, T
87443780	*Fcrl5*	T	G	Missense variant	V/G	0.12, T
87444264	*Fcrl5*	A	G	Missense variant	K/R	0.13, T
87444307	*Fcrl5*	T	A	Missense variant	S/R	0.92, T
87446385	*Fcrl5*	A	G	Missense variant	K/E	0.27, T
87446463	*Fcrl5*	T	C	Missense variant	Y/H	0.02, D
87446476	*Fcrl5*	A	C	Missense variant	N/T	0.01, D
87536340	*Etv3*	G	T	Missense variant	M/I	0.61, T
87536471	*Etv3*	T	C	Missense variant	V/A	1, T low confidence
87847667	*Sh2d2a* (b)	A	G	Missense variant	N/S	1, T
88854680	*Gon4l*	C	T	Missense variant	P/L	0.01, D
88895267	*Gon4l*	G	T	Missense variant	A/S	0.06, T
88908282	*Gon4l*	T	C	Missense variant	S/P	1, T low confidence
88718080	*Rit1* (c)	T	C	NMD transcript variant	-	-
94933406	*Selenbp1* (d)	G	A	NMD transcript variant	-	-
94959097	*Rfx5* (e)	G	A*	Missense variant NMD transcript variant	R/Q	0.2, T low confidence
95734876	*Ecm1*	T	C	Missense variant	I/V	0.13, T
95932170	*Anp32e* (f)	T	A	NMD transcript variant	-	-
96805720	*Cd160*	T	C	Missense variant	N/S	1, T
100138730	*Wdr3* (g)	T	C	Missense variant	K/R	1, T
100153578	*Wdr3*	C	T*	Missense variant NMD transcript variant	V/M	0.12, T
100928128	*Trim45*	A	G	Missense variant	I/V	0.39, T
100930059	*Trim45*	G	A	Missense variant	-	-
100931711	*Trim45*	A	G	Missense variant	D/G	-
100931837	*Trim45*	T	C	Missense variant	L/S	-
102163294	*Vangl1*	C	A	Splice region variant	-	-
103746072	*Hipk1* (h)	A	C	NMD transcript variant	-	-
103862050	*Ptpn22* (i)	A	G	NMD transcript variant	-	-
104865646	*St7l* (j)	C	T	NMD transcript variant	-	-

*Table 93: Single nucleotide polymorphisms in genes related to the pathogenesis of cancer and lymphocyte biology identified in the QTL. The differences in nucleotides at specific positions between C57BL/6 and A/J mice genes are shown. In AA (amino acid) column, the amino acid replacement is indicated, followed by the SIFT score on how the substitution in amino acid is predicted to affect protein function: T (tolerated), D (deleterious, <0.05). *Multiple consequences; (a, b): two additional splice region variants were found, (c) 26 additional NMD transcript variants were found, (d) 56 additional NMD transcript variants, (e) 3 additional NMD transcript variants, (f) 2 additional NMD transcript variants, (g) 27 additional NMD transcript variants, (h) 71 NMD transcript variants, (i) 266 additional NMD transcript variants, and (j) 89 additional NMD transcript variants.*

3.5.3.2. Insertions/deletions

Using the same resources described for SNPs, insertions and deletion variants in A/J genes, located in the QTL and related to the pathogenesis of cancer and lymphocyte biology, were identified. The differences in nucleotides at specific positions between C57BL/6 and A/J mice genes are shown. In AA (amino acid) column, the amino acid replacement would be indicated, followed by the SIFT score on how the substitution in amino acid was likely to affect protein function, but given they are all located in introns, that information does not apply and is difficult to predict, respectively. Nine variants where found for *Rit1*, 18 for *Selenbp1*, 4 for *Anp32e*, 6 for *Wdr3*, 2 for *Nras*, 24 for *Hipk1*, 75 for *Ptpn22* and 36 for *St7l*. Detailed information about each variant is shown in Appendix 2 - Tables and figures, Table 123.

4. Discussion

4.1. ENU Protocol

4.1.1. Introduction

During the treatment of the first cohort, mice showed a gradual and unexpected weight loss two to three days following the second ENU injection, whereas no weight decrease was seen in control animals. No data on ENU toxicity specifically in the F2 (C57BL/6J x A/J) intercross was available at the MRC or published in the literature. Based on the evidence available, 3 x 100 mg/kg was considered a balanced dose to use in this study. This section is aimed to discuss the results obtained from the euthanized animals and the set of measures introduced to find a balance between animal welfare and scientific output.

4.1.2. Pathology findings

Stem cells, including haematopoietic stem cells, are particularly susceptible to the toxic effects of ENU, which can explain the haematology findings. The white cell population seemed to be more affected than the red population probably because the cellular turn over in the latter is faster. Unlike in many other species in which neutrophils occupy that rank, lymphocytes are the most common leukocyte population in mice, and it was exactly this population that showed a considerable decrease after the second treatment with ENU.

Clinical chemistry and necropsy did not reveal any outstanding findings. Decreased cellularity in the bone marrow and lymph nodes seen at histological evaluation was considered to be related to ENU administration.

The investigation as to what may have caused an increased weight loss the F2 intercross was not conclusive. Given that this unexpected phenomenon happened half way through the execution of first treatment, treatment protocol had to be changed in order to avoid a similar situation when treating the remaining cohorts.

4.1.3. Animal welfare

Although the body weight loss was significant in a considerable number of animals, at the clinical exam they did not show the classical signs of ill-health, such as hunched posture, inactivity, labored breathing and piloerection.

The following measures were immediately put in place to minimize pain, suffering, distress and lasting harm: (1) body weight monitoring (all animals with less than 15% of body weight loss had their weight assessed every other day and all with 15% or more were weighed daily; furthermore, animals with a loss of 19% were euthanized), (2) extra clinical assessment at weight control (clinical signs were recorded and their evolution assessed on a daily basis), (3) improved access to food and water (meshed pellets were placed on cage floor), and (4) modification of treatment protocol (the interval between injections was increased from one to two weeks, and ENU dose of third treatment was decreased to 80 mg/kg, down from 100 mg/kg).

4.1.4. Changes in treatment protocol

There was a positive outcome following the implementation of the set of measures described above, and they were the foundation to the protocol used in cohorts 2 and 3. The major changes included: weight monitoring, diet regimen, treatment dosage, time between treatments, age at commencement and selection of animals to carry through treatment, as explained below.

4.1.4.1. Weight control

All mice, including controls, were weighted before each injection. In the first week after treatment, body weight was recorded every 48 hours unless in presence of a decrease of 15% or higher, in which case mice were weighed every 24 hours.

4.1.4.2. Diet

In addition to regular food pellets, TransBreed® formula pellets, with increased fat content and higher palatability, were added to cage floor to both treated and control animals two days before first ENU injection and kept until at least one week after last injection.

4.1.4.3. Treatment dosage

A dose of 100 mg/kg on first treatment was kept based how the first group tolerated this dose even being 12 weeks old. Decreasing doses for second and third treatments, of 90 and 80 mg/kg, respectively, were established as an attempt to counterbalance the cumulative detrimental effects of ENU.

4.1.4.4. Time between treatments

Instead of one week, two weeks of recovering time were allowed between treatments.

4.1.4.5. Age at commencement

Animals from cohorts 2 and 3 received first treatment at 14 weeks of age, instead of 12, as they would be, in principle, more resilient.

4.1.4.6. Selection of animals to carry through treatment

All animals received the first treatment of 100 mg/kg. Only animals with body weight decrease not higher than 10% received a second injection of 90 mg/kg. Following the same rationale, only animals with body weight decrease not higher than 10% received a third injection of 80 mg/kg.

This combination of measures resulted in a decrease in morbidity and mortality from cohort 1 to the next cohorts. The higher mortality seen at (100+90) mg/kg than at (100+90+80) mg/kg is potentially explained by the fact these mice were more

susceptible – they were not select for a 3rd treatment given their body weight decrease higher than 10% after the second treatment

4.1.5. Impact on the study

This study was designed to compare lymphoma positive and negative mice and is arguable whether how lymphoma was induced is a critical factor or not. Ideally, all animals would have received the same treatment but, for the reasons explained above, there was a deviation in the treatment protocol between cohort 1 and the other two cohorts. Furthermore, within each cohort, 3 different treatment doses were administered.

For biometric and haematology data analysis, it was acknowledged that different ENU dosages may have accounted, on their own, for differences in the variables evaluated. Therefore, "lymphoma status" as well as "treatment dose" and their interaction were taken into account while performing the relevant statistical tests.

For the purpose of the mapping analysis, differences in ENU dose did not have a significant impact on the findings - upon being treated with a higher ENU dose, mice are more likely suffer, for example, a higher body weight loss, but any dose that was enough to induce DNA mutations conductive to lymphoma would have exposed the susceptibility factors that were investigated in this study.

The experience reported here shows how advisable it is to test the ENU protocol in a pilot study before implementing it, particularly when using animal models for which there is no data in the literature.

4.2. Pathology

4.2.1. Histology

According to Swerdlow et al. (2008), precursor T-cell lymphoblastic lymphoma is more frequent in adolescent males. In this study, no significant difference between sexes was found.

According to Morse et al. (2002a), precursor and mature T-cell neoplasms in mice have very identical behaviour in terms of organs and tissues involved and a leukemic phase is seen in one third of lymphoblastic lymphomas. A leukaemic phase is an indication of the invasive behaviour and malignancy of this tumour. The colonisation of other organs is facilitated by the spread of tumour cells to the blood stream and in this study a high metastization rate was seen in the spleen.

Increased splenic extramedullary haematopoiesis potentially means that a compensatory production of RBC took place in the spleen following the deleterious effects of ENU in bone marrow hematopoietic stem cells.

4.2.2. Necropsy

Lymph node enlargement seen at necropsy was probably related to the infiltration of lymph nodes with neoplastic cells and/or activation of the immune system in response to pathologies triggered by treatment. Growths of pale colouration in the lungs and growths in the gastrointestinal tract seen at necropsy were likely to be lung adenoma/adenocarcinoma and gastrointestinal adenoma/adenocarcinoma, respectively, as seen in other studies using ENU (Smith et al., 2009, Fenske et al., 2006b). At macroscopic examination, the intestinal growths seemed to be ulcerated and were probably related to the presence of blood in the perianal area. Insidious blood loss can lead to anaemia and thrombocytopenia. Nevertheless, a histological evaluation of the lesions would have to be done to reach a definitive conclusion.

4.3. Biometric and Haematology

4.3.1. Biometric data

4.3.1.1. Body weight

It was not surprising to observe a significant difference in body weight at culling in ENU-treated animals given the well-known detrimental effects of ENU, which include body weight loss (Justice et al., 2000).

4.3.1.2. Organ weight

4.3.1.2.1. Thymus

As expected, in both males and females the presence of a thymic lymphoma had a strong impact on increasing thymus weight because of the significant expansion of a subset of T-cells within this organ.

4.3.1.2.2. Spleen

Although splenomegaly can be caused by neoplastic infiltration of acute lymphoblastic lymphomas (Kumar et al., 2010a), the main cause that potentially explains the increased weight in spleens of treated mice seems to be related with the high frequency of splenic extramedullary haematopoiesis (EMH), seen in 60% of treated mice. Splenic EMH is relatively small and tends to decline with age of the mouse but when prominent it can result in a marked increase in splenic size (Van Etten, 2008). Anaemia, as described further ahead, was a very common finding in treated mice and might have been at the origin of increased compensatory EMH.

4.3.2. Haematology data

4.3.2.1. White blood cell-related parameters

Immunosuppression, as result of the mutagen effect of ENU on hematopoietic stem cells, as stated in Justice et al. (2000), was not found in treated animals at culling, but seemed to be present in animals culled on welfare grounds one to two weeks after treatment (section 3.1.6, Table 20).

Extramedullary haematopoiesis, present in 60% of treated mice, might have accounted for the increase in neutrophils. While some degree of EMH is present in normal rodents, especially in mice, increased EMH can result from hematotoxic insult (Suttie, 2006).

Lymphocytosis can potentially be explained by a leukaemic status at terminal blood collection. Lymphomas are circumscribed masses by definition, although they can become leukemic as they grow, in which case is expected to see an increase in absolute count of circulating lymphocytes. In some cases, there seemed to be a clear spreading of the thymic neoplasm into the blood stream with pronounced lymphocytosis and colonization of other organs such as the spleen and lymph nodes.

Increased absolute monocyte count can occur to any condition involving significant tissue destruction, such as widespread inflammation (Robert L. Hall, 2013). Apart from not being a particularly specific biomarker, there were many necropsy findings that could have been associated with increased inflammation (section 3.2.5, Table 22), and that could have accounted for the monocytosis seen here. Furthermore, mutations affecting *Nras* have also been implicated if increase in leucocyte, neutrophils and monocyte number (Xu et al., 2013).

As for eosinophils, the fact that the effect was not seen in both sexes and that a dose-effect was not present, suggests that the difference can be attributed to biologic variation. In any case, eosinophil decrease can be potentially explained by ENU toxicity - being an alkylating agent, ENU may induce agranulocytosis because of generalised suppression of the bone marrow, also affecting red blood cells and platelets (Kumar et al., 2010a). Although in the current study leukopenia was seen in

the first weeks after treatment and not at culling, ENU might have caused DNA damage to eosinophil precursor cells.

Large unstained cells are generally thought to represent large lymphocytes or monocytes (Robert L. Hall, 2013). In the current study, large unstained cells seemed to be large lymphocytes, rather than monocytes, since monocyte count in females was not increased at all. The analysis of cellular size carried out on T-cells from control and lymphoma positive mice based on forward scatter measured by flow cytometry has revealed that CD4+ and CD8+CD4+ cells were significantly larger in lymphoma positive mice (section 3.4.1.2.1, Table 78).

As already hypothesised above, ENU is a stem cell mutagen, it also affects haematopoietic stem cells (Justice et al., 2000) and could have induced mutations in the myeloid cell line resulting in an increase in basophil count. Basophilia is rare and often indicative of a myeloproliferative disease (e.g., chronic myeloid leukaemia), (Kumar et al., 2010a). The significant increase found in this study might be associated with mutations caused by ENU in bone marrow pluripotent haematopoietic stem cells, affecting both lymphoid and myeloid cell lines. Furthermore, chronic myeloid leukaemia transformation to lymphoblastic leukaemia, (term used interchangeably with lymphoblastic lymphoma/thymic lymphoma), is seen, indicating that it originates from a transformed pluripotent haematopoietic stem cell (Kumar et al., 2010a).

4.3.2.2. Red blood cell-related parameters and platelets

The data suggest that ENU was associated with a decrease whereas thymic lymphoma was associated with an increase in red blood cell-related parameters. This might be hypothetically related to the impact of ENU treatment on hematopoietic pluripotent stem cells, having caused mutations in the myeloid cell line and affected blood

cellular constituents such as RBC and basophils that were increased in lymphoma positive animals.

The difference in MCV between treated and control animals is possibly explained as an attempt to regenerate red blood cells, which might possibly correlate with the high incidence of splenic increased extramedullary haematopoiesis. The pattern of haematological alterations seen here are suggestive of a regenerative, macrocytic anaemia, although the analyser used during the project does not measure reticulocytes and therefore a definitive classification is not given.

As for platelet count, presence of blood in the perianal area, which were not rare amongst ENU-treated mice, might have accounted for the decrease seen in treated animals. The blood loss in some occasions could also have been associated with other pathologies of the gastrointestinal and female reproductive tracts observed during necropsy such as tumours, intussusception and prolapse.

4.4. Flow Cytometry

4.4.1. Thymus

According to Morse et al. (2002b), chemically induced lymphomas are precursor T-cell lymphoblastic lymphomas (Pre-TLBL), also called lymphoblastic lymphomas or thymic lymphomas, and have a phenotype characterized by immature T-cells, CD4-CD8- double negative, CD4+CD8+ double positive, CD4 single positive or CD8 single positive.

According to Uyttebroeck et al. (2007), although there is a considerable overlap between the immunophenotype of T-cell lymphoblastic neoplasms, T-cell lymphoblastic leukaemias (T-ALL) have a more immature phenotype and T-cell acute lymphoblastic lymphomas (T-LBL) have a more mature phenotype. This may suggest that T-ALL derive from a T-cell progenitor in the bone marrow, while thymocytes represent the normal counterpart in T-LBL, which offers a possible explanation for the differential patterns in both disease distribution (bone marrow involvement versus mediastinal mass) and immunophenotype (earlier versus latter stages of T-cell differentiation). According to Kumar et al. (2010a), the more immature tumours are usually negative for surface CD3, CD4, and CD8, whereas “late” pre-T cell tumours are positive for these markers.

In the current study, ENU-induced thymic lymphomas were of varied immunophenotypes. The majority (57.5%) were predominantly of cells with some co-expression of both CD4 and CD8 markers while only 5% were of double negative cells. In most cases the co-expression of CD4 and CD8 was not clearly positive or negative - there was a range of intermediate states. Indeed, according to Swerdlow et al. (2008), CD4 and CD8 are frequently co-expressed on the blasts in T-ALL/LBL. Single positive CD8 lymphomas were 2.6 times more common than CD4 and 10%

were of mixed cells. Even though most malignant tumours are monoclonal in origin, by the time they become clinically evident their constituent cells are extremely heterogeneous (Kumar et al., 2010d).

Although an attempt to label and group lymphomas by phenotype was made, by establishing and using reference intervals based on the immunophenotype of thymi from control mice, the classification used here is open to discussion - each tumour has a unique profile.

There was a considerable degree of variation in the dataset, which is not uncommon in flow cytometry, particularly when dealing with cells that have a departure from their original state and do not necessarily express the same surface antigens as their non-neoplastic counterparts. For that reason, the analysis was focused on Median, and not Mean, Fluorescence Intensity, since medians are a better representation of the centre in these cases.

Neoplastic cells can have a different size from their healthy counterparts. Variation in cellular size, and consequently in cellular membrane area, may in theory have an impact on the number of antigens expressed on the cell surface. Since the antigens measured in this study are all expressed at the cellular membrane, the size of each cell type was measured by Mean Forward Scatter. When compared to controls, double positive and CD4 single positive neoplastic T-lymphocytes were significantly larger, double negative neoplastic T-lymphocytes were significantly smaller, and CD8 single positive showed no significant difference. It was beyond the objectives of this study to understand exactly how neoplastic cells differ from healthy cells in the number of surface antigens expressed on the cellular membrane and the sample size was too

small for a statistical analysis. Nevertheless, the data suggest that the number of surface antigens in CD4 lymphocytes followed the variation in cellular size: bigger CD4+ neoplastic (N= 2) seemed to have more CD4 antigen (8953.5±580.5) than control (7291±1104, N= 21). Double positive neoplastic cells (N= 6), that were significantly larger than control, seemed to have more CD4 (7121.5±4095.5) but less CD8 (2130.33±609.4) than control (N= 21), (5345±894.4) and (2341±440.7), respectively. CD8+ neoplastic lymphocytes (N= 2), that were not significantly different in size from control CD8+, showed a mean MFI captured in APC-Cy7 channel of 1636+-306.9, lower than in control (2730±613.6, N= 21). CD8 tumours were more common than CD4 but they were mostly of lymphocytes with intermediate expression of CD8 antigen. Neoplastic cells with intermediate expression cannot be compared since there were no equivalent controls for comparison. Results presented here comparing expression on neoplastic cells with controls are merely speculative - a larger sample would be required to assess whether the suggested differences were significant.

4.4.2. Spleen

A possible limitation of performing flow cytometry on solely the thymus was revealed by comparing the phenotypes of the primary tumours and respective metastases. This limitation, identification of which cell type has become neoplastic, holds particularly true when the thymic tumour has a similar proportion of double positive, double negative and single positive cells as a normal thymus. This is particularly apparent in mouse 26.1e (section 3.4.2.2.2, Figure 33), in which 69.7% were DP, 5.03% were DN, 6.13% were CD8+ and 19.1% were CD4+. When looking at the flow cytometry profile of the metastasis in the spleen, it becomes clear that the predominant neoplastic

cells were DP, since they accounted for 54.4% of all lymphocytes, whereas in normal spleens they are almost not present at all. Although flow cytometry and other techniques with adjunctive roles in diagnosis and classification of hematopoietic neoplasms provide valuable information, they must be reconciled with morphology for diagnostic purposes (Kaleem, 2006).

Flow cytometry analysis of spleens was carried out with the intention of having a first look at correlation between the immunophenotype found in the thymus and the immunophenotype that had spread to the spleen, and to assess if there was a specific phenotype which had spread more frequently. From 6 cases of metastasis to the spleen presented here, only one was of CD8+ cells, while five CD8CD4 subtypes accounted for the remaining metastases. These two subgroups were the first (57.5%) and second (20%) most common phenotypes found in the thymus. More than showing any particular trait in terms of invasion rate, these figures might simply be reflecting the higher incidence of the primary tumour – a larger sample would be needed for a conclusive result.

Although CD44PE-CF594 and CD25PE were included in the panel of antibodies used to phenotype both splenic and thymic T-lymphocytes, their expression have a different meaning in the two organs. In the spleen, CD44 is used to distinguish CD4 naïve (CD44 low) from those that are antigen-experienced (CD44 high) (Zeng et al., 2008), whereas in the thymus, as previously stated, CD44 can be used to differentiate different stages of immature lymphocytes, which are CD4-. Furthermore, CD25 detects an activation antigen (IL-2 receptor alpha chain) on T cells and B cells (Parker A. et al., 2010), conferring on it a different interpretation in immature (thymic) and mature (splenic) T-lymphocytes. For these reasons, and in retrospective analysis,

results for splenic metastases presented here were limited to T-cells versus B-cells and CD4 versus CD8 gates, with no further investigation on the nature of DN based on the expression of CD44 and CD25.

The DN classification in the spleen should be interpreted differently to that in the thymus. Given that lymphocytes were selected from an FSC/SSC gate and polymorphonuclear cells with a higher FSC were excluded, it is unexpected to have such a high percentage of genuine immature CD4-CD8- T-lymphocytes in the spleen. This is because CD4-CD8- T-lymphocytes are released in the peripheral circulation, and eventually colonise the spleen as CD4 or CD8 mature single positive cells. Therefore, the DN gate in the spleen contains cells that have a similar FSC/SSC pattern to lymphocytes, are CD19 negative and therefore not B cells, are CD4-CD8-, and hence should not represent genuine DN lymphocytes. The refined analysis of this DN CD4CD8 splenic population is beyond the scope of this study.

4.5. Genetic analysis

4.5.1. Physical distance and linkage distance

The genotyping data was generated in base pair (bp) and for the QTL analysis had to be converted to centimorgan (cM). The relationship between linkage distance and physical distance can vary greatly in different parts of the genome as well as in crosses between different strains of mice. Nevertheless, and according to Lee M. Silver (1995), one can derive an average equivalence value between the two metrics of genome measurement, kilobases and centimorgans of approximately 2000 kb (or 2000000 bp) per centimorgan. Therefore, for the QTL analysis, the position of each SNP was converted to cM by dividing by 2000000.

4.5.2. Selection of the quantitative trait to analyse

After receiving ENU, only some animals developed thymic lymphoma. The phenotype studied here, thymic lymphoma, seems, at first glance, a categorical trait: there were lymphoma positive and lymphoma negative mice. Nevertheless, within a lymphoma positive status, there are several degrees of severity of the disease.

While phenotyping the experimental population studied here, continuous variables such as adjusted thymus weight at culling and absolute lymphocyte count at culling, were strongly associated with thymic lymphoma and were therefore potentially considered as good quantitative traits for the QTL analysis. Ideally, adjusted thymus weight to body weight at culling would have been better to use instead of absolute thymus weight since it would take into account the variation in thymus weight attributable to variation in body weight, but adjusted organ weight is performed at the group level, not allowing to get the individual measurements crucial for the QTL analysis. Lymphocyte count, although significantly associated with the presence of thymic lymphoma, was not considered as an optimal quantitative trait. Lymphomas

are circumscribed masses by nature and only at later stages become leukaemic. Additionally, there may have been other causes of lymphocytosis that would not be possible to identify and would lead to false positive results. Absolute thymus weight was, therefore, the quantitative trait selected for the QTL analysis. According to Jacoby et al. (2002b), the thymus reaches maximum size around the time of sexual maturity and involutes between 35 and 80 days of age. In this study, the age of mice at culling was well above 80 days, when no further considerable involution was expected to occur. Additionally, thymus weight is a good indicator of whether a proliferative process is present (Deschepper CF and Gallo-Payet N, 2004).

4.5.3. A QTL in chromosome 3

According to Fenske et al. (2006b), lymphoma susceptibility mapped to two regions on chromosomes 3 and 15, one of which contains the gene encoding Sprouty1, according to same authors, an antagonist of fibroblast growth factor signalling. In this study, a QTL in chromosome 3 was found using an Interval Mapping analysis at 48.3 cM, which correlates to approximately 96525953 bp, between SNPs "UNCHS009289 chr3:87248346" and "UNC5893653 chr3:105034644".

In the QTL, genetic variants between C57BL/6J and A/J were selected. These sequence differences will contribute to the susceptibility of C57BL/6 mice to ENU-induced lymphomas. The ENU will affect individual cells and cause mutations in particular genes which interact in some way with the susceptibility loci to result in lymphoma. The loci could be a result of a sequence in A/J that results in resistance or a sequence in C57BL/6 that results in susceptibility.

In theory, Composite Interval Mapping (CIM) gives more power and precision than simple Interval Mapping because the effects of other QTL are not present as residual

variance (Wang S. et al., 2012). Although the CMI carried out here did not identify the peak in chromosome 3 as statistically significant, it was nevertheless the highest peak found. Furthermore, there was a good correspondence between the peaks found using both methodologies.

4.5.4. Single nucleotide polymorphisms

In this section, genes found on the locus of interest are discussed. The type of variant and its impact on protein function are assessed. A missense variant is a sequence variant that changes one or more bases, resulting in a different amino acid sequence but where the length is preserved. It is considered to have a moderate impact and might change protein effectiveness. In splice region variants, the change has occurred within the region of the splice site, either within 1-3 bases of the exon or 3-8 bases of the intron. A nonsense-mediated decay (NMD) transcript variant is a variant in a transcript that is predicted to be a target of NMD (Yates et al., 2016), a surveillance pathway that reduces errors in gene expression by eliminating mRNA transcripts that encode incomplete proteins (Baker and Parker, 2004). NMD transcript variants are usually non-coding variants or variants affecting non-coding genes, where predictions on protein function are difficult or there is no evidence of impact. Finally, synonymous variants result in no change to the encoded amino acid.

4.5.4.1. *Fcrls, Fcrl1* and *Fcrl5*

In the published literature, there are references to the role this gene plays in B cell differentiation but its relevance to T cell biology is not clear. Research published in Davis et al. (2001) and Miller et al. (2002), showed that *FCRL1-5* expression increases as a function of B cell differentiation and peaks among circulating cells and those located in secondary lymphoid tissues (Li et al., 2014). Members of the

extended Fc receptor-like family in humans and mice are preferentially expressed by B cells but *Fcrls*, specifically, is not present in the human genome (Li et al., 2014). Fc receptor-like homologs (FcRH1-5) are differentially expressed during B cell differentiation in humans and the mouse orthologs moFcRH1 and moFcRH3 are preferentially expressed at different stages in B cell differentiation (Davis et al., 2004).

Mouse *Fcrl1* and *Fcrl5* encode type I transmembrane proteins with moderately different features to equivalents in humans. Mouse FCRL5, present in B cells located in the marginal zone of lymph nodes, shares greater structural similarity to human FCRL2 and FCRL3 (Li et al., 2014). Although FCRL3 is present in human T cells, both naturally occurring CD4+ regulatory cells (Nagata et al., 2009, Swainson et al., 2010) and CD8+ cells (Li et al., 2014), the FCRL3 gene is not present in mice (Nagata et al., 2009). Both in humans and mice, FCRL1 protein is present in B cells (Li et al., 2014).

Given their preferential expression on B cells, the role of FCRL family members in disease pathogenesis is being investigated and multiple groups have detected their expression and dysregulation in various lymphoproliferative disorders (Li et al., 2014). Upregulation of FCRL was shown in diffuse large B cell lymphoma, follicular lymphoma and chronic lymphocytic leukaemia (Alizadeh et al., 2000). Furthermore, monoclonal antibodies confirmed the FCRL1-5 protein surface expression on diffuse large B cell lymphoma, follicular lymphoma, chronic lymphocytic leukaemia, Burkitt lymphoma, hairy cell leukaemia and mantle cell lymphoma (Ise et al., 2005, Polson et al., 2006, Du et al., 2008).

In *Fcrl1*, no deleterious effects on protein function seem to result from the replacement in amino acids. As for *Fcrl5*, ten missense variants were found in A/J mice, two of which resulting in amino acid substitutions, from tyrosine to histidine and from asparagine to threonine, that can have a deleterious effect on protein function. Nevertheless, no associations to T cell lymphomas were found in the literature.

4.5.4.2. *Cd5l*

CDL5 protein is expressed mostly by macrophages in lymphoid and inflamed tissues, and it is known to play major role in lipid homeostasis (Sanjurjo et al., 2015). Concerning its tissue expression, Northern blot analysis identified 3 distinct RNAs hybridizing to human CD5L in bone marrow, spleen, lymph node, thymus and foetal liver but not in non-lymphoid tissues (Gebe et al., 1997).

Phenotypes related to the hematopoietic system and the immune system are described for *Cd5l*. Apoptosis inhibitor expressed by macrophages (AIM) inhibits apoptosis of CD4+CD8+ double positive thymocytes and supports the viability of DP thymocytes before thymic selection (Miyazaki et al., 1999). Although there is evidence in (Kuwata et al. (2003) suggesting that in $CD5l^{tm1Nto}/CD5l^{tm1Nto}$ mice, synonym to $AIM^{-/-}$, T cell apoptosis was prevented in *Corynobacterium parvum* infection. Furthermore, recombinant AIM protein significantly inhibited apoptosis of T cells obtained from C. parvum-stimulated livers *in vitro*. In another study Miyazaki et al. (1999), AIM-deficient mice had thymocyte numbers diminished to half of those in wild-type mice, and CD4/CD8 double positive thymocytes were more susceptible to apoptosis induced by dexamethasone and irradiation *in vivo*. Still according to the same authors,

numbers of either CD4/CD8 double-negative and single-positive thymocytes were grossly normal.

It has been hypothesised that differences in glycosylation patterns between human and mouse proteins result in distinct functional activities. Furthermore, the mutation of 2 N-glycosylation sites in the mouse protein affect its secretion and enhance its lipolytic activity (Mori et al., 2012). Further studies would be necessary to ascertain if other functional aspects of CD5L, for example inhibition of apoptosis, are also influenced.

Mutations in genes that modulate apoptosis might be implicated in the pathogenesis of cancer (Kumar et al., 2010b, Elmore, 2007). Additionally, according to Sanjurjo et al. (2015), evidence shows that both mouse and human CD5L forms can be defined as apoptosis inhibitors that support the survival of macrophages and other cell types when challenged by various apoptosis-inducing insults of infectious and chemical origin. It is therefore possible to speculate whether a sequence variant in *Cd5l* could have accounted for the abnormal survivability of T lymphocytes, in particular of CD4+CD8+ lymphocytes in ENU-induced thymic lymphomas.

The missense variant found in A/J causes an asparagine to be replaced by a serine but this substitution seems to be well tolerated and have no deleterious effect on protein function.

4.5.4.3. *Etv3*

Also named Ets variant 3, this gene is known to be involved in cell differentiation and proliferation (Eppig et al., 2015). Most Ets family protein, including Etv-1 and 2, transcription factors are nuclear targets for activation of Ras-MAP kinase signalling pathway and some of them affect proliferation of cells by regulating the immediate

early response genes and other growth-related genes (Oikawa and Yamada, 2003). Likewise, Ets1 have been shown to be required for survival and activation of T cells (Muthusamy et al., 1995), and the pro-apoptotic and anti-apoptotic roles of Ets-1 and Ets-2 (Oikawa and Yamada, 2003) are but no references were found associating Etv3 to T cell biology. Other Ets family proteins, including Ets-1, Ets-2, Erg, Fli-1, Elf-1, GABPα, PU.1 and Spi-B are expressed in lymphoid cells (Bassuk and Leiden, 1997, Anderson et al., 1999), but no reference is made to Etv3 variant. Furthermore, some *Ets* family genes can be activated and become oncogenic by retroviral insertion in animal tumours. For example, in Friend virus-induced erythroleukaemia, PU.1 is activated (Moreau-Gachelin, 1994). The *Ets* family genes are also involved in chromosome translocations, frequently associated with leukaemia and solid tumours (Look, 1995) and T cell lymphoblastic lymphomas (Lones et al., 2007, Thomas and Kantarjian, 2001). One well-known example is a translocation found in 95% of human Ewing's (EWS) sarcomas (Delattre et al., 1992). The expression of EWS-Fli-1, an *Ets* variant, leads to a strong up-regulation of the *c-myc* oncogene and a considerable down-regulation of the $p57^{KIP2}$ tumour suppressor gene (Dauphinot et al., 2001). According to de Leval et al. (2009), a translocation involving *myc* is encountered in 35% of T-ALL/LBL.

In conclusion, there is evidence for the association of Ets genes with biological processes linked to cancer but no clear information concerning the role of Etv3 on thymic lymphoma was found. Furthermore, the two missense variants found in A/J are unlikely to have deleterious consequences to the protein.

4.5.4.4. *Sh2d2a*

This gene, also known as RIBP, is expressed in T and natural killer cells. RIBP-disrupted knockout mice displayed apparently normal T cell development, however, T cell receptor mediated activation was impaired, suggesting that RIBP plays a role in the regulation of T cell differentiation (Rajagopal et al., 1999). It is therefore possible to speculate about its role on cellular arrest on the course of lymphocyte differentiation in neoplastic thymi. Nevertheless, the missense variant found in A/J is well tolerated and the splice region variants relate to intronic regions, which, not ruling out the possibility of having had an impact on the phenotype studied here via gene regulation mechanisms, makes difficult any prediction.

4.5.4.5. *Gon4l*

Mice homozygous for an ENU-induced allele exhibit arrested B cell development at the early pro-B cell stage (Lu et al., 2010), but no phenotype, other than a decrease by approximately twofold in mature CD3+ in spleens, was found in T cells. Of three missense variants found in A/J mice, one is predicted to have a deleterious effect on protein function. It affects bp 88854680, consists of a change from cytosine to thymine on the codon, causing proline to be replaced with leucine on the protein.

4.5.4.6. *Ecm1*

Extracellular matrix 1 (ECM1) was statistically-significantly elevated in Diffuse Large B-cell Lymphoma patient sera as compared to controls (Riby et al., 2016). It has also been implicated in other tumours, such as laryngeal carcinoma, in which case it ECMI1 expression was associated with tumour cell growth, metastasis and angiogenesis (Meng et al., 2015). Here, the missense variant found in A/J is likely to have no deleterious effect on the coded protein and therefore unlikely to have been implicated in the phenotype.

4.5.4.7. *Cd160*

CD160 antigen is expressed on activated NK or T cells in humans but its function is unknown and in Tu et al. (2015), CD160-deficient mice were generated to probe its function. According to their data, although CD160 (-/-) mice showed no abnormalities in lymphocyte development, the control of NK-sensitive tumours was severely compromised. Therefore, CD160 functionally controls cytokine production by NK cells and is important for early control of tumour growth. Nevertheless, the missense variant found in A/J is likely to have no deleterious effect on the coded protein and therefore unlikely to have been implicated in the phenotype.

4.5.4.8. *Trim45*

Tripartite motif-containing 45, one of the TRIM family ubiquitin ligases, suppresses transcriptional activities of Elk-1 and AP-1, which are targets of the MAPK signalling pathway (Shibata et al., 2012). Moreover, the same authors found that TRIM45 overexpression suppresses cell growth by acting as a repressor for the NF-κB signal, which plays an important role in cell survival, immunity, inflammation, carcinogenesis, and organogenesis. The gene variants in A/J are unlikely to affect protein function.

4.5.4.9. *Vangl1*

Vang-like 1 (van gogh, Drosophila), also called KITENIN, promotes tumour progression by enhancing angiogenesis in colorectal cancer (Oh et al., 2016). The variant in A/J mice is intronic and therefore difficult to predict whether it may have played a role in the pathogenesis of thymic lymphoma.

4.5.5. Insertions/deletions

4.5.5.1. *Nras*

Nras, also known as neuroblastoma ras oncogene, is associated with several phenotypes close to lymphoma in general and with acute lymphoblastic leukaemia (Eppig et al., 2015). Ras genes are the most common targets for somatic gain-of-function mutations in human cancer (Schubbert et al., 2007). Within the haematopoietic system, several genotypes were described in association with modification of leucocyte biology: Homozygous mice carrying a genetic modification which increased the level of wild type *Nras* mRNA, $Nras^{tm1.1Emfu}$/ $Nras^{tm1.1Emfu}$, developed granulocytosis and T-cell expansion, whereas heterozygous mice showed a moderate of T cells and granulocytes. This indicates that *Nras* overexpression alone is sufficient to cause dose-dependent granulocytosis and T-cell expansion (Lassen et al., 2012).

As shown in Wang et al. (2011), 100% of recipient mice transplanted with $Nras^{G12D/G12D}$, a normal oncogenic *Nras* allele, bone marrow cells, develop acute T-cell lymphoblastic leukaemia/lymphoma, whereas approximately 8% of recipient mice transplanted with $Nras^{G12D/+}$ developed that same neoplasm. These findings were consistent with results published in Xu et al. (2013).

Research has suggested that wild type *Ras* exerts tumour suppression activity (Bremner and Balmain, 1990, To et al., 2008, Li et al., 2011, Zhang et al., 2001). Nevertheless, data published in Xu et al. (2013), suggest that although this possibility remains viable in tissues such as skin and lung, where normal RAS genes are likely to function as tumour suppressors, restoring or enhancing normal *Ras* expression will be ineffective in leukaemias with oncogenic NRAS mutations.

Both variants in A/J are nonsense-mediated decay transcript variants, one of which located in intron 4-5, a non-coding region, which makes difficult to predict how this could impact on gene expression and therefore on the phenotype studied here.

4.5.6. Single nucleotide polymorphisms and insertions/deletions

4.5.6.1. *Rit1*

Ras-like without CAAX 1 mediates several cellular functions, including prominent roles in the control of mitogen-activated protein kinase (MAPK) cascades (Cai et al., 2011), cell proliferation, survival, differentiation and may play crucial oncogenic role in human cancer (Xu et al., 2015). Still according to the last authors, elevated expression of RIT1 was associated with poor prognosis in endometrial cancer and in Berger et al. (2014), RIT1 was identified as a driver oncogene in a specific subset of lung adenocarcinomas. Both SNP and insertion/deletion variants in A/J are nonsense-mediated decay transcript variants located in introns, not allowing to predict here their consequences at functional level.

4.5.6.2. *Selenbp1*

Selenium-binding protein 1 is suggested to play a role in tumour suppression and in *Selenbp1*$^{(-/-)}$ mice, the thymus weight was significantly higher than in wild type (Tsujimoto et al., 2013). Nevertheless, according to the same authors, a reduction in *Selenbp1* in *Selenbp1*$^{(-/-)}$ mice appears not to be the sole determinant for tumorigenesis. Other authors, Ansong et al. (2015), have found evidence to support that selenium binding protein 1 is a tumour suppressor in prostate cancer. Nevertheless, both SNP and insertion/deletion variants in A/J are nonsense-mediated decay transcript variants located in introns not allowing to predict here their consequences at functional level, but it is possible to speculate they might have resulted in a lower expression of this gene.

4.5.6.3. *Rfx5*

Regulatory factor X, 5 is related to MHC - II expression. $Rfx5^{tm1.1Ifo}/Rfx5^{tm1.1Ifo}$ mice thymus is almost completely devoid of MHC- II expression, as well as a decrease in CD4+ alpha beta T cell number and decreased single positive T cell number. Furthermore, the lack of MCH II expression causes an immunodeficiency syndrome, the bare lymphocyte syndrome (Elhasid and Etzioni, 1996).

Genetic deletions of MHC genes appear to be common in extranodal lymphomas at immune-privileged sites, in particular the central nervous system and testes. In one study, 60% of immune-privileged site lymphomas had a total loss of MHC class I genes as compared with 10% of intranodal cases. Additionally, MHC class II expression was lost in 56% of immune-privileged lymphomas compared with only 5% of nodal lymphomas (Riemersma et al., 2000). Loss of MHC class II in these particular types of lymphomas is due to both homozygous and heterozygous deletions as well as point mutations (Jordanova et al., 2002, Jordanova et al., 2003). In Rimsza et al. (2004), the authors have found evidence that diminished MHC class II gene expression with consequent loss of immunosurveillance is an important factor related to patient survival in diffuse large B-cell lymphomas.

Published data suggest that it is possible to speculate about the role of *Rfx5* in the phenotype studied here, although both SNP and insertion/deletion variants found in A/J mice are mostly uninformative, as they relate to non-coding regions. There is a missense SNP variant that results in the replacement of arginine with glutamine but with no predicted deleterious effect on protein function.

4.5.6.4. *Anp32e*

Acidic (leucine-rich) nuclear phosphoprotein 32 family, member E, is involved in the regulation apoptotic process (Gaudet et al., 2010) in zebrafish. Furthermore, a high expression of ANP32E, amongst other genes, was associated with better survival rate in patients with follicular lymphoma (Bjorck et al., 2005). Nevertheless, mice homozygous for a knock-out allele are phenotypically normal, including no defects no thymocyte apoptosis (Eppig et al., 2015, Reilly et al., 2010). The variants found in A/J mice are of nonsense-mediated decay transcript type.

4.5.6.5. *Wdr3*

Proteins belonging to the WD repeat family are involved in a variety of cellular processes, including cell cycle progression, signal transduction, apoptosis, and gene regulation (NCBI, 2016). Furthermore, as described in McMahon et al. (2010), WDR3 has an essential function in p53-mediated regulation of cell cycle progression in cancer cells. No specific phenotypes were associated with lymphoma and from most of the genetic variants in A/J are of nonsense-mediated decay transcript type and thus not very informative as whether this gene could have played a role in the pathogenesis of thymic lymphoma. There are two missense variants but none seems to have a deleterious effect on protein function.

4.5.6.6. *Hipk1*

Homozygous null mice are viable and fertile, do not develop spontaneous tumours, and are resistant to DMBA-induced skin tumour formation (Eppig et al., 2015). In (Kondo et al. (2003), homeodomain-interacting protein kinase 1 (HIPK1) was used as a p53-binding protein and deletion analysis showed that amino acids 100–370 of p53 and amino acids 885-1093 of HIPK1 were sufficient for HIPK1–p53 interaction. Moreover, gene-targeted HIPK1-/- mice were grossly normal but oncogenically

transformed HIPK1 -/- mouse embryonic fibroblasts exhibited reduced transcription of Mdm2 and were more susceptible than transformed HIPK1+/+ cells to apoptosis induced by DNA damage. Furthermore, carcinogen-treated HIPK1 -/- mice developed fewer and smaller skin tumours than HIPK1+/+ mice. The authors concluded that HIPK1 may play a role in tumorigenesis, perhaps by means of the regulation of p53 and/or Mdm2.

More than 70 SNP and 20 insertion/deletion nonsense-mediated decay transcript variants were found in A/J mice, but given their nature, it is difficult to speculate on their effect on gene regulation.

4.5.6.7. *Ptpn22*

Homozygous null mice display antigen dependent increases in T cell proliferation and cytokine production, enlarged spleens and lymph nodes, increased spontaneous germinal centre formation, increased B cell numbers, and increased serum IgG and IgE levels (Eppig et al., 2015). There are several B and T cell phenotypes associated with this gene, most of them related to auto-immune diseases, including type 1 diabetes, rheumatoid arthritis, Graves' disease, and systemic lupus erythematosus, which are associated with an allelic variant of protein tyrosine phosphatase nonreceptor 22 (*PTPN22*) (Dai et al., 2013), more than with cancer. Furthermore, in A/J this is a nonsense-mediated decay variant, which usually are non-coding variants or variants that affect non-coding genes, where predictions are difficult or there is no evidence of impact (Yates et al., 2016).

4.5.6.8. *St7l*

In their study, Hooi et al. (2006), have provided evidence that ST7 functions as a tumour suppressor in both prostate and breast cancer cells, but as with Ptpn22, the

gene variants in A/J are nonsense-mediated decay variants, not allowing for predictions in terms of consequences for the function of the coded protein.

4.5.7. Conclusion

In conclusion, just in this QTL it was possible to identify at least 20 genes that are directly or indirectly implicated in tumorigenesis. Genes such as *Nras* and *Cd5L* seem to be strong candidates in explaining the differences in phenotype found between ENU-treated C57BL/6J and A/J mice. In other cases, such as in *Fcrls*, *Ets* families, *Rfx5*, the variants were found to be more directly implicated in cancer-related processes affecting either other lymphocyte subsets or involving gene variants other than the one found in the QTL vicinity. In most situations, the gene variants in A/J did not relate to modification in protein function, except in the case of *Fcrl5* and Gon4l. Nevertheless, it seems that rather than one gene of strong effect, there are multiple genes that could be implicated in the pathogenesis of thymic lymphoma.

5. Conclusions and future work

Starting from the evidence that different inbred strains of mice had very distinct degrees of susceptibility to ENU-induced lymphoma, this study was designed with the major objective of identifying candidate loci associated with susceptibility to lymphoma. The incidence is higher in C57BL/6J than in A/J mice and, since external factors such as diet, temperature, humidity and light intensity are generally well controlled in biomedical research settings and therefore should not have accounted for the difference, we have hypothesised that there are specific loci associated with increased susceptibility in C57BL/6J mice and have carried out a QTL analysis to test our hypothesis.

The resistant inbred strain (A/J) was crossed with the susceptible strain (C57BL/6J) to generate an experimental F2 intercross model in which genes from both progenitors are thoroughly mixed. Those animals were then challenged with ENU and the incidence of lymphoma across the experimental population was used to identify and map potential candidate loci related to increased susceptibility to ENU-induced thymic lymphoma.

The ENU protocol initially planned to induce thymic lymphoma in this study was designed based on evidence described in the literature and a wealth of experience held at the MRC Harwell. Nevertheless, there was an unexpected drop in body weight flowing ENU administration to the F2 intercross, which resulted in having to reach a new compromise between the welfare of the mice and scientific output, with the side effect of introducing variability to the study. This did not have an impact on biometric and haematology results since appropriate statistical tests were employed where different ENU regimens might have accounted for differences in the variables measured, but overall, it has reduced the power of the experiment. Retrospectively,

and to anyone interested in conducting a similar study, it is advisable to perform a pilot study and assess the tolerance to ENU administration on the specific animal model to be studied. At a dose regimen of (100+90+80) mg/kg, 36% of mice developed thymic lymphoma (N= 178), and no significant difference was seen between sexes.

The phenotype – thymic lymphoma – was studied according to haematological and other biometric variables measured and analysed between lymphoma negative and positive mice. Thymus enlargement was clearly associated with thymic lymphoma but splenomegaly was seen in lymphoma negative animals and attributed to increased extramedullary haematopoiesis rather than to metastasis arising from the primary tumour. Haematological findings included an increase in RBC in lymphoma positive mice, counteracting the tendency to develop anaemia associated with ENU administration, possibly explained by mutations caused by treatment not only on lymphoid medullary precursors, leading to the neoplastic transformation of the thymus, but also to myeloid stem cells, causing an increase in RBC. Basophils, also myeloid-derived cells, were also found to be increased in association with thymic lymphoma. Despite being exclusively associated with thymic lymphoma, lymphocytosis was attributed to the evasion of the neoplastic cells from the primary tumour into the blood stream, given the elevated metastization rate (49%) found at the histological examination of the spleens.

Flow cytometry analysis of thymic lymphomas has revealed a diversity of phenotypes, the most frequent (57.5%) of which was composed of lymphocytes with variable degrees of CD4 and CD8 co-expression. Only 5% of the lymphomas had an immature phenotype, composed of double negative CD4CD8 cells. The results found here

indicate that ENU-induced lymphomas have a more mature phenotype, as according to (Kumar et al. (2010a), the more immature tumours are usually negative for surface CD3, CD4, and CD8, whereas "late" pre-T cell tumours are positive for these markers. This suggests that ENU-induced lymphomas in this study were T-cell acute lymphoblastic lymphomas (T-LBL), with a more mature phenotype, rather than T-cell lymphoblastic leukaemias (T-ALL), which have a more immature phenotype. According to (Wood et al. (2007), the international panel of scientists with expertise in mouse and human haematopathology together with the haematopathology subcommittee of the Mouse Models for Human Cancers Consortium (MMHCC) classified precursor T cell neoplasms uniquely as precursor T-cell lymphoblastic lymphoma/leukaemia (pre-T LBL), making no distinction between lymphoma and leukaemia forms. The results obtained here, showing that only 5% of ENU-induced lymphomas had an immature phenotype, provide some evidence that there is place for a distinct classification of these two types of precursor T cell neoplasms. Furthermore, it would be interesting to carry out a detailed comparison of H&E stained slides of thymic lymphoma according to their flow cytometry profile and assess whether there are any outstanding differences in the cellular morphology of these tumours.

The null hypothesis that "No quantitative trait loci (QTL) exist that can explain the increased susceptibility to thymic lymphoma in ENU-treated C57BL/6J mice" was tested. A QTL was found by Interval Mapping on Chromosome 3 in the vicinity of a QTL found by Fenske et al. (2006b). These same authors acknowledged the need for their results to be validated and complemented using traditional intercross mapping strategies, which were carried out in here.

Several genes of interest, already identified as oncogenes, tumours suppressor genes, major players in regulation of apoptosis and genes intervening in lymphocyte biology are present in the region of the QTL. When comparing to C57BL/6J mice, most of the gene variants identified in A/J were in non-coding regions, where predictions of the impact the variant has on the phenotype are difficult. Deleterious effects on protein function are likely to occur as a consequence of missense mutations in *Fcrl5* and *Gon4l*. Although these genes are not described as being implicated in the pathogenesis of thymic lymphoma, they have been described in association with B cell lymphomas and lymphocyte biology. Other gene variants, such as the nonsense-mediated decay transcript variant affecting oncogene *Nras*, well described across the literature as an oncogene in lymphomas in C57BL/6 in response to ENU treatment (Shimada et al., 2003a), where found in the QTL. A close relative of *Nras*, *Rit1*, was also within the QTL. In both cases and in many other, their intronic positioning does not facilitate the process of speculating about their implication of the phenotype studied here.

Although the QTL in chromosome 3 reached statistical significance, there are 14 other peaks of minor expression along the whole genome, which suggests that ENU-induced thymic lymphoma, as other cancers in general, is a complex disease and that more than being associated to a single QTL of strong effect, there are multiple QTLs of weaker effect accounting for the phenotype, as stated in Demant (2003).

The initial analysis carried out in this study compared mice that did or did not develop lymphoma within the screening period, but a more detailed analysis comparing cell types and oncogene mutations can also be performed. Tissue samples of grossly altered tissues found at necropsy were archived for posterior fine mapping. Data collected during this study allow to investigate possible mutations according to

different flow cytometric immunophenotypes. Lymphoma clones or T cells can be isolated by FACS sorting and the expression levels of various genes within the QTL can be evaluated to see if any are different between the C57BL/6 and A/J.

For further analysis, consomic strains where individual chromosomes from the A/J strain have been introduced onto the C57BL/6J strain could be studied to confirm the relationship between the QTL and the phenotypes. Furthermore, mutations in genes that are affected by ENU, such as *K-ras* (Shimada et al., 2003a) could be investigated.

The results of this project will help with future investigation on the genetic component of precursor T cell lymphoblastic lymphoma, on refining the group of genes and underlying mutations that intervene on its pathogenesis and on research leading to the development of new therapeutic solutions for this pathology.

6. References

ACEVEDO-AROZENA, A., WELLS, S., POTTER, P., KELLY, M., COX, R. D. & BROWN, S. D. M. 2008. ENU Mutagenesis, a Way Forward to Understand Gene Function. *The Annual Review of Genomics and Human Genetics.* Medical Research Council.

ADAMSON, P., BRAY, F., COSTANTINI, A. S., TAO, M. H., WEIDERPASS, E. & ROMAN, E. 2007. Time trends in the registration of Hodgkin and non-Hodgkin lymphomas in Europe. *Eur J Cancer,* 43**,** 391-401.

AIFANTIS, I., MANDAL, M., SAWAI, K., FERRANDO, A. & VILIMAS, T. 2006. Regulation of T-cell progenitor survival and cell-cycle entry by the pre-T-cell receptor. *Immunological Reviews,* 209**,** 159-169.

AIFANTIS, I., RAETZ, E. & BUONAMICI, S. 2008. Molecular pathogenesis of T-cell leukaemia and lymphoma. *Nat Rev Immunol,* 8**,** 380-90.

ALIZADEH, A. A., EISEN, M. B., DAVIS, R. E., MA, C., LOSSOS, I. S., ROSENWALD, A., BOLDRICK, J. C., SABET, H., TRAN, T., YU, X., POWELL, J. I., YANG, L., MARTI, G. E., MOORE, T., HUDSON, J., JR., LU, L., LEWIS, D. B., TIBSHIRANI, R., SHERLOCK, G., CHAN, W. C., GREINER, T. C., WEISENBURGER, D. D., ARMITAGE, J. O., WARNKE, R., LEVY, R., WILSON, W., GREVER, M. R., BYRD, J. C., BOTSTEIN, D., BROWN, P. O. & STAUDT, L. M. 2000. Distinct types of diffuse large B-cell lymphoma identified by gene expression profiling. *Nature,* 403**,** 503-11.

ANDERSON, M. K., HERNANDEZ-HOYOS, G., DIAMOND, R. A. & ROTHENBERG, E. V. 1999. Precise developmental regulation of Ets family transcription factors during specification and commitment to the T cell lineage. *Development,* 126**,** 3131-3148.

ANGERVALL, L. & CARLSTRÖM, E. 1963. Theoretical criteria for the use of relative organ weights and similar ratios in biology. *Journal of Theoretical Biology,* 4**,** 254-259.

ANSONG, E., YING, Q., EKOUE, D. N., DEATON, R., HALL, A. R., KAJDACSY-BALLA, A., YANG, W., GANN, P. H. & DIAMOND, A. M. 2015. Evidence that selenium binding protein 1 is a tumor suppressor in prostate cancer. *PLoS One,* 10**,** e0127295.

ASNAFI, V., BELDJORD, K., LIBURA, M., VILLARESE, P., MILLIEN, C., BALLERINI, P., KUHLEIN, E., LAFAGE-POCHITALOFF, M., DELABESSE, E., BERNARD, O. & MACINTYRE, E. 2004. Age-related phenotypic and oncogenic differences in T-cell acute lymphoblastic leukemias may reflect thymic atrophy. *Blood,* 104**,** 4173-4180.

BAKER, K. E. & PARKER, R. 2004. Nonsense-mediated mRNA decay: terminating erroneous gene expression. *Current Opinion in Cell Biology,* 16**,** 293-299.

BASSUK, A. G. & LEIDEN, J. M. 1997. The role of Ets transcription factors in the development and function of the mammalian immune system. *Advances in Immunology.*

BERGER, A. H., IMIELINSKI, M., DUKE, F., WALA, J., KAPLAN, N., SHI, G. X., ANDRES, D. A. & MEYERSON, M. 2014. Oncogenic RIT1 mutations in lung adenocarcinoma. *Oncogene,* 33**,** 4418-4423.

BERGER, A. H., KNUDSON, A. G. & PANDOLFI, P. P. 2011. A continuum model for tumour suppression. *Nature,* 476**,** 163-9.

BERNARD, A., BOUMSELL, L., REINHERZ, E. L., NADLER, L. M., RITZ, J., COPPIN, H., RICHARD, Y., VALENSI, F., DAUSSET, J., FLANDRIN, G., LEMERLE, J. & SCHLOSSMAN, S. F. 1981. CELL-SURFACE CHARACTERIZATION OF MALIGNANT T-CELLS FROM LYMPHOBLASTIC LYMPHOMA USING MONOCLONAL-ANTIBODIES - EVIDENCE FOR PHENOTYPIC DIFFERENCES BETWEEN MALIGNANT T-CELLS FROM PATIENTS WITH ACUTE LYMPHOBLASTIC-LEUKEMIA AND LYMPHOBLASTIC LYMPHOMAHO. *Blood,* 57**,** 1105-1110.

BETTERS, D. M. 2015. Use of Flow Cytometry in Clinical Practice. *J Adv Pract Oncol,* 6**,** 435-40.

BJORCK, E., EK, S., LANDGREN, O., JERKEMAN, M., EHINGER, M., BJORKHOLM, M., BORREBAECK, C. A., PORWIT-MACDONALD, A. & NORDENSKJOLD, M. 2005. High

expression of cyclin B1 predicts a favorable outcome in patients with follicular lymphoma. *Blood,* 105**,** 2908-15.

BLACKWELL, B. N., BUCCI, T. J., HART, R. W. & TURTURRO, A. 1995. LONGEVITY, BODY-WEIGHT, AND NEOPLASIA IN AD LIBITUM-FED AND DIET-RESTRICTED C57BL6 MICE FED NIH-31 OPEN FORMULA DIET. *Toxicologic Pathology,* 23**,** 570-582.

BOROWSKY, A. D., MUNN, R. J., GALVEZ, J. J., CARDIFF, R. D., WARD, J. M., MORSE, H. C., 3RD, KOGAN, S. C., ALDAPE, K. D., LOUIS, D. N. & BOSENBERG, M. W. 2004. Mouse models of human cancers (part 3). *Comp Med,* 54**,** 258-70.

BOULTON, E., COLE, C., KNIGHT, A., CLEARY, H., SNOWDEN, R. & PLUMB, M. 2003. Low-penetrance genetic susceptibility and resistance loci implicated in the relative risk for radiation-induced acute myeloid leukemia in mice. *Blood,* 101**,** 2349-54.

BRAYTON, C. F., TREUTING, P. M. & WARD, J. M. 2012. Pathobiology of Aging Mice and GEM: Background Strains and Experimental Design. *Veterinary Pathology Online,* 49**,** 85-105.

BREMNER, R. & BALMAIN, A. 1990. Genetic changes in skin tumor progression: correlation between presence of a mutant ras gene and loss of heterozygosity on mouse chromosome 7. *Cell,* 61**,** 407-17.

BREUER, M., SLEBOS, R., VERBEEK, S., VAN LOHUIZEN, M., WIENTJENS, E. & BERNS, A. 1989. Very high frequency of lymphoma induction by a chemical carcinogen in pim-1 transgenic mice. *Nature,* 340**,** 61-3.

BRUNNING RD, M. BOROWITZ, E. MATUTES, G. FLANDRIN, S. H. SWERDLOW & J. M. BENNET 2008. Precursor T lymphoblastic leukaemia/ lymphoblastic lymphoma (Precursor T-cell acute lymphoblastic leukaemia). *In:* SWERDLOW, S. H., CAMPO, E., HARRIS N. L., JAFFE, E. S., PILERI, S. A., STEIN, H., THIEL, J. & VARDIMAN, J. W. (eds.) *WHO Classification of Tumours of Haematopoietic and Lymphoid Tissues.* 4th ed.: WHO Press.

CAI, W., RUDOLPH, J. L., HARRISON, S. M. W., JIN, L., FRANTZ, A. L., HARRISON, D. A. & ANDRES, D. A. 2011. An evolutionarily conserved Rit GTPase–p38 MAPK signaling pathway mediates oxidative stress resistance. *Molecular Biology of the Cell,* 22**,** 3231-3241.

CANCER RESEARCH UK 2013. Cancer Statistics Report: Non-Hodgkin Lymphoma. Cancer Research UK.

CARTER NP & ORMEROD MG 2000. Introduction to the principles of flow cytometry. *In:* MG, O. (ed.) *Flow Cytometry.* 3rd ed.: NY: Oxford University Press.

CARTWRIGHT, R., BRINCKER, H., CARLI, P. M., CLAYDEN, D., COEBERGH, J. W., JACK, A., MCNALLY, R., MORGAN, G., DE SANJOSE, S., TUMINO, R. & VORNANEN, M. 1999. The rise in incidence of lymphomas in Europe 1985-1992. *Eur J Cancer,* 35**,** 627-33.

CHIARETTI, S. & FOÀ, R. 2009. T-cell acute lymphoblastic leukemia. *Haematologica,* 94**,** 160.

CLAIJ, N., VAN DER WAL, A., DEKKER, M., JANSEN, L. & TE RIELE, H. 2003. DNA mismatch repair deficiency stimulates N-ethyl-N-nitrosourea-induced mutagenesis and lymphomagenesis. *Cancer Res,* 63**,** 2062-6.

CLARKE, C. A. & GLASER, S. L. 2002. Changing incidence of non-Hodgkin lymphomas in the United States. *Cancer,* 94**,** 2015-2023.

CORTELAZZO, S., PONZONI, M., FERRERI, A. J. & HOELZER, D. 2011. Lymphoblastic lymphoma. *Crit Rev Oncol Hematol,* 79**,** 330-43.

CURTIS, R. E., BOICE, J. D., JR., STOVALL, M., BERNSTEIN, L., GREENBERG, R. S., FLANNERY, J. T., SCHWARTZ, A. G., WEYER, P., MOLONEY, W. C. & HOOVER, R. N. 1992. Risk of leukemia after chemotherapy and radiation treatment for breast cancer. *N Engl J Med,* 326**,** 1745-51.

DAI, X., JAMES, R. G., HABIB, T., SINGH, S., JACKSON, S., KHIM, S., MOON, R. T., LIGGITT, D., WOLF-YADLIN, A., BUCKNER, J. H. & RAWLINGS, D. J. 2013. A disease-associated PTPN22 variant promotes systemic autoimmunity in murine models. *J Clin Invest,* 123**,** 2024-36.

DAUPHINOT, L., DE OLIVEIRA, C., MELOT, T., SEVENET, N., THOMAS, V., WEISSMAN, B. E. & DELATTRE, O. 2001. Analysis of the expression of cell cycle regulators in Ewing cell lines: EWS-FLI-1 modulates p57KIP2 and c-Myc expression. *Oncogene,* 20**,** 3258-3265.

DAVIS, R. S., STEPHAN, R. P., CHEN, C. C., DENNIS, G., JR. & COOPER, M. D. 2004. Differential B cell expression of mouse Fc receptor homologs. *Int Immunol,* 16**,** 1343-53.

DAVIS, R. S., WANG, Y. H., KUBAGAWA, H. & COOPER, M. D. 2001. Identification of a family of Fc receptor homologs with preferential B cell expression. *Proc Natl Acad Sci U S A,* 98**,** 9772-7.

DE LEVAL, L., BISIG, B., THIELEN, C., BONIVER, J. & GAULARD, P. 2009. Molecular classification of T-cell lymphomas. *Crit Rev Oncol Hematol,* 72**,** 125-43.

DELATTRE, O., ZUCMAN, J., PLOUGASTEL, B., DESMAZE, C., MELOT, T., PETER, M., KOVAR, H., JOUBERT, I., DE JONG, P., ROULEAU, G., AURIAS, A. & THOMAS, G. 1992. Gene fusion with an ETS DNA-binding domain caused by chromosome translocation in human tumours. *Nature,* 359**,** 162-165.

DEMANT, P. 2003. Cancer susceptibility in the mouse: genetics, biology and implications for human cancer. *Nat Rev Genet,* 4**,** 721-34.

DESCHEPPER CF & GALLO-PAYET N. 2004. *Systolic blood pressure and multi-organ morphologic characterization in 13 inbred strains of mice* [Online]. Mouse Phenome Database web site: The Jackson Laboratory. Available: http://phenome.jax.org/db/qp?rtn=views/measplot&brieflook=10415&projhint=Deschepper1 [Accessed 2014].

DONEHOWER, L. A., HARVEY, M., SLAGLE, B. L., MCARTHUR, M. J., MONTGOMERY, C. A., JR., BUTEL, J. S. & BRADLEY, A. 1992. Mice deficient for p53 are developmentally normal but susceptible to spontaneous tumours. *Nature,* 356**,** 215-21.

DU, X., NAGATA, S., ISE, T., STETLER-STEVENSON, M. & PASTAN, I. 2008. FCRL1 on chronic lymphocytic leukemia, hairy cell leukemia, and B-cell non-Hodgkin lymphoma as a target of immunotoxins. *Blood,* 111**,** 338-43.

DUDGEON, C., CHAN, C., KANG, W., SUN, Y., EMERSON, R., ROBINS, H. & LEVINE, A. J. 2014. The evolution of thymic lymphomas in p53 knockout mice. *Genes & Development,* 28**,** 2613-2620.

DUNN, G. P., KOEBEL, C. M. & SCHREIBER, R. D. 2006. Interferons, immunity and cancer immunoediting. *Nat Rev Immunol,* 6**,** 836-48.

ELHASID, R. & ETZIONI, A. 1996. Major histocompatibility complex class II deficiency: a clinical review. *Blood Rev,* 10**,** 242-8.

ELMORE, S. 2007. Apoptosis: a review of programmed cell death. *Toxicol Pathol,* 35**,** 495-516.

EPPIG, J. T., BLAKE, J. A., BULT, C. J., KADIN, J. A. & RICHARDSON, J. E. 2015. The Mouse Genome Database (MGD): facilitating mouse as a model for human biology and disease. *Nucleic Acids Res,* 43**,** D726-36.

FENSKE, T. S., MCMAHON, C., EDWIN, D., JARVIS, J. C., CHEVERUD, J. M., MINN, M., MATHEWS, V., BOGUE, M. A., PROVINCE, M. A., MCLEOD, H. L. & GRAUBERT, T. A. 2006a. Identification of candidate alkylator-induced cancer susceptibility genes by whole genome scanning in mice. *Cancer Res,* 66**,** 5029-38.

FENSKE, T. S., MCMAHON, C., EDWIN, D., JARVIS, J. C., CHEVERUD, J. M., MINN, M., MATHEWS, V., BOGUE, M. A., PROVINCE, M. A., MCLEOD, H. L. & GRAUBERT, T. A.

2006b. Identification of Candidate Alkylator-Induced Cancer Susceptibility Genes by Whole Genome Scanning in Mice. *Cancer Research,* 66**,** 5029-5038.

FERRANDO, A. A. 2009. The role of NOTCH1 signaling in T-ALL. *Hematology / the Education Program of the American Society of Hematology. American Society of Hematology. Education Program***,** 353-61.

FERRANDO, A. A. & LOOK, A. T. 2003. Gene expression profiling in T-cell acute lymphoblastic leukemia. *Semin Hematol,* 40**,** 274-80.

FERRANDO, A. A., NEUBERG, D. S., STAUNTON, J., LOH, M. L., HUARD, C., RAIMONDI, S. C., BEHM, F. G., PUI, C. H., DOWNING, J. R., GILLILAND, D. G., LANDER, E. S., GOLUB, T. R. & LOOK, A. T. 2002. Gene expression signatures define novel oncogenic pathways in T cell acute lymphoblastic leukemia. *Cancer Cell,* 1**,** 75-87.

FLEX, E., PETRANGELI, V., STELLA, L., CHIARETTI, S., HORNAKOVA, T., KNOOPS, L., ARIOLA, C., FODALE, V., CLAPPIER, E., PAOLONI, F., MARTINELLI, S., FRAGALE, A., SANCHEZ, M., TAVOLARO, S., MESSINA, M., CAZZANIGA, G., CAMERA, A., PIZZOLO, G., TORNESELLO, A., VIGNETTI, M., BATTISTINI, A., CAVE, H., GELB, B. D., RENAULD, J. C., BIONDI, A., CONSTANTINESCU, S. N., FOA, R. & TARTAGLIA, M. 2008. Somatically acquired JAK1 mutations in adult acute lymphoblastic leukemia. *Journal of Experimental Medicine,* 205**,** 751-758.

FLINT, J., VALDAR, W., SHIFMAN, S. & MOTT, R. 2005. Strategies for mapping and cloning quantitative trait genes in rodents. *Nat Rev Genet,* 6**,** 271-86.

FRITH, C. H., WARD, J. M., HARLEMAN, P. C., HALM, S., INOUE, T. & WRIGHT, J. A. 2001. Hematopoietic System. *In:* MOHR, U. (ed.) *International Classification of Rodent Tumors, The Mouse.* Springer.

GAUDET, P., LIVSTONE, M. & THOMAS, P. 2010. The Reference Genome Project (2010) Annotation inferences using phylogenetic trees. The Zebrafish Model Organism Database.

GEBE, J. A., KIENER, P. A., RING, H. Z., LI, X., FRANCKE, U. & ARUFFO, A. 1997. Molecular cloning, mapping to human chromosome 1 q21-q23, and cell binding characteristics of Spalpha, a new member of the scavenger receptor cysteine-rich (SRCR) family of proteins. *J Biol Chem,* 272**,** 6151-8.

GODFREY, D. I., KENNEDY, J., SUDA, T. & ZLOTNIK, A. 2012. Pillars article: a developmental pathway involving four phenotypically and functionally distinct subsets of CD3-CD4-CD8- triple-negative adult mouse thymocytes defined by CD44 and CD25 expression. J. Immunol. 1993. 150: 4244-4252. *J Immunol,* 189**,** 4203-11.

GOLDSBY, R. E., LAWRENCE, N. A., HAYS, L. E., OLMSTED, E. A., CHEN, X., SINGH, M. & PRESTON, B. D. 2001. Defective DNA polymerase-delta proofreading causes cancer susceptibility in mice. *Nat Med,* 7**,** 638-9.

GRULICH, A. E., VAN LEEUWEN, M. T., FALSTER, M. O. & VAJDIC, C. M. 2007. Incidence of cancers in people with HIV/AIDS compared with immunosuppressed transplant recipients: a meta-analysis. *The Lancet,* 370**,** 59-67.

HALEY, P. J. 2013. Lymphoid System. *In:* PRITAM S. SAHOTA, JAMES A. POPP, JERRY F. HARDISTY & GOPINATH, C. (eds.) *Toxicologic Pathology: Nonclinical Safety Assessment.* 1st ed.: CRC Press.

HANAHAN, D. & WEINBERG, R. A. 2000. The hallmarks of cancer. *Cell,* 100**,** 57-70.

HARRIS, N. L., JAFFE, E. S., DIEBOLD, J., FLANDRIN, G., MULLER-HERMELINK, H. K., VARDIMAN, J., LISTER, T. A. & BLOOMFIELD, C. D. 1999a. The World Health Organization classification of neoplastic diseases of the hematopoietic and lymphoid tissues. Report of the Clinical Advisory Committee meeting, Airlie House, Virginia, November, 1997. *Ann Oncol,* 10**,** 1419-32.

HARRIS, N. L., JAFFE, E. S., DIEBOLD, J., FLANDRIN, G., MULLER-HERMELINK, H. K., VARDIMAN, J., LISTER, T. A. & BLOOMFIELD, C. D. 1999b. World Health Organization classification of neoplastic diseases of the hematopoietic and lymphoid tissues: report of the Clinical Advisory Committee meeting-Airlie House, Virginia, November 1997. *J Clin Oncol,* 17**,** 3835-49.

HASHIMOTO, M., YAMASHITA, Y. & MORI, N. 2002. Immunohistochemical detection of CD79a expression in precursor T cell lymphoblastic lymphoma/leukaemias. *Journal of Pathology,* 197**,** 341-347.

HERBERT C. MORSE, MIRIAM R. ANVER, TORGNY N. FREDRICKSON, DIANA C. HAINES, ALAN W. HARRIS, NANCY L. HARRIS, ELAINE S. JAFFE, SCOTT C. KOGAN, IAN C. M. MACLENNAN & WARD, J. M. 2002. Bethesda proposals for classification of lymphoid neoplasms in mice- SUPPLEMENTARY INFORMATION.

HITOTSUMACHI, S., CARPENTER, D. A. & RUSSELL, W. L. 1985. DOSE-REPETITION INCREASES THE MUTAGENIC EFFECTIVENESS OF N-ETHYL-N-NITROSOUREA IN MOUSE SPERMATOGONIA. *Proceedings of the National Academy of Sciences of the United States of America,* 82**,** 6619-6621.

HOELZER, D. & GOKBUGET, N. 2009. T-cell lymphoblastic lymphoma and T-cell acute lymphoblastic leukemia: a separate entity? *Clin Lymphoma Myeloma,* 9 Suppl 3**,** S214-21.

HOELZER, D. & GÖKBUGET, N. 2009. T-Cell Lymphoblastic Lymphoma and T-Cell Acute Lymphoblastic Leukemia: A Separate Entity? *Clinical Lymphoma and Myeloma,* 9, Supplement 3**,** S214-S221.

HOFFMANN, R. & MELCHERS, F. 2003. A genomic view of lymphocyte development - Opinion. *Current Opinion in Immunology,* 15**,** 239-245.

HOOI, C.-F., BLANCHER, C., QIU, W., REVET, I. M., WILLIAMS, L. H., CIAVARELLA, M. L., ANDERSON, R. L., THOMPSON, E. W., CONNOR, A., PHILLIPS, W. A. & CAMPBELL, I. G. 2006. ST7-mediated suppression of tumorigenicity of prostate cancer cells is characterized by remodeling of the extracellular matrix. *Oncogene,* 25**,** 3924-3933.

HORI, M., XIANG, S., QI, C.-F., CHATTOPADHYAY, S. K., FREDRICKSON, T. N., HARTLEY, J. W., KOVALCHUK, A. L., BORNKAMM, G. W., JANZ, S., COPELAND, N. G., JENKINS, N. A., WARD, J. M. & MORSE III, H. C. 2001. Non-Hodgkin Lymphomas of Mice. *Blood Cells, Molecules, and Diseases,* 27**,** 217-222.

ISE, T., MAEDA, H., SANTORA, K., XIANG, L., KREITMAN, R. J., PASTAN, I. & NAGATA, S. 2005. Immunoglobulin superfamily receptor translocation associated 2 protein on lymphoma cell lines and hairy cell leukemia cells detected by novel monoclonal antibodies. *Clin Cancer Res,* 11**,** 87-96.

IUPAC-IUB 1984. IUPAC-IUB Joint Commission on Biochemical Nomenclature (JCBN). Nomenclature and symbolism for amino acids and peptides. Recommendations 1983. *Eur J Biochem,* 138**,** 9-37.

JABBOUR, E., KOSCIELNY, S., SEBBAN, C., PESLIN, N., PATTE, C., GARGI, T., BIRON, P., FERME, C., BOURHIS, J. H., VANTELON, J. M., ARNAUD, P. & RIBRAG, V. 2006. High survival rate with the LMT-89 regimen in lymphoblastic lymphoma (LL), but not in T-cell acute lymphoblastic leukemia (T-ALL). *Leukemia,* 20**,** 814-9.

JACOBY, R. O., FOX, J. G. & DAVISSON, M. 2002a. Biology and Diseases of Mice. *In:* FOX, J. G., ANDERSON, L. C., LOEW, F. L. & QUIMBY, F. W. (eds.) *Laboratory Animal Medicne* 2nd ed.: American College of Laboratory Animal Medicine.

JACOBY, R. O., FOX, J. G. & DAVISSON, M. 2002b. Biology and Diseases of Mice. *In:* FOX, J. G., ANDERSON, L. C., LOEW, F. M. & QUIMBY, F. W. (eds.) *Laboratory Animal Medicine* 2nd ed.: Elsevier.

JORDANOVA, E. S., PHILIPPO, K., GIPHART, M. J., SCHUURING, E. & KLUIN, P. M. 2003. Mutations in the HLA class II genes leading to loss of expression of HLA-DR and HLA-DQ in diffuse large B-cell lymphoma. *Immunogenetics,* 55**,** 203-9.

JORDANOVA, E. S., RIEMERSMA, S. A., PHILIPPO, K., GIPHART-GASSLER, M., SCHUURING, E. & KLUIN, P. M. 2002. Hemizygous deletions in the HLA region account for loss of heterozygosity in the majority of diffuse large B-cell lymphomas of the testis and the central nervous system. *Genes Chromosomes Cancer,* 35**,** 38-48.

JUSTICE, M. J., CARPENTER, D. A., FAVOR, J., NEUHAUSER-KLAUS, A., HRABE DE ANGELIS, M., SOEWARTO, D., MOSER, A., CORDES, S., MILLER, D., CHAPMAN, V., WEBER, J. S., RINCHIK, E. M., HUNSICKER, P. R., RUSSELL, W. L. & BODE, V. C. 2000. Effects of ENU dosage on mouse strains. *Mamm Genome,* 11**,** 484-8.

KAKINUMA, S., NISHIMURA, M., KUBO, A., NAGAI, J. Y., AMASAKI, Y., MAJIMA, H. J., SADO, T. & SHIMADA, Y. 2005a. Frequent retention of heterozygosity for point mutations in p53 and Ikaros in N-ethyl-N-nitrosourea-induced mouse thymic lymphomas. *Mutat Res,* 572**,** 132-41.

KAKINUMA, S., NISHIMURA, M., KUBO, A., NAGAI, J. Y., AMASAKI, Y., MAJIMA, H. J., SADO, T. & SHIMADA, Y. 2005b. Frequent retention of heterozygosity for point mutations in p53 and Ikaros in N-ethyl-N-nitrosourea-induced mouse thymic lymphomas. *Mutation Research - Fundamental and Molecular Mechanisms of Mutagenesis,* 572**,** 132-141.

KALDOR, J. M., DAY, N. E., CLARKE, E. A., VAN LEEUWEN, F. E., HENRY-AMAR, M., FIORENTINO, M. V., BELL, J., PEDERSEN, D., BAND, P., ASSOULINE, D., KOCH, M., CHOI, W., PRIOR, P., BLAIR, V., LANGMARK, F., KIRN, V. P., NEAL, F., PETERS, D., PFEIFFER, R., KARJALAINEN, S., CUZICK, J., SUTCLIFFE, S. B., SOMERS, R., PELLAE-COSSET, B., PAPPAGALLO, G. L., FRASER, P., STORM, H. & STOVALL, M. 1990. Leukemia Following Hodgkin's Disease. *New England Journal of Medicine,* 322**,** 7-13.

KALEEM, Z. 2006. Flow cytometric analysis of lymphomas: current status and usefulness. *Arch Pathol Lab Med,* 130**,** 1850-8.

KALEEM, Z., WHITE, G. & ZUTTER, M. M. 2001. Aberrant expression of T-cell-associated antigens on B-cell non-Hodgkin lymphomas. *Am J Clin Pathol,* 115**,** 396-403.

KEANE, T. M., GOODSTADT, L., DANECEK, P., WHITE, M. A., WONG, K., YALCIN, B., HEGER, A., AGAM, A., SLATER, G., GOODSON, M., FURLOTTE, N. A., ESKIN, E., NELLÅKER, C., WHITLEY, H., CLEAK, J., JANOWITZ, D., HERNANDEZ-PLIEGO, P., EDWARDS, A., BELGARD, T. G., OLIVER, P. L., MCINTYRE, R. E., BHOMRA, A., NICOD, J., GAN, X., YUAN, W., VAN DER WEYDEN, L., STEWARD, C. A., BALA, S., STALKER, J., MOTT, R., DURBIN, R., JACKSON, I. J., CZECHANSKI, A., GUERRA-ASSUNÇAO, J., DONAHUE, L. R., REINHOLDT, L. G., PAYSEUR, B. A., PONTING, C. P., BIRNEY, E., FLINT, J. & ADAMS, D. J. 2011. Mouse genomic variation and its effect on phenotypes and gene regulation. *Nature,* 477**,** 289-294.

KEREM, B., ROMMENS, J. M., BUCHANAN, J. A., MARKIEWICZ, D., COX, T. K., CHAKRAVARTI, A., BUCHWALD, M. & TSUI, L. C. 1989. Identification of the cystic fibrosis gene: genetic analysis. *Science,* 245**,** 1073-80.

KIM, R., EMI, M. & TANABE, K. 2007. Cancer immunoediting from immune surveillance to immune escape. *Immunology,* 121**,** 1-14.

KNOWLTON, R. G., COHEN-HAGUENAUER, O., VAN CONG, N., FREZAL, J., BROWN, V. A., BARKER, D., BRAMAN, J. C., SCHUMM, J. W., TSUI, L. C., BUCHWALD, M. & ET AL. 1985. A polymorphic DNA marker linked to cystic fibrosis is located on chromosome 7. *Nature,* 318**,** 380-2.

KNUDSON, A. G. 1993. Antioncogenes and human cancer. *Proc Natl Acad Sci U S A,* 90**,** 10914-21.

KNUDSON, A. G., JR. 1971. Mutation and cancer: statistical study of retinoblastoma. *Proc Natl Acad Sci U S A,* 68**,** 820-3.

KONDO, S., LU, Y., DEBBAS, M., LIN, A. W., SAROSI, I., ITIE, A., WAKEHAM, A., TUAN, J., SARIS, C., ELLIOTT, G., MA, W., BENCHIMOL, S., LOWE, S. W., MAK, T. W. & THUKRAL, S. K. 2003. Characterization of cells and gene-targeted mice deficient for the p53-binding kinase homeodomain-interacting protein kinase 1 (HIPK1). *Proc Natl Acad Sci U S A,* 100**,** 5431-6.

KONN, Z. J., MARTINEAU, M., BOWN, N., RICHARDS, S., SWANSBURY, J., TALLEY, P., WRIGHT, S. L. & HARRISON, C. J. 2010. Cytogenetics of Long-Term Survivors of ETV6-RUNX1 Fusion Positive Acute Lymphoblastic Leukemia. *Genes Chromosomes & Cancer,* 49**,** 253-259.

KRUPKE, D. M., BEGLEY, D. A., SUNDBERG, J. P., BULT, C. J. & EPPIG, J. T. 2008. The Mouse Tumor Biology database. *Nature reviews. Cancer,* 8**,** 459-465.

KUMAR, V., ABBAS, A. K., FAUSTO, N. & ASTER, J. C. 2010a. Diseases of White Blood Cells, Lymph Nodes, Spleen, and Thymus. *Robbins & Cotran Pathology Basis of Disease.* 8th ed. Philadelphia: Saunders Elsevier.

KUMAR, V., ABBAS, A. K., FAUSTO, N. & ASTER, J. C. 2010b. Diseases of White Blood Cells, Lymph Nodes, Spleen, and Thymus. *Robbins & Cotran Pathology Basis of Disease.* 8th ed. Philadelphia: Saunders Elsevier.

KUMAR, V., ABBAS, A. K., FAUSTO, N. & ASTER, J. C. 2010c. *Pathology Basis of Disease* Saunders Elsevier

KUMAR, V., ABBAS, A. K., FAUSTO, N. & ASTER, J. C. 2010d. *Robbins & Cotran Pathology Basis of Disease*, Saunders Elsevier.

KUMAR, V., ABBAS, A. K., FAUSTO, N. & ASTER, J. C. 2010e. *Robbins & Cotran Pathology Basis of Disease*, Saunders Elsevier.

KUNDER, S., CALZADA-WACK, J., HOLZLWIMMER, G., MULLER, J., KLOSS, C., HOWAT, W., SCHMIDT, J., HOFLER, H., WARREN, M. & QUINTANILLA-MARTINEZ, L. 2007. A comprehensive antibody panel for immunohistochemical analysis of formalin-fixed, paraffin-embedded hematopoietic neoplasms of mice: analysis of mouse specific and human antibodies cross-reactive with murine tissue. *Toxicol Pathol,* 35**,** 366-75.

KUNDU, M., COMPTON, S., GARRETT-BEAL, L., STACY, T., STAROST, M. F., ECKHAUS, M., SPECK, N. A. & LIU, P. P. 2005a. Runx1 deficiency predisposes mice to T-lymphoblastic lymphoma. *Blood,* 106**,** 3621-3624.

KUNDU, M., COMPTON, S., GARRETT-BEAL, L., STACY, T., STAROST, M. F., ECKHAUS, M., SPECK, N. A. & LIU, P. P. 2005b. Runx1 deficiency predisposes mice to T-lymphoblastic lymphoma. *Blood,* 106**,** 3621-4.

KUWATA, K., WATANABE, H., JIANG, S.-Y., YAMAMOTO, T., TOMIYAMA-MIYAJI, C., ABO, T., MIYAZAKI, T. & NAITO, M. 2003. AIM Inhibits Apoptosis of T Cells and NKT Cells in Corynebacterium-Induced Granuloma Formation in Mice. *The American Journal of Pathology,* 162**,** 837-847.

LAI, L., ALAVERDI, N., MALTAIS, L. & MORSE, H. C., 3RD 1998. Mouse cell surface antigens: nomenclature and immunophenotyping. *J Immunol,* 160**,** 3861-8.

LASSEN, L. B., BALLARÍN-GONZÁLEZ, B., SCHMITZ, A., FÜCHTBAUER, A., PEDERSEN, F. S. & FÜCHTBAUER, E. M. 2012. Nras overexpression results in granulocytosis, T-cell expansion and early lethality in mice. *PLoS One,* 7**,** e42216.

LE VOYER, T., LU, Z., BABB, J., LIFSTED, T., WILLIAMS, M. & HUNTER, K. 2000. An epistatic interaction controls the latency of a transgene-induced mammary tumor. *Mammalian Genome,* 11**,** 883-889.

LEE M. SILVER 1995. *Mouse genetics: Concepts and applications*, Oxford University Press, Walton Street, Oxford OX2 6DP, England.

LEVENE, H. 1960. Robust tests for equality of variances. *In:* AL, O. E. (ed.) *Contributions to Probability and Statistics.* USA: Stanford University Press.

LI, F. J., WON, W. J., BECKER, E. J., EASLICK, J. L., TABENGWA, E., LI, R., SHAKHMATOV, M., BURROWS, P. D. & DAVIS, R. S. 2014. Emerging Roles for FCRL Family Members in Lymphocyte Biology and Disease. *Current topics in microbiology and immunology,* 382**,** 29-50.

LI, Q., HAIGIS, K. M., MCDANIEL, A., HARDING-THEOBALD, E., KOGAN, S. C., AKAGI, K., WONG, J. C., BRAUN, B. S., WOLFF, L., JACKS, T. & SHANNON, K. 2011. Hematopoiesis and leukemogenesis in mice expressing oncogenic NrasG12D from the endogenous locus. *Blood,* 117**,** 2022-32.

LOEB, L. A., LOEB, K. R. & ANDERSON, J. P. 2003. Multiple mutations and cancer. *Proceedings of the National Academy of Sciences,* 100**,** 776-781.

LONES, M. A., HEEREMA, N. A., LE BEAU, M. M., SPOSTO, R., PERKINS, S. L., KADIN, M. E., KJELDSBERG, C. R., MEADOWS, A., SIEGEL, S., BUCKLEY, J., ABROMOWITCH, M., KERSEY, J., BERGERON, S., CAIRO, M. S. & SANGER, W. G. 2007. Chromosome abnormalities in advanced stage lymphoblastic lymphoma of children and adolescents: a report from CCG-E08. *Cancer Genetics and Cytogenetics,* 172**,** 1-11.

LOOK, A. T. 1995. Oncogenic role of "master" transcription factors in human leukemias and sarcomas: A developmental model. *Advances in Cancer Research,* 67**,** 25-57.

LU, P., HANKEL, I. L., KNISZ, J., MARQUARDT, A., CHIANG, M. Y., GROSSE, J., CONSTIEN, R., MEYER, T., SCHROEDER, A., ZEITLMANN, L., AL-ALEM, U., FRIEDMAN, A. D., ELLIOTT, E. I., MEYERHOLZ, D. K., WALDSCHMIDT, T. J., ROTHMAN, P. B. & COLGAN, J. D. 2010. The Justy mutation identifies Gon4-like as a gene that is essential for B lymphopoiesis. *J Exp Med,* 207**,** 1359-67.

MACEY, M. G. 1988. Flow cytometry: principles and clinical applications. *Med Lab Sci,* 45**,** 165-73.

MALKINSON, A. M. 1989. THE GENETIC-BASIS OF SUSCEPTIBILITY TO LUNG-TUMORS IN MICE. *Toxicology,* 54**,** 241-271.

MCCORMACK, M. P., YOUNG, L. F., VASUDEVAN, S., DE GRAAF, C. A., CODRINGTON, R., RABBITTS, T. H., JANE, S. M. & CURTIS, D. J. 2010. The Lmo2 Oncogene Initiates Leukemia in Mice by Inducing Thymocyte Self-Renewal. *Science,* 327**,** 879-883.

MCCOY, J. P., JR. 2001. Handling, storage, and preparation of human blood cells. *Curr Protoc Cytom,* Chapter 5**,** Unit 5.1.

MCKENNA, K. C., BEATTY, K. M., VICETTI MIGUEL, R. & BILONICK, R. A. 2009. Delayed processing of blood increases the frequency of activated CD11b+ CD15+ granulocytes which inhibit T cell function. *J Immunol Methods,* 341**,** 68-75.

MCMAHON, M., AYLLON, V., PANOV, K. I. & O'CONNOR, R. 2010. Ribosomal 18 S RNA processing by the IGF-I-responsive WDR3 protein is integrated with p53 function in cancer cell proliferation. *J Biol Chem,* 285**,** 18309-18.

MENG, X. Y., LIU, J., LV, F., LIU, M. Q. & WAN, J. M. 2015. Study on the correlation between extracellular matrix protein-1 and the growth, metastasis and angiogenesis of laryngeal carcinoma. *Asian Pac J Cancer Prev,* 16**,** 2313-6.

MILES, C. & WAYNE, M. 2008. Quantitative trait locus (QTL) analysis. *Nature Education,* 1**,** 208.

MILLER, I., HATZIVASSILIOU, G., CATTORETTI, G., MENDELSOHN, C. & DALLA-FAVERA, R. 2002. IRTAs: a new family of immunoglobulinlike receptors differentially expressed in B cells. *Blood,* 99**,** 2662-9.

MIYAZAKI, T., HIROKAMI, Y., MATSUHASHI, N., TAKATSUKA, H. & NAITO, M. 1999. Increased susceptibility of thymocytes to apoptosis in mice lacking AIM, a novel murine

macrophage-derived soluble factor belonging to the scavenger receptor cysteine-rich domain superfamily. *J Exp Med,* 189**,** 413-22.

MOREAU-GACHELIN, F. 1994. Spi-1/PU.1: an oncogene of the Ets family. *BBA - Reviews on Cancer,* 1198**,** 149-163.

MORI, M., KIMURA, H., IWAMURA, Y., ARAI, S. & MIYAZAKI, T. 2012. Modification of N-glycosylation modulates the secretion and lipolytic function of apoptosis inhibitor of macrophage (AIM). *FEBS Lett,* 586**,** 3569-74.

MORSE, H. C., ANVER, M. R., FREDRICKSON, T. N., HAINES, D. C., HARRIS, A. W., HARRIS, N. L., JAFFE, E. S., KOGAN, S. C., MACLENNAN, I. C. & M, W. J. 2002a. Bethesda proposals for classification of lymphoid neoplasms in mice- SUPPLEMENTARY INFORMATION.

MORSE, H. C., ANVER, M. R., FREDRICKSON, T. N., HAINES, D. C., HARRIS, A. W., HARRIS, N. L., JAFFE, E. S., KOGAN, S. C., MACLENNAN, I. C., PATTENGALE, P. K. & WARD, J. M. 2002b. Bethesda proposals for classification of lymphoid neoplasms in mice. *Blood,* 100**,** 246-58.

MORSE, H. C., QI, C. F., CHATTOPADHYAY, S. K., HORI, M., TADDESSE-HEATH, L., OZATO, K., HARTLEY, J. W., TAYLOR, B. A., WARD, J. M., JENKINS, N. A., COPELAND, N. G. & FREDRICKSON, T. N. 2001. Combined histiologic and molecular features reveal previously unappreciated subsets of lymphoma in AKXD recombinant inbred mice. *Leukemia Research,* 25**,** 719-733.

MUCENSKI, M. L., BEDIGIAN, H. G., SHULL, M. M., COPELAND, N. G. & JENKINS, N. A. 1988a. Comparative molecular genetic analysis of lymphomas from six inbred mouse strains. *J Virol,* 62**,** 839-46.

MUCENSKI, M. L., BEDIGIAN, H. G., SHULL, M. M., COPELAND, N. G. & JENKINS, N. A. 1988b. COMPARATIVE MOLECULAR GENETIC-ANALYSIS OF LYMPHOMAS FROM 6 INBRED MOUSE STRAINS. *Journal of Virology,* 62**,** 839-846.

MUSTAFA, A., GILLMEISTER, L., HERNANDEZ, W. P., LARSEN, C. T., WITONSKY, S., HOLLADAY, S. D., KERR, R. P., AHMED, S. A., SANTO, A. & GOGAL, R. M. 2008. Viability and function in lymphocytes cultured from the horse, chicken, and mouse: Effects of different leukocyte enrichment techniques. *Journal of Immunoassay & Immunochemistry,* 29**,** 370-389.

MUTHUSAMY, N., BARTON, K. & LEIDEN, J. M. 1995. Defective activation and survival of T cells lacking the Ets-1 transcription factor. *Nature,* 377**,** 639-642.

NAF, D., KRUPKE, D. M., SUNDBERG, J. P., EPPIG, J. T. & BULT, C. J. 2002. The mouse tumor biology database: A public resource for cancer genetics and pathology of the mouse. *Cancer Research,* 62**,** 1235-1240.

NAGATA, S., ISE, T. & PASTAN, I. 2009. Fc receptor-like 3 protein expressed on IL-2 nonresponsive subset of human regulatory T cells. *J Immunol,* 182**,** 7518-26.

NAH, E. H., KING, D. E. & CRAIG, F. E. 1997. CD4 and CD8 antigen coexpression: a flow cytometric study of peripheral blood, bone marrow, body fluid, and solid lymphoreticular specimens. *Arch Pathol Lab Med,* 121**,** 381-4.

NCBI. 2016. *NCBI* [Online]. National Center for Biotechnology Information, U.S. National Library of Medicine. Available: https://www.ncbi.nlm.nih.gov/ [Accessed 2016].

NICKLAS, W., BANEUX, P., BOOT, R. & DECELLE, T. 2001. Recommendations for the health monitoring of rodent and rabbit colonies in breeding and experimental units. Laboratory Animals.

OH, H. H., PARK, K. J., KIM, N., PARK, S. Y., PARK, Y. L., OAK, C. Y., MYUNG, D. S., CHO, S. B., LEE, W. S., KIM, K. K. & JOO, Y. E. 2016. Impact of KITENIN on tumor angiogenesis and lymphangiogenesis in colorectal cancer. *Oncol Rep,* 35**,** 253-60.

OIKAWA, T. & YAMADA, T. 2003. Molecular biology of the Ets family of transcription factors. *Gene,* 303**,** 11-34.

OLIVER, S., TAYLOR, F., BOLTON, E., BROOK, C., FERGUSON, B., ROSS, H., WOOD, C. & TATAREK-GINTOWT, R. 2013. Haematological malignancies in England Cancers Diagnosed 2001-2008 NHS- Northern and Yorkshire Cancer Registry and Information Service

ORMEROD MG 2000. Fluorescence and fluorochromes. *In:* MG, O. (ed.) *Flow Cytometry.* 3rd ed. New York: NY: Oxford University Press.

PARKER A., BAIN B., DEVEREUX S., GATTER K., JACK A., MATUTES E., ROONEY N., ROSS F., WILKINS B., WOTHERSPOON A. & RAMSAY A. 2010. Best Practice in Lymphoma Diagnosis and Reporting. London, UK: British Committee for Standards in Haematology, Royal College of Pathologists.

PATAER, A., KAMOTO, T., LU, L. M., YAMADA, Y. & HIAI, H. 1996. Two dominant host resistance genes to pre-B lymphoma in wild-derived inbred mouse strain MSM/Ms. *Cancer Res,* 56**,** 3716-20.

PEDREIRA, C. E., COSTA, E. S., LECREVISSE, Q., VAN DONGEN, J. J. & ORFAO, A. 2013. Overview of clinical flow cytometry data analysis: recent advances and future challenges. *Trends Biotechnol,* 31**,** 415-25.

PERCY D.H. & S.W., B. 2007. *Pathology of Laboratory Rodents and Rabbits*, Iowa State University Press.

PERCY, D. H. & BARTHOLD, S. W. 2007. *Pathology of Laboratory Rodents and Rabbits*, Iowa State University Press.

PILOZZI, E., PULFORD, K., JONES, M., MULLER-HERMELINK, H. K., FALINI, B., RALFKIAER, E., PILERI, S., PEZZELLA, F., DE WOLF-PEETERS, C., ARBER, D., STEIN, H., MASON, D. & GATTER, K. 1998. Co-expression of CD79a (JCB117) and CD3 by lymphoblastic lymphoma. *J Pathol,* 186**,** 140-3.

POLSON, A. G., ZHENG, B., ELKINS, K., CHANG, W., DU, C., DOWD, P., YEN, L., TAN, C., HONGO, J. A., KOEPPEN, H. & EBENS, A. 2006. Expression pattern of the human FcRH/IRTA receptors in normal tissue and in B-chronic lymphocytic leukemia. *Int Immunol,* 18**,** 1363-73.

QIAGEN. 2015. *DNeasy Blood & Tissue Kit* [Online]. Available: https://www.qiagen.com/gb/resources/resourcedetail?id=6b09dfb8-6319-464d-996c-79e8c7045a50(=en [Accessed 2015].

QUWAILID, M. M., HUGILL, A., DEAR, N., VIZOR, L., WELLS, S., HORNER, E., FULLER, S., WEEDON, J., MCMATH, H., WOODMAN, P., EDWARDS, D., CAMPBELL, D., RODGER, S., CAREY, J., ROBERTS, A., GLENISTER, P., LALANNE, Z., PARKINSON, N., COGHILL, E. L., MCKEONE, R., COX, S., WILLAN, J., GREENFIELD, A., KEAYS, D., BRADY, S., SPURR, N., GRAY, I., HUNTER, J., BROWN, S. D. & COX, R. D. 2004. A gene-driven ENU-based approach to generating an allelic series in any gene. *Mamm Genome,* 15**,** 585-91.

RAETZ, E. A., PERKINS, S. L., BHOJWANI, D., SMOCK, K., PHILIP, M., CARROLL, W. L. & MIN, D. J. 2006. Gene expression profiling reveals intrinsic differences between T-cell acute lymphoblastic leukemia and T-cell lymphoblastic lymphoma. *Pediatric Blood & Cancer,* 47**,** 130-140.

RAJAGOPAL, K., SOMMERS, C. L., DECKER, D. C., MITCHELL, E. O., KORTHAUER, U., SPERLING, A. I., KOZAK, C. A., LOVE, P. E. & BLUESTONE, J. A. 1999. RIBP, a novel Rlk/Txk- and itk-binding adaptor protein that regulates T cell activation. *J Exp Med,* 190**,** 1657-68.

RANA, T. M. 2007. Illuminating the silence: understanding the structure and function of small RNAs. *Nat Rev Mol Cell Biol,* 8**,** 23-36.

REGGETI, F. & BIENZLE, D. 2011. Flow cytometry in veterinary oncology. *Vet Pathol,* 48**,** 223-35.

REHG, J. E., BUSH, D. & WARD, J. M. 2012. The Utility of Immunohistochemistry for the Identification of Hematopoietic and Lymphoid Cells in Normal Tissues and

Interpretation of Proliferative and Inflammatory Lesions of Mice and Rats. *Toxicologic Pathology,* 40**,** 345-374.

REILLY, P. T., AFZAL, S., WAKEHAM, A., HAIGHT, J., YOU-TEN, A., ZAUGG, K., DEMBOWY, J., YOUNG, A. & MAK, T. W. 2010. Generation and characterization of the Anp32e-deficient mouse. *PLoS One,* 5**,** e13597.

RIBY, J., MOBLEY, J., ZHANG, J., BRACCI, P. M. & SKIBOLA, C. F. 2016. Serum protein profiling in diffuse large B-cell lymphoma. *Proteomics Clin Appl*.

RIEMERSMA, S. A., JORDANOVA, E. S., SCHOP, R. F., PHILIPPO, K., LOOIJENGA, L. H., SCHUURING, E. & KLUIN, P. M. 2000. Extensive genetic alterations of the HLA region, including homozygous deletions of HLA class II genes in B-cell lymphomas arising in immune-privileged sites. *Blood,* 96**,** 3569-77.

RIMSZA, L. M., ROBERTS, R. A., MILLER, T. P., UNGER, J. M., LEBLANC, M., BRAZIEL, R. M., WEISENBERGER, D. D., CHAN, W. C., MULLER-HERMELINK, H. K., JAFFE, E. S., GASCOYNE, R. D., CAMPO, E., FUCHS, D. A., SPIER, C. M., FISHER, R. I., DELABIE, J., ROSENWALD, A., STAUDT, L. M. & GROGAN, T. M. 2004. Loss of MHC class II gene and protein expression in diffuse large B-cell lymphoma is related to decreased tumor immunosurveillance and poor patient survival regardless of other prognostic factors: a follow-up study from the Leukemia and Lymphoma Molecular Profiling Project. *Blood,* 103**,** 4251-8.

ROBERT L. HALL 2013. Principles of Clinical Pathology. *In:* PRITAM S. SAHOTA, JAMES A. POPP, JERRY F. HARDISTY & GOPINATH, C. (eds.) *Toxicologic Pathology Nonclinical Safety Assessment.* CRC Press Taylor & Francis Group.

ROSENQUIST, R., LINDH, J., ROOS, G. & HOLMBERG, D. 1997. Immunoglobulin V-H gene replacements in a T-cell lymphoblastic lymphoma. *Molecular Immunology,* 34**,** 305-313.

SAITO, T. & WATANABE, N. 1998. Positive and negative thymocyte selection. *Critical Reviews in Immunology,* 18**,** 359-370.

SANJURJO, L., ARAN, G., ROHER, N., VALLEDOR, A. F. & SARRIAS, M.-R. 2015. AIM/CD5L: a key protein in the control of immune homeostasis and inflammatory disease. *Journal of Leukocyte Biology,* 98**,** 173-184.

SAS, I. 2002. SAS OnlineDoc® Version Nine. *In:* INC., S. I. (ed.). Cary, NC, USA.

SCHUBBERT, S., SHANNON, K. & BOLLAG, G. 2007. Hyperactive Ras in developmental disorders and cancer. *Nat Rev Cancer,* 7**,** 295-308.

SEWELL, F., RAGAN, I., MARCZYLO, T., ANDERSON, B., BRAUN, A., CASEY, W., DENNISON, N., GRIFFITHS, D., GUEST, R., HOLMES, T., VAN HUYGEVOORT, T., INDANS, I., KENNY, T., KOJIMA, H., LEE, K., PRIETO, P., SMITH, P., SMEDLEY, J., STOKES, W. S., WNOROWSKI, G. & HORGAN, G. 2015. A global initiative to refine acute inhalation studies through the use of 'evident toxicity' as an endpoint: Towards adoption of the fixed concentration procedure. *Regul Toxicol Pharmacol,* 73**,** 770-9.

SHAPIRO, H. M. 2003. *Practical flow cytometry,* Hoboken, N.J., Hoboken, N.J. : Wiley-Liss.

SHIBATA, M., SATO, T., NUKIWA, R., ARIGA, T. & HATAKEYAMA, S. 2012. TRIM45 negatively regulates NF-kappaB-mediated transcription and suppresses cell proliferation. *Biochem Biophys Res Commun,* 423**,** 104-9.

SHIMADA, Y., NISHIMURA, M., KAKINUMA, S., OGIU, T., FUJIMOTO, H., KUBO, A., NAGAI, J., KOBAYASH, K., TANO, K., YOSHINAGA, S. & BHAKAT, K. K. 2003a. Genetic susceptibility to thymic lymphomas and K-ras gene mutation in mice after exposure to X-rays and N-ethyl-N-nitrosourea. *International Journal of Radiation Biology,* 79**,** 423-430.

SHIMADA, Y., NISHIMURA, M., KAKINUMA, S., OGIU, T., FUJIMOTO, H., KUBO, A., NAGAI, J., KOBAYASH, K., TANO, K., YOSHINAGA, S. & BHAKAT, K. K. 2003b. Genetic

susceptibility to thymic lymphomas and K-ras gene mutation in mice after exposure to X-rays and N-ethyl-N-nitrosourea. *Int J Radiat Biol,* 79**,** 423-30.

SHISA, H., YAMADA, Y., KAWARAI, A., TERADA, N., KAWAI, M., MATSUSHIRO, H. & HIAI, H. 1996. Genetic and epigenetic resistance of SL/Ni mice to lymphomas. *Jpn J Cancer Res,* 87**,** 258-62.

SILVER, L. M. & SILVER, L. M. 1995. *Mouse genetics: Concepts and applications*, Oxford University Press, Inc., 200 Madison Avenue, New York, New York 10016, USA; Oxford University Press, Walton Street, Oxford OX2 6DP, England.

SIM, N.-L., KUMAR, P., HU, J., HENIKOFF, S., SCHNEIDER, G. & NG, P. C. 2012. SIFT web server: predicting effects of amino acid substitutions on proteins. *Nucleic Acids Research*.

SKIBOLA, C. F., CURRY, J. D. & NIETERS, A. 2007. Genetic susceptibility to lymphoma. *Haematologica,* 92**,** 960-9.

SMITH, A. P. L., POLLEY, S., WELLS, S., STEWART, M., VIZOR, L., HUMPHREYS, J., WARREN, M. V., DEAR, N. & CHEESEMAN, M. T. 2009. Analysis of breeding and pathology helps refine management practices of a large-scale N'-ethyl-N'-nitrosourea mouse mutagenesis programme. *Laboratory Animals,* 43**,** 1-10.

SOULIER, J., CLAPPIER, E., CAYUELA, J. M., REGNAULT, A., GARCIA-PEYDRO, M., DOMBRET, H., BARUCHEL, A., TORIBIO, M. L. & SIGAUX, F. 2005. HOXA genes are included in genetic and biologic networks defining human acute T-cell leukemia (TALL). *Blood,* 106**,** 274-286.

STEINIGER, B., BARTH, P. & HELLINGER, A. 2001. The perifollicular and marginal zones of the human splenic white pulp : do fibroblasts guide lymphocyte immigration? *Am J Pathol,* 159**,** 501-12.

STEINIGER, B., TIMPHUS, E. M. & BARTH, P. J. 2006. The splenic marginal zone in humans and rodents: an enigmatic compartment and its inhabitants. *Histochem Cell Biol,* 126**,** 641-8.

SUTTIE, A. W. 2006. Histopathology of the spleen. *Toxicol Pathol,* 34**,** 466-503.

SWAINSON, L. A., MOLD, J. E., BAJPAI, U. D. & MCCUNE, J. M. 2010. Expression of the autoimmune susceptibility gene FcRL3 on human regulatory T cells is associated with dysfunction and high levels of programmed cell death-1. *J Immunol,* 184**,** 3639-47.

SWERDLOW, S., CAMPO, E., HARRIS, N. L., JAFFE, E. S., PILERI, S., STEIN, H., THIELE, J. & VARDIMAN, J. 2008. *WHO classification of tumours of haematopoietic and lymphoid tissues,* Lyon, Lyon : International Agency for Research on Cancer.

SWERDLOW, S. H., CAMPO, E., PILERI, S. A., HARRIS, N. L., STEIN, H., SIEBERT, R., ADVANI, R., GHIELMINI, M., SALLES, G. A., ZELENETZ, A. D. & JAFFE, E. S. 2016. The 2016 revision of the World Health Organization classification of lymphoid neoplasms. *Blood,* 127**,** 2375-90.

SZCZEPANSKI, T., PONGERS-WILLEMSE, M. J., LANGERAK, A. W., HARTS, W. A., WIJKHUIJS, A. J. M., VAN WERING, E. R. & VAN DONGEN, J. J. M. 1999. Ig heavy chain gene rearrangements in T-cell acute lymphoblastic leukemia exhibit predominant DH6-19 and DH7-27 gene usage, can result in complete V-D-J rearrangements, and are rare in T-cell receptor alpha beta lineage. *Blood,* 93**,** 4079-4085.

THOMAS, D. A. & KANTARJIAN, H. M. 2001. Lymphoblastic lymphoma. *Hematology-Oncology Clinics of North America,* 15**,** 51-+.

TO, M. D., WONG, C. E., KARNEZIS, A. N., DEL ROSARIO, R., DI LAURO, R. & BALMAIN, A. 2008. Kras regulatory elements and exon 4A determine mutation specificity in lung cancer. *Nat Genet,* 40**,** 1240-4.

TRAVIS, L. B., CURTIS, R. E., BOICE, J. D., JR., HANKEY, B. F. & FRAUMENI, J. F., JR. 1991. Second cancers following non-Hodgkin's lymphoma. *Cancer,* 67**,** 2002-9.

TSUJIMOTO, S., ISHIDA, T., TAKEDA, T., ISHII, Y., ONOMURA, Y., TSUKIMORI, K., TAKECHI, S., YAMAGUCHI, T., UCHI, H., SUZUKI, S. O., YAMAMOTO, M., HIMENO, M., FURUE, M. & YAMADA, H. 2013. Selenium-binding protein 1: Its physiological function, dependence on aryl hydrocarbon receptors, and role in wasting syndrome by 2,3,7,8-tetrachlorodibenzo-p-dioxin. *Biochimica et Biophysica Acta (BBA) - General Subjects,* 1830**,** 3616-3624.

TU, T. C., BROWN, N. K., KIM, T. J., WROBLEWSKA, J., YANG, X., GUO, X., LEE, S. H., KUMAR, V., LEE, K. M. & FU, Y. X. 2015. CD160 is essential for NK-mediated IFN-gamma production. *J Exp Med,* 212**,** 415-29.

UCKUN, F. M., GAYNON, P. S., SENSEL, M. G., NACHMAN, J., TRIGG, M. E., STEINHERZ, P. G., HUTCHINSON, R., BOSTROM, B. C., SATHER, H. N. & REAMAN, G. H. 1997. Clinical features and treatment outcome of childhood T-lineage acute lymphoblastic leukemia according to the apparent maturational stage of T-lineage leukemic blasts: a Children's Cancer Group study. *J Clin Oncol,* 15**,** 2214-21.

UYTTEBROECK, A., VANHENTENRIJK, V., HAGEMEIJER, A., BOECKX, N., RENARD, M., WLODARSKA, I., VANDENBERGHE, P., DEPAEPE, P. & DE WOLF-PEETERS, C. 2007. Is there a difference in childhood T-cell acute lymphoblastic leukaemia and T-cell lymphoblastic lymphoma? *Leuk Lymphoma,* 48**,** 1745-54.

VAN DONGEN, J. J., LHERMITTE, L., BOTTCHER, S., ALMEIDA, J., VAN DER VELDEN, V. H., FLORES-MONTERO, J., RAWSTRON, A., ASNAFI, V., LECREVISSE, Q., LUCIO, P., MEJSTRIKOVA, E., SZCZEPANSKI, T., KALINA, T., DE TUTE, R., BRUGGEMANN, M., SEDEK, L., CULLEN, M., LANGERAK, A. W., MENDONCA, A., MACINTYRE, E., MARTIN-AYUSO, M., HRUSAK, O., VIDRIALES, M. B. & ORFAO, A. 2012. EuroFlow antibody panels for standardized n-dimensional flow cytometric immunophenotyping of normal, reactive and malignant leukocytes. *Leukemia,* 26**,** 1908-75.

VAN ETTEN, R. A. 2008. Murine Models of Haematopoietic Disease: Pathologic Analysis and Characterization. *In:* SHAOGUANG LI (ed.) *Mouse Models of Human Blood Cancers: Basic Reseacrh and Pre-clinical Applications.* NY, USA: Springer.

VAN LEEUWEN, F. E., KLOKMAN, W. J., HAGENBEEK, A., NOYON, R., VAN DEN BELT-DUSEBOUT, A. W., VAN KERKHOFF, E. H., VAN HEERDE, P. & SOMERS, R. 1994. Second cancer risk following Hodgkin's disease: a 20-year follow-up study. *J Clin Oncol,* 12**,** 312-25.

VAN VLIERBERGHE, P., PIETERS, R., BEVERLOO, H. B. & MEIJERINK, J. P. P. 2008. Molecular-genetic insights in paediatric T-cell acute lymphoblastic leukaemia. *British Journal of Haematology,* 143**,** 153-168.

VON BOEHMER, H., AIFANTIS, I., GOUNARI, F., AZOGUI, O., HAUGHN, L., APOSTOLOU, I., JAECKEL, E., GRASSI, F. & KLEIN, L. 2003. Thymic selection revisited: how essential is it? *Immunological Reviews,* 191**,** 62-78.

WAINWRIGHT, B. J., SCAMBLER, P. J., SCHMIDTKE, J., WATSON, E. A., LAW, H. Y., FARRALL, M., COOKE, H. J., EIBERG, H. & WILLIAMSON, R. 1985. Localization of cystic fibrosis locus to human chromosome 7cen-q22. *Nature,* 318**,** 384-5.

WANG, J., LIU, Y., LI, Z., WANG, Z., TAN, L. X., RYU, M. J., MELINE, B., DU, J., YOUNG, K. H., RANHEIM, E., CHANG, Q. & ZHANG, J. 2011. Endogenous oncogenic Nras mutation initiates hematopoietic malignancies in a dose- and cell type-dependent manner. *Blood,* 118**,** 368-79.

WANG S., C. J. BASTEN & ZENG', Z.-B. 2012. *Windows QTL Cartographer 2.5.* [Online]. North Carolina, Raleigh, NC: Department of Statistics, North Carolina State University, Raleigh, NC. Available: http://statgen.ncsu.edu/qtlcart/WQTLCart.htm [Accessed 2016].

WANG, Y., EDINGER, M., MITTAR, D. & MCINTYRE, C. 2012a. Studying Mouse Thymocyte Developmeent using Multiparametric Flow Cytometry: An Efficent Method to Improve an 8-Color Panel on the BDFACSVerse (tm) Sustem. *BD Biosciences Application Note*.

WANG, Y., EDINGER, M., MITTAR, D. & MCINTYRE, C. 2012b. Studying Mouse Thymocyte Developmeent using Multiparametric Flow Cytometry: An Efficent Method to Improve an 8-Color Panel on the BDFACSVerse (tm) System. *BD Biosciences Application Note*.

WARD, J. M. 2006. Lymphomas and leukemias in mice. *Experimental and Toxicologic Pathology,* 57**,** 377-381.

WARD, J. M., MANN, P. C., MORISHIMA, H. & FRITH, C. H. 1999. Thymus, Spleen, and Lymph Nodes. *In:* MARONPOT, R. R. (ed.) *Pathology of The Mouse.* Cache River Press.

WARD, J. M., REHG, J. E. & MORSE, H. C. 2012. Differentiation of rodent immune and hematopoietic system reactive lesions from neoplasias. *Toxicol Pathol,* 40**,** 425-34.

WEBER, J. S., SALINGER, A. & JUSTICE, M. J. 2000. Optimal N-ethyl-N-nitrosourea (ENU) doses for inbred mouse strains. *Genesis,* 26**,** 230-3.

WELLCOME TRUST SANGER INSTITUTE. 2011. *Mouse Genomes Project - Query SNPs, indels or SVs* [Online]. Available: http://www.sanger.ac.uk/sanger/Mouse_SnpViewer/rel-1410 [Accessed 2016].

WENG, A. P., FERRANDO, A. A., LEE, W., MORRIS, J. P., SILVERMAN, L. B., SANCHEZ-IRIZARRY, C., BLACKLOW, S. C., LOOK, A. T. & ASTER, J. C. 2004. Activating mutations of NOTCH1 in human T cell acute lymphoblastic leukemia. *Science,* 306**,** 269-271.

WILLIAMS RW. 2015. *Web QTL - GeneNetwork Resource* [Online]. Available: www.genenetwork.org/glossary.html [Accessed 2016].

WOOD, B. L., ARROZ, M., BARNETT, D., DIGIUSEPPE, J., GREIG, B., KUSSICK, S. J., OLDAKER, T., SHENKIN, M., STONE, E. & WALLACE, P. 2007. 2006 Bethesda International Consensus recommendations on the immunophenotypic analysis of hematolymphoid neoplasia by flow cytometry: optimal reagents and reporting for the flow cytometric diagnosis of hematopoietic neoplasia. *Cytometry B Clin Cytom,* 72 Suppl 1**,** S14-22.

XU, F., SUN, S., YAN, S., GUO, H., DAI, M. & TENG, Y. 2015. Elevated expression of RIT1 correlates with poor prognosis in endometrial cancer. *Int J Clin Exp Pathol,* 8**,** 10315-24.

XU, J., HAIGIS, K. M., FIRESTONE, A. J., MCNERNEY, M. E., LI, Q., DAVIS, E., CHEN, S. C., NAKITANDWE, J., DOWNING, J., JACKS, T., LE BEAU, M. M. & SHANNON, K. 2013. Dominant role of oncogene dosage and absence of tumor suppressor activity in Nras-driven hematopoietic transformation. *Cancer Discov,* 3**,** 993-1001.

YALCIN, B., WONG, K., AGAM, A., GOODSON, M., KEANE, T. M., GAN, X., NELLAKER, C., GOODSTADT, L., NICOD, J., BHOMRA, A., HERNANDEZ-PLIEGO, P., WHITLEY, H., CLEAK, J., DUTTON, R., JANOWITZ, D., MOTT, R., ADAMS, D. J. & FLINT, J. 2011. Sequence-based characterization of structural variation in the mouse genome. *Nature,* 477**,** 326-329.

YANG, Y. L., LIN, S. R., CHEN, J. S., LIN, S. W., YU, S. L., CHEN, H. Y., YEN, C. T., LIN, C. Y., LIN, J. F., LIN, K. H., JOU, S. T., HU, C. Y., CHANG, S. K., LU, M. Y., CHANG, H. H., CHANG, W. H., LIN, K. S. & LIN, D. T. 2010. Expression and prognostic significance of the apoptotic genes BCL2L13, Livin, and CASP8AP2 in childhood acute lymphoblastic leukemia. *Leukemia Research,* 34**,** 18-23.

YATES, A., AKANNI, W., AMODE, M. R., BARRELL, D., BILLIS, K., CARVALHO-SILVA, D., CUMMINS, C., CLAPHAM, P., FITZGERALD, S., GIL, L., GIRÓN, C. G., GORDON, L., HOURLIER, T., HUNT, S. E., JANACEK, S. H., JOHNSON, N., JUETTEMANN, T., KEENAN,

S., LAVIDAS, I., MARTIN, F. J., MAUREL, T., MCLAREN, W., MURPHY, D. N., NAG, R., NUHN, M., PARKER, A., PATRICIO, M., PIGNATELLI, M., RAHTZ, M., RIAT, H. S., SHEPPARD, D., TAYLOR, K., THORMANN, A., VULLO, A., WILDER, S. P., ZADISSA, A., BIRNEY, E., HARROW, J., MUFFATO, M., PERRY, E., RUFFIER, M., SPUDICH, G., TREVANION, S. J., CUNNINGHAM, F., AKEN, B. L., ZERBINO, D. R. & FLICEK, P. 2016. Ensembl 2016. *Nucleic Acids Research,* 44**,** D710-D716.

YOSHIHIRO YAMADA, HAYASE SHISA, HISANORI MATSUSHIRO, TOSHIYUKI KAMOTO, YASUHITO KOBAYASH, ATSUKO KAWARAI & HIROSHI HIAI 1994. T lymphomagenesis is determined by a dominant host gene thymic lymphoma susceptible mouse-1 (TLSM-1) in mouse models. *The Journal of Experimental Medicine,* 180**,** 2155-2162.

YOU, M. J., MEDEIROS, L. J. & HSI, E. D. 2015. T-Lymphoblastic Leukemia/Lymphoma. *American Journal of Clinical Pathology,* 144**,** 411-422.

YUAN, Y., ZHOU, L., MIYAMOTO, T., IWASAKI, H., HARAKAWA, N., HETHERINGTON, C. J., BUREL, S. A., LAGASSE, E., WEISSMAN, I. L., AKASHI, K. & ZHANG, D. E. 2001a. AML1-ETO expression is directly involved in the development of acute myeloid leukemia in the presence of additional mutations. *Proceedings of the National Academy of Sciences of the United States of America,* 98**,** 10398-10403.

YUAN, Y., ZHOU, L., MIYAMOTO, T., IWASAKI, H., HARAKAWA, N., HETHERINGTON, C. J., BUREL, S. A., LAGASSE, E., WEISSMAN, I. L., AKASHI, K. & ZHANG, D. E. 2001b. AML1-ETO expression is directly involved in the development of acute myeloid leukemia in the presence of additional mutations. *Proc Natl Acad Sci U S A,* 98**,** 10398-403.

ZENG, H., CHEN, Y., YU, M., XUE, L., GAO, X., MORRIS, S. W., WANG, D. & WEN, R. 2008. T Cell Receptor-mediated Activation of CD4(+)CD44(hi) T Cells Bypasses Bcl10: AN IMPLICATION OF DIFFERENTIAL NF-κB DEPENDENCE OF NAïVE AND MEMORY T CELLS DURING T CELL RECEPTOR-MEDIATED RESPONSES. *The Journal of Biological Chemistry,* 283**,** 24392-24399.

ZHANG, W., DAHLBERG, J. E. & TAM, W. 2007. MicroRNAs in tumorigenesis: a primer. *Am J Pathol,* 171**,** 728-38.

ZHANG, Z., WANG, Y., VIKIS, H. G., JOHNSON, L., LIU, G., LI, J., ANDERSON, M. W., SILLS, R. C., HONG, H. L., DEVEREUX, T. R., JACKS, T., GUAN, K. L. & YOU, M. 2001. Wildtype Kras2 can inhibit lung carcinogenesis in mice. *Nat Genet,* 29**,** 25-33.

ZITVOGEL, L., TESNIERE, A. & KROEMER, G. 2006. Cancer despite immunosurveillance: immunoselection and immunosubversion. *Nat Rev Immunol,* 6**,** 715-27.

7. Appendix 1 - List of materials and reagents

Product (including reagents and labware)	Manufacturer
ADVIA Haematology Analyzer	Siemens Healthineers
Beckam Coulter AU680	Beckam Coulter
Buffer for organ preservation during transport: RPMI with 2% FCS (v/v)	Prepared in house
C Tubes	BD Biosciences
CD117 APC	BD Biosciences
CD16	BD Biosciences
CD19 BV510	BD Biosciences
CD25 PE	BD Biosciences
CD3 Pac Blue	BD Biosciences
CD4 FITC	BD Biosciences
CD44 PerCP-Cy5.5	BD Biosciences
CD45 PECy7	BD Biosciences
CD8a APC-Cy7	BD Biosciences
Collagenase D	Roche
DNeasy Blood & Tissue Kit	Qiagen
EDTA 5mM	Sigma
ENU ISOPAC®	Sigma
FACSCanto II	BD Biosciences
FACSDiva™	BD Biosciences
Falcon Filters	BD Biosciences
FC buffer: PBS 1X (Sigma); EDTA 5mM; 0.5% FCS (v/v)	Prepared in house
FloJo™	FloJo
GigaMUGA array	GeneSeek
Macs Gentle Cell Dissociator	Miltenyibiotec
Moxi Z cell counter	Bio-Rad
NanoDrop Thermo 8000	Thermo Scientific
New-born Calf Serum, New Zealand origin	Life Technologies
PBS	Sigma
Rapid- Diff II	Bios Europe
Red blood cell lysis buffer (1:10 dilution required)	eBiosciences
RPMI buffer	Sigma
Stopping reaction buffer: PBS 1X/EDTA 0.1 M (37.5g in one litre)	Prepared in house
Sytox Blue	BD Biosciences

8. Appendix 2 - Tables and figures

1st Value	2nd Value	Average	Concentration	Average Value at end	Loss in value	Concentration 2	Batch number	Vol ethanol
1.646	1.645	1.6455	11.8476	1.6325	-0.01300	11.8476	267 AJ 100mg/kg	10ml
1.432	1.444	1.4380	10.3536	1.4250	-0.01300	10.3536	267 AJ 100mg/kg	10ml
1.501	1.505	1.5030	10.8216	1.4980	-0.00500	10.8216	267 AJ 80mg/kg	10ml
1.549	1.557	1.5530	11.1816	1.5505	-0.00250	11.1816	269 AJ 100mg/kg	10ml
1.492	1.500	1.4960	10.7712	1.4810	-0.01500	10.7712	269 AJ 90mg/kg	10ml
1.419	1.418	1.4185	10.2132	1.4090	-0.00950	10.2132	269 AJ 80mg/kg	10ml
1.026	1.035	1.0305	7.4196	1.0150	-0.01550	7.4196	271 AJ 100mg/kg	10ml
1.076	1.094	1.0850	7.8120	1.0770	-0.00800	7.8120	271 AJ 100mg/kg	8ml
1.143	1.148	1.1455	8.2476	1.1330	-0.01250	8.2476	271 AJ 90mg/kg	8ml
1.097	1.109	1.1030	7.9416	1.0960	-0.00700	7.9416	271 AJ 90mg/kg	8ml
1.452	1.463	1.4575	10.4940	1.4485	-0.00900	10.4940	271 AJ 80mg/kg	6ml

Table 94: ENU concentration at each treatment. Spectrometer adjusted to 398.

P1 Stock	Panel 1:	Fluorochrome	Recommended Dilution	Stock for FMO	Antibody (µl)	Buffer (µl)				
S1	**CD3**	Pac Blue	1:100	1:10	12	108				
S2	**CD4**	FITC	1:1600	1:160	1	159				
S3	**CD8**	APC-Cy7	1:200	1:20	6	114				
S4	**CD25**	PE	1:200	1:20	6	114				
S5	**CD44**	PE-CF594	1:1600	1:160	1	159				
S6	**CD45**	PECy7	1:8000	1:800	1	799				
S7	**CD117**	APC	1:100	1:10	12	108				
P1 Single Stains			**Buffer**	**CD3**	**CD4**	**CD8**	**CD25**	**CD44**	**CD45**	**CD117**
A1	**CD3**	Pac Blue	108 µl	12µl	**x**	**x**	**x**	**x**	**x**	**x**
A2	**CD4**	FITC	108 µl	**x**	12µl	**x**	**x**	**x**	**x**	**x**
A3	**CD8**	APC-Cy7	108 µl	**x**	**x**	12µl	**x**	**x**	**x**	**x**
A4	**CD25**	PE	108 µl	**x**	**x**	**x**	12µl	**x**	**x**	**x**
A5	**CD44**	PE-CF594	108 µl	**x**	**x**	**x**	**x**	12µl	**x**	**x**
A6	**CD45**	PECy7	108 µl	**x**	**x**	**x**	**x**	**x**	12µl	**x**
A7	**CD117**	APC	108 µl	**x**	**x**	**x**	**x**	**x**	**x**	12µl
P1 FMO			**Buffer**	**CD3**	**CD4**	**CD8**	**CD25**	**CD44**	**CD45**	**CD117**
C1	**CD3**	Pac Blue	48µl	**x**	12µl	12µl	12µl	12µl	12µl	12µl
C2	**CD4**	FITC	48µl	12µl	**x**	12µl	12µl	12µl	12µl	12µl
C3	**CD8**	APC-Cy7	48µl	12µl	12µl	**x**	12µl	12µl	12µl	12µl
C4	**CD25**	PE	48µl	12µl	12µl	12µl	**x**	12µl	12µl	12µl
C5	**CD44**	PE-CF594	48µl	12µl	12µl	12µl	12µl	**x**	12µl	12µl
C6	**CD45**	PECy7	48µl	12µl	12µl	12µl	12µl	12µl	**x**	12µl
C7	**CD117**	APC	48µl	12µl	12µl	12µl	12µl	12µl	12µl	**x**

Table 95: Antibody preparation for thymus antibody conjugate panel FMO experiment. S= stock solutions, A= single stain solutions, C= FMO cocktails

P1 Stock	Panel 1:	Fluorochrome	Recommended Dilution	Stock for FMO	Antibody (µl)	Buffer (µl)					
S1	**CD3**	Pac Blue	1:100	1:10	12	108					
S2	**CD4**	FITC	1:800	1:80	2	158					
S3	**CD8**	APC-Cy7	1:200	1:20	6	114					
S4	**CD19**	AmCyan	1:200	1:20	6	114					
S5	**CD25**	PE	1:200	1:20	6	114					
S6	**CD44**	PE-CF594	1:1600	1:160	1	159					
S7	**CD45**	PECy7	1:8000	1:800	1	799					
S8	**CD117**	APC	1:200	1:20	6	114					
P1 Single Stains			**Buffer**	**CD3**	**CD4**	**CD8**	**CD19**	**CD25**	**CD44**	**CD45**	**CD117**
A1	**CD3**	Pac Blue	108µl	12µl	**x**	**x**	**x**	**x**	**x**	**x**	x
A2	**CD4**	FITC	108µl	**x**	12µl	**x**	**x**	**x**	**x**	**x**	x
A3	**CD8**	APC-Cy7	108µl	**x**	**x**	12µl	**x**	**x**	**x**	**x**	**x**
A4	**CD19**	AmCyan	108µl	**x**	**x**	**x**	12µl	**x**	**x**	**x**	**x**
A5	**CD25**	PE	108µl	**x**	**x**	**x**	**x**	12µl	**x**	**x**	x
A6	**CD44**	PE-CF594	108µl	**x**	**x**	**x**	**x**	**x**	12µl	**x**	x
A7	**CD45**	PECy7	108µl	**x**	**x**	**x**	**x**	**x**	**x**	12µl	x
A8	**CD117**	APC	108µl	**x**	**x**	**x**	**x**	**x**	**x**	**x**	12µl
P1 FMO			**Buffer**	**CD3**	**CD4**	**CD8**	**CD19**	**CD25**	**CD44**	**CD45**	**CD117**
C1	**CD3**	Pac Blue	36µl	**x**	12µl	12µl	12µl	12µl	12µl	12µl	12µl
C2	**CD4**	FITC	36µl	12µl	**x**	12µl	12µl	12µl	12µl	12µl	12µl
C3	**CD8**	APC-Cy7	36µl	12µl	12µl	**x**	12µl	12µl	12µl	12µl	12µl
C4	**CD19**	AmCyan	36µl	12µl	12µl	12µl	**x**	12µl	12µl	12µl	12µl
C5	**CD25**	PE	36µl	12µl	12µl	12µl	12µl	**x**	12µl	12µl	12µl
C6	**CD44**	PE-CF594	36µl	12µl	12µl	12µl	12µl	12µl	**x**	12µl	12µl
C7	**CD45**	PECy7	36µl	12µl	12µl	12µl	12µl	12µl	12µl	**x**	12µl
C8	**CD117**	APC	36µl	12µl	12µl	12µl	12µl	12µl	12µl	12µl	**x**

Table 96: Antibody preparation for spleen antibody conjugate panel FMO experiment. S= stock solutions, A= single stain solutions, C= FMO cocktails

	Flow in time	**Live leucocytes**	**FSC singlets**	**SSC singlets**
Minimum	82.5	77.1	97.5	290581
25% Percentile	90.35	86.1	98.03	345412
Median	93.1	87.1	98.3	374505
75% Percentile	96.2	89.03	98.5	386699
Maximum	96.8	94.5	99	407000
IQR				
RI high (Q3+1.5*IQR)				
RI low (Q1-1.5*IQR)				
Mean	92.46	87.2	98.28	366447
Std. Deviation	4.1	3.896	0.3412	29931
Mean + 2SD	100.66	94.992	98.9624	426309
Mean - 2SD	84.26	79.408	97.5976	306585
P value	0.0846	0.109	0.6359	0.1044
Passed normality test (alpha=0.05)?	Yes	Yes	Yes	Yes

Table 97: Flow cytometry of control thymi, general profile

	CD4+ | Freq. of Parent (%)	CD4+ | Mean (FSC-A)	CD4+ | Median (Comp-FITC-A)
Minimum	8.63	73164	5474
25% Percentile	9.69	78046	6377
Median	11.4	80014	7663
75% Percentile	12.9	83408	8281
Maximum	17.1	88353	8834
IQR			1904
RI high (Q3+1.5*IQR)			11137
RI low (Q1-1.5*IQR)			3521
Mean	11.62	80634	7291
Std. Deviation	2.323	3732	1104
Mean + 2SD	16.266	88098	
Mean - 2SD	6.974	73170	
P value	0.174	0.9535	0.0395
Passed normality test (alpha=0.05)?	Yes	Yes	No

Table 98: Flow cytometry of control thymi, CD4+ group results

	CD8+ | Freq. of Parent (%)	CD8+ | Mean (FSC-A)	CD8+ | Median (Comp-APC-Cy7-A)
Minimum	2.03	79224	892
25% Percentile	2.49	84616	2385
Median	2.86	88016	2804
75% Percentile	3.29	91060	3059
Maximum	3.93	95371	4041
IQR			674
RI high (Q3+1.5*IQR)			4070
RI low (Q1-1.5*IQR)			1374
Mean	2.887	87901	2730
Std. Deviation	0.5193	4045	613.6
Mean + 2SD	3.9256	95991	
Mean - 2SD	1.8484	79811	
P value	0.8244	0.8712	0.0081
Passed normality test (alpha=0.05)?	Yes	Yes	No

Table 99: Flow cytometry of control thymi, CD8+ group results

	CD8+CD4+ | Freq. of Parent (%)	CD8+CD4+ | Mean (FSC-A)	CD8+CD4+ | Median (Comp-APC-Cy7-A)	CD8+CD4+ | Median (Comp-FITC-A)
Minimum	75.3	66423	937	3746
25% Percentile	79.1	69979	2103	4615
Median	81.2	72352	2323	5291
75% Percentile	82.2	73480	2637	6317
Maximum	84.5	77925	2963	6645
IQR			534	
RI high (Q3+1.5*IQR)			3438	
RI low (Q1-1.5*IQR)			1302	
Mean	80.66	71917	2341	5345
Std. Deviation	2.281	2843	440.7	894.4
Mean + 2SD	85.222	77603		7133.8
Mean - 2SD	76.098	66231		3556.2
P value	0.3643	0.7177	0.0009	0.1251
Passed normality test (alpha=0.05)?	Yes	Yes	No	Yes

Table 100: Flow cytometry of control thymi, DP group results

	CD8-CD4- | Freq. of Parent (%)	CD8-CD4- | Mean (FSC-A)	CD8-CD4- | Median (Comp-APC-Cy7-A)	CD8-CD4- | Median (Comp-FITC-A)
Minimum	3.73	85573	18	77.1
25% Percentile	4.4	93354	67.75	156.5
Median	5.37	94813	86.1	186.5
75% Percentile	5.61	97069	100.3	198
Maximum	6.79	101817	155	299
IQR				
RI high (Q3+1.5*IQR)				
RI low (Q1-1.5*IQR)				
Mean	5.229	94822	85.71	175.9
Std. Deviation	0.8366	4322	28.26	51.91
Mean + 2SD	6.9022	103466	142.23	279.72
Mean - 2SD	3.5558	86178	29.19	72.08
P value	0.8588	0.7607	0.2166	0.51
Passed normality test (alpha=0.05)?	Yes	Yes	Yes	Yes

Table 101: Flow cytometry of control thymi, DN group results

	DN1 | Freq. of Parent (%)	DN1 | Mean (FSC-A)	DN1 | Median (Comp-PE-A)	DN1 | Median (Comp-PE-CF594-A)
Minimum	30.7	82230	-407	4791
25% Percentile	48.4	86760	-269.5	14487
Median	53.4	90476	-213	17845
75% Percentile	58.5	92211	-181.3	22457
Maximum	92	97663	7.7	32409
IQR	10.1			
RI high (Q3+1.5*IQR)	73.65			
RI low (Q1-1.5*IQR)	33.25			
Mean	53.77	90078	-215.9	18346
Std. Deviation	14.84	3938	83.36	6988
Mean + 2SD		97954	-49.18	32322
Mean - 2SD		82202	-382.62	4370
P value	0.0456	0.9925	0.0916	0.8208
Passed normality test (alpha=0.05)?	No	Yes	Yes	Yes

Table 102: Flow cytometry of control thymi, DN1 group results

	DN2 | Freq. of Parent (%)	DN2 | Mean (FSC-A)	DN2 | Median (Comp-PE-A)	DN2 | Median (Comp-PE-CF594-A)
Minimum	0.57	100946	2917	4643
25% Percentile	0.66	116566	4237	11967
Median	0.92	122100	5451	14635
75% Percentile	1.035	125634	6432	17096
Maximum	1.26	134757	6926	18158
IQR				
RI high (Q3+1.5*IQR)				
RI low (Q1-1.5*IQR)				
Mean	0.8795	120923	5236	13890
Std. Deviation	0.2029	7620	1210	3841
Mean + 2SD	1.2853	136163	7656	21572
Mean - 2SD	0.4737	105683	2816	6208
P value	0.32	0.1283	0.4885	0.083
Passed normality test (alpha=0.05)?	Yes	Yes	Yes	Yes

Table 103: Flow cytometry of control thymi, DN2 group results

	DN3 | Freq. of Parent (%)	DN3 | Mean (FSC-A)	DN3 | Median (Comp-PE-A)	DN3 | Median (Comp-PE-CF594-A)
Minimum	3.51	92077	2670	596
25% Percentile	17.75	98126	3739	753.5
Median	22.4	103154	4444	892
75% Percentile	25.45	106141	5093	1087
Maximum	33.1	107323	6660	1432
IQR				
RI high (Q3+1.5*IQR)				
RI low (Q1-1.5*IQR)				
Mean	21.69	101963	4483	916.3
Std. Deviation	7.334	4638	976.9	231.9
Mean + 2SD	36.358	111239	6436.8	1380.1
Mean - 2SD	7.022	92687	2529.2	452.5
P value	0.189	0.2953	0.8232	0.4467
Passed normality test (alpha=0.05)?	Yes	Yes	Yes	Yes

Table 104: Flow cytometry of control thymi, DN3 group results

	DN4 | Freq. of Parent (%)	DN4 | Mean (FSC-A)	DN4 | Median (Comp-PE-A)	DN4 | Median (Comp-PE-CF594-A)
Minimum	3.42	82814	-195	282
25% Percentile	20.15	95014	-152.3	338
Median	23.6	97965	-118.5	370
75% Percentile	29.5	103364	-100	478.5
Maximum	40	111761	10.3	546
IQR			52.3	
RI high (Q3+1.5*IQR)			-21.55	
RI low (Q1-1.5*IQR)			-230.75	
Mean	23.65	98339	-117.5	396.9
Std. Deviation	8.264	6366	45.42	79.63
Mean + 2SD	40.178	111071		556.16
Mean - 2SD	7.122	85607		237.64
P value	0.106	0.4392	0.0346	0.2042
Passed normality test (alpha=0.05)?	Yes	Yes	No	Yes

Table 105: Flow cytometry of control thymi, DN4 group results

	Flow in time	Live leucocytes	Lymphocytes	FSC singlets	SSC singlets
Minimum	80.7	70.1	78.1	98.7	207004
25% Percentile	89.45	74.65	81.4	99	239450
Median	91.3	77.9	83.95	99.5	251043
75% Percentile	92.3	82.58	85.25	99.6	260982
Maximum	97.2	85.4	88.1	99.8	288331
IQR					
RI high (Q3+1.5*IQR)					
RI low (Q1-1.5*IQR)					
Mean	90.33	77.99	83.29	99.37	249355.00
Std. Deviation	4.238	4.948	2.766	0.3083	16628
Mean + 2SD	98.81	87.89	88.82	99.99	282611.00
Mean - 2SD	81.85	68.09	77.76	98.75	216099.00
P value	0.0781	0.4871	0.7509	0.3623	0.1232
Passed normality test (alpha=0.05)?	Yes	Yes	Yes	Yes	Yes

Table 106: Flow cytometry of control spleens, general profile

	B-lymphocytes | Freq. of Parent (%)	B-lymphocytes | Mean (FSC-A)	B-lymphocytes | Median (Comp-AmCyan-A)
Minimum	57.3	84235	3420
25% Percentile	62.88	90683	4040
Median	68.25	93306	4403
75% Percentile	72.35	102672	5341
Maximum	76.3	105447	5964
IQR			
RI high (Q3+1.5*IQR)			
RI low (Q1-1.5*IQR)			
Mean	67.56	95174.00	4594.00
Std. Deviation	5.755	6278	748.6
Mean + 2SD	79.07	107730.00	6091.20
Mean - 2SD	56.05	82618.00	3096.80
P value	0.5089	0.4489	0.5473
Passed normality test (alpha=0.05)?	Yes	Yes	Yes

Table 107: Flow cytometry of control spleens, B-lymphocyte group results

	T-lymphocytes | Freq. of Parent (%)	T-lymphocytes | Mean (FSC-A)	T-lymphocytes | Median (Comp-AmCyan-A)
Minimum	23.7	86922	195
25% Percentile	27.65	94914	259.5
Median	31.75	97017	300.5
75% Percentile	37.13	103194	340
Maximum	42.8	108683	360
IQR			
RI high (Q3+1.5*IQR)			
RI low (Q1-1.5*IQR)			
Mean	32.46	98271.00	295.70
Std. Deviation	5.773	5297	48.25
Mean + 2SD	44.01	108865.00	392.20
Mean - 2SD	20.91	87677.00	199.20
P value	0.5107	0.7989	0.4629
Passed normality test (alpha=0.05)?	Yes	Yes	Yes

Table 108: Flow cytometry of control spleens, T-lymphocyte group results

	CD8+CD4+ | Freq. of Parent (%)	CD8+CD4+ | Mean (FSC-A)	CD8+CD4+ | Median (Comp-APC-Cy7-A)	CD8+CD4+ | Median (Comp-FITC-A)
Minimum	0.23	92119	301	3413
25% Percentile	0.27	97581	1907	4316
Median	0.38	101832	2448	4812
75% Percentile	0.52	108683	2812	5348
Maximum	1.13	112983	3511	9449
IQR	0.25			1032.00
RI high (Q3+1.5*IQR)	0.90			6896.00
RI low (Q1-1.5*IQR)	-0.11			2768.00
Mean	0.45	102770.00	2279.00	5039.00
Std. Deviation	0.237	6385	882.8	1362
Mean + 2SD		115540.00	4044.60	
Mean - 2SD		90000.00	513.40	
P value	0.0021	0.4393	0.2332	<0.0001
Passed normality test (alpha=0.05)?	No	Yes	Yes	No

Table 109: Flow cytometry of control spleens, DP group results

	CD8+| Freq. of Parent (%)	CD8+ | Mean (FSC-A)	CD8+ | Median (Comp-APC-Cy7-A)	CD8+ | Median (Comp-FITC-A)
Minimum	16.3	87539	653	156
25% Percentile	25.2	94948	2944	183
Median	29.35	96555	3883	198.5
75% Percentile	33.08	102141	4226	219.3
Maximum	37.2	108917	4903	250
IQR				
RI high (Q3+1.5*IQR)				
RI low (Q1-1.5*IQR)				
Mean	28.72	98053.00	3407.00	199.90
Std. Deviation	5.12	5142	1333	28.12
Mean + 2SD	38.96	108337.00	6073.00	256.14
Mean - 2SD	18.48	87769.00	741.00	143.66
P value	0.364	0.8198	0.077	0.8299
Passed normality test (alpha=0.05)?	Yes	Yes	Yes	Yes

Table 110: Flow cytometry of control spleens, CD8 group results

	CD4+ | Freq. of Parent (%)	CD4+ | Mean (FSC-A)	CD4+ | Median (Comp-APC-Cy7-A)	CD4+ | Median (Comp-FITC-A)
Minimum	42.4	84756	-5.13	8411
25% Percentile	46.85	91972	15.73	9188
Median	51.55	94787	21.15	10099
75% Percentile	54.25	98527	24.4	11430
Maximum	57.3	105489	37.2	12467
IQR				
RI high (Q3+1.5*IQR)				
RI low (Q1-1.5*IQR)				
Mean	50.75	95268.00	18.68	10294.00
Std. Deviation	4.338	4858	10.47	1215
Mean + 2SD	59.43	104984.00	39.62	12724.00
Mean - 2SD	42.07	85552.00	-2.26	7864.00
P value	0.5059	0.6781	0.0815	0.3473
Passed normality test (alpha=0.05)?	Yes	Yes	Yes	Yes

Table 111: Flow cytometry of control spleens, CD4 group results

	CD8-CD4- | Freq. of Parent (%)	CD8-CD4- | Mean (FSC-A)	CD8-CD4- | Median (Comp-APC-Cy7-A)	CD8-CD4- | Median (Comp-FITC-A)
Minimum	10.9	94319	5.13	165
25% Percentile	16.15	101311	18.33	186.8
Median	18.65	103969	23.75	200
75% Percentile	23.08	110480	25.7	235
Maximum	37.8	117702	29.5	252
IQR	6.93		7.37	
RI high (Q3+1.5*IQR)	33.48		36.76	
RI low (Q1-1.5*IQR)	5.76		7.28	
Mean	20.08	105540.00	21.40	207.20
Std. Deviation	6.454	5882	6.446	25.72
Mean + 2SD		117304.00		258.64
Mean - 2SD		93776.00		155.76
P value	0.016	0.5869	0.0282	0.4299
Passed normality test (alpha=0.05)?	No	Yes	No	Yes

Table 112: Flow cytometry of control spleens, DN group results

	DN1 | Freq. of Parent (%)	DN1 | Mean (FSC-A)	DN1 | Median (Comp-PE-A)	DN1 | Median (Comp-PE-CF594-A)
Minimum	91.9	94834	-8.98	8581
25% Percentile	95.3	101930	211.3	10400
Median	97.35	104670	243.5	13144
75% Percentile	98	110901	301.5	16951
Maximum	98.7	118248	587	31039
IQR				6551.00
RI high (Q3+1.5*IQR)				26777.50
RI low (Q1-1.5*IQR)				573.50
Mean	96.58	105987.00	270.10	14765.00
Std. Deviation	2.03	5821	127.4	6143
Mean + 2SD	100.64	117629.00	524.90	
Mean - 2SD	92.52	94345.00	15.30	
P value	0.0686	0.5741	0.06	0.0025
Passed normality test (alpha=0.05)?	Yes	Yes	Yes	No

Table 113: Flow cytometry of control spleens, DN1 group results

	DN2 | Freq. of Parent (%)	DN2 | Mean (FSC-A)	DN2 | Median (Comp-PE-A)	DN2 | Median (Comp-PE-CF594-A)
Minimum	0.016	99008	1400	2766
25% Percentile	0.04025	111331	2373	9701
Median	0.0785	116530	2617	22085
75% Percentile	0.1525	119883	4179	29430
Maximum	0.49	126371	7365	53955
IQR	0.11			
RI high (Q3+1.5*IQR)	0.32			
RI low (Q1-1.5*IQR)	-0.13			
Mean	0.11	114309.00	3499.00	21978.00
Std. Deviation	0.1108	8208	1820	13828
Mean + 2SD		130725.00	7139.00	49634.00
Mean - 2SD		97893.00	-141.00	-5678.00
P value	<0.0001	0.2128	0.0927	0.4353
Passed normality test (alpha=0.05)?	No	Yes	Yes	Yes

Table 114: Flow cytometry of control spleens, DN2 group results

	DN3 | Freq. of Parent (%)	DN3 | Mean (FSC-A)	DN3 | Median (Comp-PE-A)	DN3 | Median (Comp-PE-CF594-A)
Minimum	0	107251	3022	-1002
25% Percentile	0	109434	3472	-422.5
Median	0.00629	113971	5971	-109.4
75% Percentile	0.022	124824	8045	183.2
Maximum	0.12	129984	11403	745
IQR	0.02			
RI high (Q3+1.5*IQR)	0.06			
RI low (Q1-1.5*IQR)	-0.03			
Mean	0.02	116190.00	6131.00	-118.50
Std. Deviation	0.02861	8088	2868	555.4
Mean + 2SD		132366.00	11867.00	992.30
Mean - 2SD		100014.00	395.00	-1229.30
P value	<0.0001	0.4365	0.4973	0.9635
Passed normality test (alpha=0.05)?	No	Yes	Yes	Yes

Table 115: Flow cytometry of control spleens, DN3 group results

	DN4 | Freq. of Parent (%)	DN4 | Mean (FSC-A)	DN4 | Median (Comp-PE-A)	DN4 | Median (Comp-PE-CF594-A)
Minimum	0.79	85006	14.1	-21.8
25% Percentile	1.96	88448	21.8	175.3
Median	2.505	90285	31.45	245
75% Percentile	4.553	93188	36.55	299.8
Maximum	7.97	100987	78.4	638
IQR			14.75	124.50
RI high (Q3+1.5*IQR)			58.68	486.55
RI low (Q1-1.5*IQR)			-0.32	-11.45
Mean	3.29	91615.00	31.45	248.60
Std. Deviation	2.061	4622	14.43	138.4
Mean + 2SD	7.41	100859.00		
Mean - 2SD	-0.83	82371.00		
P value	0.0843	0.1541	<0.0001	0.0182
Passed normality test (alpha=0.05)?	Yes	Yes	No	No

Table 116: Flow cytometry of control spleens, DN4 group results

Cytometer Baseline Report																
Cytometer:	FACSCantoII	User:	Administrator													
Cytometer Name:	FACSCantoII	Institution:	N/A													
Serial Number:	V96300196	Software:	BD FACSDiva 8.0													
Input Device:	HTS	Date:	04/24/2014 03:22 PM													
Tube Loaded Manually:	Yes															
Cytometer Configuration:	IMPC															
Setup Beads																
Bead Product:	CST Setup Beads	Part #:	910858													
Lot ID:	71774	Expiration Date:	03/31/2015													
Bead Lot Information:	Available															
Detector Settings																
Laser	Detector	Parameter	PMTV	New Target Value	Old Target Value	Bright Bead %Robust CV	Mid Bead Median Channel	Mid Bead %Robust CV	Dim Bead Median Channel	Dim Bead %Robust CV						
Blue	FSC	FSC	542	125000	N/A	2.09	132804	2.08	19498	10.87						
Blue	F	SSC	402	125000	N/A	2.09	120602	2.17	58486	1.67						
Blue	E	Alexa Fluor 488	486	22116	N/A	2.21	447	16.64	91	50.22						
Blue	D	PE	429	34937	N/A	1.59	789	12.47	172	41.82						
Blue	B	PE-CF594	464	27806	N/A	2.31	636	15.82	138	41.01						
Blue	A	PE-Cy7	554	30864	N/A	6.2	654	36.81	88	113.67						
Red	C	APC	554	57710	N/A	2.4	1824	13.41	346	31.81						
Red	A	APC-Cy7	582	31577	N/A	3.6	882	18.85	118	63.09						
Violet	B	Pacific Blue	343	11829	N/A	3.8	414	13.12	72	57.8						
Violet	A	AmCyan	434	41035	N/A	3.68	823	9.46	155	28.02						
Detector Settings (Continued)																
Laser	Detector	Parameter	Linearity Min Channel	Linearity Max Channel	Slope	Intercept	Electronic Noise Robust SD	Qr	Br		Target	Current	Current	AppSet	AppSet	
Blue	FSC	FSC	N/A	N/A	0.0039	3	N/A	N/A	N/A		rSD	PMTV	rSD	PMTV	rSD	
Blue	F	SSC	N/A	N/A	7.5862	-14.7	N/A	N/A	N/A							
Blue	E	Alexa Fluor 488	168	238175	7.3747	-15.5	30.6	0.0289	123		76.5	493	71	505	80	
Blue	D	PE	67	236077	7.4045	-14.9	29.5	0.2262	324		73.75	343	80	434	80	
Blue	B	PE-CF594	100	235894	7.4225	-15.3	30.8	0.0186	133		77	470	51	520	82	
Blue	A	PE-Cy7	149	242368	7.664	-16.5	31.7	0.0151	15		79.25	557	49	673	80	
Red	C	APC	140	240547	7.4203	-15.6	26.1	0.0218	81		65.25	54	53	585	72	
Red	A	APC-Cy7	93	238489	7.5067	-16.3	24.4	0.0025	817		61	583	51	615	68	
Violet	B	Pacific Blue	77	239862	7.7782	-15.7	25.2	0.0958	1354		63	344	62	350	67	
Violet	A	AmCyan	45	237295	7.5379	-15.3	24.5	0.0341	753		61.25	434	123	400	69	
Specifications																
Violet Laser Primary Channel Bright Bead %Robust CV:	6.00 (Recommended)															
Blue Laser Primary Channel Bright Bead %Robust CV:	6.00 (Recommended)															
Red Laser Primary Channel Bright Bead %Robust CV:	6.00 (Recommended)															
Laser Settings																
Laser	Power (mW)	Power Spec. (mW)	Current (mA)	Current Guidelines (mA)	Delay (Trigger on FSC)	Delay (Trigger on Fluorescence)	Area Scaling Factor									
Violet	59.8	45.88 - 68.82	N/A	N/A	-29.47	-29.27	1.22									
Blue	20.43	16.36 - 24.54	1.22	0.97 - 1.45	0	0	1.48									
Red	15.03	13.43 - 20.15	N/A	N/A	30.59	30.94	1.26									
Window Extension:	7															
FSC Area Scaling Factor:	0.9															
Threshold																
Threshold (FSC):	11670															
Fluidics																
FACSFlow Pressure:	4.2	Sample Pressure:	3.9													
Spec.:	4.10 - 4.30															
Comments																
Research Use Only																

Table 117: Application settings used during FC analysis of thymus.

Cytometer Baseline Report																
Cytometer:	FACSCantoII	User:	Administrator													
Cytometer Name:	FACSCantoII	Institution:	N/A													
Serial Number:	V96300196	Software:	BD FACSDiva 8.0													
Input Device:	HTS	Date:	04/24/2014 03:22 PM													
Tube Loaded Manually:	Yes															
Cytometer Configuration:	IMPC															
Setup Beads																
Bead Product:	CST Setup Beads	Part #:	910858													
Lot ID:	71774	Expiration Date:	03/31/2015													
Bead Lot Information:	Available															
Detector Settings																
Laser	Detector	Parameter	PMTV	New Target Value	Old Target Value	Bright Bead %Robust CV	Mid Bead Median Channel	Mid Bead %Robust CV	Dim Bead Median Channel	Dim Bead %Robust CV						
Blue	FSC	FSC	542	125000	N/A	2.09	132804	2.08	19498	10.87						
Blue	F	SSC	402	125000	N/A	2.09	120602	2.17	58486	1.67						
Blue	E	Alexa Fluor 488	486	22116	N/A	2.21	447	16.64	91	50.22						
Blue	D	PE	429	34937	N/A	1.59	789	12.47	172	41.82						
Blue	B	PE-CF594	464	27806	N/A	2.31	636	15.82	138	41.01						
Blue	A	PE-Cy7	554	30864	N/A	6.2	654	36.81	88	113.67						
Red	C	APC	554	57710	N/A	2.4	1824	13.41	346	31.81						
Red	A	APC-Cy7	582	31577	N/A	3.6	882	18.85	118	63.09						
Violet	B	Pacific Blue	343	11829	N/A	3.8	414	13.12	72	57.8						
Violet	A	AmCyan	434	41035	N/A	3.68	823	9.46	155	28.02						
Detector Settings (Continued)																
Laser	Detector	Parameter	Linearity Min Channel	Linearity Max Channel	Slope	Intercept	Electronic Noise Robust SD	Qr	Br		Target	Current	Current	AppSet	AppSet	
Blue	FSC	FSC	N/A	N/A	0.0039	3	N/A	N/A	N/A		rSD	PMTV	rSD	PMTV	rSD	
Blue	F	SSC	N/A	N/A	7.5862	-14.7	N/A	N/A	N/A							
Blue	E	Alexa Fluor 488	168	238175	7.3747	-15.5	30.6	0.0289	123		76.5	495	107	489	89	
Blue	D	PE	67	236077	7.4045	-14.9	29.5	0.2262	324		73.75	436	93	426	78	
Blue	B	PE-CF594	100	235894	7.4225	-15.3	30.8	0.0186	133		77	472	60	506	87	
Blue	A	PE-Cy7	149	242368	7.664	-16.5	31.7	0.0151	15		79.25	558	60	605	82	
Red	C	APC	140	240547	7.4203	-15.6	26.1	0.0218	81		65.25	555	69	560	67	
Red	A	APC-Cy7	93	238489	7.5067	-16.3	24.4	0.0025	817		61	583	54	605	65	
Violet	B	Pacific Blue	77	239862	7.7782	-15.7	25.2	0.0958	1354		63	344	72	350	67	
Violet	A	AmCyan	45	237295	7.5379	-15.3	24.5	0.0341	753		61.25	435	152	406	72	
Specifications																
Violet Laser Primary Channel Bright Bead %Robust CV:	6.00 (Recommended)															
Blue Laser Primary Channel Bright Bead %Robust CV:	6.00 (Recommended)															
Red Laser Primary Channel Bright Bead %Robust CV:	6.00 (Recommended)															
Laser Settings																
Laser	Power (mW)	Power Spec. (mW)	Current (mA)	Current Guidelines (mA)	Delay (Trigger on FSC)	Delay (Trigger on Fluorescence)	Area Scaling Factor									
Violet	59.8	45.88 - 68.82	N/A	N/A	-29.47	-29.27	1.22									
Blue	20.43	16.36 - 24.54	1.22	0.97 - 1.45	0	0	1.48									
Red	15.03	13.43 - 20.15	N/A	N/A	30.59	30.94	1.26									
Window Extension:	7															
FSC Area Scaling Factor:	0.9															
Threshold																
Threshold (FSC):	11670															
Fluidics																
FACSFlow Pressure:	4.2	Sample Pressure:	3.9													
Spec.:	4.10 - 4.30															
Comments																
Research Use Only																

Table 118: Application settings used during FC analysis of spleen.

CD8-CD4- | Freq. of Parent (%)	CD8-CD4- | Mean (FSC-A)	CD8-CD4- | Median (Comp-APC-Cy7-A)	CD8-CD4- | Median (Comp-FITC-A)	DN4 | Freq. of Parent (%)	DN4 | Mean (FSC-A)	DN4 | Median (Comp-PE-A)	DN4 | Median (Comp-PE-CF594-A)
99.93	75440.43	-6.05	135.81	99.96	75449.57	22.91	27.13
0.13	4759.42	0.63	48.71	0.08	4766.53	10.22	13.00

Table 119: FC of thymus, control mice, FSC and MFI of unstained cells.

	CD8-CD4- | Freq. of Parent (%)	CD8-CD4- | Mean (FSC-A)	CD8-CD4- | Median (Comp-APC-Cy7-A)	CD8-CD4- | Median (Comp-FITC-A)	DN4 | Freq. of Parent (%)	DN4 | Mean (FSC-A)	DN4 | Median (Comp-PE-A)	DN4 | Median (Comp-PE-CF594-A)
Mean	95.80	101245.43	-4.10	297.68	99.98	100503.90	47.60	60.55
SD	14.32	17710.33	2.08	94.73	0.09	12680.94	18.90	29.58

Table 120: FC of thymus, treated mice, FSC and MFI of unstained cells.

Position	Gene	C57BL/6	A_J	Consequences	AA	SIFT
87257389	Fcrls	T	C	Missense variant	-	-
87367745	Cd5l	A	G	Missense variant	N/S	0.58, T
87384839	Fcrl1	C	G	Missense variant	P/A	0.22, T
87385323	Fcrl1	C	T	Splice region variant	-	-
87385732	Fcrl1	T	C	Missense variant	L/P	0.17, T
87389383	Fcrl1	C	T	Missense variant	P/S	1, T
87443666	Fcrl5	C	A	Missense variant	P/H	0.13, T
87443680	Fcrl5	T	C	Missense variant	F/L	0.57, T
87443684	Fcrl5	A	C	Missense variant	Y/S	0.41, T
87443693	Fcrl5	G	A	Missense variant	R/H	0.76, T
87443780	Fcrl5	T	G	Missense variant	V/G	0.12, T
87444264	Fcrl5	A	G	Missense variant	K/R	0.13, T
87444307	Fcrl5	T	A	Missense variant	S/R	0.92, T
87446385	Fcrl5	A	G	Missense variant	K/E	0.27, T
87446463	Fcrl5	T	C	Missense variant	Y/H	0.02, D
87446476	Fcrl5	A	C	Missense variant	N/T	0.01, D
87446531	Fcrl5	G	A	Splice region variant	-	-
87457108	Fcrl5	G	A	Splice region variant	-	-
87536340	Etv3	G	T	Missense variant	M/I	0.61, T
87536471	Etv3	T	C	Missense variant	V/A	1, T low confidence
87847112	Sh2d2a	G	T	Splice region variant	-	-
87847114	Sh2d2a	A	G	Splice region variant	-	-
87847667	Sh2d2a	A	G	Missense variant	N/S	1, T
88854680	Gon4l	C	T	Missense variant	P/L	0.01, D
88895267	Gon4l	G	T	Missense variant	A/S	0.06, T
88908282	Gon4l	T	C	Missense variant	S/P	1, T low confidence

88718080	Rit1	T	C	NMD transcript variant	-	-
88718914	Rit1	G	T	NMD transcript variant	-	-
88720331	Rit1	G	A	NMD transcript variant	-	-
88720850	Rit1	T	C	NMD transcript variant	-	-
88723006	Rit1	G	C	NMD transcript variant	-	-
88723159	Rit1	G	A	NMD transcript variant	-	-
88723196	Rit1	T	C	NMD transcript variant	-	-
88723313	Rit1	T	A	NMD transcript variant	-	-
88723553	Rit1	T	C	NMD transcript variant	-	-
88723637	Rit1	C	T	NMD transcript variant	-	-
88723767	Rit1	T	C	NMD transcript variant	-	-
88724207	Rit1	A	C	NMD transcript variant	-	-
88724430	Rit1	T	C	NMD transcript variant	-	-
88724977	Rit1	A	G	NMD transcript variant	-	-
88725351	Rit1	C	T	NMD transcript variant	-	-
88725539	Rit1	C	T	NMD transcript variant	-	-
88726187	Rit1	G	A*	Splice region variant NMD transcript variant	-	-
88726620	Rit1	G	A	NMD transcript variant	-	-
88727071	Rit1	A	C	NMD transcript variant	-	-
88727398	Rit1	A	G	NMD transcript variant	-	-
88727925	Rit1	T	C	NMD transcript variant	-	-
88729061	Rit1	C	T	NMD transcript variant	-	-
88729080	Rit1	T	C	NMD transcript variant	-	-
88729773	Rit1	A	C	NMD transcript variant	-	-
88729940	Rit1	G	A	NMD transcript variant	-	-
88730254	Rit1	T	C	NMD transcript variant	-	-
94933406	Selenbp1	G	A	NMD transcript variant	-	-
94933721	Selenbp1	G	A	NMD transcript variant	-	-
94933954	Selenbp1	G	c	NMD transcript variant	-	-
94934756	Selenbp1	G	A	NMD transcript variant	-	-
94935736	Selenbp1	T	C	NMD transcript variant	-	-
94936270	Selenbp1	G	C	NMD transcript variant	-	-
94936362	Selenbp1	T	C	NMD transcript variant	-	-
94936947	Selenbp1	T	C	NMD transcript variant	-	-
94937071	Selenbp1	C	T	NMD transcript variant	-	-
94937576	Selenbp1	T	C	NMD transcript variant	-	-
94938228	Selenbp1	T	G	NMD transcript variant	-	-
94938505	Selenbp1	T	A	NMD transcript variant	-	-
94938654	Selenbp1	T	A	NMD transcript variant	-	-
94938919	Selenbp1	G	T	NMD transcript variant	-	-
94938962	Selenbp1	G	T	NMD transcript variant	-	-

94939213	Selenbp1	T	G	NMD transcript variant	-	-
94939262	Selenbp1	C	T	NMD transcript variant	-	-
94939317	Selenbp1	T	C	NMD transcript variant	-	-
94939328	Selenbp1	A	G	NMD transcript variant	-	-
94939335	Selenbp1	G	A	NMD transcript variant	-	-
94939339	Selenbp1	G	T	NMD transcript variant	-	-
94939370	Selenbp1	T	C	NMD transcript variant	-	-
94939427	Selenbp1	T	C	NMD transcript variant	-	-
94939590	Selenbp1	T	C	NMD transcript variant	-	-
94939604	Selenbp1	G	A	NMD transcript variant	-	-
94939609	Selenbp1	T	C	NMD transcript variant	-	-
94939785	Selenbp1	C	T	NMD transcript variant	-	-
94939852	Selenbp1	C	G	NMD transcript variant	-	-
94939859	Selenbp1	T	C	NMD transcript variant	-	-
94939901	Selenbp1	C	T	NMD transcript variant	-	-
94940145	Selenbp1	C	A	NMD transcript variant	-	-
94940377	Selenbp1	C	T	NMD transcript variant	-	-
94940442	Selenbp1	C	T	NMD transcript variant	-	-
94940446	Selenbp1	G	C	NMD transcript variant	-	-
94940486	Selenbp1	C	T	NMD transcript variant	-	-
94940528	Selenbp1	T	G	NMD transcript variant	-	-
94940551	Selenbp1	A	G	NMD transcript variant	-	-
94940574	Selenbp1	C	T	NMD transcript variant	-	-
94940586	Selenbp1	A	T	NMD transcript variant	-	-
94941061	Selenbp1	A	T	NMD transcript variant	-	-
94941114	Selenbp1	A	G	NMD transcript variant	-	-
94941120	Selenbp1	C	T	NMD transcript variant	-	-
94941510	Selenbp1	A	G	NMD transcript variant	-	-
94941535	Selenbp1	T	A	NMD transcript variant	-	-
94941607	Selenbp1	T	C	NMD transcript variant	-	-
94941706	Selenbp1	A	C	NMD transcript variant	-	-
94941858	Selenbp1	G	A	NMD transcript variant	-	-
94942254	Selenbp1	T	c	NMD transcript variant	-	-
94942337	Selenbp1	C	t	NMD transcript variant	-	-
94942364	Selenbp1	G	C	NMD transcript variant	-	-
94942372	Selenbp1	A	G	NMD transcript variant	-	-
94943021	Selenbp1	C	T	NMD transcript variant	-	-
94943045	Selenbp1	C	A	NMD transcript variant	-	-
94943071	Selenbp1	C	T	NMD transcript variant	-	-
94943280	Selenbp1	C	A	NMD transcript variant	-	-
94944281	Selenbp1	T	G	NMD transcript variant	-	-
94944538	Selenbp1	G	A	NMD transcript variant	-	-

94955672	Rfx5	G	C	NMD transcript variant	-	-
94959097	Rfx5	G	A*	Missense variant NMD transcript variant	R/Q	0.2, T low confidence
94959817	Rfx5	A	G	NMD transcript variant	-	-
94961247	Rfx5	T	A	NMD transcript variant	-	-
95734876	Ecm1	T	C	Missense variant	I/V	0.13, T
95932170	Anp32e	T	A	NMD transcript variant	-	-
95935823	Anp32e	G	A	NMD transcript variant	-	-
95936250	Anp32e	A	G	NMD transcript variant	-	-
96805720	Cd160	T	C	Missense variant	N/S	1, T
100138730	Wdr3	T	C	Missense variant	K/R	1, T
100142747	Wdr3	A	G	NMD transcript variant	-	-
100142749	Wdr3	T	A	NMD transcript variant	-	-
100143308	Wdr3	C	T	NMD transcript variant	-	-
100144268	Wdr3	A	G	NMD transcript variant	-	-
100148521	Wdr3	T	C	NMD transcript variant	-	-
100150992	Wdr3	T	C	NMD transcript variant	-	-
100151144	Wdr3	A	G	NMD transcript variant	-	-
100153578	Wdr3	C	T*	Missense variant NMD transcript variant	V/M	0.12, T
100155709	Wdr3	C	T	NMD transcript variant	-	-
100157544	Wdr3	A	G	NMD transcript variant	-	-
100157669	Wdr3	G	T	NMD transcript variant	-	-
100158327	Wdr3	G	A	NMD transcript variant	-	-
100158959	Wdr3	T	t/a	NMD transcript variant	-	-
100160415	Wdr3	G	A	NMD transcript variant	-	-
100160529	Wdr3	A	T	NMD transcript variant	-	-
100160580	Wdr3	T	C	NMD transcript variant	-	-
100161192	Wdr3	C	T	NMD transcript variant	-	-
100161207	Wdr3	A	G	NMD transcript variant	-	-
100161429	Wdr3	T	C	NMD transcript variant	-	-
100161460	Wdr3	T	C	NMD transcript variant	-	-
100161694	Wdr3	A	G	NMD transcript variant	-	-
100161776	Wdr3	A	C	NMD transcript variant	-	-
100161804	Wdr3	A	G	NMD transcript variant	-	-
100162068	Wdr3	C	A	NMD transcript variant	-	-
100162203	Wdr3	A	G	NMD transcript variant	-	-
100162227	Wdr3	T	C	NMD transcript variant	-	-
100162307	Wdr3	C	T	NMD transcript variant	-	-
100162349	Wdr3	T	C	NMD transcript variant	-	-
100928128	Trim45	A	G	Missense variant	I/V	0.39, T
100930059	Trim45	G	A	Missense variant	-	-

100931711	Trim45	A	G	Missense variant	D/G	-
100931837	Trim45	T	C	Missense variant	L/S	-
102163294	Vangl1	C	A	Splice region variant	-	-
103746072	Hipk1	A	C	NMD transcript variant	-	-
103746125	Hipk1	A	G	NMD transcript variant	-	-
103746170	Hipk1	T	A	NMD transcript variant	-	-
103747593	Hipk1	G	A	NMD transcript variant	-	-
103748156	Hipk1	C	T	NMD transcript variant	-	-
103750022	Hipk1	C	T	NMD transcript variant	-	-
103751264	Hipk1	A	T	NMD transcript variant	-	-
103751896	Hipk1	T	C	NMD transcript variant	-	-
103751914	Hipk1	A	G	NMD transcript variant	-	-
103754710	Hipk1	C	T	NMD transcript variant	-	-
103755734	Hipk1	C	G	NMD transcript variant	-	-
103756279	Hipk1	A	G	NMD transcript variant	-	-
103757210	Hipk1	T	G	NMD transcript variant	-	-
103757683	Hipk1	A	T	NMD transcript variant	-	-
103757684	Hipk1	T	A	NMD transcript variant	-	-
103758448	Hipk1	G	A	NMD transcript variant	-	-
103758851	Hipk1	G	A	NMD transcript variant	-	-
103759206	Hipk1	T	C	NMD transcript variant	-	-
103760137	Hipk1	G	T	NMD transcript variant	-	-
103761381	Hipk1	C	T	NMD transcript variant	-	-
103761474	Hipk1	C	T	NMD transcript variant	-	-
103761866	Hipk1	G	A	NMD transcript variant	-	-
103762338	Hipk1	A	G	NMD transcript variant	-	-
103765834	Hipk1	A	G	NMD transcript variant	-	-
103766009	Hipk1	G	A	NMD transcript variant	-	-
103766169	Hipk1	G	T	NMD transcript variant	-	-
103767756	Hipk1	T	G	NMD transcript variant	-	-
103768007	Hipk1	C	A	NMD transcript variant	-	-
103768076	Hipk1	C	T	NMD transcript variant	-	-
103768851	Hipk1	T	C	NMD transcript variant	-	-
103768899	Hipk1	A	C	NMD transcript variant	-	-
103769037	Hipk1	C	G	NMD transcript variant	-	-
103769064	Hipk1	A	G	NMD transcript variant	-	-
103769116	Hipk1	A	G	NMD transcript variant	-	-
103769806	Hipk1	T	C	NMD transcript variant	-	-
103770665	Hipk1	G	A	NMD transcript variant	-	-
103770669	Hipk1	T	C	NMD transcript variant	-	-
103771075	Hipk1	C	T	NMD transcript variant	-	-
103771159	Hipk1	G	T	NMD transcript variant	-	-

103771160	Hipk1	T	C	NMD transcript variant	-	-
103771363	Hipk1	A	G	NMD transcript variant	-	-
103771413	Hipk1	A	G	NMD transcript variant	-	-
103771826	Hipk1	A	T	NMD transcript variant	-	-
103771834	Hipk1	C	T	NMD transcript variant	-	-
103773855	Hipk1	A	T	NMD transcript variant	-	-
103773975	Hipk1	G	A	NMD transcript variant	-	-
103774142	Hipk1	C	A	NMD transcript variant	-	-
103774264	Hipk1	C	T	NMD transcript variant	-	-
103774267	Hipk1	A	G	NMD transcript variant	-	-
103774269	Hipk1	G	A	NMD transcript variant	-	-
103774336	Hipk1	A	G	NMD transcript variant	-	-
103774390	Hipk1	G	T	NMD transcript variant	-	-
103774497	Hipk1	G	A	NMD transcript variant	-	-
103774773	Hipk1	G	T	NMD transcript variant	-	-
103774774	Hipk1	A	G	NMD transcript variant	-	-
103775283	Hipk1	G	A	NMD transcript variant	-	-
103775514	Hipk1	T	C	NMD transcript variant	-	-
103775775	Hipk1	C	A	NMD transcript variant	-	-
103776454	Hipk1	A	G	NMD transcript variant	-	-
103776903	Hipk1	A	G	NMD transcript variant	-	-
103777195	Hipk1	G	A	NMD transcript variant	-	-
103779290	Hipk1	G	A	NMD transcript variant	-	-
103780021	Hipk1	A	G	NMD transcript variant	-	-
103780352	Hipk1	A	G	NMD transcript variant	-	-
103783506	Hipk1	T	C	NMD transcript variant	-	-
103784173	Hipk1	A	G	NMD transcript variant	-	-
103784206	Hipk1	A	C	NMD transcript variant	-	-
103789644	Hipk1	T	A	NMD transcript variant	-	-
103789750	Hipk1	A	C	NMD transcript variant	-	-
103791109	Hipk1	C	G	NMD transcript variant	-	-
103791217	Hipk1	T	G	NMD transcript variant	-	-
103791540	Hipk1	C	G	NMD transcript variant	-	-
103862050	Ptpn22	A	G	NMD transcript variant	-	-
103862572	Ptpn22	A	G	NMD transcript variant	-	-
103863052	Ptpn22	C	T	NMD transcript variant	-	-
103863800	Ptpn22	G	A	NMD transcript variant	-	-
103863995	Ptpn22	G	A	NMD transcript variant	-	-
103864502	Ptpn22	C	G	NMD transcript variant	-	-
103865052	Ptpn22	A	G	NMD transcript variant	-	-
103865196	Ptpn22	C	T	NMD transcript variant	-	-
103865644	Ptpn22	C	A	NMD transcript variant	-	-

103865691	Ptpn22	G	A	NMD transcript variant	-	-
103865957	Ptpn22	G	A	NMD transcript variant	-	-
103866223	Ptpn22	T	C	NMD transcript variant	-	-
103866294	Ptpn22	G	C	NMD transcript variant	-	-
103866564	Ptpn22	T	C	NMD transcript variant	-	-
103866607	Ptpn22	C	T	NMD transcript variant	-	-
103866782	Ptpn22	T	C	NMD transcript variant	-	-
103866882	Ptpn22	C	T	NMD transcript variant	-	-
103867835	Ptpn22	G	A	NMD transcript variant	-	-
103867854	Ptpn22	T	C	NMD transcript variant	-	-
103867993	Ptpn22	C	T	NMD transcript variant	-	-
103868468	Ptpn22	C	T	NMD transcript variant	-	-
103868512	Ptpn22	A	C	NMD transcript variant	-	-
103868861	Ptpn22	T	C	NMD transcript variant	-	-
103869678	Ptpn22	C	T	NMD transcript variant	-	-
103870168	Ptpn22	A	G	NMD transcript variant	-	-
103870181	Ptpn22	C	T	NMD transcript variant	-	-
103871416	Ptpn22	C	T	NMD transcript variant	-	-
103871590	Ptpn22	T	C	NMD transcript variant	-	-
103871883	Ptpn22	G	A	NMD transcript variant	-	-
103871932	Ptpn22	A	G	NMD transcript variant	-	-
103871948	Ptpn22	A	G	NMD transcript variant	-	-
103871990	Ptpn22	G	A	NMD transcript variant	-	-
103871991	Ptpn22	A	T	NMD transcript variant	-	-
103871995	Ptpn22	G	A	NMD transcript variant	-	-
103872053	Ptpn22	A	G	NMD transcript variant	-	-
103872149	Ptpn22	C	T	NMD transcript variant	-	-
103872150	Ptpn22	C	T	NMD transcript variant	-	-
103872217	Ptpn22	C	T	NMD transcript variant	-	-
103872738	Ptpn22	C	T	NMD transcript variant	-	-
103872911	Ptpn22	A	a/t	NMD transcript variant	-	-
103872913	Ptpn22	G	C	NMD transcript variant	-	-
103872941	Ptpn22	A	a/c	NMD transcript variant	-	-
103872949	Ptpn22	C	G	NMD transcript variant	-	-
103873046	Ptpn22	A	T	NMD transcript variant	-	-
103873048	Ptpn22	G	C	NMD transcript variant	-	-
103873053	Ptpn22	T	C	NMD transcript variant	-	-
103873119	Ptpn22	C	T	NMD transcript variant	-	-
103873202	Ptpn22	C	T	NMD transcript variant	-	-
103873349	Ptpn22	C	c/t	NMD transcript variant	-	-
103873373	Ptpn22	T	C	NMD transcript variant	-	-
103873527	Ptpn22	C	T	NMD transcript variant	-	-

103874257	Ptpn22	T	C	NMD transcript variant	-	-
103874307	Ptpn22	A	C	NMD transcript variant	-	-
103874309	Ptpn22	A	G	NMD transcript variant	-	-
103874844	Ptpn22	T	G	NMD transcript variant	-	-
103874919	Ptpn22	A	G	NMD transcript variant	-	-
103875021	Ptpn22	T	C	NMD transcript variant	-	-
103875759	Ptpn22	A	G	NMD transcript variant	-	-
103876511	Ptpn22	A	G	NMD transcript variant	-	-
103876807	Ptpn22	A	T	NMD transcript variant	-	-
103877043	Ptpn22	T	G	NMD transcript variant	-	-
103877388	Ptpn22	A	T	NMD transcript variant	-	-
103877982	Ptpn22	C	T	NMD transcript variant	-	-
103878030	Ptpn22	G	A	NMD transcript variant	-	-
103878173	Ptpn22	G	A	NMD transcript variant	-	-
103878264	Ptpn22	C	A	NMD transcript variant	-	-
103878269	Ptpn22	C	T	NMD transcript variant	-	-
103878271	Ptpn22	C	T	NMD transcript variant	-	-
103878273	Ptpn22	C	T	NMD transcript variant	-	-
103878275	Ptpn22	C	T	NMD transcript variant	-	-
103878297	Ptpn22	T	C	NMD transcript variant	-	-
103878710	Ptpn22	C	T	NMD transcript variant	-	-
103878771	Ptpn22	G	A	NMD transcript variant	-	-
103878905	Ptpn22	G	A	NMD transcript variant	-	-
103878933	Ptpn22	C	T	NMD transcript variant	-	-
103878971	Ptpn22	C	T	NMD transcript variant	-	-
103878972	Ptpn22	G	A	NMD transcript variant	-	-
103879092	Ptpn22	C	T	NMD transcript variant	-	-
103879186	Ptpn22	A	G	NMD transcript variant	-	-
103879265	Ptpn22	A	G	NMD transcript variant	-	-
103879530	Ptpn22	G	T	NMD transcript variant	-	-
103879668	Ptpn22	G	C	NMD transcript variant	-	-
103879673	Ptpn22	T	C	NMD transcript variant	-	-
103879850	Ptpn22	C	T	NMD transcript variant	-	-
103879858	Ptpn22	C	T	NMD transcript variant	-	-
103879860	Ptpn22	T	C	NMD transcript variant	-	-
103879994	Ptpn22	A	G	NMD transcript variant	-	-
103880234	Ptpn22	C	T	NMD transcript variant	-	-
103880265	Ptpn22	G	C	NMD transcript variant	-	-
103880272	Ptpn22	T	C	NMD transcript variant	-	-
103880295	Ptpn22	C	T	NMD transcript variant	-	-
103880316	Ptpn22	G	A	NMD transcript variant	-	-
103880366	Ptpn22	C	T	NMD transcript variant	-	-

103880505	Ptpn22	C	T	NMD transcript variant	-	-
103880509	Ptpn22	G	A	NMD transcript variant	-	-
103880566	Ptpn22	G	A	NMD transcript variant	-	-
103880746	Ptpn22	C	T	NMD transcript variant	-	-
103880751	Ptpn22	A	G	NMD transcript variant	-	-
103880759	Ptpn22	C	A	NMD transcript variant	-	-
103880796	Ptpn22	G	A	NMD transcript variant	-	-
103880901	Ptpn22	C	T	NMD transcript variant	-	-
103880905	Ptpn22	C	T	NMD transcript variant	-	-
103880912	Ptpn22	G	A	NMD transcript variant	-	-
103880915	Ptpn22	G	T	NMD transcript variant	-	-
103880925	Ptpn22	A	C	NMD transcript variant	-	-
103881180	Ptpn22	T	C	NMD transcript variant	-	-
103881420	Ptpn22	A	G	NMD transcript variant	-	-
103881684	Ptpn22	C	T	NMD transcript variant	-	-
103881713	Ptpn22	C	T	NMD transcript variant	-	-
103881804	Ptpn22	C	T	NMD transcript variant	-	-
103881831	Ptpn22	T	C	NMD transcript variant	-	-
103882018	Ptpn22	T	A	NMD transcript variant	-	-
103882409	Ptpn22	G	C	NMD transcript variant	-	-
103882525	Ptpn22	A	G	NMD transcript variant	-	-
103882539	Ptpn22	A	T	NMD transcript variant	-	-
103882540	Ptpn22	T	C	NMD transcript variant	-	-
103882556	Ptpn22	C	T	NMD transcript variant	-	-
103882557	Ptpn22	A	G	NMD transcript variant	-	-
103882627	Ptpn22	C	T	NMD transcript variant	-	-
103882695	Ptpn22	C	A	NMD transcript variant	-	-
103882718	Ptpn22	C	T	NMD transcript variant	-	-
103882730	Ptpn22	T	C	NMD transcript variant	-	-
103882883	Ptpn22	C	T	NMD transcript variant	-	-
103882915	Ptpn22	G	T	NMD transcript variant	-	-
103883048	Ptpn22	A	G	NMD transcript variant	-	-
103883067	Ptpn22	G	A	NMD transcript variant	-	-
103883068	Ptpn22	T	C	NMD transcript variant	-	-
103883127	Ptpn22	T	C	NMD transcript variant	-	-
103883152	Ptpn22	A	G	NMD transcript variant	-	-
103883154	Ptpn22	G	A	NMD transcript variant	-	-
103883155	Ptpn22	A	T	NMD transcript variant	-	-
103883188	Ptpn22	T	G	NMD transcript variant	-	-
103883222	Ptpn22	C	T	NMD transcript variant	-	-
103883298	Ptpn22	G	A	NMD transcript variant	-	-
103883311	Ptpn22	G	A	NMD transcript variant	-	-

103883315	Ptpn22	C	T	NMD transcript variant	-	-
103883351	Ptpn22	G	A	NMD transcript variant	-	-
103883372	Ptpn22	C	A	NMD transcript variant	-	-
103883416	Ptpn22	C	G	NMD transcript variant	-	-
103883441	Ptpn22	G	C	NMD transcript variant	-	-
103883452	Ptpn22	G	T	NMD transcript variant	-	-
103883469	Ptpn22	C	T	NMD transcript variant	-	-
103883483	Ptpn22	T	G	NMD transcript variant	-	-
103883601	Ptpn22	G	A	NMD transcript variant	-	-
103883619	Ptpn22	T	C	NMD transcript variant	-	-
103883674	Ptpn22	T	C	NMD transcript variant	-	-
103883854	Ptpn22	T	C	NMD transcript variant	-	-
103883868	Ptpn22	A	C	NMD transcript variant	-	-
103883911	Ptpn22	T	C	NMD transcript variant	-	-
103884013	Ptpn22	A	G	NMD transcript variant	-	-
103884071	Ptpn22	C	T	NMD transcript variant	-	-
103884357	Ptpn22	G	T	NMD transcript variant	-	-
103884673	Ptpn22	G	T	NMD transcript variant	-	-
103885203	Ptpn22	T	C	NMD transcript variant	-	-
103885439	Ptpn22	T	C	NMD transcript variant	-	-
103887222	Ptpn22	T	C	NMD transcript variant	-	-
103887378	Ptpn22	T	C	NMD transcript variant	-	-
103887613	Ptpn22	G	A	NMD transcript variant	-	-
103887904	Ptpn22	C	A	NMD transcript variant	-	-
103888070	Ptpn22	G	A	NMD transcript variant	-	-
103888106	Ptpn22	T	C	NMD transcript variant	-	-
103888370	Ptpn22	A	T	NMD transcript variant	-	-
103888508	Ptpn22	T	A*	Splice region variant NMD transcript variant	-	-
103888669	Ptpn22	G	C	NMD transcript variant	-	-
103888917	Ptpn22	C	T	NMD transcript variant	-	-
103889075	Ptpn22	G	T	NMD transcript variant	-	-
103889133	Ptpn22	A	G	NMD transcript variant	-	-
103889154	Ptpn22	G	A	NMD transcript variant	-	-
103889181	Ptpn22	C	T	NMD transcript variant	-	-
103889249	Ptpn22	C	A	NMD transcript variant	-	-
103889322	Ptpn22	A	G	NMD transcript variant	-	-
103889404	Ptpn22	C	T	NMD transcript variant	-	-
103889434	Ptpn22	G	A	NMD transcript variant	-	-
103889463	Ptpn22	G	A	NMD transcript variant	-	-
103889546	Ptpn22	C	T	NMD transcript variant	-	-
103889547	Ptpn22	C	G	NMD transcript variant	-	-

103889807	Ptpn22	C	T	NMD transcript variant	-	-
103890236	Ptpn22	T	C	NMD transcript variant	-	-
103890613	Ptpn22	G	A	NMD transcript variant	-	-
103890835	Ptpn22	T	C	NMD transcript variant	-	-
103890858	Ptpn22	C	A	NMD transcript variant	-	-
103890951	Ptpn22	A	C	NMD transcript variant	-	-
103890961	Ptpn22	A	G	NMD transcript variant	-	-
103891148	Ptpn22	A	G	NMD transcript variant	-	-
103891284	Ptpn22	A	G	NMD transcript variant	-	-
103891342	Ptpn22	A	T	NMD transcript variant	-	-
103891678	Ptpn22	T	A	NMD transcript variant	-	-
103891777	Ptpn22	A	T	NMD transcript variant	-	-
103891990	Ptpn22	C	T	NMD transcript variant	-	-
103892004	Ptpn22	A	C	NMD transcript variant	-	-
103892034	Ptpn22	T	C	NMD transcript variant	-	-
103892043	Ptpn22	T	C	NMD transcript variant	-	-
103892047	Ptpn22	T	C	NMD transcript variant	-	-
103892059	Ptpn22	T	A	NMD transcript variant	-	-
103892061	Ptpn22	T	G	NMD transcript variant	-	-
103892187	Ptpn22	A	G	NMD transcript variant	-	-
103892197	Ptpn22	T	C	NMD transcript variant	-	-
103892440	Ptpn22	T	C	NMD transcript variant	-	-
103892458	Ptpn22	A	G	NMD transcript variant	-	-
103892463	Ptpn22	C	T	NMD transcript variant	-	-
103892469	Ptpn22	A	G	NMD transcript variant	-	-
103892503	Ptpn22	T	C	NMD transcript variant	-	-
103892574	Ptpn22	C	T	NMD transcript variant	-	-
103892649	Ptpn22	C	T	NMD transcript variant	-	-
103892774	Ptpn22	T	C	NMD transcript variant	-	-
103893057	Ptpn22	A	G	NMD transcript variant	-	-
103893066	Ptpn22	G	C	NMD transcript variant	-	-
103895618	Ptpn22	T	A	NMD transcript variant	-	-
103895619	Ptpn22	A	G	NMD transcript variant	-	-
103896056	Ptpn22	G	T	NMD transcript variant	-	-
103896108	Ptpn22	A	T	NMD transcript variant	-	-
103896283	Ptpn22	A	G	NMD transcript variant	-	-
103896400	Ptpn22	G	C	NMD transcript variant	-	-
103896815	Ptpn22	C	T	NMD transcript variant	-	-
103897266	Ptpn22	A	G	NMD transcript variant	-	-
103897322	Ptpn22	G	T	NMD transcript variant	-	-
103897439	Ptpn22	C	T	NMD transcript variant	-	-
103897632	Ptpn22	G	A	NMD transcript variant	-	-

103897947	Ptpn22	C	T	NMD transcript variant	-	-
103897993	Ptpn22	T	C	NMD transcript variant	-	-
103898156	Ptpn22	G	A	NMD transcript variant	-	-
103898216	Ptpn22	A	G	NMD transcript variant	-	-
103898273	Ptpn22	T	C	NMD transcript variant	-	-
103898445	Ptpn22	A	C	NMD transcript variant	-	-
103898511	Ptpn22	G	A	NMD transcript variant	-	-
103898814	Ptpn22	T	C	NMD transcript variant	-	-
103898980	Ptpn22	T	G	NMD transcript variant	-	-
103899017	Ptpn22	G	A	NMD transcript variant	-	-
103899156	Ptpn22	A	C	NMD transcript variant	-	-
103899178	Ptpn22	T	C	NMD transcript variant	-	-
103899196	Ptpn22	T	C	NMD transcript variant	-	-
103899205	Ptpn22	T	C	NMD transcript variant	-	-
103899432	Ptpn22	C	T	NMD transcript variant	-	-
103899510	Ptpn22	T	C	NMD transcript variant	-	-
103899541	Ptpn22	C	A	NMD transcript variant	-	-
103899740	Ptpn22	G	C	NMD transcript variant	-	-
103900939	Ptpn22	A	C	NMD transcript variant	-	-
103901055	Ptpn22	C	A	NMD transcript variant	-	-
103901063	Ptpn22	A	C	NMD transcript variant	-	-
103901887	Ptpn22	G	C	NMD transcript variant	-	-
103902308	Ptpn22	A	G	NMD transcript variant	-	-
103902713	Ptpn22	T	G	NMD transcript variant	-	-
103902764	Ptpn22	C	T	NMD transcript variant	-	-
103904280	Ptpn22	T	C	NMD transcript variant	-	-
103905079	Ptpn22	T	C	NMD transcript variant	-	-
103905223	Ptpn22	G	A	NMD transcript variant	-	-
103905932	Ptpn22	G	A	NMD transcript variant	-	-
103906375	Ptpn22	A	C	NMD transcript variant	-	-
103906404	Ptpn22	A	C	NMD transcript variant	-	-
103906553	Ptpn22	G	C	NMD transcript variant	-	-
103906564	Ptpn22	T	C	NMD transcript variant	-	-
103906642	Ptpn22	C	T	NMD transcript variant	-	-
103906989	Ptpn22	G	A	NMD transcript variant	-	-
103907300	Ptpn22	T	C	NMD transcript variant	-	-
103907574	Ptpn22	A	G	NMD transcript variant	-	-
103907613	Ptpn22	T	A	NMD transcript variant	-	-
103908205	Ptpn22	A	G	NMD transcript variant	-	-
103908574	Ptpn22	A	G	NMD transcript variant	-	-
103909478	Ptpn22	T	G	NMD transcript variant	-	-
103909560	Ptpn22	A	G	NMD transcript variant	-	-

103909636	Ptpn22	A	G	NMD transcript variant	-	-
103909858	Ptpn22	G	A	NMD transcript variant	-	-
103910510	Ptpn22	T	A	NMD transcript variant	-	-
103910525	Ptpn22	A	G	NMD transcript variant	-	-
103910934	Ptpn22	T	C	NMD transcript variant	-	-
103911747	Ptpn22	T	C	NMD transcript variant	-	-
104865646	St7l	C	T	NMD transcript variant	-	-
104865681	St7l	C	T	NMD transcript variant	-	-
104866827	St7l	A	G	NMD transcript variant	-	-
104868454	St7l	A	G	NMD transcript variant	-	-
104869204	St7l	T	C	NMD transcript variant	-	-
104869891	St7l	C	G	NMD transcript variant	-	-
104872446	St7l	T	C	NMD transcript variant	-	-
104873738	St7l	T	C	NMD transcript variant	-	-
104874119	St7l	T	C	NMD transcript variant	-	-
104875321	St7l	A	T	NMD transcript variant	-	-
104875633	St7l	G	C	NMD transcript variant	-	-
104876926	St7l	G	A	NMD transcript variant	-	-
104877115	St7l	G	C	NMD transcript variant	-	-
104877748	St7l	G	A	NMD transcript variant	-	-
104877775	St7l	A	g	NMD transcript variant	-	-
104878663	St7l	G	A	NMD transcript variant	-	-
104879483	St7l	A	G	NMD transcript variant	-	-
104879716	St7l	A	G	NMD transcript variant	-	-
104882163	St7l	G	A	NMD transcript variant	-	-
104884200	St7l	T	C	NMD transcript variant	-	-
104884585	St7l	A	G	NMD transcript variant	-	-
104885637	St7l	C	G	NMD transcript variant	-	-
104885696	St7l	C	T	NMD transcript variant	-	-
104886073	St7l	G	A	NMD transcript variant	-	-
104886369	St7l	G	A	NMD transcript variant	-	-
104888881	St7l	C	T	NMD transcript variant	-	-
104891332	St7l	T	C	NMD transcript variant	-	-
104891612	St7l	A	G	NMD transcript variant	-	-
104893757	St7l	C	T	NMD transcript variant	-	-
104895397	St7l	G	A	NMD transcript variant	-	-
104896846	St7l	T	A	NMD transcript variant	-	-
104896981	St7l	T	G	NMD transcript variant	-	-
104897009	St7l	A	G	NMD transcript variant	-	-
104897826	St7l	C	T	NMD transcript variant	-	-
104899029	St7l	G	g/a	NMD transcript variant	-	-
104899243	St7l	T	C	NMD transcript variant	-	-

104901510	St7l	G	A	NMD transcript variant	-	-
104902530	St7l	C	T	NMD transcript variant	-	-
104904813	St7l	G	C	NMD transcript variant	-	-
104905611	St7l	A	G	NMD transcript variant	-	-
104906445	St7l	C	T	NMD transcript variant	-	-
104906831	St7l	A	T	NMD transcript variant	-	-
104907655	St7l	A	G	NMD transcript variant	-	-
104908296	St7l	A	G	NMD transcript variant	-	-
104908563	St7l	C	A	NMD transcript variant	-	-
104908993	St7l	C	T	NMD transcript variant	-	-
104909822	St7l	T	C	NMD transcript variant	-	-
104910136	St7l	G	T	NMD transcript variant	-	-
104910347	St7l	G	A	NMD transcript variant	-	-
104910405	St7l	A	C	NMD transcript variant	-	-
104910688	St7l	A	G	NMD transcript variant	-	-
104910808	St7l	A	G	NMD transcript variant	-	-
104911012	St7l	G	T	NMD transcript variant	-	-
104911155	St7l	G	T	NMD transcript variant	-	-
104911566	St7l	G	A	NMD transcript variant	-	-
104912439	St7l	A	G	NMD transcript variant	-	-
104913142	St7l	C	T	NMD transcript variant	-	-
104913163	St7l	C	T	NMD transcript variant	-	-
104913677	St7l	C	T	NMD transcript variant	-	-
104913800	St7l	C	T	NMD transcript variant	-	-
104913986	St7l	C	T	NMD transcript variant	-	-
104914127	St7l	G	T	NMD transcript variant	-	-
104915072	St7l	T	C	NMD transcript variant	-	-
104915912	St7l	A	G	NMD transcript variant	-	-
104916086	St7l	C	T	NMD transcript variant	-	-
104916275	St7l	G	A	NMD transcript variant	-	-
104916981	St7l	T	C	NMD transcript variant	-	-
104917461	St7l	C	G	NMD transcript variant	-	-
104917790	St7l	A	G	NMD transcript variant	-	-
104917905	St7l	G	A	NMD transcript variant	-	-
104918031	St7l	C	A	NMD transcript variant	-	-
104918694	St7l	T	G	NMD transcript variant	-	-
104919747	St7l	A	G	NMD transcript variant	-	-
104920464	St7l	T	C	NMD transcript variant	-	-
104920650	St7l	G	A	NMD transcript variant	-	-
104920785	St7l	G	C	NMD transcript variant	-	-
104921546	St7l	C	A	NMD transcript variant	-	-
104922391	St7l	G	T	NMD transcript variant	-	-

104922510	St7l	G	A	NMD transcript variant	-	-
104923225	St7l	C	T	NMD transcript variant	-	-
104923420	St7l	C	T	NMD transcript variant	-	-
104923669	St7l	G	A	NMD transcript variant	-	-
104925082	St7l	T	C	NMD transcript variant	-	-
104925584	St7l	A	G	NMD transcript variant	-	-
104927034	St7l	G	A	NMD transcript variant	-	-
104927352	St7l	T	C	NMD transcript variant	-	-
104927358	St7l	G	A	NMD transcript variant	-	-
104927384	St7l	T	C	NMD transcript variant	-	-
104927422	St7l	A	T	NMD transcript variant	-	-
104927626	St7l	T	C	NMD transcript variant	-	-

*Table 121: Single nucleotide polymorphisms in genes related to the pathogenesis of cancer and lymphocyte biology identified in the QTL. The differences in nucleotides at specific positions between C57BL/6 and A/J mice genes are shown. In AA (amino acid) column, the amino acid replacement is indicated, followed by the SIFT score on how the substitution in amino acid is predicted to affect protein function: T (tolerated), D (deleterious, <0.05). *Multiple consequences.*

Abbreviation	**Amino acid name**
A	Alanine
R	Arginine
N	Asparagine
D	Aspartic acid (Aspartate)
C	Cysteine
Q	Glutamine
E	Glutamic acid (Glutamate)
G	Glycine
H	Histidine
I	Isoleucine
L	Leucine
K	Lysine
M	Methionine
F	Phenylalanine
P	Proline
S	Serine
T	Threonine
W	Tryptophan
Y	Tyrosine
V	Valine
B	Aspartic acid or Asparagine
Z	Glutamine or Glutamic acid
X	Any amino acid
TERM	termination codon

Table 122: Nomenclature and symbolism for amino acids, (IUPAC-IUB, 1984).

Position	Gene	C57BL/6	A_J	Consequences	A/A	SIFT
88717089	Rit1	TG	T	NMD transcript variant	-	-
88718966	Rit1	G	GCA	NMD transcript variant	-	-
88720828	Rit1	G	GGGCGTGGT	NMD transcript variant	-	-
88721564	Rit1	CT	C	NMD transcript variant	-	-
88724401	Rit1	T	TCTGCCTGCCTGC	NMD transcript variant	-	-
88724473	Rit1	CT	CTT	NMD transcript variant	-	-
88725392	Rit1	AAATAATAAT	A	NMD transcript variant	-	-
88725693	Rit1	A	AACAG	NMD transcript variant	-	-
88728690	Rit1	CAA	caaa	NMD transcript variant	-	-
94933993	Selenbp1	TC	t	NMD transcript variant	-	-
94934958	Selenbp1	CT	c	NMD transcript variant	-	-
94935163	Selenbp1	CTTTT	CTT	NMD transcript variant	-	-
94935957	Selenbp1	A	agtgtgt/agtgt	NMD transcript variant	-	-
94938457	Selenbp1	TACACACACACACAC	tacacac/tacac	NMD transcript variant	-	-
94938694	Selenbp1	T	TTTG	NMD transcript variant	-	-
94939085	Selenbp1	TAAAAAA	TA	NMD transcript variant	-	-
94939221	Selenbp1	G	GTTTGT	NMD transcript variant	-	-
94939868	Selenbp1	C	CTTGGTCCACAGCCCT	NMD transcript variant	-	-
94941130	Selenbp1	AC	A	NMD transcript variant	-	-
94941189	Selenbp1	AACC	A	NMD transcript variant	-	-
94941779	Selenbp1	G	GA	NMD transcript variant	-	-

94941791	Selenbp1	CAAAAAAA	C	NMD transcript variant	-	-
94941842	Selenbp1	C	CAAA	NMD transcript variant	-	-
94943005	Selenbp1	C	CACACACAT	NMD transcript variant	-	-
94943303	Selenbp1	TAAA	T	NMD transcript variant	-	-
94943357	Selenbp1	A	AG	NMD transcript variant	-	-
94943595	Selenbp1	GGTGTGT	GGTGT	NMD transcript variant	-	-
94954668	Rfx5	TGGGGG	tggg	NMD transcript variant	-	-
95933317	Anp32e	GTCTCTCTCTCTCTCTCTCTCTCTC	gtctctctctctctctctctc/gtctctctctctctctctctctctc	NMD transcript variant	-	-
95933688	Anp32e	CA	C	NMD transcript variant	-	-
95936265	Anp32e	GC	G	NMD transcript variant	-	-
95936317	Anp32e	GA	G	NMD transcript variant	-	-
100149749	Wdr3	CA	C	NMD transcript variant	-	-
100151311	Wdr3	GCACACACACACA	GCACACACACACACA	NMD transcript variant	-	-
100158467	Wdr3	A	AT	NMD transcript variant	-	-
100160095	Wdr3	A	AACACAT	NMD transcript variant	-	-
100160823	Wdr3	T	TAAG	NMD transcript variant	-	-
100161288	Wdr3	C	ctttttttttt/cttttttttt	NMD transcript variant	-	-
103062700	Nras	AC	ACC	NMD transcript variant	-	-
103066490	Nras	CGTGTGTGTGTGT	cgtgtgt/cgtgt	NMD transcript variant	-	-
103748101	Hipk1	CTT	CTTT	NMD transcript variant	-	-
103749889	Hipk1	CCACACACACACACATACACACACACACACA	CCA	NMD transcript variant	-	-
103751266	Hipk1	T	TA	NMD transcript variant	-	-
103754140	Hipk1	CT	CTTT	NMD transcript variant	-	-
103755197	Hipk1	TAA	TAAA	NMD transcript variant	-	-

103756285	Hipk1	GC	G	NMD transcript variant	-	-
103757605	Hipk1	T	TCACACA	NMD transcript variant	-	-
103757621	Hipk1	A	acacaca/acacatactcact	NMD transcript variant	-	-
103759001	Hipk1	A	AT	NMD transcript variant	-	-
103759877	Hipk1	G	GTT	NMD transcript variant	-	-
103760975	Hipk1	G	GACT	NMD transcript variant	-	-
103765864	Hipk1	T	TA	NMD transcript variant	-	-
103767572	Hipk1	CTTTT	CTT	NMD transcript variant	-	-
103771183	Hipk1	CCAACCAAA	C	NMD transcript variant	-	-
103771399	Hipk1	G	g/gaaagaaagaa	NMD transcript variant	-	-
103773152	Hipk1	CTGCA	C	NMD transcript variant	-	-
103774079	Hipk1	T	TA	NMD transcript variant	-	-
103774324	Hipk1	GTGT	G	NMD transcript variant	-	-
103775265	Hipk1	GA	G	NMD transcript variant	-	-
103775533	Hipk1	AGGAAT	A	NMD transcript variant	-	-
103784404	Hipk1	T	TCTCTGAG	NMD transcript variant	-	-
103784505	Hipk1	CA	C	NMD transcript variant	-	-
103789182	Hipk1	A	AT	NMD transcript variant	-	-
103791225	Hipk1	GAGCGCTC	G	NMD transcript variant	-	-
103860656	Ptpn22	C	CTG	NMD transcript variant	-	-
103861105	Ptpn22	C	CG	NMD transcript variant	-	-
103861234	Ptpn22	GTGTT	GTGTTTGTT	NMD transcript variant	-	-
103861606	Ptpn22	GATT	G	NMD transcript variant	-	-
103862692	Ptpn22	ACCCAC	A	NMD transcript variant	-	-
103863538	Ptpn22	CTGGGACCTCAGCAAACACAGCAAG	C	NMD transcript variant	-	-

103863799	Ptpn22	AG	A	NMD transcript variant	-	-
103863945	Ptpn22	TGTGAGA	T	NMD transcript variant	-	-
103863980	Ptpn22	G	GAGAGAC	NMD transcript variant	-	-
103864067	Ptpn22	G	GT	NMD transcript variant	-	-
103864344	Ptpn22	TTG	T	NMD transcript variant	-	-
103864423	Ptpn22	CAA	CA	NMD transcript variant	-	-
103864735	Ptpn22	CT	C	NMD transcript variant	-	-
103866797	Ptpn22	TA	T	NMD transcript variant	-	-
103867519	Ptpn22	A	AT	NMD transcript variant	-	-
103868223	Ptpn22	GA	G	NMD transcript variant	-	-
103869756	Ptpn22	G	GCCT	NMD transcript variant	-	-
103870085	Ptpn22	GA	G	NMD transcript variant	-	-
103871742	Ptpn22	A	AGGC	NMD transcript variant	-	-
103871886	Ptpn22	ACAAAAACAAACAACCAAACAAC	A	NMD transcript variant	-	-
103872123	Ptpn22	A	ATGCAGTAAACATT	NMD transcript variant	-	-
103872511	Ptpn22	A	AGTCT	NMD transcript variant	-	-
103872540	Ptpn22	G	GA	NMD transcript variant	-	-
103873496	Ptpn22	C	CA	NMD transcript variant	-	-
103876025	Ptpn22	GTGTGTGTGTT	G	NMD transcript variant	-	-
103876070	Ptpn22	TGA	T	NMD transcript variant	-	-
103876589	Ptpn22	T	TTTTA*	Splice region variant NMD transcript variant	-	-
103877886	Ptpn22	ATGTGTG	atgtgtg/atgtgtgtg	NMD transcript variant	-	-
103878898	Ptpn22	C	CAATGAAAAT	NMD transcript variant	-	-
103878945	Ptpn22	G	GTCACAGCA	NMD transcript variant	-	-
103879220	Ptpn22	AT	A	NMD transcript variant	-	-

103879433	Ptpn22	T	TAGAG	NMD transcript variant	-	-
103879460	Ptpn22	T	TC	NMD transcript variant	-	-
103879892	Ptpn22	C	CAACAA	NMD transcript variant	-	-
103879973	Ptpn22	CCTT	C	NMD transcript variant	-	-
103880767	Ptpn22	GTTA	G	NMD transcript variant	-	-
103881205	Ptpn22	A	AT	NMD transcript variant	-	-
103881859	Ptpn22	GA	G	NMD transcript variant	-	-
103881913	Ptpn22	A	AG	NMD transcript variant	-	-
103882199	Ptpn22	ATTT	A	NMD transcript variant	-	-
103882691	Ptpn22	C	CTG	NMD transcript variant	-	-
103882795	Ptpn22	A	AACAT	NMD transcript variant	-	-
103884029	Ptpn22	TA	T	NMD transcript variant	-	-
103884281	Ptpn22	TC	T	NMD transcript variant	-	-
103887563	Ptpn22	A	AGAGAGAGAGAGAGAGG	NMD transcript variant	-	-
103888005	Ptpn22	T	TG	NMD transcript variant	-	-
103888153	Ptpn22	CAAAAAAAAAAAAAAAA	caaaaa/caaaaaa	NMD transcript variant	-	-
103888861	Ptpn22	G	GTCAC*	Splice region variant NMD transcript variant	-	-
103888987	Ptpn22	C	CT	NMD transcript variant	-	-
103889253	Ptpn22	AG	A	NMD transcript variant	-	-
103889294	Ptpn22	CAAA	C	NMD transcript variant	-	-
103889379	Ptpn22	GATAC	G	NMD transcript variant	-	-
103889474	Ptpn22	G	GCTGATT	NMD transcript variant	-	-
103889487	Ptpn22	T	TCAAGGC	NMD transcript variant	-	-
103889817	Ptpn22	TC	T	NMD transcript variant	-	-
103890471	Ptpn22	TA	T	NMD transcript variant	-	-

103890540	Ptpn22	AC	A	NMD transcript variant	-	-
103890581	Ptpn22	AACTAC	A	NMD transcript variant	-	-
103892012	Ptpn22	CCCTGCCCTCT	C	NMD transcript variant	-	-
103892579	Ptpn22	TC	T	NMD transcript variant	-	-
103893042	Ptpn22	CT	ctt	NMD transcript variant	-	-
103895079	Ptpn22	AT	A	NMD transcript variant	-	-
103896667	Ptpn22	CT	CTTT	NMD transcript variant	-	-
103897518	Ptpn22	AGGGG	AGG	NMD transcript variant	-	-
103898016	Ptpn22	AGT	A	NMD transcript variant	-	-
103898485	Ptpn22	TTC	T	NMD transcript variant	-	-
103898791	Ptpn22	G	GCATA	NMD transcript variant	-	-
103899387	Ptpn22	C	CACACA	NMD transcript variant	-	-
103902353	Ptpn22	GTCTCTCTCTCTC	gtctctctctctc/gtctctctctctctc	NMD transcript variant	-	-
103902707	Ptpn22	CT	C	NMD transcript variant	-	-
103906952	Ptpn22	GGTGTGTGT	GGTGTGTGTGT	NMD transcript variant	-	-
103907170	Ptpn22	CAA	C	NMD transcript variant	-	-
103907182	Ptpn22	CAAAAAAACAA	C	NMD transcript variant	-	-
103908727	Ptpn22	A	ATATG	NMD transcript variant	-	-
103909183	Ptpn22	TC	T	NMD transcript variant	-	-
104872873	St7l	G	GTTGTTTGCTTGCTTGC	NMD transcript variant	-	-
104875905	St7l	TACACACACAC	TACAC	NMD transcript variant	-	-
104876633	St7l	GATGAATGAATGAATGA	GATGAATGAATGAATGAATGAATGAATGA	NMD transcript variant	-	-
104884273	St7l	T	TTC	NMD transcript variant	-	-
104885039	St7l	CA	CAA	NMD transcript variant	-	-
104892123	St7l	GTTTTTT	gttttt	NMD transcript variant	-	-

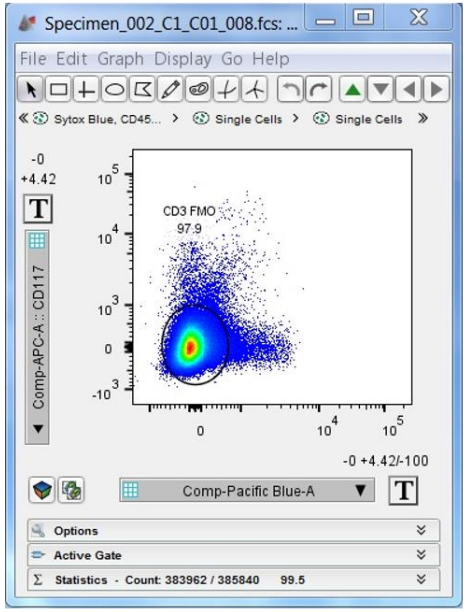
104892137	St7l	TG	T	NMD transcript variant	-	-
104892164	St7l	GTTTT	gttt	NMD transcript variant	-	-
104894332	St7l	CTGTG	C	NMD transcript variant	-	-
104894850	St7l	GA	G	NMD transcript variant	-	-
104899036	St7l	C	CGTGTGT	NMD transcript variant	-	-
104900424	St7l	CA	C	NMD transcript variant	-	-
104900708	St7l	G	GT	NMD transcript variant	-	-
104901051	St7l	GC	GCC	NMD transcript variant	-	-
104905356	St7l	GTATAT	G	NMD transcript variant	-	-
104905606	St7l	T	TG	NMD transcript variant	-	-
104908522	St7l	A	AAAG	NMD transcript variant	-	-
104909839	St7l	GCACA	GCA	NMD transcript variant	-	-
104912083	St7l	ATGTGTGTGTGTGTGTGTGTG	atgtgtgtgtgtgtgtg/atgtgtgtgtgtg	NMD transcript variant	-	-
104912776	St7l	TTTGTTGTTG	T	NMD transcript variant	-	-
104912816	St7l	GGTTTTTTT	GTTTTT	NMD transcript variant	-	-
104913110	St7l	CCTTCCTTT	C	NMD transcript variant	-	-
104915226	St7l	CAA	C	NMD transcript variant	-	-
104915782	St7l	ACATTATACATTT	A	NMD transcript variant	-	-
104916047	St7l	A	AT	NMD transcript variant	-	-
104916340	St7l	A	AT	NMD transcript variant	-	-
104916561	St7l	C	CT	NMD transcript variant	-	-
104917342	St7l	CTT	C	NMD transcript variant	-	-
104917654	St7l	G	GCC	NMD transcript variant	-	-
104918867	St7l	T	TTA	NMD transcript variant	-	-
104918906	St7l	G	GT	NMD transcript variant	-	-

104919044	St7l	TTTTATACTTAATTG	T	NMD transcript variant	-	-
104922461	St7l	ATG	ATGTG	NMD transcript variant	-	-
104923207	St7l	CGTGTGCGTGTGCGTGTGCGTGTGT	CGTGCGTGTGCGTGTGT	NMD transcript variant	-	-
104923209	St7l	TGTGCGTGTGCGTGTGC	tgtgtgcgtgtgc	NMD transcript variant	-	-
104927417	St7l	AG	A	NMD transcript variant	-	-

*Table 123: Insertions and deletions in genes related to the pathogenesis of cancer and lymphocyte biology identified in the QTL. The differences in nucleotides at specific positions between C57BL/6 and A/J mice genes are shown. In AA (amino acid) column, the amino acid replacement would be indicated, followed by the SIFT score on how the substitution in amino acid was predicted to affect protein function, but given they are all located in introns, that information does not apply/is difficult to predict. *Multiple consequences.*

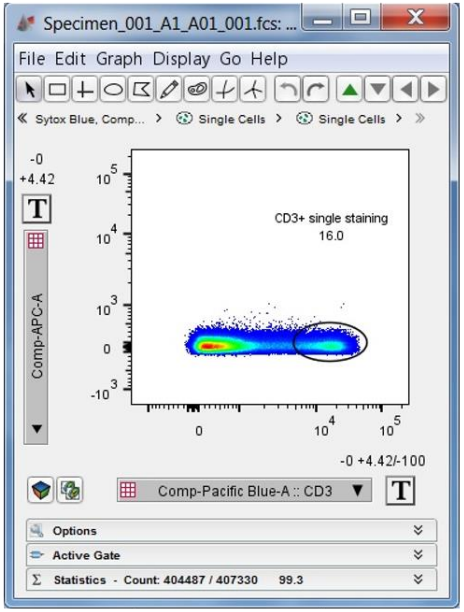
CD3-Pacific Blue

FMO



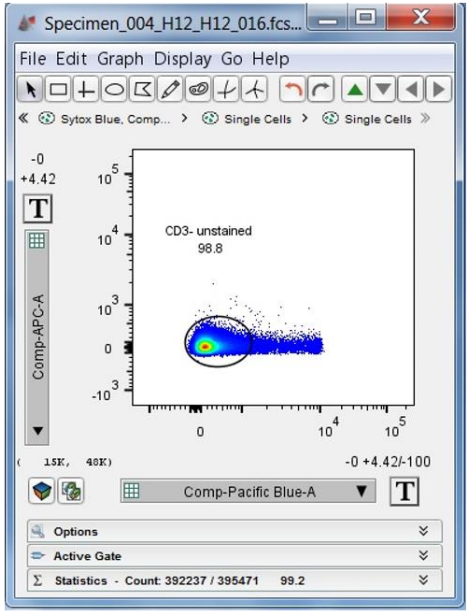
% parent	MFI
97.9	-89.4

Single staining



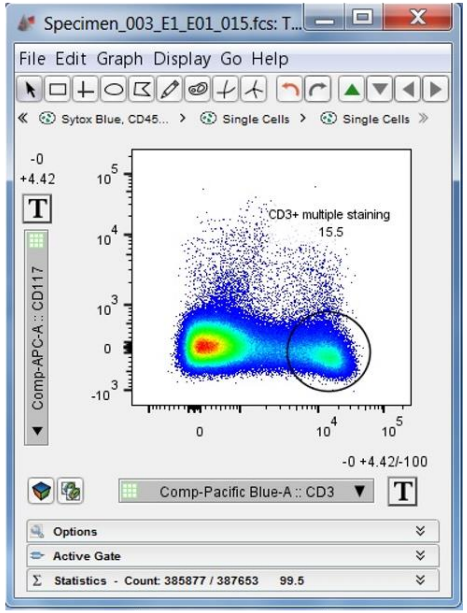
% parent	MFI
16	14177

No staining



% parent	MFI
98.8	224

Multiple staining

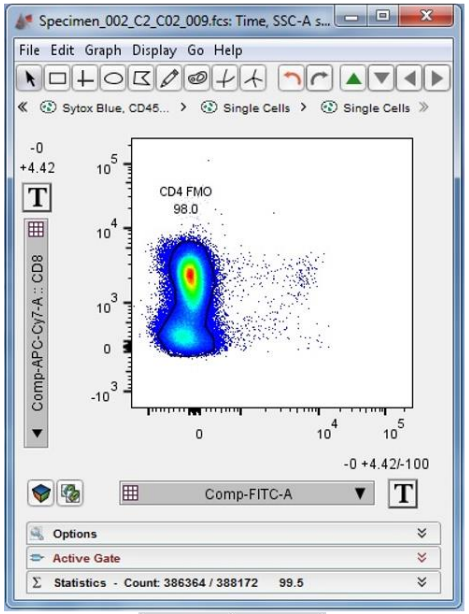


% parent	MFI
15.5	11992

Figure 40: Thymus FMO analysis of CD3-Pacific blue

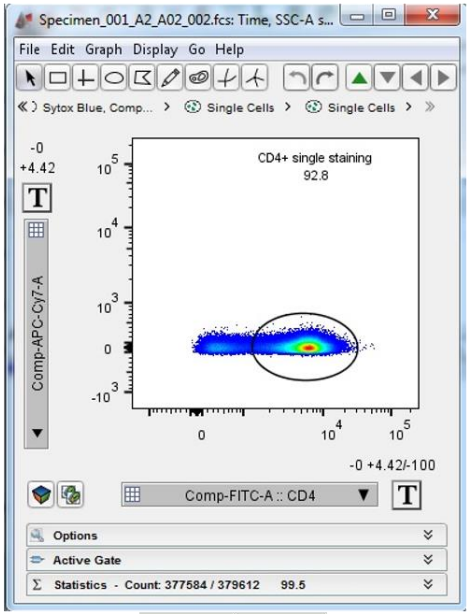
CD4- FITC

FMO



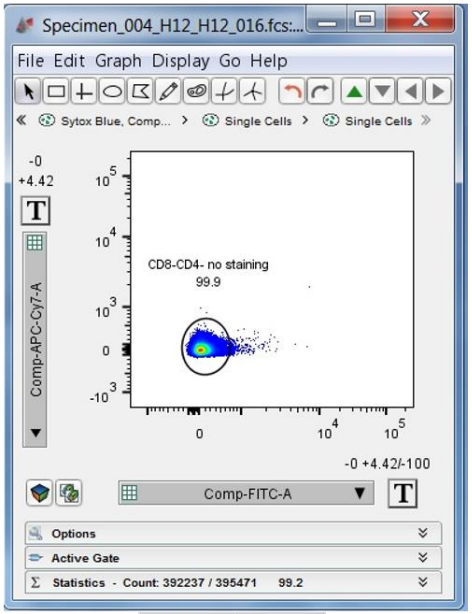
% parent	MFI
97.9	-89.4

Single staining



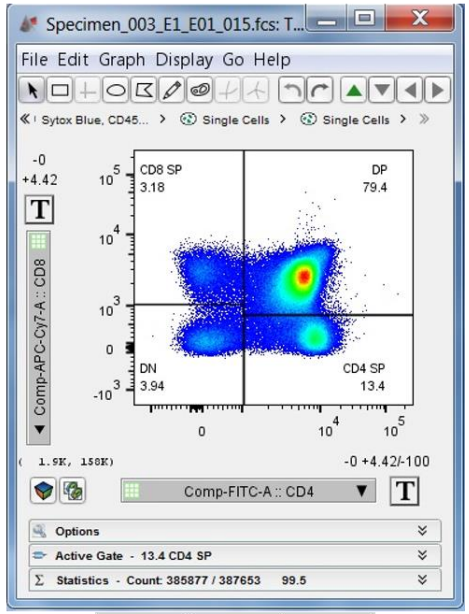
% parent	MFI
92.8	6138

No staining



% parent	MFI
99.9	137

Multiple staining

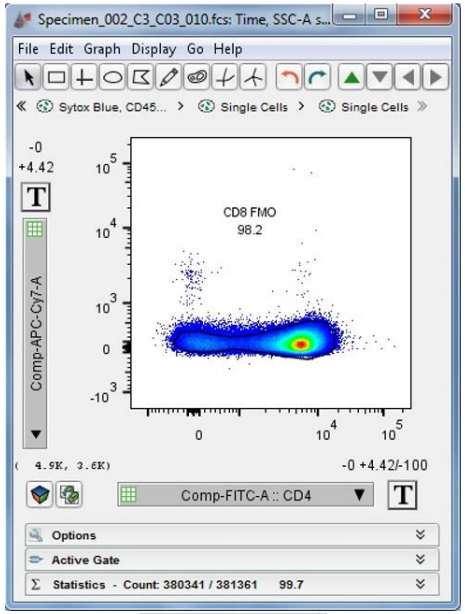


Cell type	% parent	MFI
DP	79.4	5591
CD4SP	13.4	7637

Figure 41: Thymus FMO analysis of CD4-FITC.

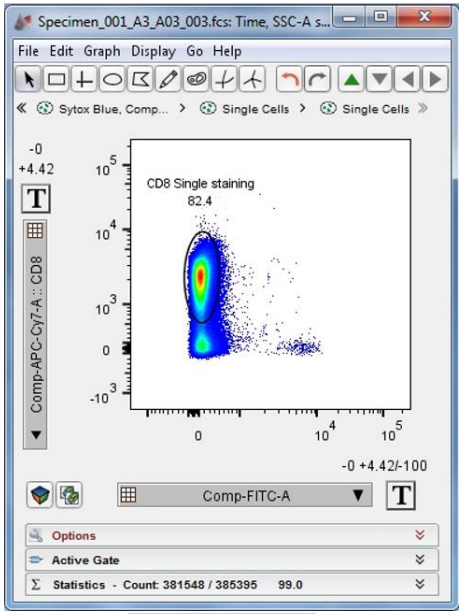
CD8-APC-Cy7

FMO



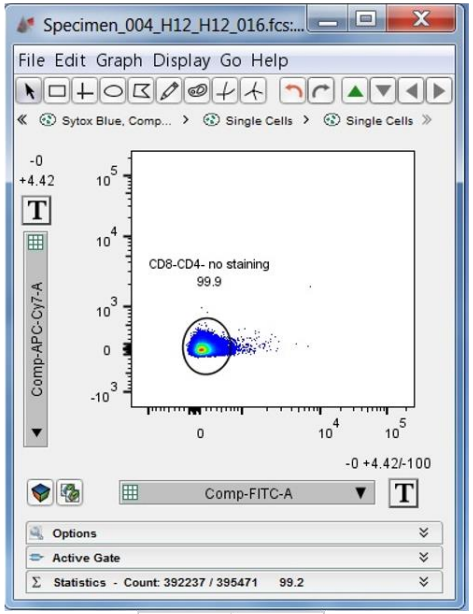
% parent	MFI
98.2	77.5

Single staining



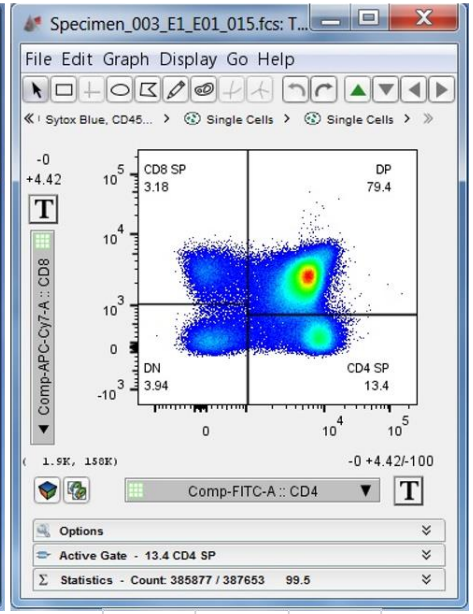
% parent	MFI
82.4	2110

No staining



% parent	MFI
99.9	2.02

Multiple staining

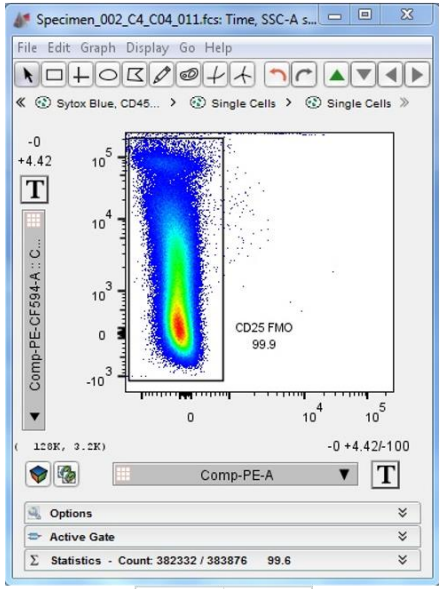


Cell type	% parent	MFI
DP	79.4	2372
CD8SP	3.18	2837

Figure 42: Thymus FMO analysis of CD8-APC-Cy7

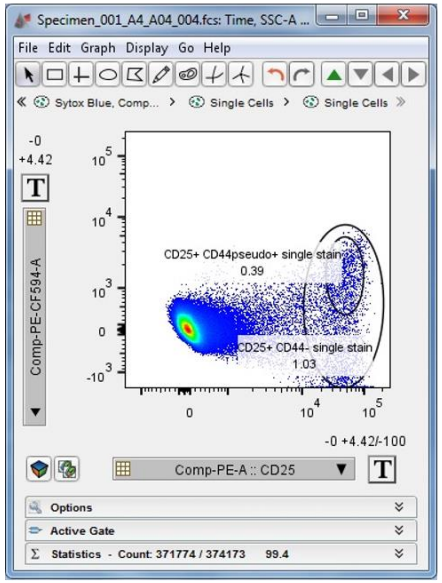
CD25- PE

FMO



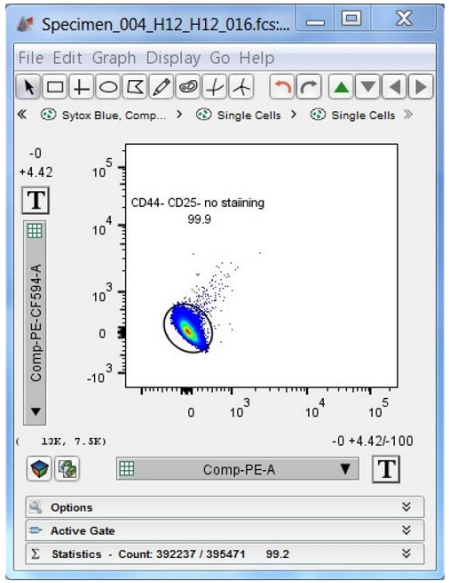
% parent	MFI
99.9	99.9

Single staining



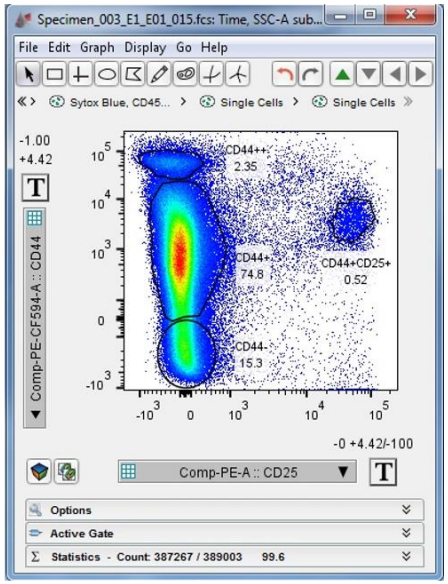
Cell type	% parent	MFI
CD25SP PE	1.03	44223
CD25SP PE-CFC594	1.03	601
pseudoDP PE	0.39	50532
pseudoDP PE-CF594	0.39	1566

No staining



% parent	MFI
99.9	2.02

Multiple staining

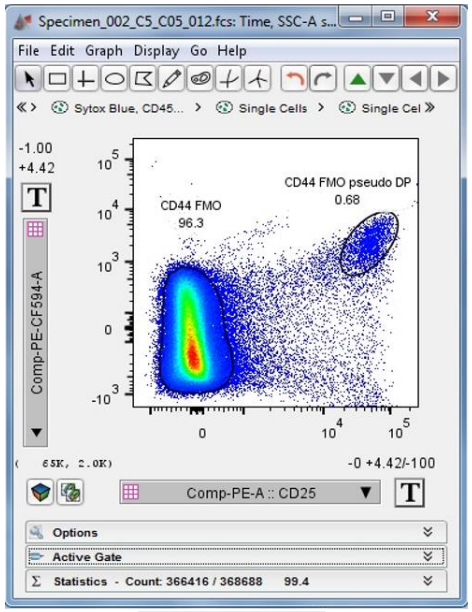


Cell type	% parent	MFI
DP PE	0.52	52385
DP PE-CF594	0.52	4217

Figure 43: Thymus FMO analysis of CD25-PE

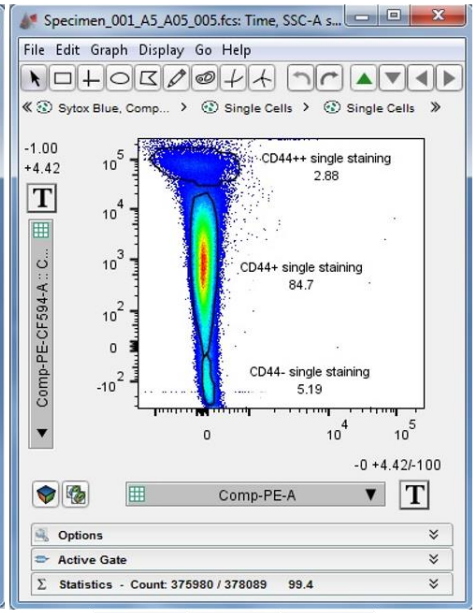
CD44-PE-CF594

FMO



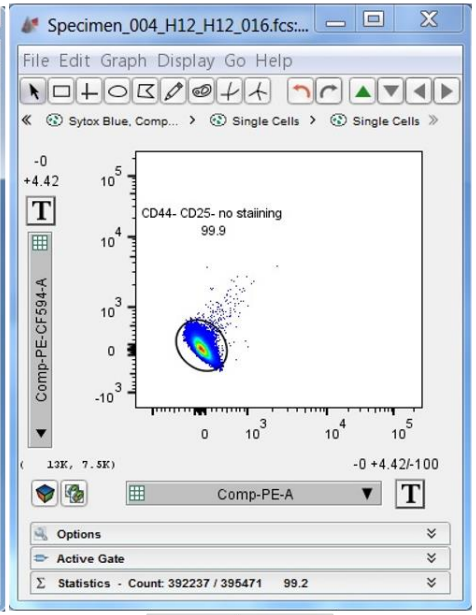
% parent	MFI
96.3	-103

Single staining



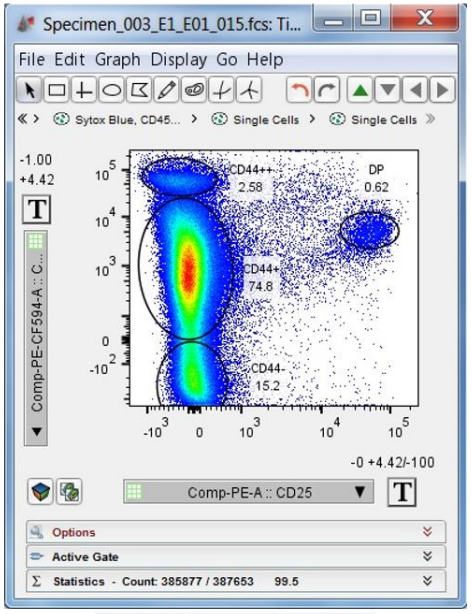
Cell type	% parent	MFI
CD44++	2.88	77913
CD44+	84.7	1894
CD44-	5.19	-97

No staining



% parent	MFI
99.9	26.9

Multiple staining

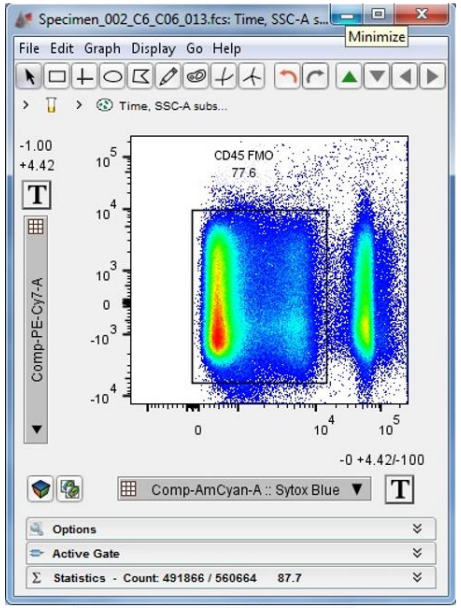


Cell type	% parent	MFI
CD44++	2.58	62555
CD44+	74.8	1775
CD44-	15.2	-213
DP (PE-CF594)	0.52	4217

Figure 44: Thymus FMO analysis of CD44-PE-CF5594

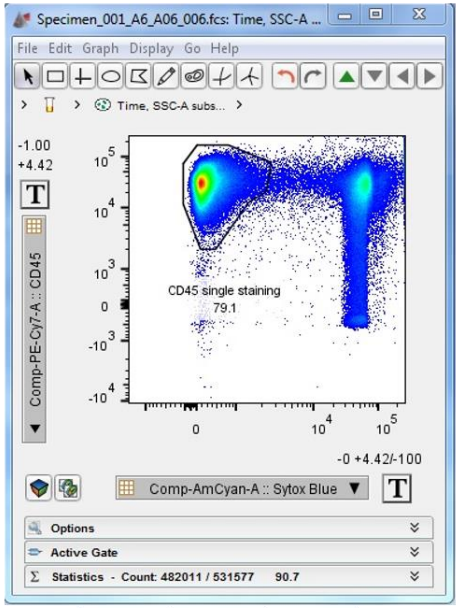
CD45-PE-Cy7

FMO



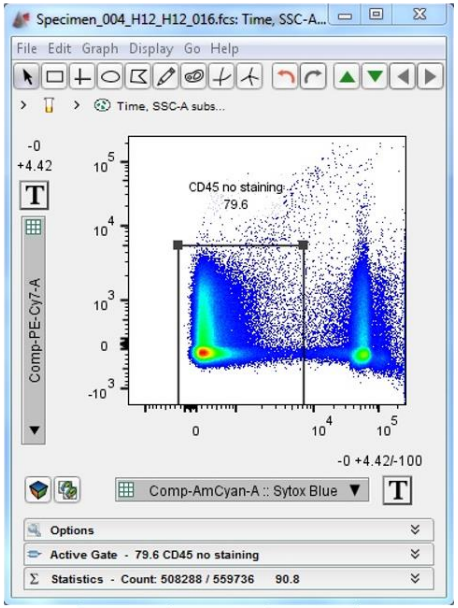
Cell type	% parent	MFI
	77.6	-21.4

Single staining



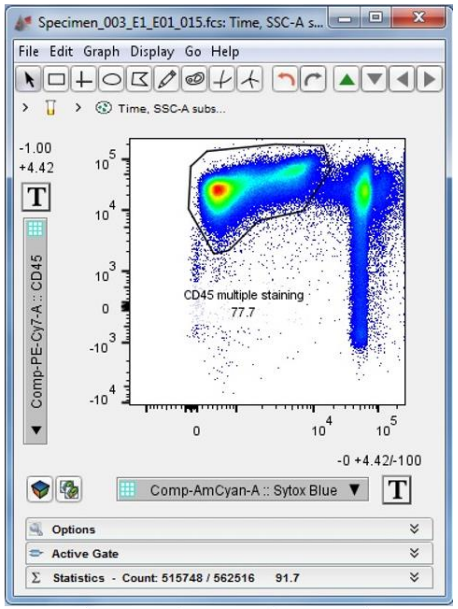
Cell type	% parent	MFI
	79.1	31217

No staining



Cell type	% parent	MFI
	79.6	60.8

Multiple staining

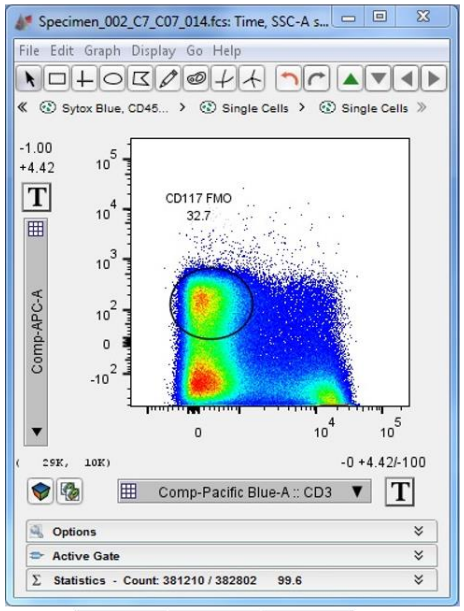


Cell type	% parent	MFI
	77.7	29102

Figure 45: Thymus FMO analysis of CD45-PE-Cy7

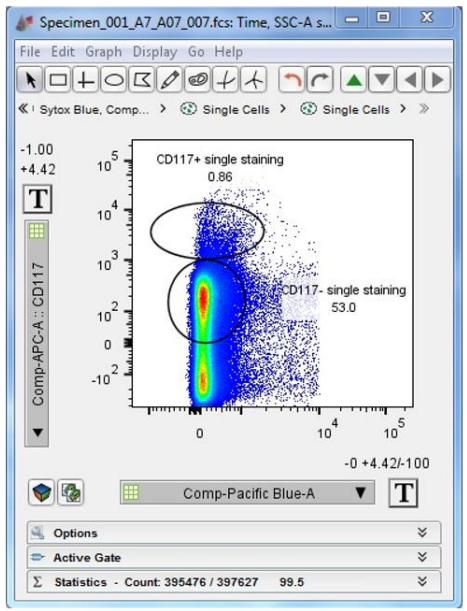
CD117-APC

FMO



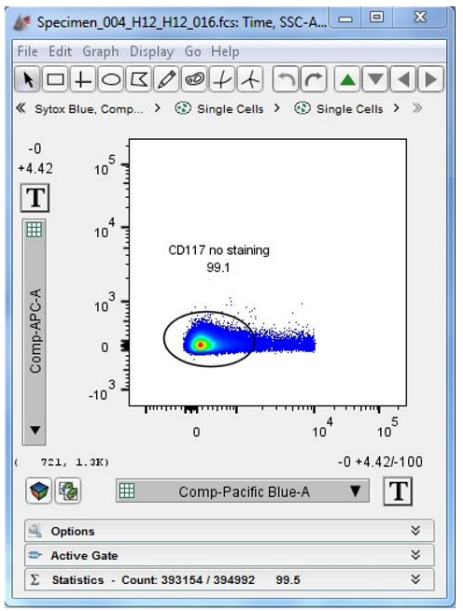
Cell type	% parent	MFI
	32.7	146

Single staining



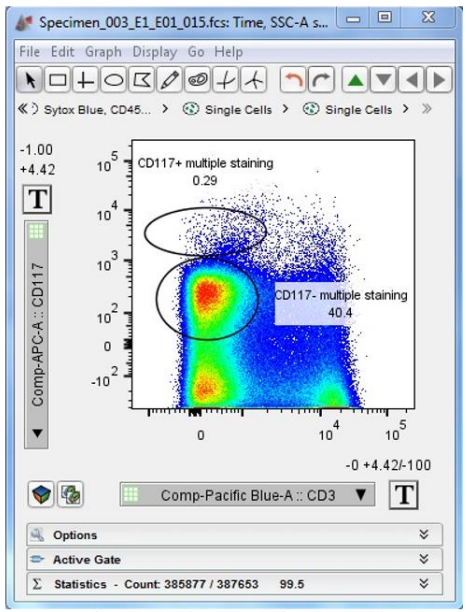
Cell type	% parent	MFI
CD117+	0.86	2862
CD117-	53	174

No staining



Cell type	% parent	MFI
	99.1	25.6

Multiple staining

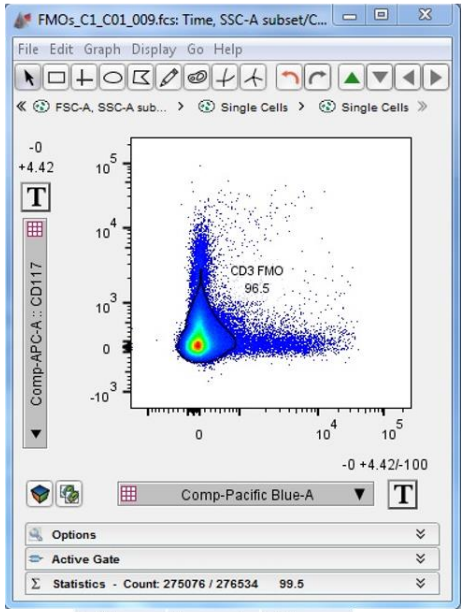


Cell type	% parent	MFI
CD117-	0.29	214
CD117+	40.4	3248

Figure 46: Thymus FMO analysis of CD117-APC

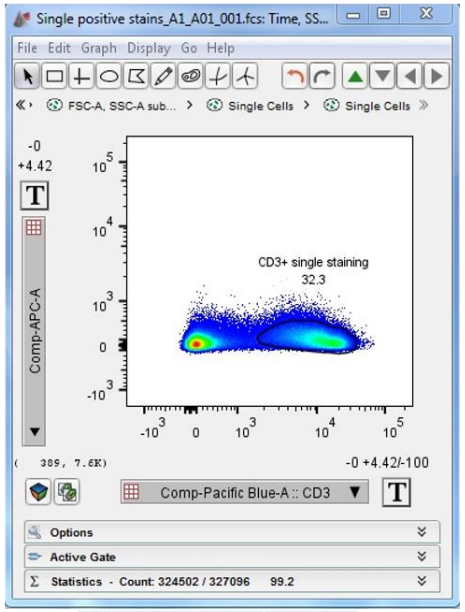
CD3-Pacific Blue

FMO



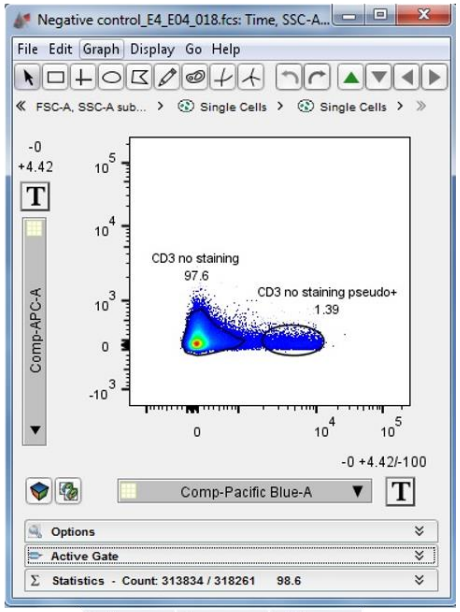
Cell type	% parent	MFI
	96.5	77.4

Single staining



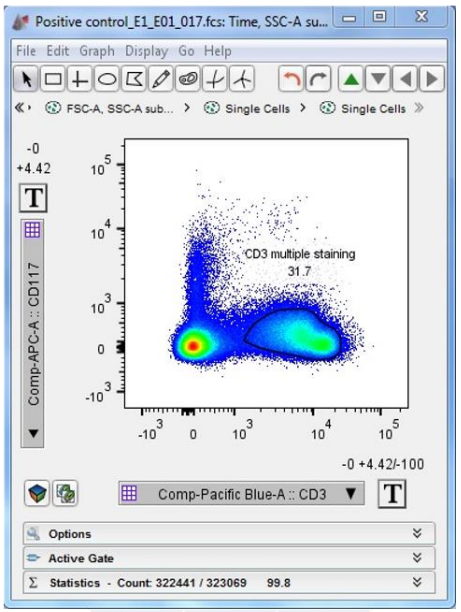
Cell type	% parent	MFI
	32.3	11616

No staining



Cell type	% parent	MFI
	100	147

Multiple staining

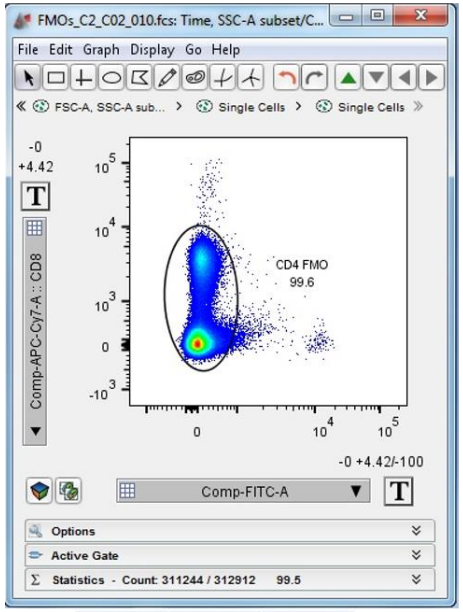


Cell type	% parent	MFI
	31.7	8598

Figure 47: Spleen FMO analysis of CD3-Pacific blue

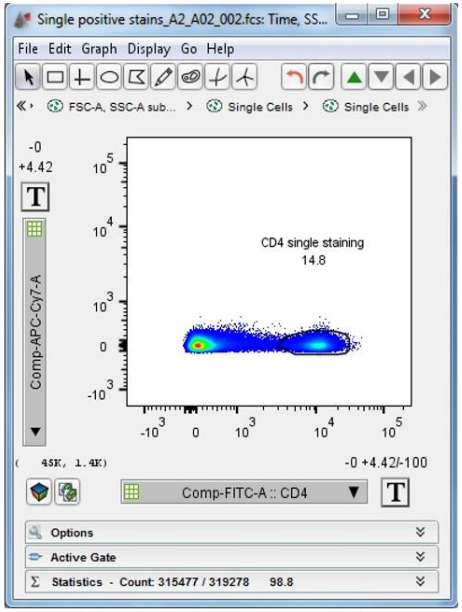
CD4-FITC

FMO



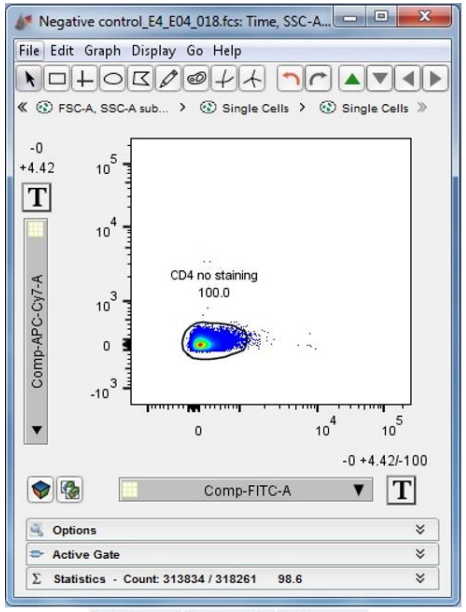
Cell type	% parent	MFI
	99.6	127

Single staining



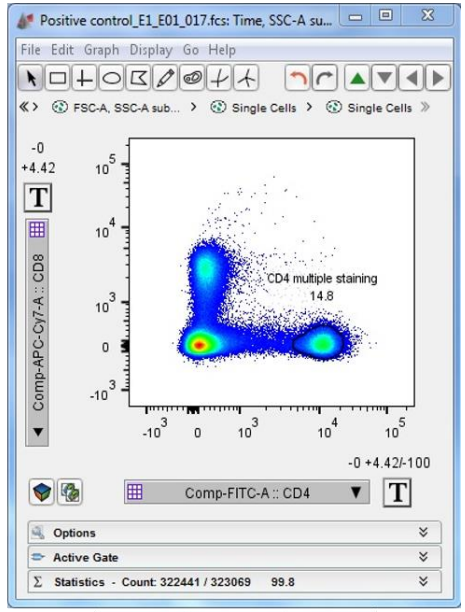
Cell type	% parent	MFI
	14.8	10405

No staining



Cell type	% parent	MFI
	100	147

Multiple staining

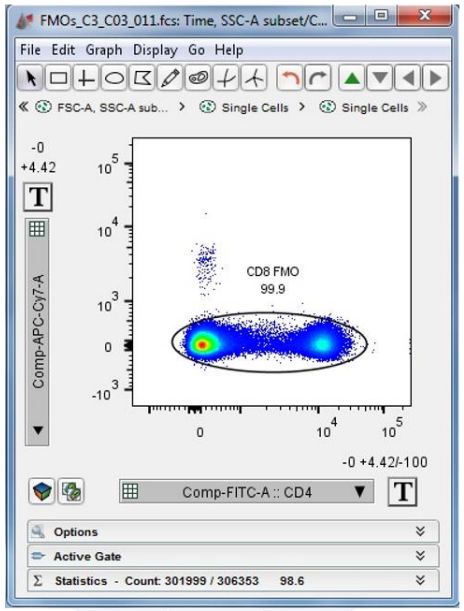


Cell type	% parent	MFI
	14.8	11151

Figure 48: Spleen FMO analysis of CD4-FITC

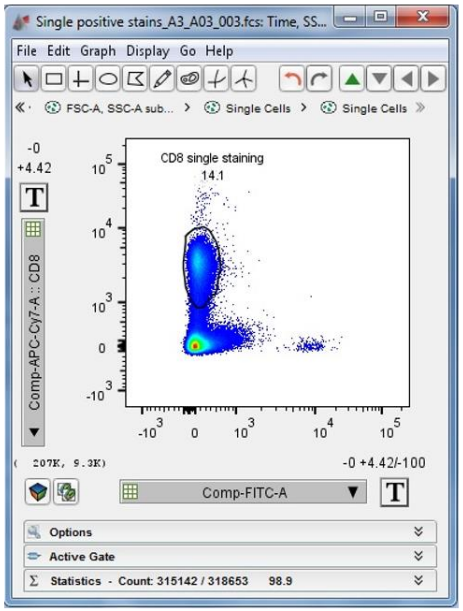
CD8-APC-Cy7

FMO



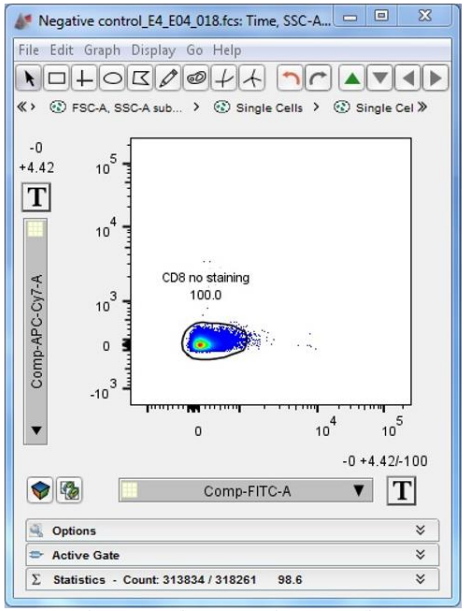
Cell type	% parent	MFI
	99.9	23

Single staining



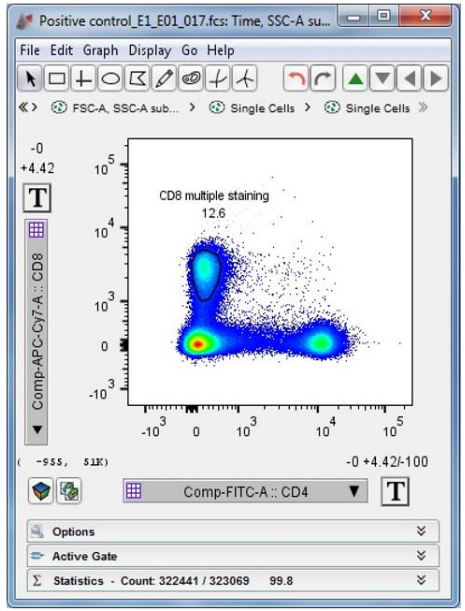
Cell type	% parent	MFI
	14.1	3081

No staining



Cell type	% parent	MFI
	100	2.6

Multiple staining

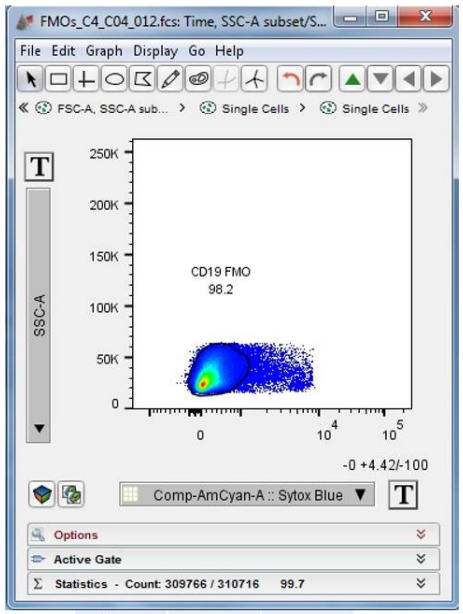


Cell type	% parent	MFI
	12.6	2538

Figure 49: Spleen FMO analysis of CD8-APC-Cy7

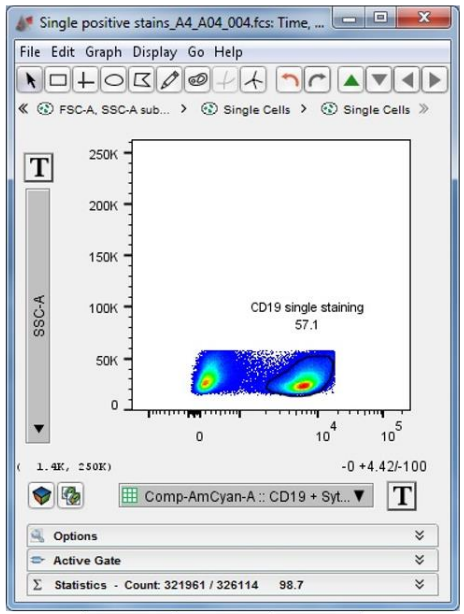
CD19-AMCyan

FMO



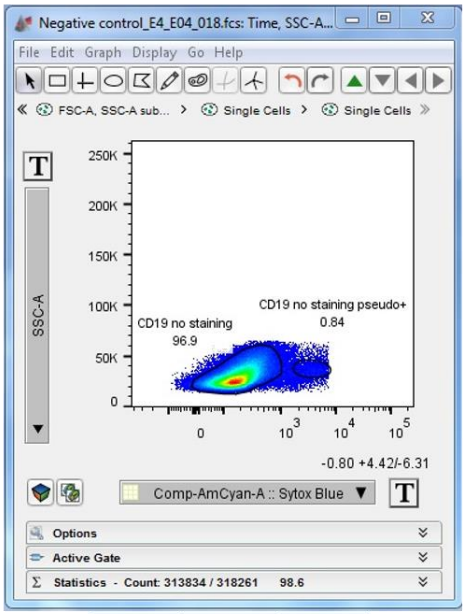
Cell type	% parent	MFI
	98.2	224

Single staining



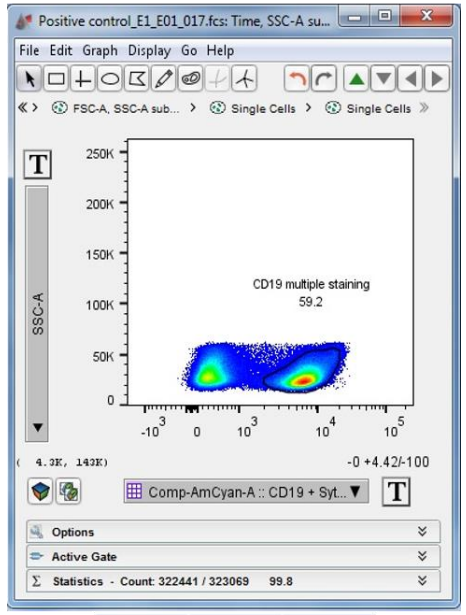
Cell type	% parent	MFI
	57.1	6607

No staining



Cell type	% parent	MFI
	96.9	197
	0.84	3625

Multiple staining

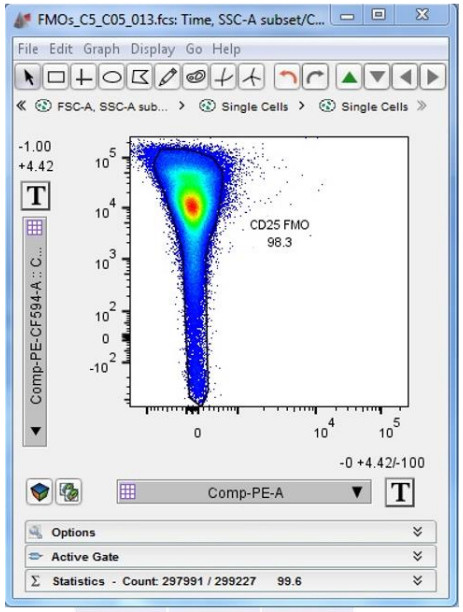


Cell type	% parent	MFI
	59.2	6685

Figure 50: Spleen FMO analysis of CD19-AmCyan

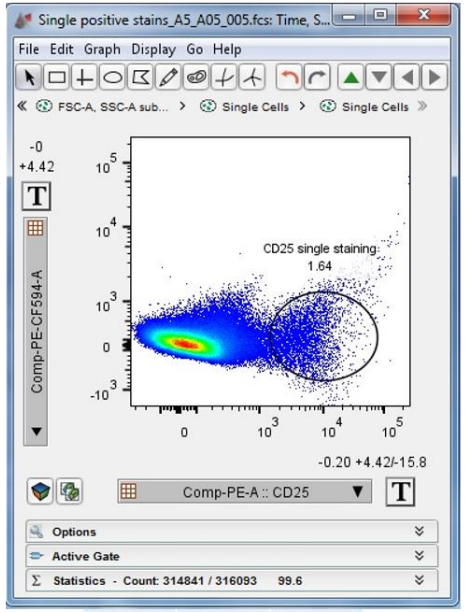
CD25-PE

FMO



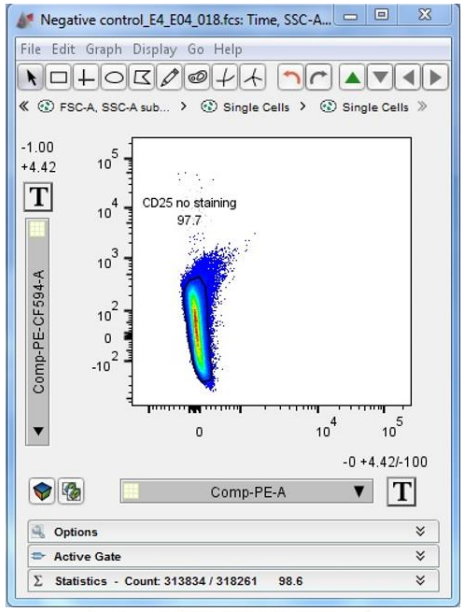
Cell type	% parent	MFI
	98.3	-32

Single staining



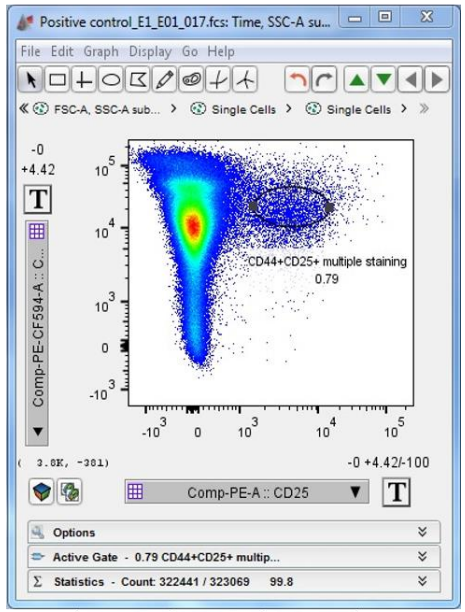
Cell type	% parent	MFI
	1.64	4862

No staining



Cell type	% parent	MFI
	97.7	27

Multiple staining

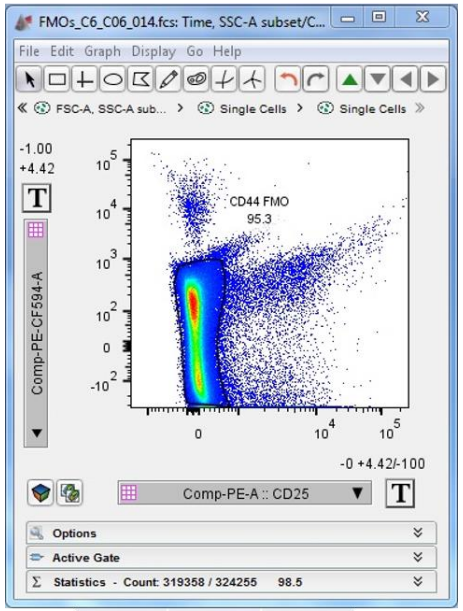


Cell type	% parent	MFI
	0.79	4644

Figure 51: Spleen FMO analysis of CD25-PE

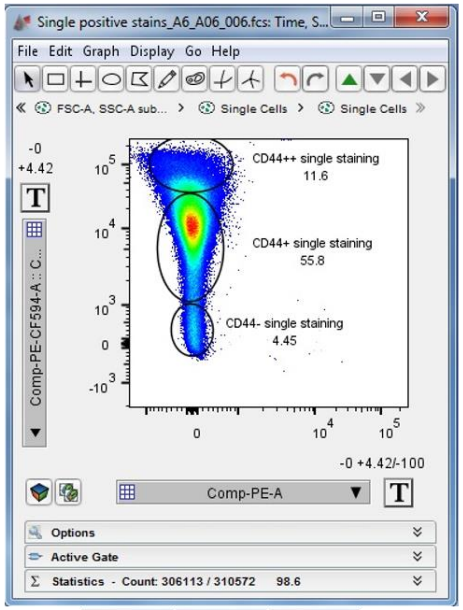
CD44-PE-CF594

FMO



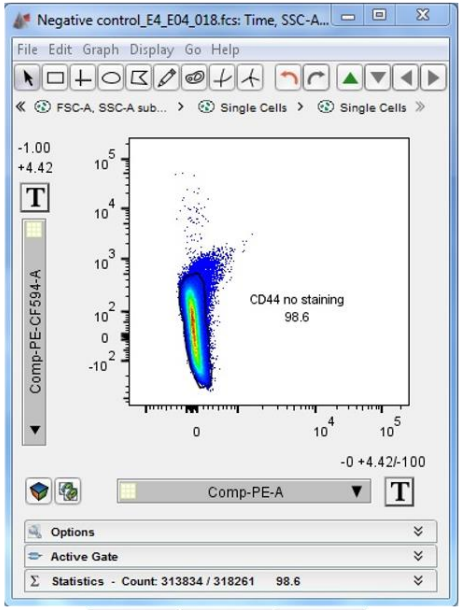
Cell type	% parent	MFI
	95.3	58.2

Single staining



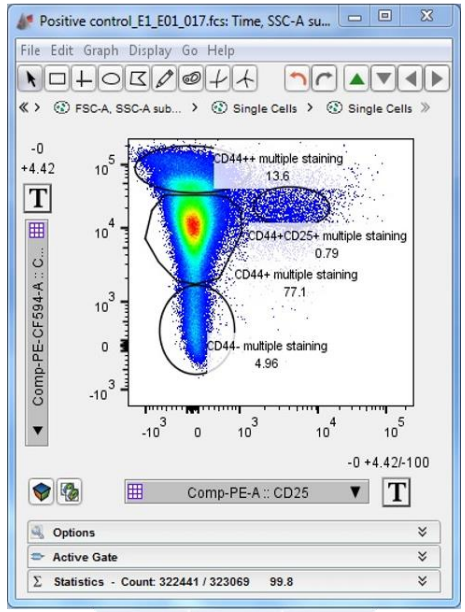
Cell type	% parent	MFI
CD44++	11.6	64524
CD44+	55.8	9406
CD44-	4.45	340

No staining



Cell type	% parent	MFI
	98.6	37.4

Multiple staining

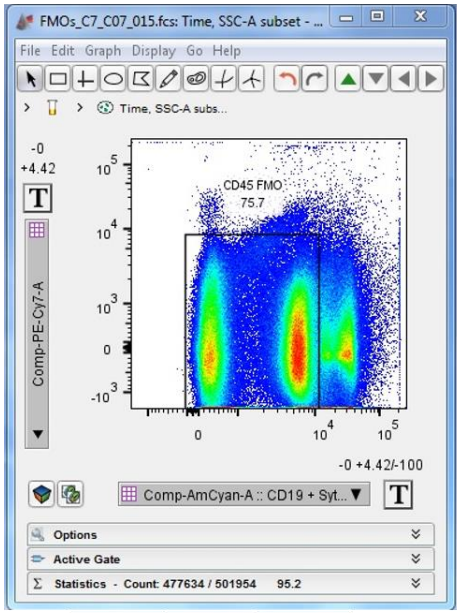


Cell type	% parent	MFI
CD44++	13.6	63009
CD44+	77.1	12637
CD44-	4.96	460
DP	0.79	21715

Figure 52: Spleen FMO analysis of CD44-PE-CF594

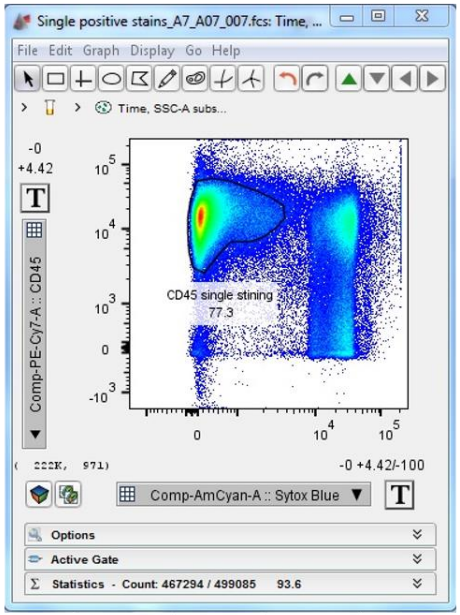
CD45-PE-Cy7

FMO



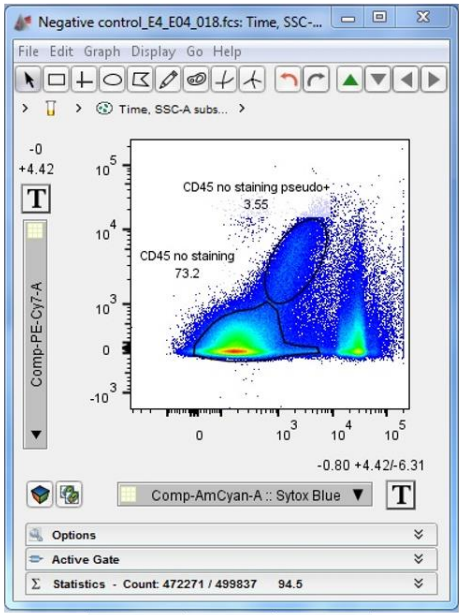
Cell type	% parent	MFI
	75.7	249

Single staining



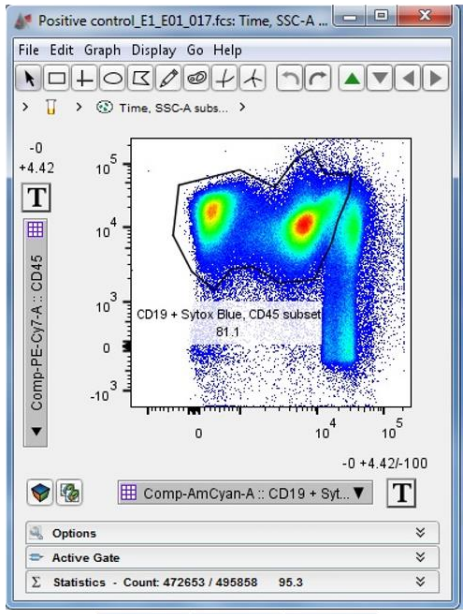
Cell type	% parent	MFI
	77.3	15754

No staining



Cell type	% parent	MFI
	73.2	35.2
pseudoCD45	3.55	3876

Multiple staining

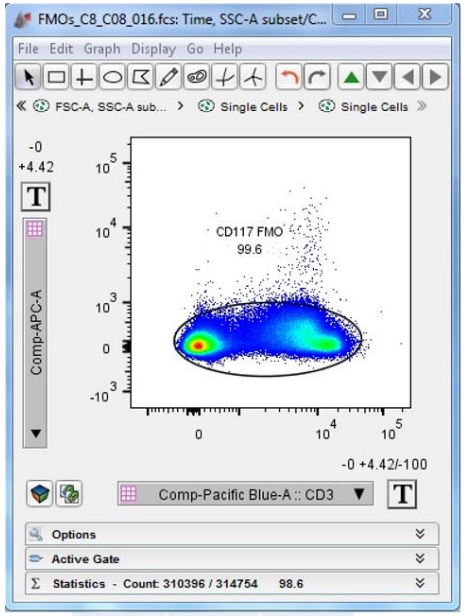


Cell type	% parent	MFI
	81.1	14353

Figure 53: Spleen FMO analysis of CD45-PE-Cy7

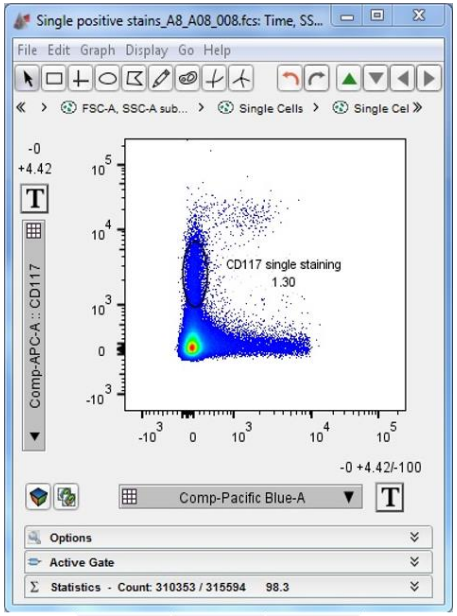
CD117-APC

FMO



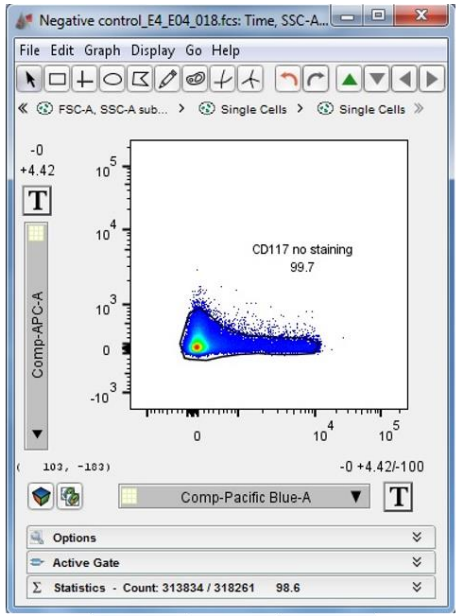
Cell type	% parent	MFI
	99.6	89.3

Single staining



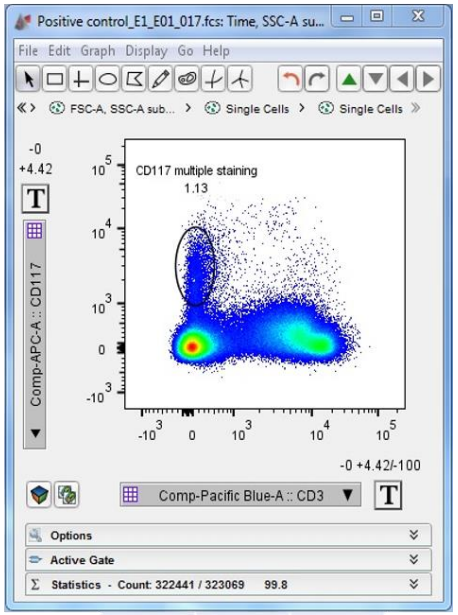
Cell type	% parent	MFI
	1.3	2533

No staining



Cell type	% parent	MFI
	99.7	70.2

Multiple staining



Cell type	% parent	MFI
	1.13	2590

Figure 54: Spleen FMO analysis of CD117-APC